UNIVERSIDAD DE MÁLAGA

Programa de Doctorado de

BIOMEDICINA, INVESTIGACIÓN TRASLACIONAL Y NUEVAS TECNOLOGÍAS EN SALUD

Facultad de Medicina
Universidad de Málaga

Tesis Doctoral

Human-Derived Blood-Brain Barrier *In Vitro* Models as Reliable Tools for Research and Therapeutics

Ana Aragón González

Agosto 2024

Directoras:

Mª Yolanda de Diego Otero
Laura Ferraiuolo

Tutora:

Mª Inmaculada Bellido Estévez

AUTOR: Ana Aragón González

https://orcid.org/0000-0002-8244-0848

EDITA: Publicaciones y Divulgación Científica. Universidad de Málaga

UNIVERSIDAD DE MÁLAGA

ANDALUCÍA TECH

DECLARACIÓN DE AUTORÍA Y ORIGINALIDAD DE LA TESIS PRESENTADA PARA OBTENER EL TÍTULO DE DOCTOR

D./Dña. **Ana Aragón González**,

estudiante del programa de doctorado **Biomedicina Investigación Traslacional y Nuevas Tecnologías en Salud** de la Universidad de Málaga, autor/a de la tesis, presentada para la obtención del título de doctor por la Universidad de Málaga, titulada:

"Human-Derived Blood-Brain Barrier In Vitro Models as Reliable Tools for Research and Therapeutics".

Realizada bajo la tutorización de Dña. **Mª Inmaculada Bellido Estévez** y dirección de Dña. **Mª Yolanda de Diego Otero** y Dña. **Laura Ferraiuolo**.

Declaro que:

La tesis presentada es una obra original y que no infringe los derechos de propiedad intelectual ni los derechos de propiedad industrial u otros, conforme al ordenamiento jurídico vigente (Real Decreto Legislativo 1/1996, de 12 de abril, por el que se aprueba el texto refundido de la Ley de Propiedad Intelectual, regularizando, aclarando y armonizando las disposiciones legales vigentes sobre la materia), modificado por la Ley 2/2019, de 1 de marzo.

Igualmente asumo, ante la Universidad de Málaga y ante cualquier otra instancia, la responsabilidad que pudiera derivarse en caso de plagio de contenido en la tesis presentada, conforme al ordenamiento jurídico vigente.

En Málaga, a 24 de agosto de 2024.

Fdo.: Ana Aragón González Doctoranda	Fdo.: M.ª Inmaculada Bellido Estévez Tutora
Fdo.: M.ª Yolanda de Diego Otero Directora	

D. / Dª **Laura Ferraiuolo**, Catedrático/a de Neurociencia Traslacional de la Facultad de Neurociencia de la Universidad de Sheffield, Reino Unido.

D. / Dª **Mª Yolanda de Diego Otero**, Doctora en Biología Molecular y Celular, Facultad de Ciencias. Universidad de Córdoba.

D. / Dª **Mª Inmaculada Bellido Estévez**, Profesora Titular Farmacología de la Facultad de Medicina, Universidad de Málaga.

CERTIFICAN Que D/Dª. **Ana Aragón González**
ha obtenido y estudiado personalmente bajo mi dirección los datos de investigación necesarios para la realización de su Tesis Doctoral, titulada: "**Human-Derived Blood-Brain Barrier In Vitro Models as Reliable Tools for Research and Therapeutics"**, que considero tiene el contenido y rigor científico necesario para ser sometido al superior juicio de la Comisión que nombre la Universidad de Málaga para optar a grado de Doctor.

Y que la publicación en coautoría que avala la presentación de esta tesis y cuyas referencias son:

Aragón-González, A.; Shaw, P.J.; Ferraiuolo, L. Blood–Brain Barrier Disruption and Its Involvement in Neurodevelopmental and Neurodegenerative Disorders. *Int. J. Mol. Sci.* 2022, 23, 15271. https://doi.org/10.3390/ijms232315271

Aragón-González, A., Shaw, A.C., Kok, J.R. *et al*. *C9ORF72* patient-derived endothelial cells drive blood-brain barrier disruption and contribute to neurotoxicity. *Fluids Barriers CNS* 21, 34 (2024). https://doi.org/10.1186/s12987-024-00528-6

no han sido utilizada en tesis anteriores ni en la Universidad de Málaga ni en otras Universidades.

Y para que conste, en cumplimiento de las disposiciones vigentes, expido el presente certificado en

Málaga, 24 de agosto de 2024.

Firman todos Director/es

Directora: Mª Yolanda de Diego Otero

Tutora: Mª Inmaculada Bellido Estévez

FUNDING

This project was funded by the 765704/European Union's Horizon 2020 research and innovation programme under the Marie Skłodowska-Curie grant agreement.

Miss Ana Aragón González was partially supported by Fulbright Spain in 2022 to investigate as a research visitor in the USA.

Funded by the Horizon 2020
Framework Programme of the
European Union

Acknowledgements

I want to express my gratitude to countless people who have played crucial roles in my journey through my PhD.

Here are some of them.

I would like to start by thanking my supervisor in Malaga, Dr Yolanda de Diego, for providing me with the opportunity to embark on this PhD path and for her continuous support. Then, I am deeply grateful to my primary supervisor, Prof. Laura Ferraiuolo, and my secondary supervisor, Prof. Dame Pamela Shaw, for their invaluable guidance and mentorship.

I am very grateful to Laura for her support, patience, positivity and honest mentoring along the years. Both, Pam and Laura helped me to grow as a scientist and as an individual for which I am truly thankful. It was an honour being part of the Ferraiuolo's team.

I also wish to extend my appreciation to Amalia for her excellent advice during my PhD journey and USA's adventure, together with Inmaculada for her assistance. Furthermore, I am thankful to Dr. Kathrin Meyer for hosting me as a Fulbright Research Visitor in her lab in Columbus, Ohio, and for her support and guidance.

Additionally, I would like to thank everyone in Ferraiuolo's lab, Andre, Allan, Sarah, Cleide, Selina, Raquel, Marianne, Monika, Jannigje, Amy; and the Meyer lab, Florence, Shrestha, Krizelle, Vera, Pipasha, Sam, Yana, Meysam, Sunshine, Shibi, Andrea, Megan, Abuzar, for their insight and encouragement along the years.

Additionally, I am grateful to all the members of the EuroNeurotrophin network for their collaborative help and support during my doctorate.

All great scientists and incredible people, I have been very lucky to have you as colleagues. I am thankful to everyone in SITraN, Sheffield, and the Nationwide Children's Hospital, Columbus (OH). In both places, I met outstanding individuals like Erika and Matt; and made long-life friends like Rachael.

I would like to extend my gratitude to the patients, their relatives and the foundations; this research was possible thanks to them.

Many thanks to my dearest friends in Spain, Elena, Marta, Celia, Carmen, Caterina and Marta: you have always been there for me, even though we no longer live in the same town.

Next, I would like to acknowledge my parents, for their infinite support and love. I would like to thank the rest of my big family, my grandparents, my dear dog Dina, for her unconditional love, and my cousins, Pili and Ana, for their constant encouragement, visits and laughs.

Lastly, special thanks to my partner Joserra, for always being there for me and believing in me during every step of my career. Doing a PhD is not an easy journey, and I am so lucky to have you by my side.

I couldn't have reached this milestone without each one of you.

Thank you all for being a part of this incredible journey with me!

Como decía Cajal en su libro sobre las reglas y consejos sobre la investigación biológica, los tónicos de la voluntad, allá por 1899:

(1) Sobre la aptitud científica e investigadora.

Como han afirmado muchos pensadores y pedagogos, el descubrimiento no es fruto de ningún talento originariamente especial, sino del sentido común mejorado y robustecido por la educación técnica y por el hábito del meditar sobre los problemas científicos. Así pues, quien disponga de regular criterio para guiarse en la vida, lo tendrá también para marchar desembarazado por el camino de la investigación.

(2) Sobre la ciencia práctica.

Cultivemos la ciencia por sí misma, sin considerar por el momento las aplicaciones. Estas llegan siempre, a veces tardan años, a veces, siglos. Poco importa que una verdad científica sea aprovechada por nuestros hijos o por nuestros nietos.

Es así que, con esta tesis, no pretendo desvelar las bases de la neurodegeneración, pero en este viaje de estudio pormenorizado sobre la barrera hematoencefálica, tanto a nivel teórico como práctico, espero que mi aportación sea de interés científico y que, con ello, ayude en un futuro a desarrollar terapias efectivas para los pacientes que tanto las necesitan.

A mi madre

Abstract

The blood-brain barrier (BBB) is a term used to describe the semipermeable cellular barrier that surrounds the microvasculature of the central nervous system (CNS). CNS vessels are continuous, non-fenestrated vessels, but they also possess a series of specific properties that allow them to strictly regulate the movement of molecules, ions, and cells between the blood and the CNS. This structure plays a fundamental role in maintaining cerebral homeostasis to enable proper neuronal function and protect the CNS from toxins, pathogens, inflammation, injuries, and diseases. The blood vessels that form the BBB are composed of two main types of cells: endothelial cells (ECs), which structure the walls of the blood vessels, and mural cells which sit on the abluminal surface of the EC layer. The properties of the BBB are largely manifested within the ECs but are induced and maintained by critical interactions with mural cells, pericytes, astrocytes, immune cells, glial cells, and neural cells, which interact and compose the neurovascular unit (NVU). The BBB allows the selective passage of molecules necessary for the brain's proper functioning while restricting the entry of potentially toxic substances, including some drugs.

In this manuscript, I will review the evidence of cerebrovascular system damage presented by others and explain its recognized importance in protecting the brain. Despite this, the exact contribution of the BBB to neurodegenerative and neurodevelopmental diseases such as amyotrophic lateral sclerosis (ALS) and Rett syndrome (RTT) remains unclear. Previous studies have suggested that BBB dysfunction may be implicated in the pathogenesis of these diseases, but a more comprehensive understanding of the underlying mechanisms is still needed.

Brain microvascular ECs (BMECs) are essential components of the BBB, characterised by the formation of tight junctions (TJs) involving various proteins: primarily Claudin-5, Occludin, and junctional adhesion molecules (JAMs), and the presence of specialised transporters such as P-glycoprotein. Together with astrocytes, they form a protective network around cerebral blood vessels; thus, actively regulating permeability and molecular exchange between the blood and the brain. Astrocytes play an essential role in BBB regulation, and their dysfunction is associated with various neurological disorders, including Alzheimer's disease (AD). However, the exact implication of BBB dysfunction in neurodegeneration is still unknown. While some studies suggest that BBB breakdown may be secondary to neurodegeneration, others propose a direct role in disease pathogenesis.

In this context, this research focuses on developing *in vitro* BBB models using human induced pluripotent stem cells (hi-PSCs) from patients with *C9ORF72* and *MECP2* mutations, linked to ALS and RTT, respectively. No similar multicellular models for both mutations have been described before. These hi-PSC models allow the study of BMEC and astrocyte dysfunction and their roles in disease pathogenesis. Our study revealed altered gene expression and decreased barrier integrity in BMECs from patients with these mutations. Astrocytes from both ALS and RTT patients showed toxicity towards BMECs, affecting permeability. Notably, ALS-astrocytes impacted BMEC function and Glut-1 expression, unlike RTT. Additionally, co-culturing BMECs with astrocytes from both models led to reduced permeability and decreased Claudin-5 and Glut-1 protein expression, as seen in ALS animal models. Moreover, both models showed altered BMEC energy metabolism, with ALS models also exhibiting motor neuron toxicity, underscoring the complexity of BBB interactions in these diseases.

In summary, this research sheds light on the crucial role of BMECs and astrocytes in BBB dysfunction in ALS and RTT. These findings have important implications for the development of new experimental therapies and treatment strategies for these diseases, as well as for a broader understanding of neurological disorders in general.

Resumen extendido en castellano

La barrera hematoencefálica (BHE) es un término utilizado para describir la barrera celular semipermeable que envuelve la microvasculatura del sistema nervioso central (SNC). Los vasos del SNC son conductos continuos no fenestrados, pero también contienen una serie de propiedades específicas que les permiten regular estrictamente el movimiento de moléculas, iones y células entre la sangre y el SNC, desempeñando un papel fundamental en el mantenimiento de la homeostasis cerebral para permitir la función neuronal adecuada, así como para proteger el SNC de toxinas, patógenos, inflamación, lesiones y enfermedades. Los vasos sanguíneos que forman la BHE, se componen de dos tipos de células principales, las células endoteliales (CE) que forman las paredes de los vasos sanguíneos y células murales que se asientan en la superficie abluminal de la capa de endotelial. Las propiedades de la BHE se manifiestan en gran medida por las CE, pero son inducidas y mantenidas por interacciones críticas con células murales, pericitos, astrocitos, células inmunes, células gliales y células neurales, que interactúan formando la unidad neurovascular (NVU). La BHE permite el paso selectivo de moléculas necesarias para el funcionamiento adecuado del cerebro, mientras que restringe la entrada de sustancias potencialmente dañinas, incluso de algunos fármacos.

A pesar de las evidencias del daño en el sistema cerebrovascular presente en la neurodegeneración, el cual comentaremos en esta investigación, y de la importancia de la BHE protegiendo el cerebro, su contribución exacta en las enfermedades neurodegenerativas y del neurodesarrollo, como la esclerosis lateral amiotrófica (ELA) y el síndrome de Rett (RTT), sigue siendo objeto de investigación. Estudios previos han sugerido que la disfunción de la BHE puede estar implicada de forma indirecta en la patogénesis de estas enfermedades, aunque se necesita una comprensión más completa de sus mecanismos subyacentes.

Las CE microvasculares cerebrales o BMECs, son elementos esenciales de la BHE, caracterizadas por la formación de uniones estrechas (TJ), con la participación de distintas proteínas, principalmente Claudina-5, Ocludina y moléculas de adhesión de la unión (JAMs), y la presencia de transportadores especializados como la glicoproteína-P, que junto a los astrocitos, forman una red protectora alrededor de los vasos sanguíneos cerebrales, regulando activamente la permeabilidad y el intercambio molecular entre la sangre y el cerebro. Los astrocitos juegan un papel esencial en esta regulación y su disfunción se asocia con diversos trastornos neurológicos, como el Alzhéimer entre otros. Sin embargo, la exacta implicación de la disfunción de la BHE en la neurodegeneración aún se desconoce. Es así que, mientras algunos estudios sugieren que la ruptura de la BHE puede ser secundaria a la neurodegeneración, otros plantean la posibilidad de un papel directo en la patogénesis de la enfermedad.

En este contexto, esta investigación se enfoca en desarrollar modelos *in vitro* de la BHE utilizando células madre pluripotentes humanas (hi-PSCs), derivadas de pacientes con mutaciones *C9ORF72* y *MECP2*, asociadas con dos enfermedades, la ELA y el RTT respectivamente. Hasta este momento, no se han descrito modelos multicelulares de similares características para ambas mutaciones. Estos modelos con hi-PSCs, nos permiten estudiar cómo la disfunción de las BMECs y los astrocitos contribuye a la patogénesis de estas enfermedades. Los resultados de este estudio han mostrado una alteración en la expresión génica y una disminución en la integridad de BHE en las BMECs derivadas de pacientes con ELA y RTT. Además, los astrocitos, elementos clave en el correcto funcionamiento la BHE, provenientes tanto de pacientes con ELA como de RTT, exhiben toxicidad hacia las BMECs, lo que altera su permeabilidad. Curiosamente, mientras que el medio condicionado de los astrocitos de pacientes con ELA puede afectar la función de las BMECs y la expresión del transportador de glucosa

GLUT1, no se observaron efectos similares para el RTT. Sin embargo, el cocultivo de BMECs con astrocitos inducibles (iAstrocitos) derivados de fibroblastos de pacientes de ambos modelos de enfermedad mostró una reducción en la permeabilidad y una disminución significativa en la expresión de las proteínas Claudina-5 y GLUT1, como se observa en modelos de ELA. Además, se evidenciaron alteraciones en el metabolismo energético de las BMECs en ambos modelos y toxicidad hacia las neuronas motoras en el contexto de ELA, destacando la complejidad de las interacciones entre los distintos componentes de la BHE en estas patologías.

En resumen, esta investigación arroja luz sobre el papel crucial de las BMECs y los astrocitos en la disfunción de la BHE en la ELA y el RTT. Estos hallazgos tienen importantes implicaciones para el desarrollo de nuevas terapias experimentales y estrategias de tratamiento para estas enfermedades, así como para una más amplia comprensión de los trastornos neurológicos en general.

En un sentido más detallado, esta tesis doctoral está dividida en cinco capítulos: en el primero, se hace una introducción teórica sobre la BHE, su función y disfunción en las etapas del neurodesarrollo y la neurodegeneración, tal y como se estudia de forma pormenorizada en mi artículo de revisión publicado sobre la materia en 2021. Seguidamente, en el capítulo dos, describo los materiales y métodos empleados, junto con la puesta a punto de estos durante el desarrollo de esta investigación. En el capítulo tercero, expongo los resultados obtenidos al modelar la BHE en el contexto neurodegenerativo de la ELA, centrándome en la mutación *C9ORF72,* incluyendo a su vez mi reciente artículo de investigación que avala estos resultados. En el cuarto, me enfoco en los resultados obtenidos al modelar la BHE en el modelo de enfermedad del neurodesarrollo del RTT y, en concreto, en la mutación *MECP2*. Por último, en el capítulo quinto expongo una discusión detallada sobre la investigación y una conclusión crítica del trabajo científico realizado.

Como se ha mencionado al principio de este resumen, la BHE es una estructura única. La formación de la BHE y su establecimiento es un proceso multietapa, que comienza prenatalmente y se completa postnatalmente. Diversas publicaciones indican la pérdida de integridad de la BHE en condiciones patológicas, desde la enfermedad de Alzhéimer, hasta enfermedades del espectro autista (ASD); sugiriendo que la disrupción de la BHE podría ser un mecanismo común en varias condiciones del neurodesarrollo y enfermedades neurodegenerativas.

El correcto funcionamiento de la BHE depende de la interacción entre diferentes tipos de células y la evolución de su comunicación e interacciones a lo largo del tiempo. La expresión controlada de las TJs, componentes de la membrana basal (BM) como el colágeno o la fibronectina, y proteínas involucradas en el mantenimiento y transporte de la BHE, entre otros los transportadores de la familia ATP-binding cassette (ABC) o los transportadores de aminoácidos excitadores (EAAT), son fundamentales para la funcionalidad de la BHE. Se ha descrito que, variantes genéticas asociadas a enfermedades neurodegenerativas y varios factores implicados en los trastornos del neurodesarrollo, desencadenan mecanismos fisiopatológicos como la neuroinflamación, el estrés oxidativo y los cambios en la homeostasis de neurotransmisores e iones. Además, estos procesos fisiopatológicos están asociados con alteraciones en la función de distintos tipos celulares presentes en la BHE, como los astrocitos, elementos clave para el soporte neuronal y la correcta función de la BHE.

Mientras que la mayoría de los estudios sobre enfermedades neurodegenerativas como el Alzhéimer, el Párkinson y la ELA, históricamente han centrado su atención en la degeneración neuronal, actualmente el foco ha cambiado, y también se realizan estudios en la disfunción de las células gliales, como los astrocitos. Estos no solo reaccionan a la muerte neuronal, sino que pueden estar

directamente afectados por los mismos factores genéticos, como el gen *APOE,* y factores ambientales, que causan la degeneración neuronal.

Asimismo, la disfunción de las BMECs, el principal soporte celular estructural de la BHE es un factor común en las primeras etapas de los trastornos neurológicos como el Alzhéimer y la demencia neurovascular. Estudios recientes sugieren una ruptura temprana de la BHE en estos pacientes, manifestándose como microhemorragias. Por lo tanto, las BMECs deben considerarse un objetivo terapéutico potencial, junto con otros componentes de la NVU.

Por otro lado, se ha realizado un esfuerzo significativo en las últimas dos décadas para desarrollar modelos humanos de la BHE *in vitro*. Estos modelos a menudo cocultivan BMECs con otras células que componen la NVU, como astrocitos o pericitos, para imitar las interacciones *in vivo*. Con el fin de evaluar la permeabilidad de la BHE y el transporte de compuestos, las BMECs se cultivan comúnmente en insertos celulares, lo que permite la evaluación de parámetros clave como resistencia eléctrica transendotelial (TEER) de la monocapa, la permeabilidad de trazadores a través de esta y el muestreo de los diferentes compartimentos. Sin embargo, estos modelos estáticos están siendo reemplazados progresivamente por otros que incluyan la circulación de un flujo continuo, como los modelos *in vitro* tipo microfluídico. Aunque estos modelos ofrecen una representación más precisa de la dinámica de fluidos de la BHE humana, su establecimiento y mantenimiento son complejos, laboriosos y más costosos que los enfoques estáticos.

En cuanto a las células utilizadas en los modelos *in vitro*, las BMECs son los principales componentes estructurales de la BHE y, por lo tanto, son el principal objetivo para su modelado *in vitro*. A lo largo de los años, se han empleado tanto líneas celulares endoteliales primarias como inmortales derivadas de animales, así como hi-PSCs. Estas últimas tienen un gran potencial debido a su origen humano, ser clínicamente relevantes y por su capacidad para modelar prácticamente cualquier patología y tejido. Los modelos basados en hi-PSCs incluyen organoides cerebrales, que pueden simular la arquitectura y funcionalidad del órgano humano. A pesar de los avances en el desarrollo de nuevos modelos más complejos, es un área aún en progreso, que cuenta con numerosas limitaciones. Entre ellas está la correcta evaluación de la permeabilidad de la BHE, que es un elemento clave en multitud de enfermedades neurodegenerativas.

Los modelos *in vivo* e *in vitro* son esenciales para comprender la BHE y evaluar el transporte de fármacos al cerebro. Aunque los modelos animales ofrecen una representación de la complejidad de la BHE humana, presentan diferencias significativas entre especies, como el metabolismo cerebral y las interacciones célula a célula dentro de la NVU. Además, debido a las consideraciones éticas y legales asociadas con los estudios *in vivo*, se recomienda el uso de modelos *in vitro* siempre que sea posible.

Como se mencionó anteriormente, este proyecto de doctorado se centra en el desarrollo de un modelo humano *in vitro* de la BHE. La BHE tiene una importancia crucial en la preservación de la salud del SNC, facilitando la demanda de energía y nutrientes del cerebro, así como protegerlo de agentes externos, incluyendo fármacos. Es por ello, que un modelo *in vitro* de la BHE se considera una herramienta muy útil en investigación básica y en ensayos clínicos. Además, como se señaló inicialmente, se conoce poco de la disfunción de la BHE en enfermedades neurodegenerativas y del neurodesarrollo.

La ELA es una enfermedad neurodegenerativa fatal, que causa la pérdida progresiva de las neuronas motoras, resultando en parálisis, atrofia muscular y muerte, generalmente 3-5 años después del diagnóstico. Los primeros síntomas, como debilidad muscular y espasmos, aparecen alrededor de los

55 años. En España, la ELA es el tercer trastorno neurodegenerativo más común, con 700 nuevos diagnósticos anuales. Afecta a personas de todos los géneros y etnias, aunque los hombres caucásicos tienen mayor predisposición. Sólo un 10% de los casos son familiares, mientras que la mayoría de ellos son esporádicos, siendo las mutaciones más comunes las que afectan los genes *C9ORF72* y *SOD1*. Desafortunadamente, no existen tratamientos efectivos para la ELA, siendo Riluzol y Edaravona los únicos medicamentos aprobados, ofreciendo beneficios modestos en sólo algunos casos.

Si bien, numerosos compuestos neuroprotectores han sido estudiados a lo largo de los años, a menudo no dan el resultado esperado en los ensayos clínicos, debido probablemente a problemas en el diseño preclínico y posiblemente afectado por la gran diversidad genética de la ELA. Además, hasta el 50% de los pacientes con ELA presentan deterioro cognitivo y el 15% desarrollan demencia frontotemporal (FTD), complicando aún más la enfermedad y su tratamiento.

Los modelos animales son fundamentales para estudiar patologías, utilizando roedores modificados genéticamente para alterar la expresión de proteínas de interés. Por ejemplo, los roedores con la mutación humana *SOD1*, presentan una BHE disfuncional y permeable, con alargamiento de los terminales de los astrocitos y una membrana basal interrumpida, lo que conduce a edema cerebral y microhemorragias; este fenotipo también se observa en pacientes, en algunos casos, puede preceder a la neurodegeneración. En ratones con la mutación *C9ORF72*, se ha observado un aumento en el transporte de glucosa.

En el caso de las enfermedades del neurodesarrollo, como el ASD o el RTT, la perspectiva respecto a la BHE es bastante similar, es por ello que realicé un estudio teórico sobre el tema, reflejado en el artículo de revisión que incorporo en el anexo primero de esta tesis doctoral.

El RTT es una patología ligada al cromosoma X que afecta casi exclusivamente a las mujeres, ya que los varones rara vez sobreviven. Con una incidencia de 1 por cada 10.000 niñas nacidas, es una de las causas más comunes de discapacidad intelectual en mujeres, con una esperanza de vida que actualmente puede llegar a los 40-50 años.

El RTT se clasifica en clásico y atípico. En el 95% de los casos clásicos, la enfermedad es causada por una deficiencia del factor de transcripción *MECP2*, esencial para el desarrollo y la función del cerebro. Las formas atípicas de RTT pueden ser más leves o severas y pueden a su vez estar asociadas con mutaciones en los genes *CDKL5* y *FOXG1*. Las mutaciones en *MECP2* presentan una amplia gama de fenotipos, desde leves hasta graves, influenciados por la inactivación del cromosoma X (XCI) y otros factores genéticos y ambientales. Las niñas con RTT se desarrollan normalmente hasta los 7-18 meses de edad, cuando comienzan a perder habilidades adquiridas. Presentan anormalidades musculares, movimientos de manos característicos, comportamientos similares al autismo, problemas respiratorios, dificultades para alimentarse, retraso en el crecimiento y convulsiones. Los varones suelen presentar síntomas más tempranos y severos.

Nuestra comprensión sobre la implicación de la BHE en el RTT es muy limitada. La eliminación condicional del gen *MECP2* en diferentes modelos animales ha demostrado ser perjudicial para las neuronas y los astrocitos, afectando la producción de factor neurotrófico derivado del cerebro (BDNF) y la comunicación celular.

Como se ha destacado, hay evidencia de disfunción de la BHE en la ELA, particularmente en casos de la mutación *SOD1*, pero muy pocos estudios se ha centrado en *C9ORF72*, aun siendo considerada la causa genética más común de ELA y demencia frontotemporal hasta la fecha. De manera similar, no se han realizado estudios sobre el deterioro de la BHE en pacientes con RTT. Además, actualmente ningún modelo humano o animal ha aclarado si el deterioro de la BHE es un evento temprano que

antecede a la neurodegeneración o es el resultado del dicho proceso. Del mismo modo, no está claro qué tipos de células y mecanismos están involucrados en esta disrupción.

Por tanto, debido al papel protector que desempeña la BHE en el cerebro, impidiendo el paso de muchos fármacos diseñados para tratar la neurodegeneración, y por otro lado enfermedades con degeneración del propio endotelio que la compone, se convierte en un área de investigación muy relevante. El estudio de la BHE en el contexto patológico nos ayuda a comprender mejor los procesos degenerativos y a explorar formas de permeabilizar la barrera para la administración de medicamentos. Además, el estudio de la BHE y su importancia en el desarrollo de patologías sigue siendo un tema poco desarrollado, lo que motiva esta investigación centrada en analizar este aspecto específico.

Por lo tanto, mi hipótesis es que la disfunción de la BHE juega un papel en el proceso neurodegenerativo que ocurre tanto en la ELA como en el RTT.

Con ello, los objetivos de esta investigación son:

1. Generar un modelo multicelular humanizado de la BHE.

2. Crear un modelo de la BHE específico para las enfermedades del ELA y el RTT.

3. Identificar la posible alteración funcional que afecta a la BHE en ambas enfermedades.

4. Investigar la contribución de los tipos de células que forman la BHE en la neurodegeneración.

Para modelar el ELA, se han usado hi-PSCs de hasta cinco pacientes portando la mutación *C9ORF72* (C9-ELA). Basándome en el estudio bibliográfico sobre los distintos modelos existentes de BHE, opté por sistema de cocultivo por medio de un inserto celular. A pesar de los retos en el establecimiento de modelos multicelulares, este enfoque ha permitido estudiar las interacciones celulares y la permeabilidad de la barrera en este estudio.

Comenzando con la optimización del protocolo de diferenciación de las BMECs, los resultados han demostrado una diferenciación exitosa de las células BMEC a partir de hi-PSCs, produciendo así células que expresan marcadores clave de la BHE y exhiben características funcionales. Este protocolo de diferenciación, desarrollado por los laboratorios Lippmann y Shusta, se aplicó para investigar los efectos de las mutaciones *C9ORF72* y *MECP2* en la morfología y función de las células BMECs.

En resumen, la investigación detallada en el Capítulo 3, explora la disfunción de la BHE en el contexto de la mutación *C9ORF72*, causa genética prevalente de la ELA. Como mencionaba previamente, la heterogeneidad de la ELA y el desconocimiento sobre la disfunción de la BHE han llevado a diversas investigaciones, pero ha quedado demostrado que la degeneración de las BMECs y la acumulación de proteínas plasmáticas como la inmunoglobulina G y el fibrinógeno, junto con la liberación de especies reactivas de oxígeno, contribuyen a la toxicidad neuronal presente en la enfermedad.

Utilizando hi-PSCs, se desarrolla un modelo de la BHE y se evalúa exhaustivamente la expresión génica y la integridad de la barrera. En nuestro modelo, se ha reportado que los genes que codifican las proteínas de TJs están regulados al alza en las células C9-ELA, contrario a los hallazgos previos de otros laboratorios en modelos de roedores portadores del gen humano *SOD1*. A través de experimentos de

cocultivo y medio condicionado, hemos registrado que los astrocitos C9-ELA empeoran la permeabilidad de la BHE establecida con células sanas, afectando la expresión de Claudina-5, la principal proteína de TJs, y GLUT1, el principal transportador de glucosa en el cerebro. Además, esta investigación demuestra que el medio condicionado de BMEC-C9-ELA tiene un impacto tóxico en las neuronas motoras sanas, llevando a una severa reducción en la longitud de las neuritas de estas. Estos hallazgos proporcionan nuevas perspectivas sobre los cambios en la BHE en C9-ELA, subrayando el papel vital de la disfunción de la BHE en las condiciones neurodegenerativas.

Seguidamente, en el Capítulo 4, esta investigación se centra en el RTT, una enfermedad pediátrica que se presenta con multitud de variantes en distintos genes, siendo las mutaciones en el gen *MECP2* la causa más común. De igual forma que para la ELA, por medio de hi-PSCs se han obtenido BMECs derivadas de pacientes con RTT y controles sanos. Las BMECs derivadas de pacientes, mostraron una expresión alterada de genes clave para el correcto funcionamiento de la BHE, como el transportador *SLC7A5* y el factor *VWF*, lo que indica que la BHE podría estar comprometida. Se han analizado cuatro mutaciones de *MECP2* diferentes, cada una afecta de manera distinta la expresión de genes relacionados con la BHE. Por ejemplo, la mutación *R133C* mostró la mayor alteración, mientras que la mutación *R255X*, aunque más severa, conservó mejor la expresión de genes implicados en la BHE.

A pesar de que añadir medio condicionado de astrocitos RTT sobre las BMECs sanas no afectó significativamente la expresión de las proteínas Claudina-5 o Glut-1, el cocultivo de astrocitos RTT sí redujo estas proteínas, comprometiendo a su vez la integridad de la barrera, como hemos podido comprobar por medio de las mediciones de TEER. Además, las BMECs, mostraron un aumento en respiración basal y glicólisis, indicando alteraciones en la respiración mitocondrial.

Sorprendentemente, al contrario que en la ELA, el medio condicionado de BMECs derivadas de pacientes, no afectó negativamente a las células neuronales (iNeurons), sugiriendo diferencias en la fisiopatología subyacente.

Finalmente, aunque al final de cada capítulo se presenta una discusión detallada sobre los principales hallazgos, en el Capítulo 5, valoro más profundamente y exploro los posibles motivos detrás de estos resultados que considero relevantes para un campo aún por expandir.

Así mismo, aunque este trabajo tiene sus limitaciones, como la gama reducida de tipos celulares analizados, considero que representa un intento innovador para desentrañar la compleja interacción entre la BHE y las enfermedades de la ELA y el RTT, especialmente en relación con las mutaciones *C9ORF72* y *MECP2*, de los cuales no se conocen modelos multicelulares similares a este. Los cambios observados en la integridad de la BHE, las firmas moleculares y las consecuencias sobre las neuronas, ofrecen evidencias convincentes y novedosas para considerar la BHE como un objetivo relevante en el desarrollo de estrategias terapéuticas en la ELA y el RTT.

Dada la función de la BHE en la protección del cerebro, la realización de ensayos clínicos para evaluar la seguridad y eficacia de los fármacos dirigidos a la BHE, así como sus propiedades de permeabilidad, en pacientes con ELA y RTT, aunque desafiante, es esencial para avanzar en nuevos tratamientos. Necesitamos una investigación más focalizada para esclarecer los mecanismos subyacentes y explorar posibles objetivos terapéuticos para estos trastornos tan devastadores.

Index

Chapter 1: Introduction
1.1. Preface 28
1.2. Components of the BBB 29
1.2.1. Basement Membrane 29
1.2.2. The NVU in the Perinatal Brain 30
1.3. BBB and ALS 30
1.3.1. ALS pathology 30
1.3.2. ALS vascular pathology and the BBB 32
1.4. BBB and Rett Syndrome 33
1.4.1. Rett Syndrome pathology 33
1.4.2. RTT vascular pathology and the BBB 36
1.5. Modelling the BBB *in vivo* and *in vitro* 36
1.6. Modelling the BBB in ALS 38
1.7. Discussion and future directions of the field 39
1.8. Hypothesis and aims 40

Chapter 2: Materials and Methods 42
Materials 45
Cell lines 47
Methods 49
2.1. Cell culture protocols 49
2.1.1. Endothelial immortalised cell lines 49
2.1.2. Hi-PSCs culture and derivatives 50
2.1.3. Fibroblast to hi-NPCs conversion 55
2.1.4. Multicellular cultures 56
2.2. Barrier tightness and transport 57
2.2.1. TEER measurements 57
2.2.2. Efflux activity: P-glycoprotein transporter 59
2.3. Protein quantification by immunocytochemistry 59
2.4. Transcription quantification by qRT-PCR 61
2.4.1. Troubleshooting: housekeeping genes 62
2.5. Cytotoxicity assay 64

2.6. Mitochondrial stress test....64
2.7. Data Analysis....65

Chapter 3: *C9ORF72* Patient-Derived Endothelial Cells Drive Blood-Brain Barrier Disruption and Contribute to Neurotoxicity in a Multicellular *In Vitro* Model....67
3.1. Preface....70
3.2. Hypothesis and Aims....71
3.3. Results....72
3.3.1. BMEC-like cells are successfully differentiated from hi-PSCs....72
3.3.2. Comment on gender differences for the healthy cell lines....75
3.4. Discussion....76

Chapter 4: A *MECP2*-Linked Mutations Blood-Brain Barrier Human-Derived *In Vitro* Model: a Valuable Resource for Researching Rett Syndrome Dynamics and Therapeutics....81
4.1. Preface....84
4.2. Hypothesis and Aims....84
4.3. Results....85
4.3.1. Juvenile and RTT-derived BMEC-like cells are successfully differentiated from hi-PSCs 85
4.3.2. MECP2-RTT BMEC-like cells monolayer displays functional abnormalities....86
4.3.3. MECP2-RTT iAstrocytes conditioned medium is toxic to BMEC-like cells....89
4.3.4. MECP2-RTT BMEC-like cells display metabolic defects....90
4.3.5. MECP2-RTT iAstrocytes interfere with the endothelial barrier's dynamics and permeability....91
4.3.6. MECP2-RTT BMEC-like cells conditioned medium is non-toxic towards healthy neurons....94
4.4. Discussion....96

Chapter 5: Discussion and Conclusions....101

References....109
Abbreviations....120
Annexes....125
Annex 1: Review Article....127

Blood–Brain Barrier Disruption and Its Involvement in Neurodevelopmental and Neurodegenerative Disorders 127

Annex 2: Research Article 161

C9ORF72 patient-derived endothelial cells drive Blood-Brain Barrier disruption and contribute to neurotoxicity 161

Index of figures

Figure 1. 1: The Neurovascular Unit 29
Figure 1. 2: *C9ORF72* gene structure, transcript variants, and protein isoforms under non-pathological and pathological conditions 31
Figure 1. 3: Blood-brain barrier breakdown and dysfunction in amyotrophic lateral sclerosis 33
Figure 1. 4: Rett Syndrome patients life expectancy 34
Figure 1. 5: Rett Syndrome development stages 35
Figure 2. 1: BMEC-like cells hi-PSCs-derived differentiation timeline for each protocol 52
Figure 2. 2: No major gene expression differences were found on BMEC-like cells when using either rat tail collagen or IV during purification 54
Figure 2. 3: Cell culture and conditioned media system 56
Figure 2. 4: Contact co-culture system 57
Figure 2. 5: TEER measurements with electrodes on transwell inserts 58
Figure 2. 6: BMECs-derived hi-PSCs differentiation timeline 59
Figure 2. 7: A combination of housekeeping genes is the most efficient approach for all cell differentiation stages 63
Figure 2. 8: Lactate dehydrogenase cytotoxicity assay 64
Figure 2. 9: Electron Transport Chain and inhibitors used during the Seahorse XF Real-Time ATP Rate Assay stress test 65
Figure 3. 1: C9ORF72 repeat sizing via Southern Blotting 71
Figure 3. 2: BMEC-like cells are successfully differentiated from hi-PSCs using protocol B 73
Figure 3. 3: Hi-PSCs derived BMECs gender differences 75
Figure 4. 1: MECP2-RTT BMEC-like cells display altered gene expression of key functional markers 87
Figure 4. 2: MECP2-RTT BMEC-like cells transcriptomic profile varies in a mutation-linked way 88
Figure 4. 3: MECP2-RTT BMEC-like cell lines form a leaky barrier 89
Figure 4. 4: MECP2-RTT iAstrocytes conditioned media is toxic but does not affect overall expression of key functional markers 90
Figure 4. 5: MECP2-RTT BMEC-like cells have an upregulated mitochondrial respiration 91
Figure 4. 6 MECP2-RTT iAstrocytes affect the endothelial barrier's permeability 93
Figure 4. 7: MECP2-RTT BMEC-like cells are non-toxic to neurons 95

Index of tables

Table 1. 1: BBB *in vitro* models Pros and Cons 37
Table 2. 1: Reagents 45
Table 2. 2: Cell lines clinical information 47
Table 2. 3: Endothelial immortalised cell lines media 49
Table 2. 4: Hi-PSCs differentiation to BMECs media 51
Table 2. 5: Collagen coating volume. 51
Table 2. 6: Cell seeding densities 53
Table 2. 7: Cell culture media volume 53
Table 2. 8: Hi-NPC and derivatives media composition 55
Table 2. 9: Primary Antibodies 59
Table 2. 10: Secondary Antibodies 60
Table 2. 11: Personalized fixation and permeabilization protocols across selected markers ..60
Table 2. 12: Primers relevant information: gene ID and sequences 61
Table 3. 1: C9-ALS cell lines repeat expansion size 70
Table 4. 1: RTT cell lines clinical information 85
Table 5. 1: Main findings summary for C9-ALS and MECP2-RTT BBB models 104

Chapter 1: Introduction

Chapter 1: Contents

1.1. Preface 28

1.2. Components of the BBB 29

1.2.1. Basement Membrane 29

1.2.2. The NVU in the Perinatal Brain 30

1.3. BBB and ALS 30

1.3.1. ALS pathology 30

1.3.2. ALS vascular pathology and the BBB 32

1.4. BBB and Rett Syndrome 33

1.4.1. Rett Syndrome pathology 33

1.4.2. RTT vascular pathology and the BBB 36

1.5. Modelling the BBB *in vivo* and *in vitro* 36

1.6. Modelling the BBB in ALS 38

1.7. Discussion and future directions of the field 39

1.8. Hypothesis and aims 40

Chapter 1: Index of figures

Figure 1. 1: The Neurovascular Unit 29
Figure 1. 2: *C9ORF72* gene structure, transcript variants, and protein isoforms under non-pathological and pathological conditions 31
Figure 1. 3: Blood-brain barrier breakdown and dysfunction in amyotrophic lateral sclerosis 33
Figure 1. 4: Rett Syndrome patients life expectancy 34
Figure 1. 5: Rett Syndrome development stages 35

Chapter 1: Index of tables

Table 1. 1: BBB *in vitro* models Pros and Cons 37

1.1. Preface

In 1885, Paul Ehrlich injected a dye into the bloodstream of animals. He noticed that all organs were stained, except the brain and spinal cord[1]. While this discovery proved the presence of a barrier protecting the brain, it was not until 1921 that Lina Stern presented the term "Barrière hématoencéphalique", the French term for blood-brain barrier (BBB). To prove the presence of such barrier, Stern and her colleague Gautier, performed several experiments in which they injected different compounds into the subarachnoid space, cerebral ventricles, and bloodstream. Additionally, Stern also demonstrated the immaturity of the BBB in the developing brain[2].

The BBB is considered a dynamic and extremely complex vascular interface capable of exerting a vast array of specialized functions. The BBB is formed by endothelial cells (ECs) of the capillary wall, astrocyte end-feet unsheathing the capillary, and pericytes embedded in the capillary basement membrane. The BBB allows the diffusion of both hydrophobic molecules such as O_2, CO_2 and hormones, as well as small polar molecules. Cells of the BBB actively transport metabolic products such as glucose across the barrier using specific transport proteins. Moreover, because of its significant barrier properties, this endothelial interface restricts uptake of neuro-therapeutic molecules. BBB disruption is a common mechanism in both neurodegenerative diseases, such as amyotrophic lateral sclerosis (ALS) and neurodevelopmental disorders, such as autism spectrum disorders (ASD). Further research is needed to understand how the BBB is altered in these disorders and the implications to BBB function.

This first introductory chapter of my thesis, addressing the BBB in health and disease, is composed of the review article published on the 3rd of December 2022, in the International Journal of Molecular Sciences, MDPI, EISSN 1422-0067, 5.6 Journal Impact Factor, Q1 by Journal Citation Reports 2022. The article titled "Blood–Brain Barrier Disruption and Its Involvement in Neurodevelopmental and Neurodegenerative Disorders" is included as Annex 1.

1.2. Components of the BBB

The BBB functional unit is known as the neurovascular unit (NVU). All components of the NVU interact with each other, contributing to its function, development, and maintenance. These cellular players in the BBB dynamics are illustrated in **Error! Reference source not found.** and their roles are described previously in my review article[3] (see Annex 1).

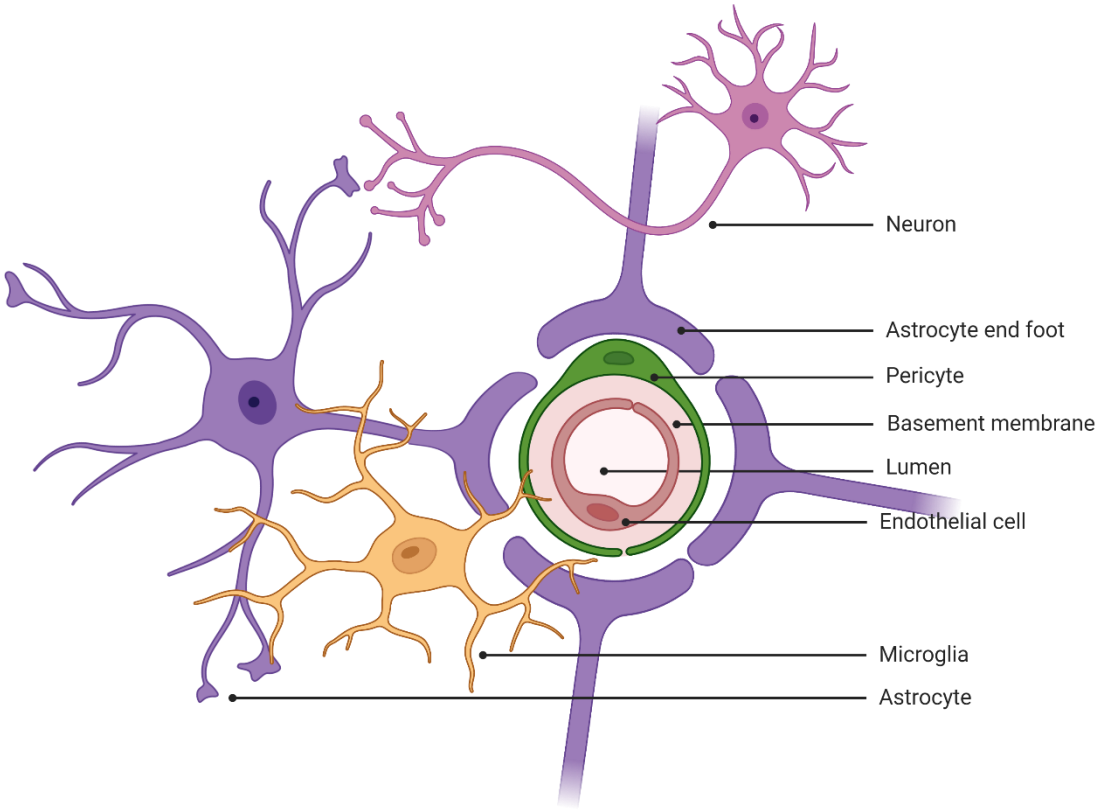

Figure 1. 1: The Neurovascular Unit

The brain endothelial cells (BMECs) are the major structural elements of the blood-brain barrier (BBB); and therefore, of the neurovascular unit (NVU). They conform the cerebral vasculature, playing an active role in the BBB that will be explored further in this chapter. The basement membrane or basal lamina is a non-cellular component that provides structural support, cell anchoring and signal transduction. Pericytes are major regulators of cerebral blood flow and regulate the expression of proteins and trafficking within the BBB. The astrocytes support the NVU by occupying a strategic position between capillaries and neurons with their end-feet. The microglia are not considered a NVU component but their role in neuroinflammation and oxidative stress balance make them an essential player. Lastly, neurons play regulatory roles within the NVU, creating feed-back mechanisms within the astrocytes. They also take part in cerebrovascular organisation.

This figure was created in Biorender.com.

1.2.1. Basement Membrane

The basement membrane (BM) is the non-cellular component of the BBB, and it is a unique form of extracellular matrix. Its main functions are structural support, cell anchoring and signal transduction. BM components are synthetized by both neurons and glial cells[4]. Collagen is the most abundant protein in mammals (approximately 30% of total proteins) and constitutes a structural framework for

other tissues such as blood vessels and most organs[5]. Collagen type I is the most abundant of the fibrils, providing structural support for all tissues and organs, playing a critical role in morphogenesis and growth, as well as homeostasis and repair[5]. Even though little is published about the regulation of collagen I expression in blood vessels, it has been identified as an excellent substrate to support the monolayer formation of ECs *in vitro*[6].

On the other hand, collagen-IV is the most abundant component of the basement membrane and maintains its stability by retaining other protein components such as laminin. Nonetheless, it was evidenced that collagen-IV is not necessary for early embryonic development, but it is indispensable for the structural integrity of the basement membranes at later stages[7]. Besides, fibronectin stimulates the proliferation and survival of the ECs in the BBB. Both collagen and fibronectin, have been extensively used in all types of EC culture to improve attachment[8].

1.2.2. The NVU in the Perinatal Brain

Despite extensive research into the mature NVU, little is known about it in the perinatal period[9]. Kozberg et al. investigated the metabolic differences in neural activity in the developing brain. They found that contrary to what happens in adults, the presence of strong and localized neural activity in the early postnatal brain does not drive cortical blood flow or hyperaemia. Instead, hemodynamic responses were observed to develop gradually, alongside the development of brain connectivity[10]. Others suggested neural activity during neurodevelopment influences the cortical microvasculature's density[11]. Furthermore, Mallard made a distinction between immature and defective BBB, with limited functions during neurodevelopment. Additionally, Mallard and her colleagues, highlighted the relevance of the brain barriers during neurodevelopment, thus protecting the foetal and neonatal brain.

To conclude, we can think of the barriers during the perinatal period to be a dynamic structure, growing and adapting to the highly demanding developing brain.

1.3. BBB and ALS

1.3.1. ALS pathology

ALS also known as motor neuron disease (MND) is a fatal neurodegenerative disorder characterised by progressive loss of upper and lower motor neurons (MNs), causing progressive paralysis, muscle atrophy (denervation atrophy) and consequently, death. The early symptoms as muscle weakness and twitches, appear at an average age of 55 years old and usually follow death 3–5 years afterwards[12].

In Spain, ALS is the third most common neurodegenerative disorder, after Alzheimer's (AD) and Parkinson's (PD), with 700 new diagnoses every year (adELA –the Spanish ALS Association[13]). In Europe, the incidence rate ranges from 2.1 to 3.8 per 100,000 people. Even though male Caucasians are most likely to develop the disease, ALS affects people of all genders, races, and ethnic backgrounds[14]. According to Traynor's team publication from 2016, the number of ALS cases across the globe will increase to approximately 377000 in 2040, representing an increase of 69%. This escalation is predominantly due to population ageing, particularly among developing nations[15].

Although most of the cases are sporadic (sALS), 10% of patients have familial ALS (fALS). More than 40 genes have been linked with fALS, but genetic studies have shown the most common mutations

are the *C9ORF72* (C9-ALS) repeat expansion followed by *SOD1*[16] (SOD1-ALS). Remarkably, fALS, and sALS are for the most part clinically indistinguishable, thus several fALS genes such as *C9ORF72* have also been reported in sALS cases. However, the main difference between sALS and fALS is the inheritance, with a most often autosomal dominant pattern, fALS's offspring have a 50% chance of developing ALS. Figure 1. 2 extracted from Smeyers et al.[17] illustrates the structure of the *C9ORF72* gene, highlighting its transcript variants and protein isoforms in both normal and pathological states. Under normal conditions, the gene produces three variants that lead to two protein isoforms (short and long). In the pathological state, abnormal expansion of the 'GGGGCC' repeat between non-coding exons can trigger three potential disease mechanisms: (1) bidirectional transcription of the hexanucleotide repeat expansion (HRE) produces sense and antisense RNAs that sequester RNA-binding proteins into RNA foci, (2) HRE transcripts undergo repeat-associated non-ATG (RAN) translation, generating dipeptide repeat proteins (DPRs), and (3) transcription is inhibited, leading to reduced C9ORF72 protein levels.

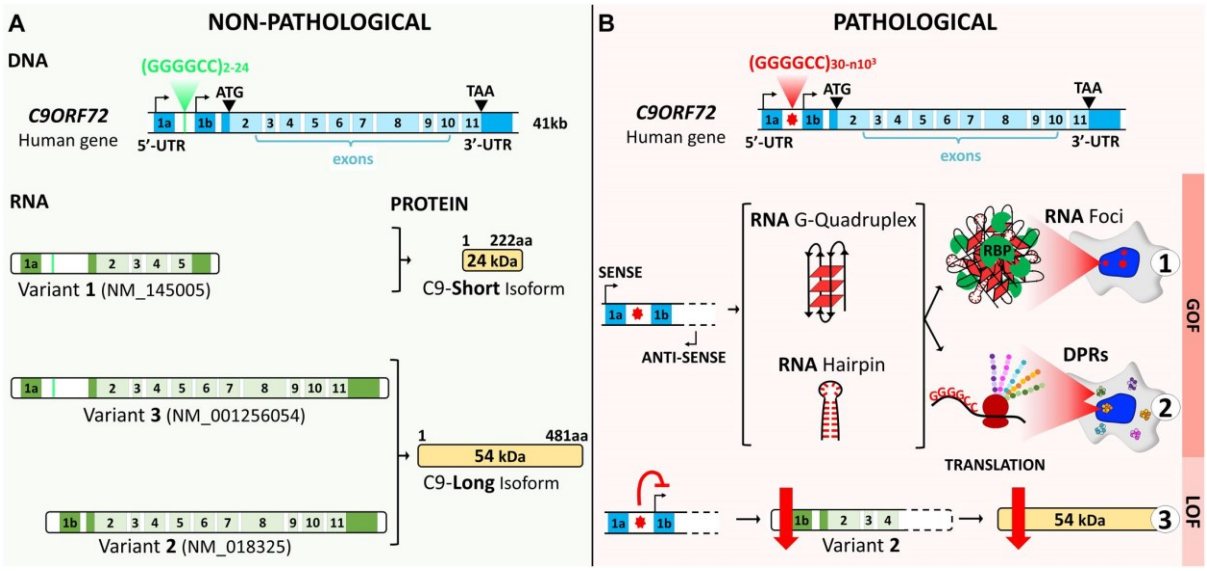

Figure 1. 2: *C9ORF72* gene structure, transcript variants, and protein isoforms under non-pathological and pathological conditions

C9ORF72 gene includes two non-coding exons (1a and 1b) and ten coding exons (2–11), producing three coding variants: Variant 1 (V1) includes exon 1a and exons 2–5; Variant 2 (V2) includes exon 1b and exons 2–11; Variant 3 (V3) includes exon 1a and exons 2–11. Alternative splicing results in two protein isoforms: a 222-amino acid (aa) isoform (C9-short, 24 kDa) encoded by V1, and a 481-aa isoform (C9-long, 54 kDa) encoded by V2 and V3. Coding exons are shown in light blue, and non-coding exons in dark blue. (B) In a pathological state, the 'GGGGCC' repeat between the non-coding exons (1a and 1b) becomes abnormally expanded, leading to three potential pathogenic mechanisms: (B1) Bidirectional transcription of the hexanucleotide repeat expansion (HRE) produces 'GGGGCC' sense and GGGGCC antisense RNAs, which form G-quadruplex and hairpin structures that sequester RNA-binding proteins (RBP) into RNA foci. (B2) HRE transcripts undergo repeat-associated non-ATG (RAN) translation, generating dipeptide repeat proteins (DPRs). (B3) The presence of the HRE inhibits transcription, reducing C9ORF72 protein levels. Figure and text extracted and adapted from Smeyers et al. 2021.

To date, there is no effective drug treatment for ALS. Riluzole and Edaravone are the only drugs approved by the US Food and Drugs Administration (FDA), providing modest benefits only in some patients[18]. Riluzole may reduce the loss of MNs and extend lifespan by about 3 months. Its mechanism of action remains unclear since it has many different targets, such as inhibition of voltage-gated Na^+ currents, inhibition of glutamatergic transmission, or increased production of brain-derived

neurotrophic factor (BDNF). Edaravone is an intravenous drug, that showed its ability to slow disease progression, potentially by reducing oxidative stress[19].

A vast array of compounds with prospective neuroprotective effects have been studied, which include antioxidants, anti-excitotoxic agents, inhibitors of apoptosis, anti-inflammatory agents, neurotrophins, chelators of metal ions and modulators of ion channels. Unfortunately, drugs that demonstrate effectiveness in animal studies often fail to show efficacy in human clinical trials. Several factors may contribute to this lack of positive translation, including inadequate preclinical study design in murine models and a lack of diverse genetic backgrounds in clinical trials to account for patients' heterogeneity[20,21].

Furthermore, up to 50% of ALS patients also have cognitive impairment [22] and 15% of patients present frontotemporal dementia (FTD), therefore the clinical spectrum of the disease goes beyond the involvement of MNs[22]. This further adds to the complexity of ALS and translation from animal models to patients.

1.3.2. ALS vascular pathology and the BBB

Transgenic rodents expressing human *SOD1* mutations develop a leaky BBB with higher permeability, enlarged astrocytic end-feet, and interrupted BM associated with a reduction of BMECs and astrocytes, thus leading to oedema and microbleeds. This pathological phenotype is also observed in ALS patients[23]. BBB's early breakdown might appear as cerebral microbleeds, which are frequently seen in AD patients[24], suggesting that BBB failure might precede neurodegeneration. Interestingly, *SOD1* dysfunction has been linked not only with ALS but also with Down Syndrome (DS). Due to the triplication of chromosome 21, this protein is highly overexpressed in the brains of patients with DS resulting in increased production of H_2O_2[25]. Historically, vascular pathology has not been studied in C9-ALS mutation carriers. However, a recent publication by Yijun Pan researched the BBB dynamics in a C9-ALS mouse model. They reported an increased glucose transport, together with an increase in the Glucose-1 (GLUT1) transporter expression, while other permeability processes such as passive diffusion or efflux transport remained unaffected. P-glycoprotein transport was not altered in the C9-ALS animals, exposing no differences when compared with wild-type ones. Regarding BMECs, mild overexpression of ZO-1 was reported in C9-ALS animals too[26].

The heterogeneity of ALS and limited knowledge of BBB dysfunction in the disease led to preliminary studies, such as Sweeney et al. 2019[27], which described BBB breakdown in multiple pathologies, including ALS. They propose that the degeneration of BMECs at the NVU leads to the BBB breakdown. Thus, a leaky BBB will drive to red blood cells extravasation (RBC) and accumulation of plasma-derived proteins as fibrinogen and Immunoglobulin G (IgG) (Figure 1. 3). As reviewed by the authors, IgG is found in the spinal cord and motor cortex both in humans with sALS and fALS, as well as in Sod1-ALS rodent models. Then, the RBC extravasation leads to the release of haemoglobin (Hb), and free iron (Fe2+) causing generation of reactive oxygen species (ROS), which is toxic to MNs. Moreover, fibrinogen can activate microglia enhancing non-autonomous MN cell death. In the same context, astrocytic end-feet become swollen and dissociate from capillaries, and the perivascular space becomes enlarged and BM breaks down. On the contrary, the effects of BBB breakdown on oligodendrocytes degeneration remained elusive at this time to the authors.

Additionally, several neuropathological studies of post-mortem brain stem and spinal cord tissue from patients with sALS and fALS found a significant reduction in tight junction (TJ) and junctional adhesion molecules (JAM) expression, transporters upregulation –as P-glycoprotein, and cells at the NVU

degeneration[28]. Moreover, Sweeney et al. suggest these findings support earlier observations showing that the BBB and blood-spinal cord barrier (BSCB) are damaged in a subset of ALS patients, as reported by the appearance of microbleeds[29].

To date, the pathogenesis of BBB/BSCB breakdown in ALS remains unclear and is an area for further investigation.

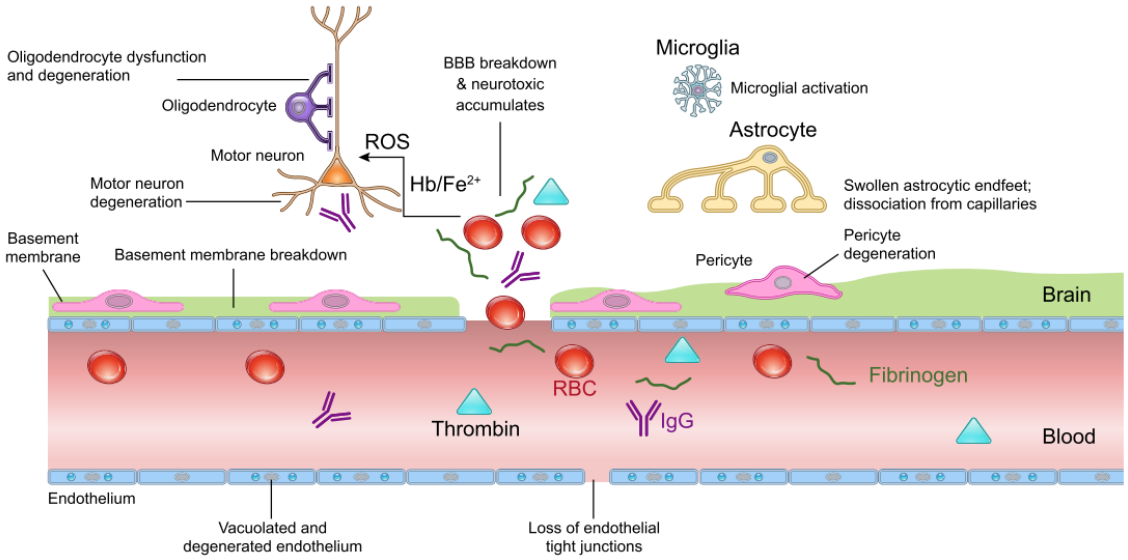

Figure 1. 3: Blood-brain barrier breakdown and dysfunction in amyotrophic lateral sclerosis

This figure, extracted from Sweeney et al. 2019, proposes a model of blood-brain barrier (BBB) breakdown in amyotrophic lateral sclerosis (ALS) based on current literature. Abbreviations in the figure include ROS (reactive oxygen species), RBC (red blood cells), IgG (Immunoglobulin G), haemoglobin (Hb), and free iron (Fe2+).

1.4. BBB and Rett Syndrome

1.4.1. Rett Syndrome pathology

Rett Syndrome (RTT) is an X-linked dominant neurodevelopmental disorder almost exclusively affecting females. Unfortunately, males affected by RTT rarely survive. Counting on an incidence of 1 per 10000 female births, RTT is one of the most common causes of intellectual disability in females. Most individuals survive into their 40s-50s (Figure 1. 4)[30–32]. However, due to the disease variability, there is very little data to make predictions about life expectancy in atypical forms of the pathology.

Cases of RTT are classified as either classical or atypical RTT. In 95% of classical RTT cases, the disease is caused by deficiency of the transcription factor methyl-CpG-binding protein 2 (*MECP2*), a key regulator of gene expression in the central nervous system (CNS). *MECP2* is essential during brain development and function, influencing neuronal differentiation, maturation, and synaptic plasticity[33]. There are five classifications of atypical RTT, which may present as milder or more severe than classical RTT cases. A small proportion of patients with signs and symptoms overlapping those of RTT syndrome have mutations in *CDKL5* and *FOXG1* genes.

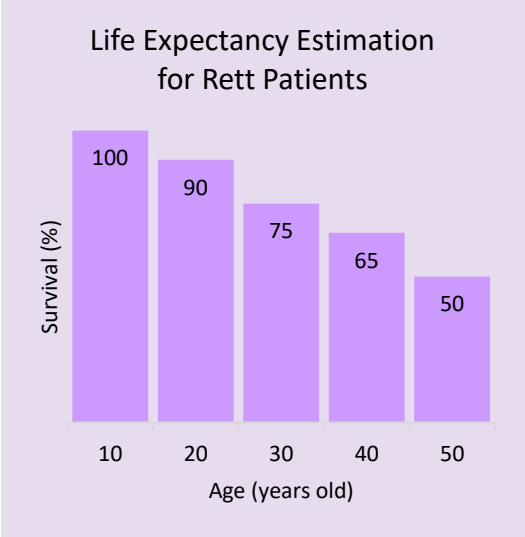

Figure 1. 4: Rett Syndrome patients life expectancy

This graph shows the chance of survival of girls suffering from Rett Syndrome (RTT) in North America. With 50% chance of reaching the age of 50. Data source: Rett Syndrome Natural History Study, 2019 report and Rett Syndrome Foundation.

Mutations in the *MECP2* gene, located on the X chromosome, can also lead to a wide range of phenotypic outcomes, from mild to severe. While it has traditionally been thought that the location, type, and severity of the *MECP2* mutation, along with the process of X chromosome inactivation (XCI) in females, can determine the severity and progression of the disease[34], some authors have suggested that factors beyond XCI, such as other polymorphisms or environmental influences, may have a greater impact on the RTT phenotype than slight variations in the XCI pattern[35].

Mammalian females (XX) carry twice as many X-linked genes on their sex chromosomes as males (XY). To correct this imbalance, females have evolved a unique mechanism of dosage compensation by the process called XCI. During early embryogenesis, mammalian females transcriptionally silence one of their two X chromosomes in a complex and highly coordinated manner[34]. The inactivated X chromosome then condenses into a stable and compact structure called a Barr body[36]. Sex-linked colour genes in cats are great examples because their cells, some with one of the X chromosomes and some with the other inactivated, will show the mottled appearance characteristic of female cats, heterozygous for those genes[37].

Even though XCI is predominantly a random process among both X chromosomes, skewed X-chromosome inactivation occurs when the X-inactivation of one X chromosome is favoured over the other. Due to its impact on X-linked diseases, this is a clinically relevant phenomenon. Skewed inactivation can alter disease phenotype, from mild to severe - if the muted allele is heavily expressed. In the context of RTT, Knudsen described how mildly affected cases appear to be more skewed than more severe ones, with a tendency of preferential inactivation of the paternally inherited X chromosome[38].

Girls with RTT generally develop normally for about 7 to 18 months after birth. At this point, they experience a developmental regression by losing previously acquired skills. Furthermore, they present muscular abnormalities such as ataxia or tremors and signature uncontrolled hand movements such as clapping. Affected children often develop autistic-like behaviours, breathing irregularities, feeding, and swallowing difficulties, growth retardation –like microcephaly, and seizures. Most males present an earlier onset of symptoms, typically with significant problems shortly after birth[39].

Classical RTT is typically described in 4 phases or stages although symptoms will often overlap between each stage. Disease´s severity varies from patient to patient, but the most common features are summarised in Figure 1. 5[30,40,41].

The severity of the disease can be also determined by specific mutations in the *MECP2* gene. Thus, distinct effects of *MECP2* mutations on clinical severity must be considered in basic research and clinical trials. There are 8 most common *MECP2* point mutations: *R106W*, *R133C*, *T158M*, *R168X*, *R255X*, *R270X*, *R294X* and *R306C*, which cause differences in ambulation, hand use, and language among patients[42]. In this study, Neul et al. described *R133C* as the less severe and *R168X* point mutation and large deletions as the most severe ones.

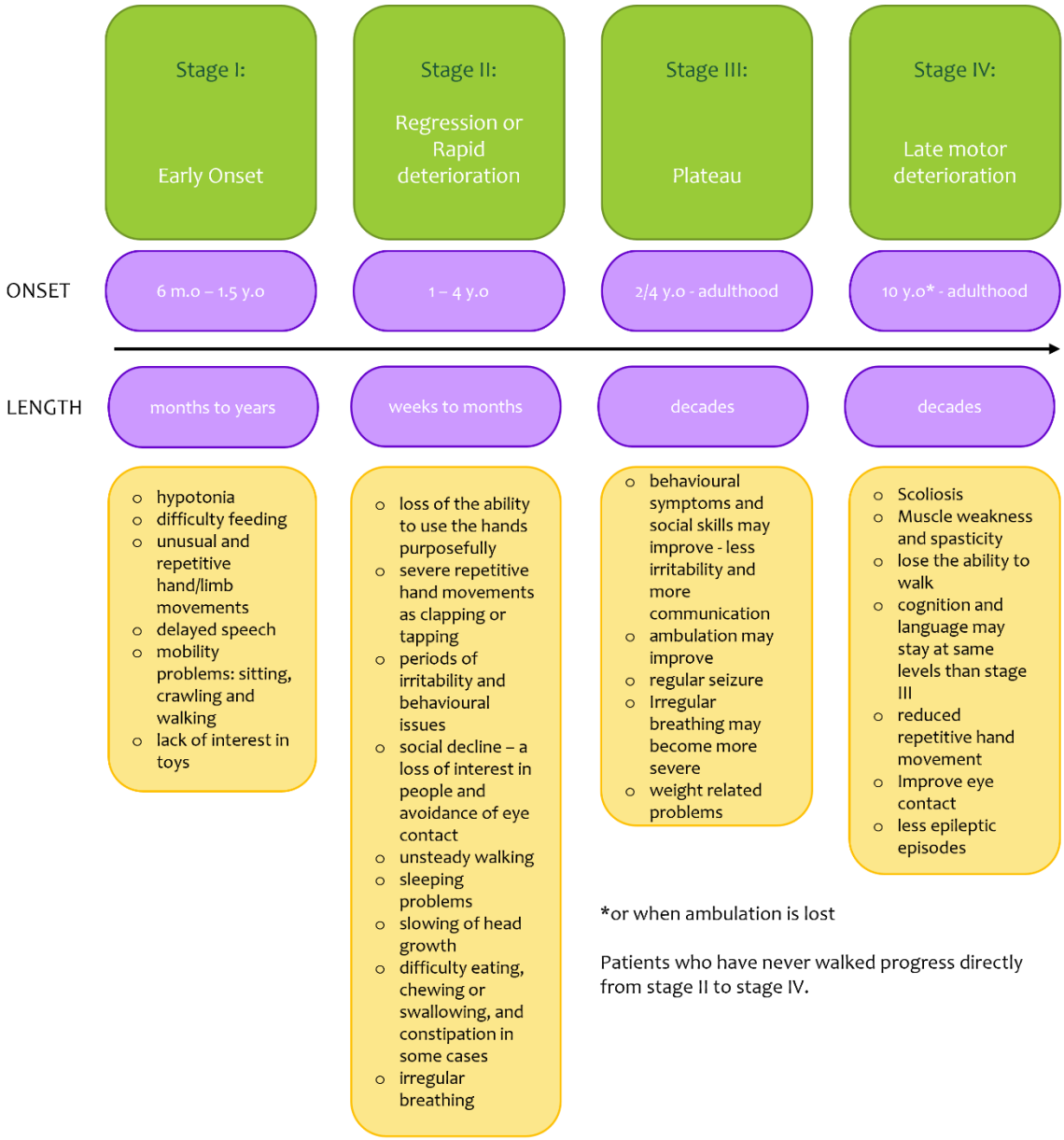

Figure 1. 5: Rett syndrome development stages

Rett syndrome (RTT) signs and symptoms differ for each person, however, there are common features in each stage that can be summarized. **Phase I:** In the early days, the child will appear to develop and grow normally for at least 6 months. There

may be subtle signs before diagnosis, such as low responsiveness. **Phase II:** during this period, the child suffers from ability regression. The infant will gradually or suddenly develop severe problems with communication, memory, mobility, coordination, etc. Some of the characteristics and behaviours might be like those of autism spectrum disorder. **Phase III:** children may stay in this phase for several years, with many of them remaining in this plateau stage for most of their lives. Various of the symptoms can improve, including behaviour, mobility, and communication, among others. **Phase IV:** similarly, patients can remain in this phase for decades. However, their muscle tone will deteriorate and patients will eventually lose their ability to walk. Sources: International Rett Syndrome Foundation, National Health Service in England (NHS) and U.S. National Institute of Health (NIH).

1.4.2. RTT vascular pathology and the BBB

Our understanding of the involvement of the BBB in RTT patients is very limited. *MECP2* has been conditionally knocked out in different animal models, tissues, brain areas, and cell types. Several studies showed particularly detrimental for neurons and astrocytes[43]. Moreover, Maezawa et al. reported *Mecp2*-deficient astrocytes have impaired BDNF and cytokine production. In addition, they showed that the *Mecp2* deficiency state can progressively spread via gap junction communications, in a novel non-cell-autonomous manner[44].

Pejhan et al. 2020, led a study of post-mortem *MECP2* degradation and brain region-specific detection in relation to RTT pathophysiology[45]. Surprisingly, *MECP2* was universally detected in hippocampus and cerebellum, with no obvious gender differences. However, lower *MECP2* detection in glial cells of the white matter, together with glial fibrillary acidic protein (GFAP) expression. Conversely, there were no *MECP2* decreases reported for neurons. Furthermore, in conflict with hypotheses concerning a deficit of BDNF signalling in RTT, the authors showed that BDNF labelling was not decreased in RTT brain samples. BMECs were also immunolabeled for MECP2, showing a variable immunoreactivity for those samples.

1.5. Modelling the BBB *in vivo* and *in vitro*

In vivo models are widely used to characterise the BBB and to evaluate drug delivery. Animal models, i.e., rodents; confer an accurate complexity of the BBB by mimicking human vasculature. Nevertheless, there exist several differences between rodents and humans including brain metabolism, vascular haemostasis, cell-to-cell interactions within the NVU and species-dependant transporters' expression. Zebrafish has many advantages as a model organism to be used in the study of BBB. Adult specimens possess a remarkably similar BBB to humans, including the presence of BMECs and astrocytic support. Unfortunately, the lack of characterisation of zebrafish transporters at the BBB is a major disadvantage when trying to translate findings.

Certainly, the ethical and legal considerations associated with *in vivo* studies reinforced the use of *in vitro* models whenever possible. For this matter, primary or immortalised animal-derived cells from various sources, such us mouse, rat, porcine, sheep or non-human primates, are broadly used. Animal *in vitro* models are highly useful for BBB characterization and drug testing, while *in vivo* models provide BBB fluid dynamics similar to those in humans. However, as reviewed in Chapter 1, translating animal model findings to human clinical studies has been challenging due to interspecies difference[46]. Thus, a renewable source of cells from the human BBB could prove to be useful for brain research and pharmaceutical development.

As a result, a big effort has been made to develop human *in vitro* models in the last two decades. Very often, BMECs are co-cultured with cells composing the NVU as astrocytes or pericytes, to mimic *in vivo* interactions. Conventional *in vitro* modelling of the BBB is generally conducted by seeding the BMECs as a flat monolayer. For studies evaluating BBB permeability or transport, BMECs are most often

cultured on a transwell insert which allows for the evaluation of transendothelial electrical resistance (TEER) of the monolayer, the permeability of tracers across the monolayer, and sampling of the different compartments. Interestingly, BMECs monolayer can be co-cultured with other cell types involved in the NVU maintenance and function, such as astrocytes, giving complexity to the transwell model.

In addition, due to the transwell statics, emerging microfluidics models are being researched. Microfluidic helps to recreate the blood flow between the body and the brain. Some examples are the organ-on-a-chip or the dynamic BBB models, adding flow to mimic the physiological conditions *in vitro*[47]. Conversely, establishment and maintenance of microfluidics models are complex, laborious, and more expensive than transwell approaches.

See Table 1. 1 for a summary of the available BBB *in vitro* models' advantages and disadvantages[48].

Table 1. 1: BBB *in vitro* models Pros and Cons

Model	Pros	Cons
Static monolayer	Easy set-up protocol	Simplistic
	Low cost and fast	No intercellular crosstalk
	High-quality imaging	Low TEER
Co-culture in Transwell	Ability to study different cell types' interactions	Difficult to establish multicellular models
	Relative low cost and fast	Reduced intercellular crosstalk in the non-contact model
	High TEER values and increased barrier stability	Difficult to establish an optimal culture media
Dynamic (DIV)	Ability to study different cell types' interactions	Difficult to set-up
	Ability to study the shear stress effects	High cost
	High TEER value	Difficult imaging
Microfluidic	3D	Difficult set-up and high maintenance
	Ability to study the shear stress effects	Low scalability
	Ability to mimic the cerebral blood flow	Hard to measure TEER
Spheroid	3D	Long culture protocols
	Innate cell-to cell interactions	Specialised maintenance
	Physiological-like conditions	Imprecise TEER measurements

Table adapted from Schreiner et al. 2022, described the main advantages (Pros) and disadvantages (Cons) of the available blood-brain barrier (BBB) *in vitro* models.

BMECs

BMECs are the main structural components of the BBB, therefore they are the main targets when modelling *in vitro*.

Due to ethical concerns and other constraints in obtaining human tissue, primary human cell lines are valuable for modelling the human BBB because they preserve many of the specific characteristics of the endothelium in vivo. However, many of these characteristics are diminished or lost after repeated passages in culture[49]. Although immortalised cell lines provide several benefits, such as low cost, ease of use, unlimited material supply, and avoidance of ethical issues associated with animal and human tissues, they often show altered phenotypes, activities, and functions due to genetic manipulation[50].

Hi-PSCs

Since Takahashi and Yamanaka discovered the four transcriptional factors, i.e., *Oct3/4*, *Sox2*, *c-Myc* and *Klf4*; that can induce pluripotency into adult somatic cells[51,52], the use of induced pluripotent stem cells (i-PSCs) in research has exponentially grown. Accordingly, human i-PSCs (hi-PSCs) based models have outstanding value due to their limitless supply of clinically relevant cells, their human origin, and their derivation potential from any individual, thus providing a resource to model theoretically any health condition and explore personalized medicine strategies[53]. In addition, these cells have also become easily accessible thanks to public biorepositories.

As a result, different approaches using hi-PSCs to reproduce the BBB *in vitro* have been published[54–56]. Initially, researchers explored the same platforms used with immortalised cell lines, including transwell or organ-on-a-chip devices. Lately, the emerging field of organoids is making strides in investigating the brain's vasculature network. An organoid is a self-organizing 3D tissue derived from hi-PSCs which can simulate the architecture and functionality of a human organ. Nowadays, protocols for developing promising brain organoids are available but this is a developing field, and more research needs to be performed to model the actual cytoarchitecture of the brain[57]. Due to the complexity of the BBB, there are no reliable organoid models but spheroids accessible. Differently to the organoids, the spheroids are formed by up to six known cellular lines such as BMECs, astrocytes or pericytes which are used as BBB models. Although promising, some of the key characteristics of the BBB, such as TEER cannot be precisely recorded on spheroids at this time.

Hence, we decided to use hi-PSCs for modelling the BBB, not only for ethical reasons but for their patient-specific origin, which is essential in modelling the heterogeneous phenotype of both ALS and RTT. Finally, after analysing the main 3D BBB models' characteristics described previously in Table 1. 1, we decided to choose a co-culture system in a transwell. The cell inserts or transwells allowed us to study each cell type individually, as well as together with their intercellular crosstalk with other cell types. The main disadvantage of this model is the optimization that needs to be addressed for each individual cell type and the conditions to grow them all together at the same time. This model is considerably low-cost and can be developed in a short time, i.e., approximately 10 days. In addition, the transwell system is suitable for testing the BBB permeability, by precisely measuring the TEER without damaging the cell monolayer.

1.6. Modelling the BBB in ALS

Animal models of disease are a common and useful tool. In ALS, many models have been developed. Different systems have contributed to the knowledge of ALS disease mechanisms. From simpler organisms such as yeast, *C. elegans* or *drosophila*; to zebrafish and rodents, are widely used.

Murine models are frequently employed for researching the pathogenesis of ALS and potential therapeutics, while other animal models are preferred for drug and genetic screening.

A key limitation of cellular models is their lack of MN complexity. Although rodent models are considered the standard for validating disease mechanisms and for providing preclinical data on therapeutics, small animal models are increasingly being used to study disease heterogeneity. They can be generated quickly, are cheaper to maintain and are liable to genetic or compound screening. One of the advantages of animal models is the ability to monitor all phases of the disease, from preclinical symptoms to death[58]. Indeed, *Sod1* models have been invaluable in understanding some of the disease mechanisms, but unfortunately, the translation to the clinic has been unsuccessful so far[18,59].

Numerous *Sod1* and other mouse models harbouring different ALS-linked mutations have been created since 1994[60], despite the different strategies, these models present degeneration and death of MNs, leading to progressive muscle atrophy and paralysis. Moreover, these animals display the same histopathological features associated with ALS in humans, such as the presence of SOD1 and ubiquitin aggregates in MNs, astrogliosis and microgliosis, implying a non-cell autonomous pathology[61].

The onset and progression of the disease vary depending on the specific mutations, the gender of the mouse, and its genetic strain. This suggests that genetic background and factors like epigenetics play a significant role in how the disease develops.

Interestingly, the mutant *Sod1* rodent models have also contributed to the concept that neurotrophic factors play a crucial role in MN degeneration. A great example is a mouse model in which the hypoxia response element (HRE) in the promoter region of the vascular endothelial growth factor (*Vegf*) gene was deleted, developing an ALS-like phenotype. Additionally, VEGF expression was lower in the spinal cords of mutant *Sod1* mice before disease onset and survival of the mutant *Sod1* rat model increased on recombinant Vegf treatment[62–64]. These findings suggest that VEGF contributes to and could modify neurodegeneration in ALS, perhaps by affecting BBB integrity.

Due to limited access to primary human brain cells, hi-PSCs are a powerful tool for modelling ALS and other neurodegenerative and neurodevelopmental disorders. These patient-derived hi-PSCs offer a significant advantage as they do not require the overexpression of transgenes with pathogenic ALS gene mutations, e.g., *C9OF72* or *SOD1.* This type of *in vitro* model has greatly contributed to understanding ALS pathogenic mechanisms, although it has some limitations. One major limitation of hi-PSCs is that inducing pluripotency in adult fibroblasts reverts cellular age to an embryonic state, removing ageing-associated signatures. Additionally, there is significant interline and clone variability due to epigenetic aberrations and reprogramming methods, although some age-related epigenetic and mitochondrial signatures can still be found in hi-PSCs. To overcome this limitation, recent studies have shown that directly reprogrammed cells from fibroblasts, without the use of pluripotency factors, retain ageing signatures[65].

1.7. Discussion and future directions of the field

As previously mentioned, there is limited knowledge about brain vasculature and the BBB in the context of ALS, particularly C9-ALS, and RTT. However, BBB breakdown has been documented in various neuropathologies, such as AD and ASD.

Despite the benefits of animal models in research, the use of patient-derived cells opens the door for personalized medicine, which might be the key to heterogeneous diseases characterized by diverse mutations and largely sporadic in origin. Hi-PSCs have the great advantage of reproducing the genetic makeup of the patient, thus reducing the genetic differences among organisms and the problems derived of protein overexpression in the animal models.

Modelling the BBB is a great challenge, but there are new resources available. The use of hi-PSCs together with permeable culture platforms as transwell inserts, allows patient-specific research with a wide range of benefits and applications. Some advantages as obtaining samples from an extended variety of patients, can help to better understand ALS and RTT vascular pathology. Besides, this model can be used for therapeutic applications, such as a resourceful tool for drug screening and brain transport research.

As the fields of BBB and neurodegeneration converge, it is clear the need for models to reproduce and better understand the implications of BBB breakdown in the course of the disease. Nowadays, it is not clear whether BBB impairment leads to the extravasation of proteins from the blood into the brain, causing neurodegeneration or whether, the brain's toxic environment may affect the brain endothelium, thus leading to permeability defects.

1.8. Hypothesis and aims

In my PhD project, I have focused on developing a BBB human-derived *in vitro* model. Due to the multiple pivotal roles of the BBB in preserving the health of the CNS, such as facilitating the brain's energy and nutrient demand, as well as protecting it from external agents, including drugs, a BBB *in vitro* model is a very useful tool for BBB-related research. Moreover, as mentioned before, BBB impairment in disease is well known. Although key aspects of BBB function and dysfunction are modelled in rodents, my project aligns with the continuous effort of replacing animal models, when possible, while reproducing specific human molecular aspects.

Specifically, my research is focused on modelling the BBB in patients affected by ALS and RTT. As highlighted previously in this Chapter, there is evidence for BBB dysfunction in ALS, particularly in mutant *SOD1* cases, but no study has focused on BBB dysfunction in C9-ALS. Since discovered in 2011, *C9ORF72* is considered the most common genetic cause of fALS, sALS and FTD to date[66]. Similarly, no studies have been conducted on BBB impairment in RTT patients. In addition, currently no human or animal model has clarified whether BBB impairment is an early event, or it is the result of the neurodegenerative process. Similarly, it is unclear which cell types and mechanisms are involved in this disruption[67].

Therefore, I hypothesise that **BBB dysfunction plays a role in the neurodegenerative process occurring in both ALS and RTT**.

Hence, the aims of this research are:

1. To generate a multicellular humanised model of the BBB
2. To generate a disease-specific model of the BBB for ALS and RTT
3. To identify the potential functional alteration affecting the BBB in both diseases
4. To dissect the contribution of the cell types forming the BBB in neurodegeneration

Specific aims and objectives will be highlighted in Chapter 3 and Chapter 4 for ALS and RTT respectively.

Chapter 2: Materials and Methods

Chapter 2: Contents

Materials 45
Cell lines 47
Methods 49
2.1. Cell culture protocols 49
2.1.1. Endothelial immortalised cell lines 49
2.1.2. Hi-PSCs culture and derivatives 50
2.1.2.1. Hi-PSCs maintenance 50
2.1.2.2. Hi-PSCs differentiation to BMEC-like cells 50
2.1.3. Fibroblast to hi-NPCs conversion 55
2.1.3.1. Hi-NPC to iAstrocytes 55
2.1.4. Multicellular cultures 56
2.1.4.1. BMECs and iAstrocytes co-culture 56
2.1.4.2. MNs treated with BMEC-like cells conditioned media 57
2.2. Barrier tightness and transport 57
2.2.1. TEER measurements 57
2.2.1.1. Troubleshooting: cell density effect on BMECs barrier properties 58
2.2.2. Efflux activity: P-glycoprotein transporter 59
2.3. Protein quantification by immunocytochemistry 59
2.4. Transcription quantification by qRT-PCR 61
2.4.1. Troubleshooting: housekeeping genes 62
2.5. Cytotoxicity assay 64
2.6. Mitochondrial stress test 64
2.7. Data Analysis 65

Chapter 2: Index of Figures

Figure 2. 1: BMEC-like cells hi-PSCs-derived differentiation timeline for each protocol.....52
Figure 2. 2: No major gene expression differences were found on BMEC-like cells when using either rat tail collagen or IV during purification 54
Figure 2. 3: Cell culture and conditioned media system 56
Figure 2. 4: Contact co-culture system.....57
Figure 2. 5: TEER measurements with electrodes on transwell inserts.....58
Figure 2. 6: BMECs-derived hi-PSCs differentiation timeline 59
Figure 2. 7: A combination of housekeeping genes is the most efficient approach for all cell differentiation stages 63
Figure 2. 8: Lactate dehydrogenase cytotoxicity assay 64
Figure 2. 9: Electron Transport Chain and inhibitors used during the Seahorse XF Real-Time ATP Rate Assay stress test 65

Chapter 2: Index of Tables

Table 2. 1: Reagents 45
Table 2. 2: Cell lines clinical information 47
Table 2. 3: Endothelial immortalised cell lines media 49
Table 2. 4: Hi-PSCs differentiation to BMECs media 51
Table 2. 5: Collagen coating volume.....51
Table 2. 6: Cell seeding densities.....53
Table 2. 7: Cell culture media volume 53
Table 2. 8: Hi-NPC and derivatives media composition.....55
Table 2. 9: Primary Antibodies 59
Table 2. 10: Secondary Antibodies 60
Table 2. 11: Personalized fixation and permeabilization protocols across selected markers ..60
Table 2. 12: Primers relevant information: gene ID and sequences.....61

Materials

Table 2. 1: Reagents

Reagent name	Brand	Code
0.5% Trypsin/EDTA solution 10x	Thermo Fisher scientific	15400-054
10 cm dish	Corning	430167
12-w cell culture insert	Falcon	3460
24-w cell culture insert	Falcon	3450
384-well plates	Corning	CLS3764
384-well plates black, clear bottom	Greiner	781079
6-well plates TC treated	Corning	CLS3506
96-well clear bottom black plates	Greiner	656171
Accutase	Sigma	A6964
Automatic haemocytometer	Life Technologies	Countess II
B-27	Gibco	17504044
Basement membrane matrix growth factor reduced Matrigel	Corning	356230
Bovine Serum Albumin (BSA)	Thermo fisher scientific	B14
Collagen IV from human placenta	Merck Millipore	C5533
Cultrex Reduced Growth Factor Basement Membrane Extract	R&D Systems	3434-005-02
CyQUANT LDH Cytotoxicity Assay	Invitrogen	C20301
CyQUANT™ LDH Cytotoxicity Assay	Thermo Fisher scientific	C20300
Dimethyl sulfoxide (DMSO)	Sigma	D8418
Donkey serum	Merck Millipore	S3-100ML
DPBS, no calcium, no magnesium	Gibco	14190144
Enzyme-free passaging reagent Relesr	Stemcell technologies	5872
EVOM2 electrode	World Precision Instruments	stx2
Fibronectin	Sigma	FC010-10MG
Fluorescein isothiocyanate–dextran (FITC-Dextran 4)	Sigma-Aldrich	46944
Foetal bovine serum (FBS)	Gibco	16000-044
Hanks' Balanced Salt Solution (HBSS), no calcium/magnesium	Thermo fisher scientific	14170161
High-Capacity cDNA Reverse Transcription Kit	Thermo Fisher Scientific	4368814
Hoechst 33342	Life technologies	62249
Human endothelial serum free medium (heSFM)	Gibco	11111044
HuMEC Basal Serum-Free Medium (1X)	Thermo fisher scientific	12753018
Knockout DMEM- Ham's F12	Gibco	12660012
Knockout DMEM-Ham’s F12, GlutaMAX supplement	Gibco	10565042
MEM non-essential amino acids	Gibco	11140050
mTeSR Plus serum-free medium (mTeSR^{+})	Stemcell technologies	100-0276
Paraformaldehyde, 32% (PFA)	Thermo fisher scientific	047377.9L
Penicillin/streptomycin mixture (Pen/Strep)	Lonza	09-757F
Phosphate-Buffered Saline (PBS)	Thermo fisher scientific	10010023
Primers (Oligos)	Merck Millipore	N.A.
Rat tail Collagen (Collagen I)	Corning	354249

Recombinant Human FGF-Basic	Peprotech	100-18B
Retinoic Acid (RA)	Merck	R2625-100MG
RNeasy Plus Mini Kit	Qiagen	74134
Saponin	Sigma-Aldrich	47036
Serum-free media TeSR-E6 (E6)	Stemcell technologies	5946
SYBR Green PCR Master Mix (SYBR Green)	Thermo Fisher scientific	4309155
T75 flask	Corning	430641U
TeSR-E8™ media (E8)	Stemcell technologies	5990
Trypan Blue Solution, 0.4% (Trypan Blue)	Gibco	15250061
XF96 Cell Culture Microplates	Agilent	101085-004
Y-27632 dihydrochloride (Rock Inhibitor)	Tocris	1254
B-mercaptoethanol	Sigma-Aldrich	M3148

Cell lines

Table 2. 2: Cell lines clinical information

Cell line	ID	Supplier	Source Tissue	Type	Rep. Method	Clinical	Mutation protein	Ethnicity	Gender	Age at sampling
GM23338	**CTR-1**	Coriell Insitute	Human fibroblast	**Hi-PSCs**	Retrovirus	**Control**	None	Cau	Male	55 years
CS14iCTR-21nxx	**CTR-2***	Cedars Sinai	Human fibroblast	**Hi-PSCs**	Episomal Plasmid	**Control**	None	Unk	Female	52 years
				hi-NPC	Retrovirus					
CS52iALS-C9nxx	**ALS-1***	Cedars-Sinai	Human fibroblast	**Hi-PSCs**	Episomal Plasmid	**ALS**	C9orf72: HRE	Cau	Male	49 years
				hi-NPC	Retrovirus					
CS29iALS-C9nxx	**ALS-2***	Cedars-Sinai	Human fibroblast	**Hi-PSCs**	Episomal Plasmid	**ALS**	C9orf72: HRE	Cau	Male	47 years
				hi-NPC	Retrovirus					
CS28iALS-C9nxx	**ALS-3**	Cedars-Sinai	Human fibroblast	**Hi-PSCs**	Episomal Plasmid	**ALS**	C9orf72: HRE	Cau	Male	47 years
ALS-183	**ALS-4***	University of Sheffield	Human fibroblast	**Hi-PSCs**	Sendai Virus	**ALS**	C9orf72: HRE	Cau	Male	50 years
				hi-NPC						
ALS-78	**ALS-5***	University of Sheffield	Human fibroblast	**Hi-PSCs**	Sendai Virus	**ALS**	C9orf72: HRE	Cau	Male	66 years
				hi-NPC						
GM23476	**CTR-3****	Coriell Insitute	Human fibroblast	**Hi-PSCs**	Lentiviral	**Control**	None	Cau	Female	20 years
WT 2036	**WT-1**	Harvard Stem Cell Institute	Erythroblasts	**Hi-PSCs**	Sendai Virus	**WT Control**	None (RTT-clone)	Cau	Female	4 years
WT 2042	**WT-2**	Harvard Stem Cell Institute	Erythroblasts	**Hi-PSCs**	Sendai Virus	**WT Control**	None (RTT-clone)	Cau	Female	7 years
WT 2047	**WT-3**	Harvard Stem Cell Institute	Erythroblasts	**Hi-PSCs**	Sendai Virus	**WT Control**	None (RTT-clone)	Cau	Female	13 years
WT 2052	**WT-4**	Harvard Stem Cell Institute	Erythroblasts	**Hi-PSCs**	Sendai Virus	**WT Control**	None (RTT-clone)	Cau	Female	18 years

RTT 2036	**RTT-1****	Harvard Stem Cell Institute	Erythroblasts	**Hi-PSCs**	Sendai Virus	**RTT**	MECP2: R133C	Cau	Female	4 years
RTT 2042	**RTT-2****	Harvard Stem Cell Institute	Erythroblasts	**Hi-PSCs**	Sendai Virus	**RTT**	MECP2: R255X	Cau	Female	7 years
RTT 2047	**RTT-3#**	Harvard Stem Cell Institute	Erythroblasts	**Hi-PSCs**	Sendai Virus	**RTT**	MECP2: R306C	Cau	Female	13 years
RTT 2052	**RTT-4#**	Harvard Stem Cell Institute	Erythroblasts	**Hi-PSCs**	Sendai Virus	**RTT**	MECP2: c.62+ 1delGT	Cau	Female	18 years
161	**CTR-4*****	NCH	Human fibroblast	**hi-NPC**	Retrovirus	**Control**	None	Cau	Male	31 years
AG8620	**CTR-5*****	NCH	Human fibroblast	**hi-NPC**	Retrovirus	**Control**	None	Cau	Female	64 years
155	**CTR-6*****	NCH	Human fibroblast	**hi-NPC**	Retrovirus	**Control**	None	Cau	Male	40 years
S3	**CTR-7*****	NCH	Human fibroblast	**hi-NPC**	Retrovirus	**Control**	None	Asian	Male	Unk
ZKW542	**CTR-8*****	NCH	Human fibroblast	**hi-NPC**	Retrovirus	**Control**	None	Unk	Female	8 years
C-003-5C (HUVECs)	**H-1**	Thermo Fisher Scientific	Human umbilical vein	**Immortalised**	N/A	**Positive Control**	N/A	Unk	Male	<14 days
A10565 (HMECs)	**H-2**	Thermo Fisher Scientific	Human Mammary Epithelia	**Immortalised**	N/A	**Positive Control**	N/A	Unk	Unk	Adult

Abbreviations: Rep. method: reprogramming method; N/A: information not available; Unk: unknown; Cau: Caucasian; HRE: Hexanucleotide repeat expansion; ALS: Amyotrophic Lateral Sclerosis; WT: Wild-Type; RTT: Rett Syndrome; NCH: Nationwide Children's Hospital, Columbus OH, USA.

WT: Non-mutant cells were clonally isolated from RTT patients.

(*)Cells available as both human induced pluripotent stem cells (hi-PSCs) and human induced neuronal progenitors (hi-NPCs).

(**)Cells available as both hi-PSCs and fibroblasts.

(***)Cells available as both hi-NPCs and fibroblasts.

(#)Cells available in all cell types: hi-PSCs, hi-NPCs and fibroblasts.

Commercial information for the reagents can be found in Table 2. 1 or, if not specified, is provided in brackets after the reagent. All cell lines and their relevant information are summarized in Table 2. 2. The endothelial immortalised cell lines, H-1 and H-2 have been used as positive controls throughout the study. CTR-1 and CTR-2, male and female respectively, were used as healthy adult controls age and gender-matched with the ALS-derived cell lines, i.e., ALS-1 to ALS-5 (Chapter 3). Later, CTR-3 and WT-1 to WT-4 are used as young controls, matching the RTT-derived cell lines (Chapter 4). In the last section of Table 2. 2, the fibroblasts used for obtaining iNeurons are also listed.

Methods

2.1. Cell culture protocols

2.1.1. Endothelial immortalised cell lines

Human mammary epithelial cells (HMECs) and human umbilical vein endothelial cells (HUVECs) were routinely seeded either in T25 or T75 flasks and 6-well or 96-well clear bottom black plates and maintenance media (Table 2. 3). The media was replaced every 48 h, or every 24 h -when cells reached 70% confluence. Cells were split when approached 85% confluence by removing the media and washing twice with HBSS no calcium/magnesium (one more wash using trypsin for HMECs). Then, cells were incubated with 1 to 5ml of trypsin for 5-10 minutes at 37°C until the cells had become completely round. Next, an equal volume of media was added to stop the enzymatic reaction and the flask was tapped vigorously. Afterwards, the cell suspension was collected in a 15ml tube and the same number of media as before was once more added to the flask and repeatedly tapped to collect the remaining HMECs. The total suspension was subsequently centrifuged either 7 min / 100 g (HUVECs) or 4 min / 200 g (HMECs) and the supernatant was discarded. Finally, the cell pellet was homogenized in 1ml of fresh media, cells were counted with an automatic haemocytometer by mixing 10µl of cell suspension with 10µl of trypan blue and seeded following the supplier recommendations (2.3x 10^3 viable cells / cm^2 for the HUVECs and 3x 10^3 viable cells/cm^2 for the HMECs). Cells were maintained at 37 °C in a saturated humidity atmosphere containing 5% CO_2.

For cryopreservation, cells were collected following the passaging protocol but transferred into a cryovial containing cryopreservation media (Table 2. 3) and stored at - 80°C or liquid nitrogen instead.

Table 2. 3: Endothelial immortalised cell lines media

Media	Component	Concentration
HUVECs maintenance	hESFM	Basal media
	Foetal Bovine Serum (FBS)	10%
HUVECs cryopreservation	maintenance	basal
	DMSO (dimethyl sulfoxide)	10%
HMECs maintenance	HuMEC Basal Serum-Free Medium (1X)	Basal media
	HuMEC Supplement	1%
	Bovine Pituitary Extract	5%
	penicillin/streptomycin	1%
HMECs cryopreservation	Fresh HMECs maintenance	46.25%
	Conditioned HMECs maintenance	46.25%
	DMSO	7.5%

Human mammary epithelial cells (HMECs) and human umbilical vein endothelial cells (HUVECs) media composition. Conditioned HMEC maintenance media need to be collected from the flask before passaging the cells. All reagents' relevant information can be found on Table 2. 1.

2.1.2. Hi-PSCs culture and derivatives

2.1.2.1. Hi-PSCs maintenance

Human induced pluripotent stem cells (hi-PSCs) were seeded in Basement Membrane Matrix Growth Factor Reduced Matrigel (83.3 µg/ml in Knockout DMEM- Ham's F12) pre-coated 6-well plates and maintained in mTeSR$^+$, replaced every 48 hours (h). Matrigel aliquots were prepared following manufacturer indications (Table 2. 1).

Hi-PSCs subculture was assessed when cells reached 70 – 80% confluence. During cell passaging, hi-PSCs were washed once with HBSS no calcium/magnesium and incubated for 1 minute (min) with the enzyme-free passaging reagent ReLeSR. Then, the dissociation reagent was removed, and cells were incubated at 37°C for 6 to 8 min, depending on cell density. To detach cells, 1 ml of mTeSR$^+$ was added per well and the plate was tapped gently. The cell suspension was seeded in a dilution factor of 1:8 to 1:12 in pre-coated matrigel plates and cells were maintained at 37°C in a saturated humidity atmosphere containing 5% CO_2. For hi-PSCs cryopreservation, cells were collected following the passaging protocol but transferred into a cryovial containing 10% DMSO and 90% mTeSR$^+$ and stored at - 80°C or liquid nitrogen instead.

2.1.2.2. Hi-PSCs differentiation to BMEC-like cells

Protocol A

At day 0 of differentiation (Figure 2. 1 top), when hi-PSCs reached more than 80% of confluence, they were seeded as described in 2.1.2.1 and resuspended in mTeSR$^+$. Differentiation was initiated when hi-PSCs reached 70 % confluence by switching the media to unconditioned media. UM was refreshed every 48 h per 7 days. Next, the cells were expanded in endothelial medium (EM$^+$) (Table 2. 4). During this phase, the media was refreshed every 48 h for 10 days. Afterwards, the cells were purified by splitting them with accutase at 37°C / 5 min and gently collected and centrifuged 4 min / 200 g. Then, the cells were subcultured in a mix of collagen I and fibronectin-coated plates (Table 2. 5) and maintained in endothelial medium (Table 2. 4). Finally, the BMEC-like cells were ready to collect 2 days after purification. The cells were routinely maintained at 37 °C in a saturated humidity atmosphere containing 5% CO_2. This protocol is an adaptation of Lippmann[54,68] and Neal[69] et al. protocols.

Protocol B

At day 0 of differentiation (Figure 2. 1 bottom), when hi-PSCs reached more than 80% of confluence, they were detached by incubating the plate with accutase, for 5 min at 37 °C. Next, cells were collected and centrifuged for 4 min / 200g and resuspended in TeSR™-E8™ media. Subsequently, cells were counted with an automatic haemocytometer as described above and seeded at appropriate density (~14 x10^3 viable cells/cm^2) in matrigel-coated 6w- plates. The cells were supplemented with 10 µM ROCK inhibitor for 24 h to improve cell survival.

Day 1 of differentiation began two days after seeding, or when cells reached 60-70% confluency, by switching the media to serum-free media TeSR™-E6™ (E6), refreshing it daily for 4 days. At day 5, during the expansion phase, the media was changed to endothelial medium (EM$^+$) and maintained for 48h. At day 7 of differentiation, cells were subcultured. Firstly, the media was removed, and cells were washed with HBSS no calcium/magnesium and 1 ml of accutase was added per well and incubated at 37°C 20 – 45 minutes until a single cell suspension was formed. Then, cells were gently collected and

centrifuged for 4 min at 200 g. Finally, cells were reseeded or subcultured (Figure 2. 1) in a mix of either collagen I or collagen IV and fibronectin pre-coated plates or cell culture inserts (Table 2. 5) and maintained one day in EM^+ (Table 2. 4) and 10 µM ROCK inhibitor. On day 8, the medium was switched to purification medium (EM^-)and one day after, the BMEC-like cells are ready to be tested. The cells were routinely maintained at 37 °C in a saturated humidity atmosphere containing 5% CO_2. This protocol is an adaptation of Lippmann and Neal et al. protocols[54,68,69].

Table 2. 4: Hi-PSCs differentiation to BMECs media

Media Code	Media	Component	Concentration
UM	Unconditioned medium	Knockout DMEM-Ham's F12, GlutaMAX supplement	Basal media
		MEM non-essential amino acids	1%
		Pen/Strep	1%
		B-27	0.5%
		β-mercaptoethanol	0.01 mM
EM^+	Endothelial medium	hESFM	Basal media
		bFGF	20 ng/mL
		RA	10 µM
		B-27	0.5%
EM^-	Purification medium	hESFM	Basal media
		B-27	0.5%

Human induced pluripotent stem cells (hi-PSCs) media composition is described in the table above. All reagents' relevant information can be found on Table 2. 1.

Table 2. 5: Collagen coating volume.

Collagen Type	Plate/Trans-well insert	Collagen I	Fibronectin	Dilution agent
I or rat tail	6-, 12-, 24- and 96-well plates	100 µg/ml	20 µg/ml	ddH_2O
	12- and 48-well trans-well inserts	400 µg/ml	100 µg/ml	ddH_2O
IV or placenta-derived	Any format	400 µg/ml	100 µg/ml	0.5 mg/ml acetic acid in H_2O

Collagen coating type and concentration used during brain endothelial cells (BMECs) differentiation. The collagen IV is prepared by diluting 1mg of collagen IV in 1 ml of 0.5 mg/ml acetic acid solution. All reagents' relevant information can be found on Table 2. 1.

Top

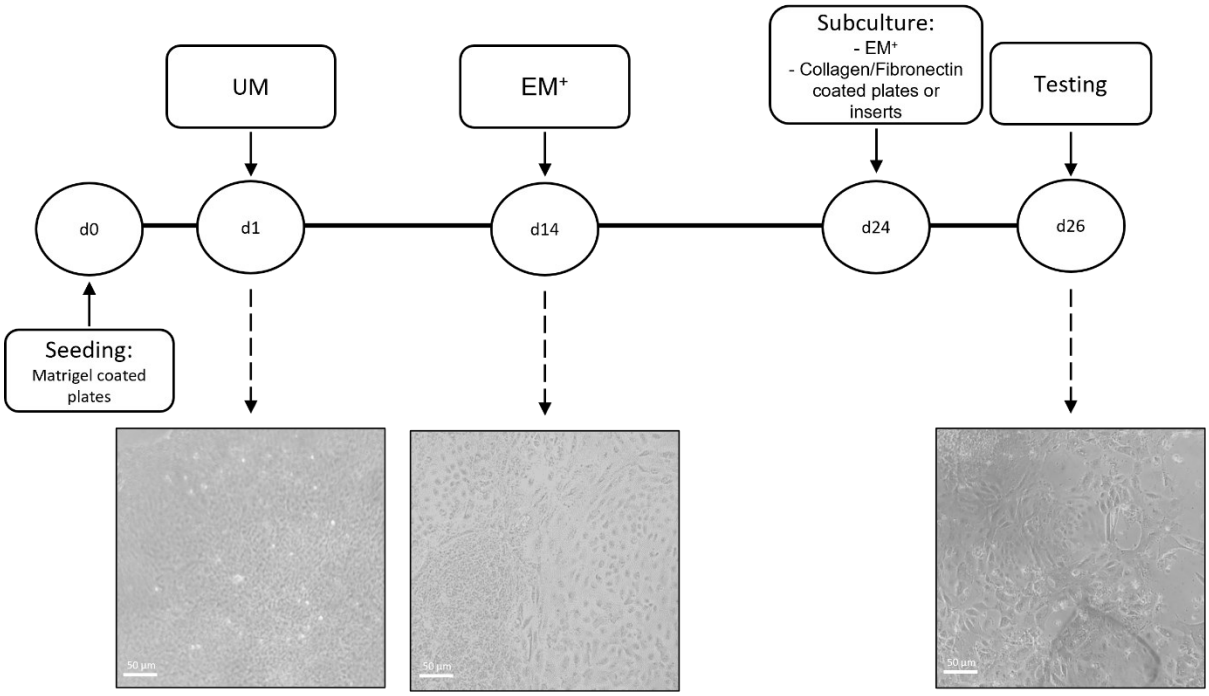

Bottom

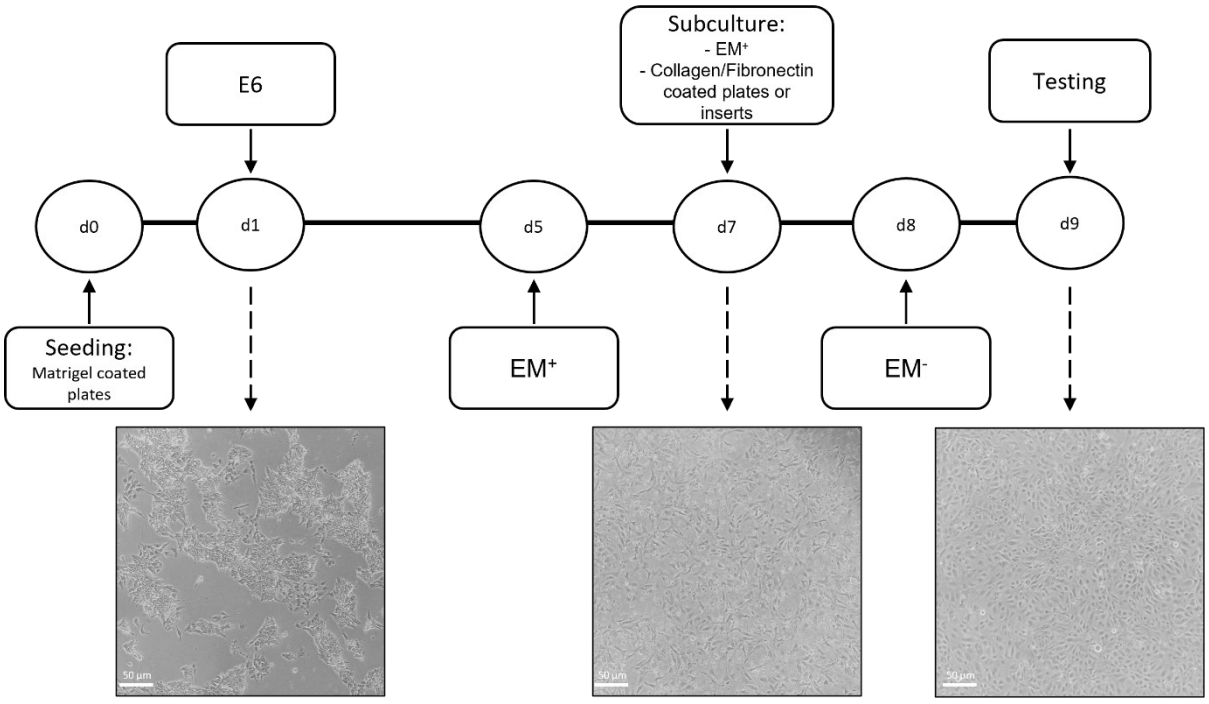

Figure 2. 1: BMEC-like cells hi-PSCs-derived differentiation timeline for each protocol

Brain endothelial (BMEC)-like cells human induced pluripotent stem cells (hi-PSCs) differentiation timeline is exposed for protocols A (Top) and B (Bottom) respectively.

(Top): The protocol A for differentiating hi-PSCs into BMEC-like cells starts when the cells reach 80% confluence. They are seeded in mTeSR+ and, at 70% confluence and switched to unconditioned media (UM) for 7 days. The cells are then expanded in endothelial medium (EM+) for 10 days, with media refreshed every 48 hours. After purification with accutase, the cells are subcultured on collagen I and fibronectin-coated plates. BMEC-like cells are ready for collection 2 days later. This protocol is

adapted from Lippmann et al. 2012, 2014. Morphology changes are significant at day 7 (d7) of the differentiation protocol. Scale bar 50 µM.

(Bottom): The protocol B for differentiating hi-PSCs into BMEC-like cells starts on d0 when hi-PSCs at over 80% confluence were detached, resuspended in TeSR™-E8™ media, and seeded onto Matrigel-coated plates. On d1, when cells reached 60-70% confluence, differentiation began by switching to serum-free TeSR™-E6™ (E6) for 4 days, then to endothelial medium (EM^+) for 48 h. On d7, cells were subcultured onto collagen-coated plates with EM^+. The next day, the medium was switched to purification medium (EM^-), and BMEC-like cells were ready for testing on d9. This protocol adapts methods from Neal et al. 2019. Morphology changes are significant at d6 of the differentiation protocol. Scale bar 50 µM.

Table 2. 6: Cell seeding densities

Cell type	Format	Cells / well
BMEC	24-well insert	330000
	6-well plate	1900000
	12-well plate	250000
	96-well plate	300000
	96-well plate (sea horse)	250000
iAstrocyte	24-well insert	9000
	24-well plate	47500
	96-well plate	9000

Brain endothelial (BMEC) and induced astrocyte (iAstrocyte) cell types seeding densities according to the cell culture format are described in the table above.

Table 2. 7: Cell culture media volume

Format	Media Volume (µl)
24-well insert (basal chamber or top)	200
24-well insert (basolateral chamber or bottom)	700
6-well plate	2000-3000
12-well plate	1000-2000
96-well plate	100-200
96-well plate (sea horse)	75

Cell culture media volumes are described in the table above, ranging from cell culture inserts to cell culture plates.

2.1.2.3. Troubleshooting: coating solutions

Establishing the hi-PSCs derived BMECs protocols is very demanding and requires several adjustments to fully developing a trustable *in vitro* model.

The hi-PSC-derived BMEC-like cells are produced through simultaneous differentiation of endothelial and neural progenitors as described by Lippmann et al. 2012, providing an environment that

recapitulates some aspects of early BBB development. At day 7 of differentiation, this mixed population is subcultured onto collagen/fibronectin-coated plates. By this method, endothelial cells (ECs) selectively attach to the plate while neural progenitor cells do not, resulting in pure BMEC monolayers when refreshing the medium on day 8[54].

As discussed previously, different approaches using rat tail collagen (collagen I) and collagen IV in combination with fibronectin have been used in the literature for culturing microvessels[70]. Hence, we explored the effect of collagen I and collagen IV on BBB markers gene expression *CDH5* (VE-Cadherin), *CLDN5*, *OCLN*, and *TJP1*. No significant differences were observed when using either of them (Figure 2. 2). TEER measurements on these cells were also quantified with no differences observed (data not shown).

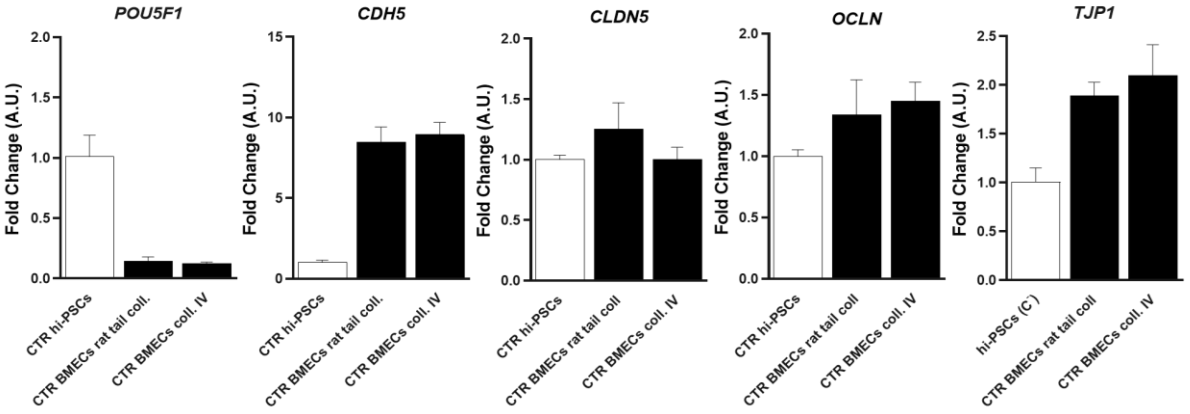

Figure 2. 2: No major gene expression differences were found on BMEC-like cells when using either rat tail collagen or IV during purification

Human induced pluripotent stem cells (hi-PSC)-derived brain endothelial (BMEC)- like cells were differentiated as described previously. However, on day 7 of differentiation (see Figure 2. 1 bottom), cells were seeded either using a mix of rat tail collagen (coll.) or collagen IV (human placenta-derived) and fibronectin. Gene expression was quantified by qRT-PCR for the following genes *CDH5*, *CLDN5*, *OCLN*, *TJP1* and *POU5F1*. Data were analysed by the non-parametrical Kruskal-Wallis test and plotted as mean ± SD, biological n = 1, technical repeats = 3. No statistical differences were found when comparing rat tail coll. Vs coll. IV.

2.1.2.4. Hi-PSCs to hi-NPCs conversion

Differentiation of hi-PSCs to hi-NPCs was performed as previously described by Du et al. 2015[71]. The cells were routinely maintained at 37°C in a saturated humidity atmosphere containing 95% air and 5% CO_2.

Hi-NPCs to motor neurons differentiation

Differentiation of hi-NPCs to motor neurons (MNs) was performed as previously described by Du et al. 2015[71]. Briefly, hi-PSCs in the presence of small molecules: ROCK inhibitor, SMAD inhibitors (SB431542 and DMH1) for 6 days and ROCK inhibitor, SB431542, DMH1, Retinoic Acid (RA) and Purmorphamine for another 6 days. At that point, all the hi-PSC lines generated more than 90% OLIG2+ Motor Neuron Progenitor Cells. Afterwards, the cells were expanded in the same media + valproic acid.

To induce MN differentiation, OLIG2+ MNPs were dissociated and cultured 1:6 in suspension in neural medium with RA and Purmorphamine. The medium was changed every other day for 6 days. Next,

they were dissociated into single cells and plated on matrigel coated plates and cultured with RA, Purmorphamine and Compound E (γ-Secretase-IN-1) for 10 days to mature into CHAT+ MNs. The cells were routinely maintained at 37 °C in a saturated humidity atmosphere containing 95% air and 5% CO_2.

2.1.3. Fibroblast to hi-NPCs conversion

Fibroblasts were reprogrammed to human induced neuronal progenitors stem cells (hi-NPCs) following Meyer et al. 2014[72]. In brief, fibroblasts were seeded in a well of a six-well plate and treated with a mixture of retroviral vectors expressing Kruppel-like factor 4 (*KLF4*), POU transcription factor Oct-3/4 (*OCT3/4*), SRY-related HMG-Box Gene 2 (*SOX2*), and c-Myc for 12 h. To promote neuroprogenitor cells conversion, the culture medium was switched 72h after to medium containing fibroblast growth factor 2 (FGF2), epidermal growth factor (EGF), and heparin, and this was continued for 18 days. Then, cells were routinely maintained at 37 °C in a saturated humidity atmosphere containing 95% air and 5% CO_2.

2.1.3.1. Hi-NPC to iAstrocytes

Hi-NPCs were seeded in 2.5 µg/ml fibronectin-coated 10cm dishes onto iAstrocyte medium (Table 2. 8) as published by Meyer and Ferraiuolo's protocol[72] for up to 7 days. The cells were routinely maintained at 37°C in a saturated humidity atmosphere containing 95% air and 5% CO_2.

Table 2. 8: Hi-NPC and derivatives media composition

Media	Component	Concentration
Hi-NPC maintenance	Knockout DMEM-Ham's F12, GlutaMAX supplement	Basal media
	100x diluted N2	1%
	B-27	1%
	bFGF	40 ng/mL
	Penicillin/Streptomycin	1%
iAstrocyte maintenance	Knockout DMEM-Ham's F12, GlutaMAX supplement	Basal media
	FBS	10%
	100x diluted N2	1.8%
	Penicillin/Streptomycin	1%

Human-induced neuronal progenitor cells (hi-NPC) and induced astrocyte (iAstrocyte) media composition is described in the table above. All reagents' relevant information can be found on Table 2. 1.

2.1.4. Multicellular cultures

To test the effect of cell types onto each other's function, hi-PSC-derived BMEC-like cells, MNs and hi-NPC-derived astrocytes were cultured together (Figure 2. 3).

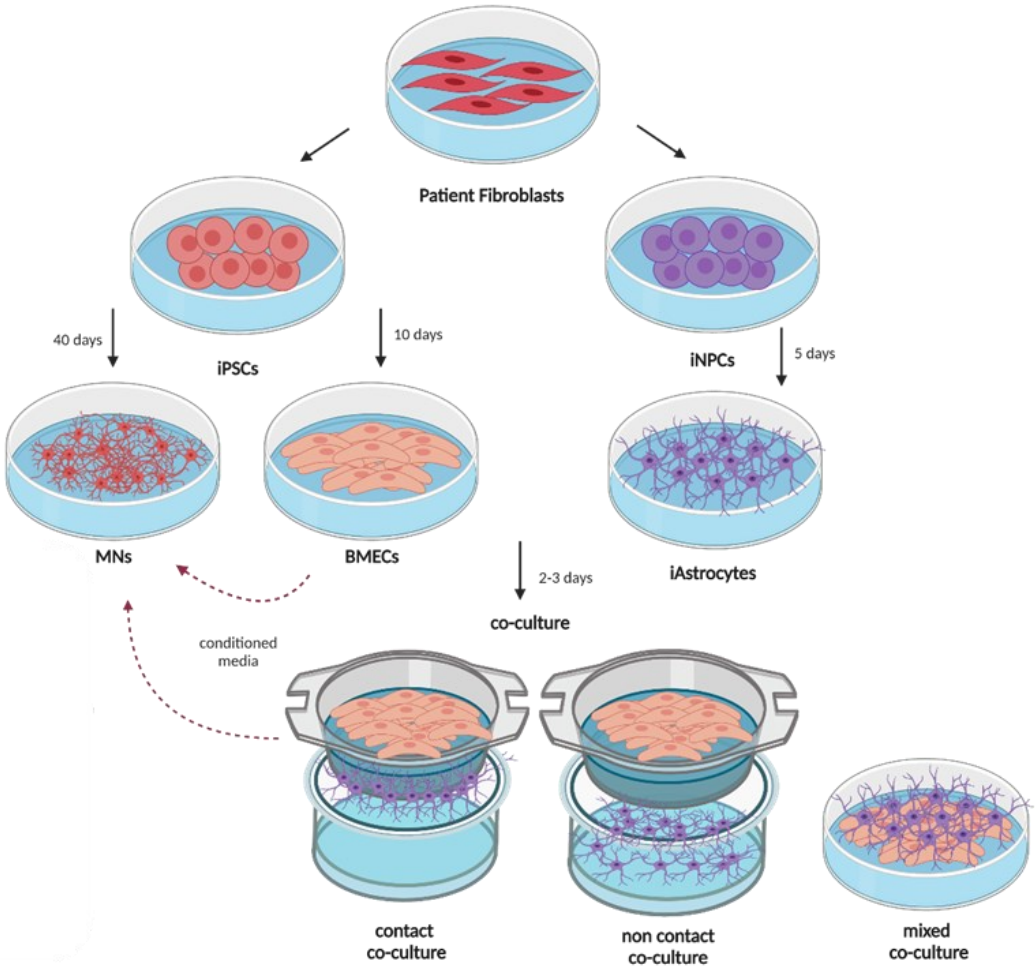

Figure 2. 3: Cell culture and conditioned media system

To explore the effect of each cell type on others, different co-culture assemblies, thus including brain endothelial cells (BMECs) and induced astrocytes (iAstrocytes) and conditioned media experiments from them were explored in every other cell type (including motor neurons -MNs) as illustrated above. Briefly, contact co-culture: iAstrocytes were plated at the bottom of the external side of a fibronectin-coated transwell insert allowing direct contact with BMEC-like cells through the end-feet, facilitating close interaction. Non-contact co-culture: iAstrocytes were plated in the well below the transwell insert, with BMEC-like cells placed on the transwell membrane above. In this format, the cells are separated by the insert, allowing interaction through soluble factors but without direct contact. Mixed co-culture: iAstrocytes were plated in the same well as BMEC-like, allowing both direct contact and interaction through soluble factors.

2.1.4.1. BMECs and iAstrocytes co-culture

On day 7 of BMEC-like cells differentiation (Figure 2. 1 bottom), cells were subcultured and seeded on the upper part of cell trans-well inserts or in 96-well clear bottom black. One day after seeding (day 8), BMEC-like cells were co-cultured with iAstrocytes at day 6 of the differentiation stage. The iAstrocytes in dishes were washed once with PBS and detached by adding accutase at 37°C. Then, the iAstrocytes suspension was collected and centrifuged for 4 min at 200 g. At that time, iAstrocytes were

replated either at the bottom of the 2.5 µg/ml fibronectin-coated transwell insert and incubated for 1 h at 37°C (contact co-culture, see Figure 2. 4), in the well below the transwell insert (non- contact co-culture) or at in a well of a 96-well plate that already contained BMEC-like cells (mixed co-culture). Finally, conditioned media and cells were tested after 2 or 3 days of co-culture (see Figure 2. 3 bottom right). The cells were routinely maintained at 37°C in a saturated humidity atmosphere containing 95% air and 5% CO_2.

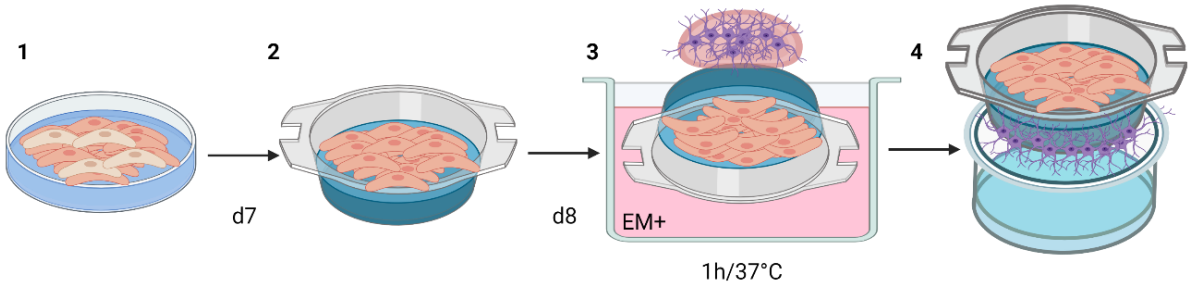

Figure 2. 4: Contact co-culture system

1-2: To perform the contact co-culture, brain endothelial (BMEC)-like cells were seeded in the transwell insert at day 7 (d7). 3: Then, on d8, the insert was placed inversely in a 12-well plate. Meanwhile, the transwell was covered with endothelial medium (EM^+) media, to keep the BMEC-like cells alive while seeding the iAstrocytes at the bottom of the insert. Then the iAstrocytes together with the BMEC-like cells are incubated for 1h/ 37 °C. 4: Finally, the cells are checked under the microscope and placed in the 24-well transwell insert plate accordingly.

2.1.4.2. MNs treated with BMEC-like cells conditioned media

At day 9 of BMEC-like cells differentiation, conditioned media were collected and added in a proportion of 50% to the day 40 MNs for 3 days (Figure 2. 3). The cells were routinely maintained at 37 °C in a saturated humidity atmosphere containing 95% air and 5% CO_2.

2.2. Barrier tightness and transport

To evaluate the barrier tightness, BMEC-like cells transendothelial resistance was measured using electrodes (Figure 2. 5). To further evaluate the active efflux activity of the BMEC-like cells, P-glycoprotein transporter was also checked.

2.2.1. TEER measurements

BMEC-like cells were differentiated following protocol B and seeded at the desired density (Figure 2. 1 and Table 2. 6) in fibronectin/collagen 0.4 µm PET transwell inserts at the subculture step (see Figure 2. 1 bottom). As previously described, the cells were maintained in EM^+ 24 h after subculture and then the medium was switched to EM^- on day 8 (Table 2. 4) and not refreshed afterwards. TEER (transendothelial resistance) measurements were monitored daily starting at day 8 of differentiation, with an EVOM2 stx2 electrode. Before the measurements, the cell monolayer was visually checked, and only intact monolayers were used. Three measurements per insert were recorded at a similar time every day by placing the electrode chopsticks on the transwell inserts containing the cells (see Figure 2. 5). One plate was recorded at a time to avoid artificially raising TEER because of having the plate a prolonged time outside the incubator as suggested by Stebbins et al. 2016[73].

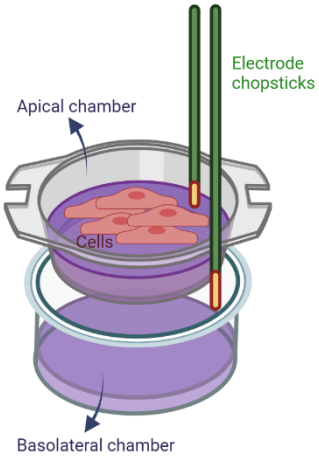

Figure 2. 5: TEER measurements with electrodes on transwell inserts

To evaluate the barrier tightness, brain endothelial (BMEC)-like cells were seeded in the apical chamber of the transwell inserts. Then, transendothelial resistance (TEER) was measured using EVOM2 stx2 electrode electrodes by placing them in both the apical and basolateral chambers of the insert. This diagram was created on Biorender.com.

2.2.1.1. Troubleshooting: cell density effect on BMECs barrier properties

Decisively, the density of hi-PSCs cultures during the differentiation process can have a significant impact on the cell phenotype. During differentiation, hi-PSCs density can affect the strength of paracrine signalling and cell-cell contacting, both involved in the regulation of differentiation fates[73]. The effect of initial seeding density affected differentiation yield in different hi-PSC differentiation protocols[74–76].

Hence, given the potential importance of initial hi-PSCs seeding density on differentiation outcome and barrier properties, different densities at day 0, before starting differentiation, and at day 7 of the differentiation process (Figure 2. 6), were compared. Cell density was also checked at day 1 of differentiation, before switching to E6 medium. As a quality check, I measured the TEER on BMEC-like cells monolayers[77].

No differences were reported among the seeding densities panel on day 0 (7.8, 10.4 or 13 thousand cells/cm^2) but on day 7 (0.875, 1 or 1.15 million cells/cm^2). Thus, while initial density may not substantially affect the barrier properties, the subculture seeding is decisive for achieving high TEER measurements (> 2000 ohms x cm^2), as also reported by Wilson et al[78]. Table 2. 6 summarizes the selected densities based on the well format, with 1 million cells/cm^2 confirmed as the most suitable on day 7 of differentiation[78].

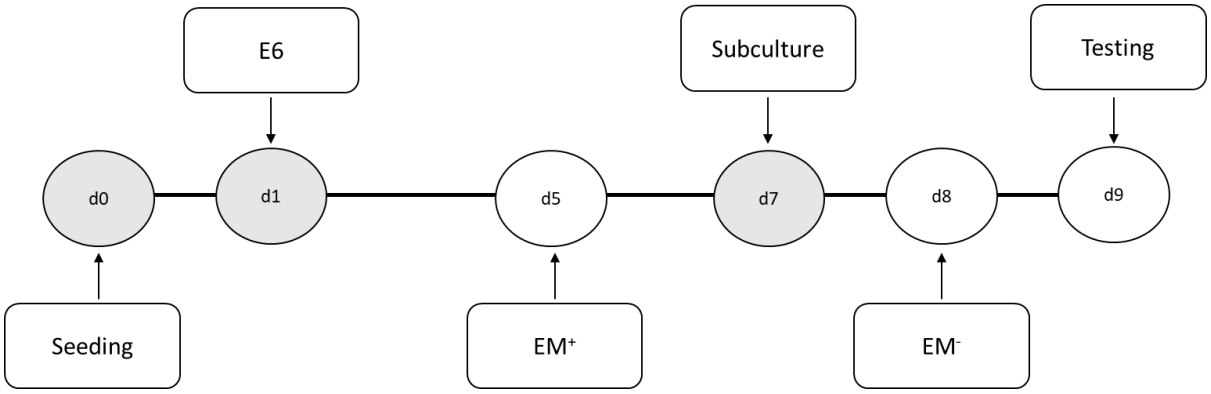

Figure 2. 6: BMECs-derived hi-PSCs differentiation timeline

Cells were seeded at day (d) 0 as described before (Chapter 2, 2.1.2.2 Protocol B) at 3 different densities: 7800, 10400 or 13000 cells/cm^2. Briefly, two days after seeding, or day 1 (d1) one well was dissociated using accutase and the cell density was registered, to determine if the hi-PSCs were ready to start the differentiation, Then E6 TeSR™-E6™ (STEMCELL Technologies) medium (E6) was refreshed daily for 4 days. On d5, during the expansion phase, the media is changed to EM+ (hESFM supplemented with Retinoic Acid, bFGF and B-27). By Day 8, the medium is switched to EM$^-$ (hESFM supplemented with B-27 only) and by d9, the BMEC-like cells are ready for testing.

2.2.2. Efflux activity: P-glycoprotein transporter

Similarly, BMEC-like cells are typically tested on day 9 of differentiation. For this assay, cells were seeded in a 24-well plate (Figure 2. 1 and Table 2. 6) at day 7. Later, on day 9, the media was aspirated, and cells were washed with HBSS no calcium/magnesium. Next, 3 wells per condition were incubated for 1 h at 37°C with HBSS only and 3 wells with HBSS + 10µM Cyclosporin A (CyA), a P-glycoprotein inhibitor. Then, the solution was aspirated, and the cells were incubated for 1 h at 37°C with HBSS + 10µM Rhodamine 123, a P-glycoprotein substrate; or with HBSS + Rhodamine 123 + CyA respectively. Afterwards, BMEC-like cells were rinsed with PBS twice and fluorescence was measured at Ex 488/ Em 530 nm with a PHERAstar® high-throughput screening microplate reader.

2.3. Protein quantification by immunocytochemistry

Cells were washed twice with PBS and fixed either with 4% paraformaldehyde (PFA) for 20 min or 100% cold methanol, 100% acetone or 50:50 methanol: acetone for 10 min. Subsequently, the cells were incubated for 1 h at RT with a blocking solution of PBS, 5% horse serum and 0.3% Triton for non-membrane epitopes. Next, cells were rinsed three times with PBS. Then, they were incubated with primary antibody (Table 2. 9) in blocking solution at 4°C overnight. After that, cells were rinsed three times with PBS and incubated 1h at RT with the secondary antibody (Table 2. 10) diluted in PBS. Nuclei were stained with 1µg/ml Hoechst 33342 for 5 min. Finally, the cells were washed three times with PBS and the images were normally acquired with a Nikon confocal microscope or with the Opera Phenix™ high-content screening system microscope.

Table 2. 9: Primary Antibodies

Antibody	Species	Company	Catalogue Number	Concentration	Fixation
CD31	Mouse	Proteintech	66065-1-Ig	1:300	MeOH
Claudin-5	Mouse	Invitrogen	35-2500	1:100	MeOH
Claudin-5	Rabbit	Abcam	Ab15106	1:100	MeOH
GLUT1	Rabbit	Proteintech	21829-1-AP	1:150	MeOH
VEGFA	Rabbit	Proteintech	19003-1-AP	1:500	MeOH

Primary antibodies used are described in the table above. Thus, including CD31 (VE-Cadherin), Claudin-5, GLUT-1 (Glucose transporter 1) and VEGFA (Vascular endothelial growth factor A).

Table 2. 10: Secondary Antibodies

Antibody	Species	Wavelength (nm)	Company	Catalogue Number	Concentration
Anti-mouse	Donkey	568	Abcam	A10037	1:500 (ICC)
Anti-rabbit	Donkey	488	Abcam	A21206	1:500 (ICC)

Secondary antibodies used are described in the table above.

2.3.1. Troubleshooting: fixation

PFA is a widely used chemical fixative[79,80]. PFA creates covalent cross-links between cell molecules, effectively sticking them together and altering their surface mechanical properties[81]. Yet, it is not adequate for all experiments, i.e., different cell types, and epitope locations (cytoplasm, cell membrane, nucleus). Thus, I tested various fixation methods and detergents such as Triton X-100 and saponin. When using organic solvents (i.e., methanol and acetone), no permeabilization was required (Table 2. 11).

Permeabilization of cell membrane lipid components facilitates antibody access to intracellular or intraorganellar antigens. Either non-specifically by Triton X-100, or specific cholesterol removal by saponin, without changing the cells' ultrastructural integrity[82]. Taking into consideration that tight junctions are our main target, organic solvents seem to be the perfect alternative to detergents, which disrupt transmembrane proteins.

Table 2. 11: Personalized fixation and permeabilization protocols across selected markers

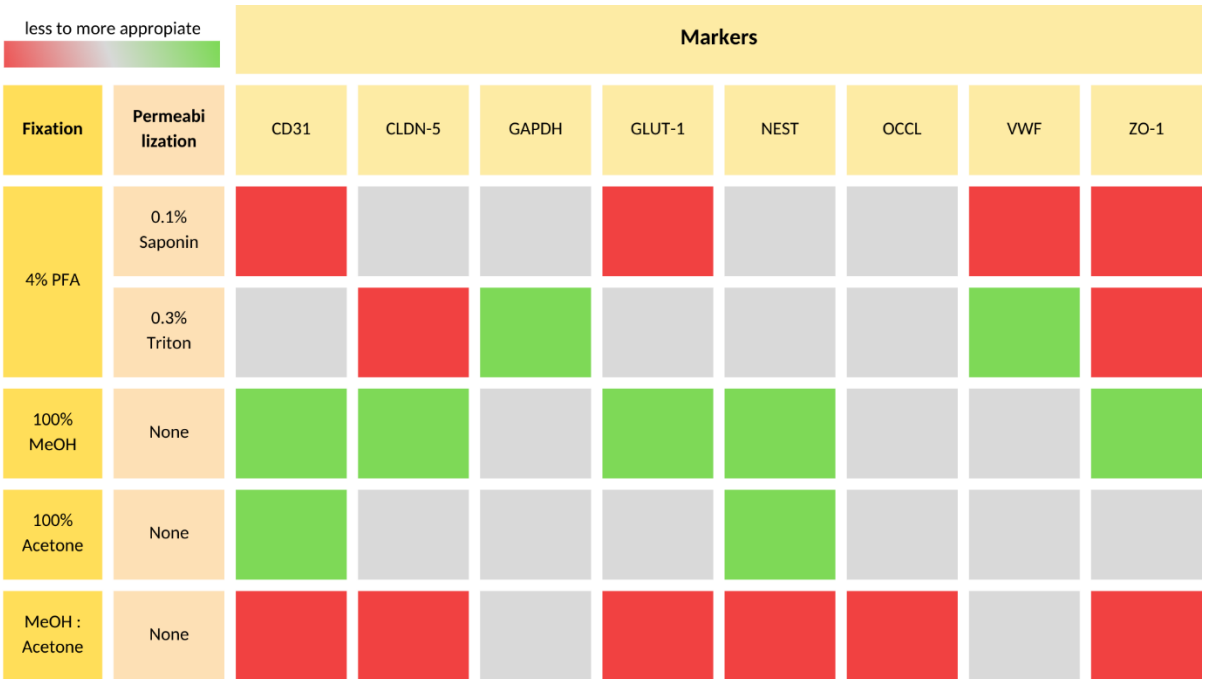

Human induced pluripotent stem cells (hi-PSCs) were differentiated into brain endothelial (BMEC)-like cells and seeded onto 96-well plates on day 7 of protocol. On day 9, they were fixed and permeabilized if required. ICC and imaging protocol were followed as previously indicated. Triplicates of two healthy and two patient cell lines were tested. Colour code: red or non-appropriate (no visible structure), grey or moderate (blurry staining) and green or appropriate (clear protein staining observable). Markers: CD31 or Platelet endothelial cell adhesion molecule (PECAM-1), Claudin-5 (CLDN-5), Glyceraldehyde

3-phosphate dehydrogenase (GAPDH), glucose transporter-1 (GLUT1), Nestin (NEST), Occludin (OCCL), Von Willebrand Factor (VWF) and Zonula Occludens-1 (ZO-1).

To summarise:

- 4% PFA + 0.1% Saponin: did not offer any adequate positive staining when imaging.
- 4% PFA + 0.3% Triton: was appropriate for some intracellular proteins (GAPDH and VWF).
- 100% MeOH: offered the best results across most transmembrane markers, CD31, CLDN-5, GLUT1, ZO-1, and NEST (intracellular).
- 100% Acetone: provided acceptable results for both, CD31 and NEST.
- MeOH: Acetone: not appropriate.

All considered, 4% PFA + 0.3% Triton and 100% MeOH protocols were selected as the most suitable protocols.

2.4. Transcription quantification by qRT-PCR

Cells were collected and washed twice with PBS and centrifuged for 4 min / 200g subsequently. RNA was extracted following the manufacturer's instructions using the RNeasyPlus MiniKit (Table 2. 1). The RNA concentration was determined with a NanoDrop and the RNA to cDNA reverse transcription was performed following the manufacturer's indications for the High-Capacity cDNA Reverse Transcription Kit. The total reaction volume per well in a 384 well plate was 10 µl, containing 2x SYBR Green, 5µM forward and reverse primers (Table 2. 12), 50ng of cDNA and ultra-pure water.

Table 2. 12: Primers relevant information: gene ID and sequences

Gene Name	Gene ID	Forward Sequence (5'-)	Reverse Sequence (5'-)
ABCB1	5243	TGAATCTGGAGGAAGACATGAC	CCAGGCACCAAAATGAAACC
ABCC1	4363	AATAGAAGTGTTGGGCTGAG	CGAGACACCTTAAAGAACAG
CDH5	1003	CGCAATAGACAAGGACATAACAC	GGTCAAACTGCCCATACTTG
CLDN5	7122	TTCGCCAACATTGTCGTCC	TCTTCTTGTCGTAGTCGCCG
INSR	3643	TGTTCATCCTCTGATTCTCTG	GCTTAGATGTTCCCAAAGTC
JAM2	58494	GCTCTAGAATAGACTTCCATGTCCTGCC	GGCAGGACATGGAAGTCTATTCTAGAG
OCLN	100506658	CTCGAGAAAGTGCTGAGTGCCTGGAC	AAGCTTTCGGTGACCAATTCACCTGA
PLVAP	83483	CAATGCAGAGATCAATTCAAGG	ACGCTTTCCTTATCCTTAGTG
POU5F1	5460	CCTGAAGCAGAAGAGGATCACC	AAAGCGGCAGATGGTCGTTTGG
RAGE	177	GTAGATTCTGCCTCTGAACTC	CTTCACAGATACTCCCTTCTC
RPL13	6137	TCAAAGCCTTCGCTAGTCTCC	GGCTCTTTTTGCCCGTATGC
RPL30	6156	GCTGGAGTCGATCAACTCTAGG	CCAATTTCGCTTTGCCTTGTC
RPL31	6160	CTCGGGCACTCAAAGAGATTC	CGGATTCGGTATGGCACATTC
RPL37	6167	CAAGCGCAAGAGAAAGTATAACTGG	CAGCTGCCCTCTTGGGTTTAG
SLC16A1	6566	GGTGTTTCTTAGTAGTTATGGG	TCTTATTGGCTTTGTGTTGG
SLC1A1	6505	GTTATTCTAGGTATTGTGCTGG	CTGATGAGATCTAACATGGC
SLC2A1	6513	ACGCTCTGATCCCTCTCAGT	GCAGTACACACCGATGATGAAG
SLC7A5	8140	TTAAAGTAGATCACCTCCTCGA	GGATGAGATTCGTACCAGAG
TGFB1	7040	AACCCACAACGAAATCTATG	CTTTTAACTTGAGCCTCAGC
TJP1	7082	ACCAGTAAGTCGTCCTGATCC	TCGGCCAAATCTTCTCACTCC
VWF	7450	CCCGAAAGGCCAGGTGTA	AGCAAGCTTCCGGGGACT

2.4.1. Troubleshooting: housekeeping genes

Glyceraldehyde 3-phosphate dehydrogenase gene (*GAPDH*) is often used as a classical housekeeping gene. However, *GAPDH* instability across ageing and different experimental conditions has been reported[83]. Several publications testing *GAPDH* gene expression stability at different environmental scenarios have been published, like oxidative stress[84]. Moreover, Desai et al. 2002 described an increased *GAPDH* expression as a survival mechanism of ECs under shear stress[85].

Hence, we first validated the appropriate housekeeping gene for these studies.

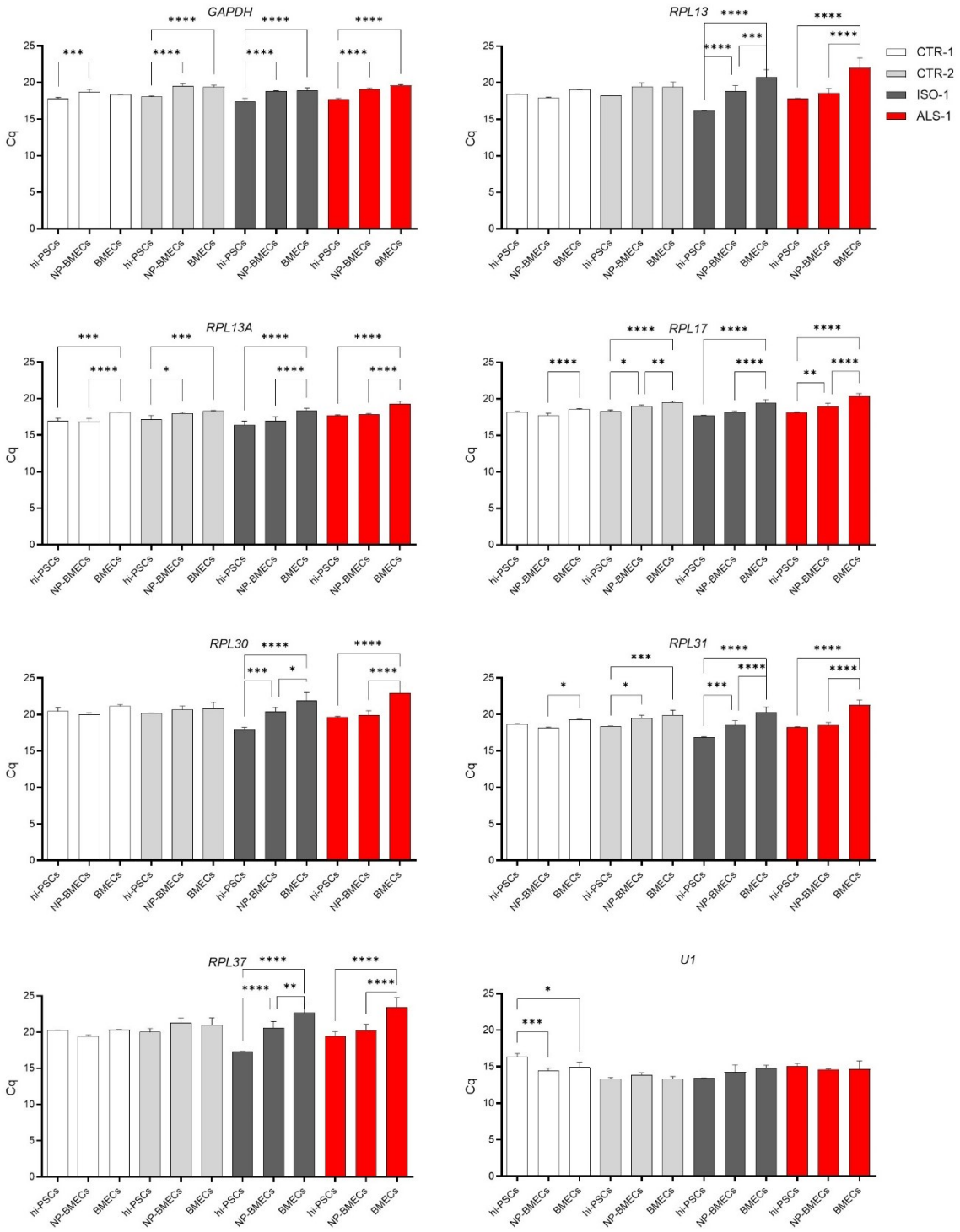

Figure 2. 7: A combination of housekeeping genes is the most efficient approach for all cell differentiation stages

Cells were collected at three points of the differentiation process, before the differentiation or d0 (hi-PSCs), at an intermediate step of the differentiation or day 7, at non-purified (NP) and at the end or day 9. Due to individual and healthy and disease stages differences, two healthy controls, one C9-ALS-isogenic control and one C9-ALS patient cell lines were tested. All samples were standardized to 50 ng of cDNA. cDNA was quantified by qRT-PCR for the following genes *GAPDH, RPL13A, RPL13, RPL17, RPL30, RPL31, RPL37* and *U1*. Quantification cycle (Cq) data were analysed by multiple one-way ANOVA and plotted as mean ±SD. ****$p < 0.001$. Technical n=3.

As exposed on the Figure 2. 7, traditional housekeeping gene (*GAPDH*), Ribosomal Protein Large subunit (*RPL*) genes (*13, 13A, 17, 30, 31* and *37*) and small nuclear ribonucleoprotein particle gene (*U1:* snRNP) were compared on different cell lines. Those genes were selected based on the last decade transcriptome analysis published on the field[86–88]. RNA expression was quantified as usual: at day 0 of the differentiation process (hi-PSCs), at day 7 (NP-BMECs) and at day 9 (BMECs). I observed a similar trend among most of them, with an increase in the gene expression through the differentiation protocol, resulting in lower expressions at hi-PSCs state than when BMECs. Nonetheless, both *RPL13A* and *U1* showed the lowest variation across all conditions. Therefore, I decided to use a combination of both markers as the most suitable housekeeping gene control for forthcoming experiments.

2.5. Cytotoxicity assay

To measure the cellular toxicity within the cells, a lactate dehydrogenase (LDH) assay was assessed following the manufacturer indications (Table 2. 1). BMEC-like cells were seeded at appropriate density in a 96-well plate (Figure 2. 1 and Table 2. 6) at day 7 of the differentiation protocol (Figure 2. 3 bottom). After 2 days, the LDH test was done, and the absorbance was measured at 490/680 nm with a PHERAstar® high-throughput screening microplate reader. To determine LDH activity, 682 nm absorbance was subtracted from the 490 nm signal (Figure 2. 8). Lysed cells were considered the Maximum LDH activity control and media without cells was used as a blank.

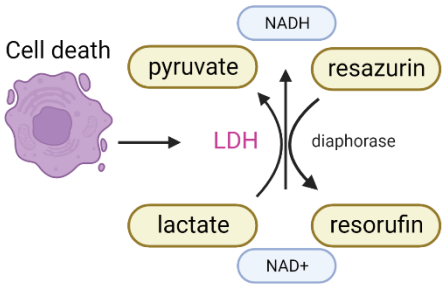

$$\%\ Cytotoxicity = \frac{LDH\ activity - Blank}{Maximum\ LDH\ activity - Blank}$$

Figure 2. 8: Lactate dehydrogenase cytotoxicity assay

Left: Lactate dehydrogenase (LDH) is rapidly released into the cell culture medium upon plasma membrane damage. Thus, LDH released from the cell oxidizes lactate to generate NADH, which then reacts with resazurin to generate a red-violet colour (682/490nm absorbance). The absorbance correlates directly with the number of lysed cells. The illustration has been created at Biorender.com. Right: See the equation for the cytotoxicity percentage (%) calculations.

2.6. Mitochondrial stress test

To test the effect of cell types on each other's function, hi-PSC-derived BMEC-like cells, motor neurons and hi-NPC-derived astrocytes were cultured together on day 7 of the differentiation protocol (Figure 2. 3 bottom), BMEC-like cells were seeded at the desired density (Figure 2. 1 and Table 2. 6) in a 96-well Agilent assay plate (Table 2. 1). The Agilent Seahorse XF Real-Time ATP Rate Assay measures key parameters of mitochondrial function by directly measuring the oxygen consumption rate (OCR) of cells on the Seahorse Analysers. It is a plate-based live cell assay that allows the monitoring of OCR in real time.

The non-mitochondrial respiration, which is the oxygen consumption that persists after the addition of rotenone and antimycin A (complex I and III electron transport chain inhibitors respectively) is used to get an accurate measure of true mitochondrial respiration. On the other hand, basal respiration which is being used to drive ATP production is measured upon injection of oligomycin (ATP synthase inhibitor). Thus, showing the ATP produced by the mitochondria (see Figure 2. 9).

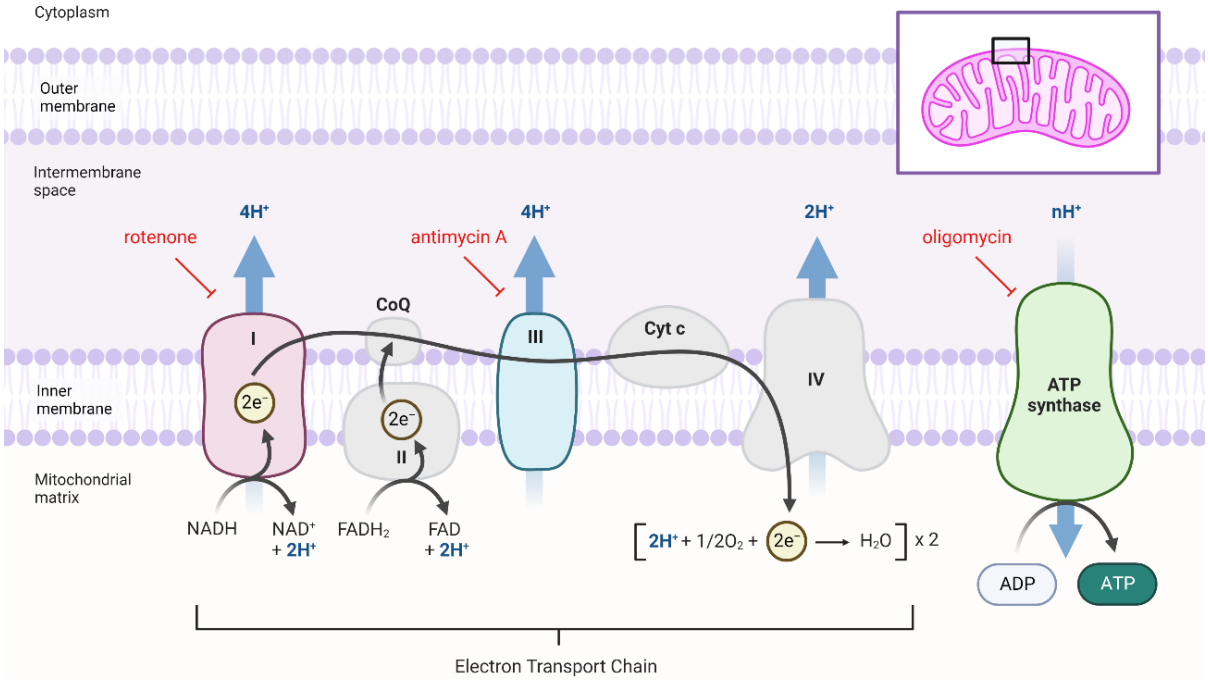

Figure 2. 9: Electron Transport Chain and inhibitors used during the Seahorse XF Real-Time ATP Rate Assay stress test

This figure illustrates the complexes of the mitochondrial electron transport chain and indicates the target of action for all the drugs included in the stress test. The mitochondrial stress test involves three injections to analyse mitochondrial respiration. First, oligomycin is added to inhibit ATP synthase, reducing oxygen consumption rate (OCR) and indicating cellular ATP production. Then, a mixture of rotenone and antimycin A is added to inhibit complexes I and III, respectively, halting mitochondrial respiration and allowing measurement of nonmitochondrial respiration. This figure has been adapted from a template at Biorender.com.

2.7. Data Analysis

All statistical analyses were undertaken with GraphPad Prism software (v.10), details of the statistical analyses have been indicated in each figure legend. Immunocytochemistry images were processed with either Columbus™ Image Data Storage and Analysis system software or Nikon NIS-Elements' software (v. 5.42).

Chapter 3: *C9ORF72* Patient-Derived Endothelial Cells Drive Blood-Brain Barrier Disruption and Contribute to Neurotoxicity in a Multicellular *In Vitro* Model

Chapter 3: Contents

3.1. Preface 70

3.2. Hypothesis and Aims 71

3.3. Results 72

3.3.1. BMEC-like cells are successfully differentiated from hi-PSCs 72

3.3.2. Comment on gender differences for the healthy cell lines 75

3.4. Discussion 76

Chapter 3: Index of Figures

Figure 3. 1: C9ORF72 repeat sizing via Southern Blotting 71
Figure 3. 2: BMEC-like cells are successfully differentiated from hi-PSCs using protocol B 73
Figure 3. 3: Hi-PSCs derived BMECs gender differences 75

Chapter 3: Index of Tables

Table 3. 1: C9-ALS cell lines repeat expansion size 70

3.1. Preface

Amyotrophic lateral sclerosis (ALS), also known as motor neuron disease (MND), is a devastating neurodegenerative condition characterized by the progressive loss of motor neurons (MNs), leading to a deathly muscle atrophy. As reviewed in Chapter 1, genetic factors play a role, with about 10% of cases being familial ALS (fALS), often due to mutations such as *C9ORF72* (C9) repeat expansion (GGGGCC). Additionally, ALS can present with cognitive impairment and frontotemporal dementia (FTD) in some cases, further complicating treatment efforts[12]. As such, addressing the complex spectrum of ALS and improving translation from research to clinical application remain significant challenges in the field.

My research focuses on C9 mutation, based on its dual significance as the primary genetic trigger for ALS and its association with FTD. Moreover, given the increasing research interest in blood-brain barrier (BBB) dysfunction in dementia, exploring the impact of this mutation on the BBB is particularly relevant. Although studies investigating the effects of *SOD1* mutations on BBB dysfunction exist, they often utilize different modelling approaches, underscoring the need for comprehensive investigation across various genetic mutations[89].

Transgenic rodents expressing human *SOD1* mutations exhibit a compromised BBB characterised by increased permeability, enlarged astrocytic end-feet, and disrupted basement membrane (BM), resulting in oedema and microbleeds. This phenomenon mirrors observations in ALS patients. The early breakdown of the BBB may manifest as cerebral microbleeds, a common occurrence in Alzheimer's disease (AD), hinting at a potential link between BBB dysfunction and neurodegeneration[89,90].

C9 mutation carrier phenotype exhibits wide heterogeneity, with conflicting evidence on the impact of repeat expansion size[91]. Hence, I explored 5 different C9-ALS patients' cell lines (Table 2. 2 and Table 3. 1) with 'GGGGCC' repeat expansion size of about 800 repeats for ALS 1, ALS-2, ALS-3[92] -as reported by Sareen et al. 2013- and ALS-4, and over 1200 repeats for the remaining ALS-5, as shown in Figure 3. 1[93–95]. While the toxicity of astrocytes towards MNs in ALS is well-documented[65,96], their impact on brain endothelial cells (BMECs) remains widely unexplored, raising questions about their influence on interactions at the BBB.

Additionally, the specific attributes of C9-ALS BMECs and their effects on astrocytes, pivotal components at the BBB; and MNs remain entirely unknown[26].

Table 3. 1: C9-ALS cell lines repeat expansion size

Cell line	ID	'GGGGCC' repeat expansion size
CS52iALS-C9nxx	ALS-1	~800
CS29iALS-C9nxx	ALS-2	~800
CS28iALS-C9nxx	ALS-3	~800
ALS-183	ALS-4	>1200
ALS-78	ALS-5	~800

C9ORF72 amyotrophic lateral sclerosis (ALS) cell lines expansion size information is detailed in the table above.

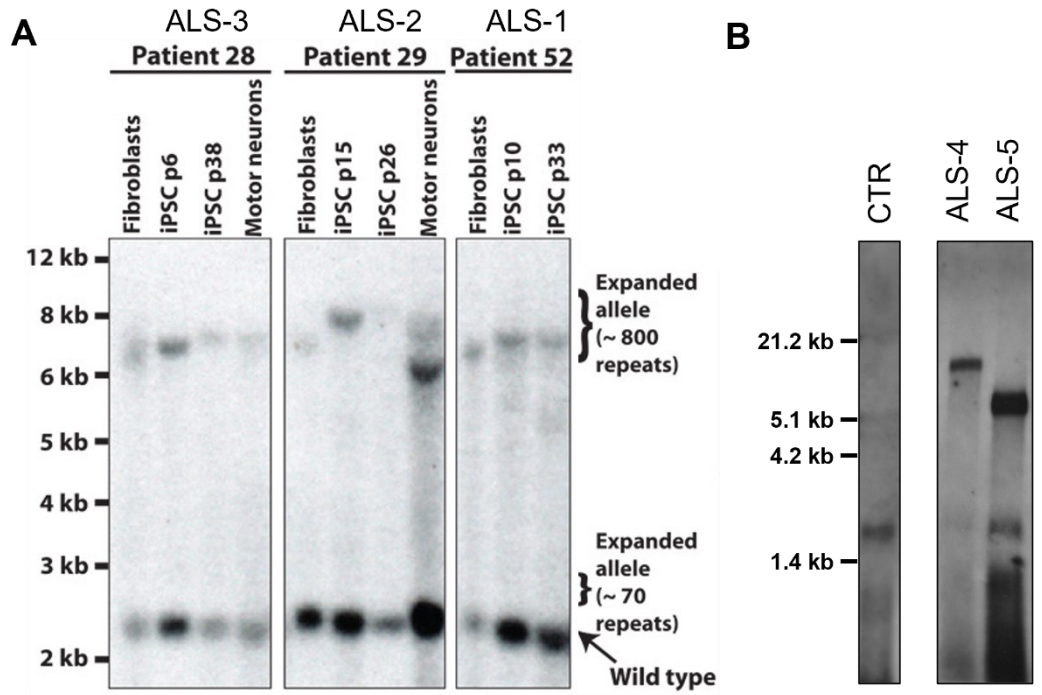

Figure 3. 1: *C9ORF72* repeat sizing via Southern Blotting

A) Examination of hexanucleotide repeat ('GGGGCC') lengths in various cell cultures (fibroblasts, pluripotent stem cells - iPSCs- and motor neuron) for ALS-1, 2 and 3 cell lines by Southern blot analysis, showing somatic instability of the repeat with both expansion (iPSCs in lines 28i,29i,52i – ALS-3, 2 and 1 respectively) and contraction (motor neurons in iPSC line derived from patient 29). Passage numbers for iPSCs are shown (p). This figure is extracted from Figure 1, panel c, Sareen et al. 2013.

B) Estimation of repeat size was performed using the DIG-labelled markers, adapted from previously published protocols (Buchman et al. 2013 and Suh et al. 2015). To convert from kilobase pairs (kb) to repeat length, the enzyme flanking regions were first subtracted and the value was divided by 6 to reflect the hexanucleotide repeat expansion ('GGGGCC'). The utilised Southern blot protocol is unable to detect the normal *C9ORF72* allele (Beck et al. 2013). The data was graciously provided by Chloé Moutin to our laboratory at the University of Sheffield.

3.2. Hypothesis and Aims

Based on the review of the literature performed in Chapter 1, we hypothesized that:

***C9ORF72* mutations affect the function of cells involved in the BBB, thus leading to permeability defects, and causing BBB disruption.**

This led to the following aims:

1. To develop a fully adult human-derived *in vitro* BBB model.
2. To assess BBB dysfunction in the context of C9-ALS.
3. To evaluate the role of the different cellular components of the BBB in relation to BBB dysfunction and neurotoxicity.

3.3. Results

3.3.1. BMEC-like cells are successfully differentiated from hi-PSCs

As mentioned previously, the research performed by Lippmann and colleagues has resulted in a few protocols that can be utilized to obtain human BMEC-like cells from hi-PSCs. Hence, my first objective was to identify which protocol would lead to the purest and most reliable source of human BMEC-like cells.

Through literature assessment, I narrowed down my tests to two protocols, both from the Lippmann team[54,69]. First of all, a BMEC-like cells monolayer was produced following and optimising specific steps in the existing protocols published by Lippmann[54,69,97,98]. One initial required adjustment was the identification of the optimal seeding density, which varies for each cell line and depends on the cell line growth capacity. To optimise this step, I tested seeding density ranges at day 0 of differentiation, from 7.8 to 13 thousand cells/cm^2 but on day 7 (0.875, 1 or 1.15 million cells/cm^2). Finally, a high density of 1 million cells/cm^2 yielded the highest purity and differentiation rate into BMEC-like cells (see Chapter 2, 2.1.2.2 protocol B and 2.2.1.1 for details).

Secondly, after completing BMEC-like cell differentiation following protocol A and protocol B (as described in Chapter 2, 2.1.2.2), I compared the transcriptional expression of endothelial (*OCLN*[99], *CLDN5* [100]), neurovascular (*NEST*[101,102]) and neuroectodermal (*PAX6*[103]) markers, as well as pluripotency markers (*POU5F1*[104]) in hi-PSC-derived BMEC-like cells from protocols A and B. Hi-PSCs are the negative control and human umbilical vein endothelial cells (HUVECs) as the positive control (see Figure 3. 2).

The results supported that both protocols were suitable, as they both led to the production of cells that expressed high levels of BMEC-like cell markers (*OCLN*, *CLDN5*) and significantly low expression of pluripotency markers (*POU5F1*). Protocol B, however, was selected to continue the study for multiple reasons: 1. The RNA expression of *CLDN5*, a key marker of BMEC-like cell differentiation, was higher in BMEC-like cells from protocol B than A, even in comparison to HUVECs, our positive control (see Figure 3. 2). The neurovascular marker *NEST* presented a higher tendency to increase in BMEC-like cells from protocol B compared to A; 3. Protocol B offered a good quality BMEC-like cells monolayer in a shorter period, presenting time and economic advantages. Therefore, protocol B was implemented in all future experiments.

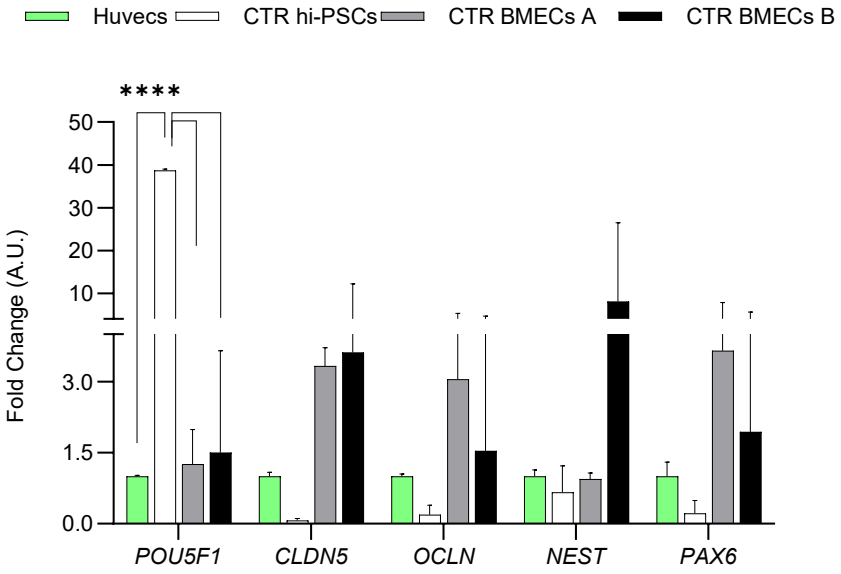

Figure 3. 2: BMEC-like cells are successfully differentiated from hi-PSCs using protocol B

Cells were collected before the differentiation as control human induced pluripotent stem cells (CTR hi-PSCs) and at the end (CTR BMEC-like cells A for protocol A and CTR BMEC-like cells B for protocol B). RNA change expression was quantified by qRT-PCR for the following genes: *POU5F3*: Oct-4; *CLDN5*: Claudin-5; *OCLN*: Occludin; *NEST*: Nestin; *PAX6*: Paired box 6. Data were analysed by multiple comparison two-way ANOVA and plotted as mean ±SD, biological n = 3, technical repeats = 3. See Chapter 2, 2.1.2.2 for a more detailed protocol and Table 2. 12 for primers details.

Once the differentiation protocol was established, BMEC-like cells from different healthy donors were differentiated (CTR-1 and CTR-2, see Chapter 2, Table 2. 2) and BBB morphology and functional characteristics were tested to establish a baseline to compare the ALS BMEC-like cells. In addition to the markers used for the comparison between protocol A and B, I assessed by qRT-PCR the expression of some genes that were expected to be expressed or suppressed at the end of BMEC-like cell differentiation compared to the hi-PSC of origin. We anticipated increased expression of:

1. Junctional proteins:
    - Tight junctions (TJs) such as Claudin-5 (*CLDN5*), Occludin (*OCLN*) and ZO-1 (*TJP1*)
    - Adherens junctions (AJs) e.g., VE-cadherin (*CDH5*).
    - Junctional adhesion molecules e.g., Jam2 (*JAM2*).
2. Transporters:
    - ATP-binding cassette (ABC) efflux transporters: as P-glucoprotein (*ABCB1*).
    - Solute carrier transporters: including glutamate transporter EAAT3 (*SLC1A1*), and to a lesser extent EAAT2 (*SLC1A2*) and EAAT1 (*SLC1A3*), which are mainly expressed by astrocytes.
3. Receptor-mediated transcytosis receptors: e.g., insulin (*INSR*), RAGE receptor (*AGER*).
4. Signalling molecules and regulators of BBB permeability such as TFG-β1 (*TFGB1*).
5. And downregulation of the pluripotency marker Oct4 (*POU5F1*).

Chapter 3: *C9ORF72* Patient-Derived Endothelial Cells Drive Blood-Brain Barrier Disruption and Contribute to Neurotoxicity in a Multicellular *In Vitro* Model

This research chapter of my thesis addressing the BBB impairment in a *C9ORF72* hi-PSC derived model was published on the 11th of April 2024 in the journal Fluids and Barriers of the CNS, EISSN 2045-8118, 7.3 Journal Impact Factor, Q1 by Journal Citation Reports 2022. The article titled "*C9ORF72* patient-derived endothelial cells drive Blood-Brain Barrier disruption and contribute to neurotoxicity" is included as Annex 2.

3.3.2. Comment on gender differences for the healthy cell lines

The BMEC-like cells were successfully obtained for two control cell lines and five C9-ALS patient-derived cells (Table 2. 2). To highlight the main results, three C9-ALS donors were used, ALS-1, ALS-2 and ALS-3. All the three patients have a similar age, repeat expansion size and same gender, male. However, CTR-1 is a male, but CTR-2 is a female. This might explain the differences I noticed between both healthy controls for some gene expressions i.e., *ABCB1*, *CDH5*, *CLDN5*, *JAM2*, *OCCL*, *SLC1A1-3* and *TGFB1* (Figure 3. 3).

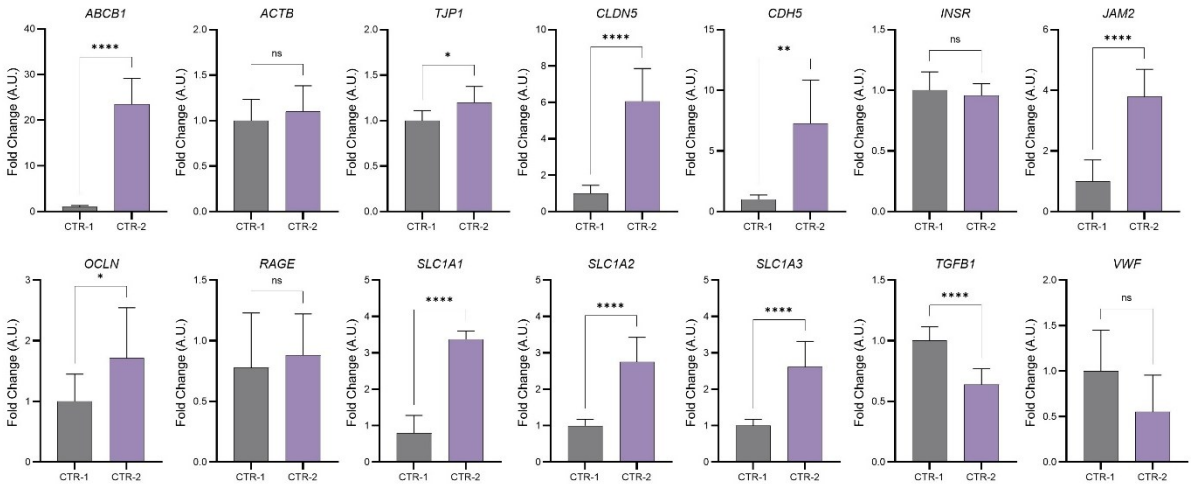

Figure 3. 3: Hi-PSCs derived BMECs gender differences

Brain endothelial (BMEC)-like cells were collected on day 9 of differentiation and the gene expression was quantified by quantitative real-time PCR (qRT-PCR). Data is plotted as Mean ± SD. N = 3, technical = 3. Statistical significance was determined using individual t-tests. CTR-1: male and CTR-2: female.

Some research has been done to investigate the sex differences among the drug transport to the brain, for example by the *ABCB1* or p-glycoprotein transporter[105]. There is controversy, especially when comparing different research models. Additionally, there is evidence that sex hormones affect the activity of p-glycoprotein, and its activity may vary across the menstrual cycle[106]. Regarding the solute carrier transporters family, *SLC1A1*, *SLC1A2*, *SLC1A3*; all of them appear to be upregulated in the female control or CTR-2. Then, *CDH5* or VE-Cadherin, which is involved in the control of vascular permeability, was found to be upregulated in CTR-2 as well. Again, there are proven sex differences in CDH5 expression, which might explain my results[107]. Similarly, *OCLN* or Occludin is upregulated in the female compared to the male control (CTR-1).

Interestingly, *JAM2* is highly expressed in CTR-2 ($p < 0.001$). JAM is involved in paracellular permeability and leukocyte extravasation across the BBB, although the functions of JAM are still largely unknown[108]. As a matter of fact, there are not many publications exploring JAM expression and sex differences. However, a previous study reported upregulation of many TJs and other BBB markers, including JAM in a BBB female mouse model[109]. Clearly, more research needs to be done on this matter.

Lastly, *TGFB1* and *VWF* were found to be down- and upregulated accordingly in the female patient. The inhibition of the transforming growth factor beta 1 or TGFB1, has been explored as a potential therapeutic to reduce BBB permeability, thus by increasing the expression of TJs as Claudin-5[110] .

In essence, due to obvious differences between CTR-1 and CTR-2, and considering all ALS patient cell lines are male, CTR-1 will be used when comparing healthy individuals versus patients (see Annex 2).

Although this is a potentially interesting observation, the differences among CTR-1 and CTR-2 might be interpersonal and not gender related. A larger number of cell lines are needed to establish a more solid hypothesis on this matter.

3.4. Discussion

In vivo models recapitulate the BBB vascular complexity and are a great tool for research. However, it is essential to recognise the differences between rodents and humans, encompassing brain metabolism, vascular haemostasis, cell-to-cell interactions within the neurovascular unit (NVU), and species-specific transporter expression[111].

The ethical and legal considerations associated with *in vivo* studies have strengthened the use of *in vitro* models whenever feasible. These models involve primary or immortalised animal-derived cells from sources such as mice or non-human primates, with applications in BBB characterisation and drug testing. However, translating findings from animal models to human clinical studies is complex due to interspecies differences[112].

Consequently, significant efforts have been directed towards developing human *in vitro* models in the last two decades. Often, BMECs are co-cultured with other NVU components, like astrocytes or pericytes, to simulate *in vivo* interactions. The conventional approach involves seeding BMECs as a flat monolayer. For BBB permeability or transport studies, BMECs are often cultured on a transwell insert, allowing assessment of TEER measurements, tracer permeability, and sampling. Attractively, BMEC monolayers can be co-cultured with other NVU cells, such as astrocytes, in a transwell model. Nevertheless, microfluidic models are gaining attraction due to their ability to recreate blood flow between the body and the brain. These models, like organ-on-a-chip or dynamic BBB models, simulate physiological conditions *in vitro*. Yet, they are complex, labour-intensive, and costlier than transwell approaches[113].

For my PhD project, I aimed to develop a human-derived *in vitro* BBB model. Given the pivotal roles of BBB in the central nervous system (CNS) in health and disease, an *in vitro* BBB model is a valuable research tool. BBB dysfunction is well-known in neurodegeneration, including ALS. While BBB impairment in ALS is evident in cases with mutant *SOD1*, little is known about the C9-ALS patients, the most common genetic cause of familial and sporadic ALS/FTD dementia[114].

I hypothesise that *C9ORF72* mutations impact BBB cell function, leading to permeability defects and disruption. Therefore, my aims were: to create a fully human-derived in vitro BBB model and to assess BBB dysfunction in the context of *C9ORF72* ALS.

Developing a model that replicated the human BBB functionality was the main challenge. Considering the potential of hi-PSCs, I chose to use them for modelling the BBB. These cells offer limitless clinically relevant cells and can be derived from any individual, facilitating personalised medicine strategies.

Various approaches were explored for BBB modelling, and I opted for a co-culture system in a transwell. Despite difficulties in establishing multicellular models, this approach allowed for studying cell interactions and barrier permeability.

Nevertheless, generating a hi-PSCs-BBB *in vitro* model might be challenging. This is why an extensive literature search on handling and purifying BMEC-like cells was made and previously published protocols were tested in our experimental setting[115–122] (Abbott, Azarin, Cicchetti, Daneman, Ghersi-Egea, Lippmann, Shusta, Stebbins; among others).

The protocols from the Lippmann team have been previously validated and applied to various cell lines, yet genomic and cell morphology analysis was not performed. However, classic endothelial markers (i.e., *CLDN5* and *OCLN*) gene expression was quantified when comparing the protocols defined as A and B. Gene expression was analysed at the beginning of the differentiation, when subculturing and when collecting the BMEC-like cell at the end of the process. No major differences were found among both protocols, thus protocol B[69] provided a good quality BMEC-like cells monolayer in a shorter period than A[54,68,97], presenting also economic advantages. Moreover, promising results regarding TEER properties for protocol B were highly referred to by Neal et al. 2019[123].

Considering the use of different collagen isoforms by others, the adequacy of those was also tested by measuring RNA data expression of endothelial markers. The results suggested that there are no significant differences when using either rat tail collagen (collagen I) or collagen derived from the human placenta (collagen IV).

As mentioned above, variability in hi-PSCs is a fact, and these dissimilarities may be inherited from donor somatic cells or arise during reprogramming or culturing, which can affect the differentiation properties of the cell lines, as reviewed by Liu et al. 2019[124]. As a quality control measure, cell density was checked and adjusted in every hi-PSC derived cell line, as described in Chapter 2.

The results demonstrated successful differentiation of BMEC-like cells from hi-PSCs using the chosen protocol. It yielded cells expressing key BBB markers and exhibiting functional characteristics. Hence, this differentiation protocol was applied to interrogate the effects of the C9 mutation on BMEC-like cell morphology and function in a C9-ALS model.

As discussed in my research paper (Annex 2), the data for the C9-ALS model suggest the following:

1. Altered Gene Expressions and Compromised Barrier Integrity:

This study reveals altered gene expressions and compromised barrier integrity in BMEC-like cells derived from C9-ALS mutated hi-PSCs. This observation underscores the crucial role of the BBB in maintaining brain homeostasis and highlights the potential contribution of BBB dysfunction to the pathogenesis of C9-ALS. The altered gene expressions could suggest molecular mechanisms underlying the disruption of barrier integrity and warrant further investigation into the specific genes involved. Additionally, elucidating the mechanisms by which the *C9ORF72* mutation influences BBB integrity can provide valuable insights into disease progression and potential therapeutic targets.

While animal models of C9-ALS have indicated downregulated TJs, my study identifies upregulation of many TJ-related genes in C9-ALS BMEC-like cells, including *CDH5* (VE-Cadherin), which plays a role in endothelial adherens junction assembly. *TJP1* (ZO-1) and *CLDN5*, crucial BBB components, display higher mRNA levels in C9-ALS BMEC-like cells, despite reports of their downregulation in other

models[26]. Notably, transporters and receptors relevant to BBB function, including P-glycoprotein, *SLC1A3* (EAAT1), *SLC1A2* (EAAT2), *SLC1A1* (EAAT3), and *INSR* (Insulin Receptor), are also overexpressed in C9-ALS BMEC-like cells. On the other hand, the upregulation of P-glycoprotein raises questions about its role in drug delivery and multidrug resistance observed in various diseases, including ALS. EAATs, critical for glutamate transport and implicated in neurodegenerative disorders, had upregulated mRNA expression in C9-ALS BMEC-like cells, potentially contributing to glutamate-induced excitotoxicity observed in ALS. Whereas many genes are upregulated in C9-ALS BMEC-like cells, *SLC2A1* (Glucose transporter-1 or GLUT1) protein expression remains consistent between healthy and patient-derived cells.

2. Impact of ALS Patient-Derived iAstrocytes:

This research further explores the impact of C9-ALS astrocytes on BMEC-like cells. Co-culture experiments reveal that C9-ALS iAstrocytes exacerbate barrier leakiness, as indicated by reduced TEER. The release of toxic factors from C9-ALS BMEC-like cells, along with the impact of C9-ALS iAstrocytes, may contribute to the disruption of BBB dynamics and integrity. Interestingly, the addition of C9-ALS iAstrocytes conditioned medium upregulates GLUT1 total expression for both healthy and C9-ALS BMEC-like cells. Nevertheless, Claudin-5 protein expression decreased upon the addition of C9-ALS iAstrocytes conditioned medium in C9-ALS BMEC-like cells. Thus, together with the diminished TEER in the C9-ALS context in our model, might indicate a failure in the BBB dynamics. As suggested previously, the controversy of upregulated mRNA expression and downregulated protein for Claudin-5 might be explained by a cell compensatory mechanism to balance the low protein production by increasing the transcriptomic gene expression.

The disruptive influence of C9-ALS patient-derived iAstrocytes on BBB function is a remarkable finding, even if expected. Astrocytes are known to play a pivotal role in maintaining the integrity of the NVU, and their interaction with BMECs is essential for proper BBB function. My results suggest that C9-ALS iAstrocytes may contribute to BBB dysfunction, potentially by affecting TJ proteins or other critical components, such as key transporters. This highlights the complex cellular interactions within the NVU and raises questions about how astrocyte dysfunction could be targeted for therapeutic interventions.

3. Energy homeostasis:

Interestingly, mitochondrial respiration is altered in C9-ALS BMEC-like cells, illustrated by a notable decline in basal glycolysis and a simultaneous rise in basal and ATP-linked respiration in C9-ALS BMECs, thus, suggesting potential disruptions in glucose metabolism, as shown by alterations at the GLUT1 protein levels, and energy homeostasis, consistent with previous research associating *C9ORF72* with mitochondrial function[125].

4. Neurite Length Reduction and Neuronal Consequences:

Moreover, C9-ALS BMEC-like cell-conditioned medium demonstrates toxicity towards MNs, resulting in a significant reduction in neurite length of 94%. The neurites detriment observed in response to C9-ALS BMEC-like cells medium suggests that BBB dysfunction could have downstream effects on neuronal health and connectivity. Further investigations should focus on the molecular signals that mediate this effect.

5. Implications for ALS Pathogenesis and Therapeutic Strategies:

While I acknowledge the limitations of this study, including the relatively small sample size, the gender imbalance and the relatively limited mechanistic insight, it nonetheless represents a pioneering effort to dissect the intricate relationship between the BBB and ALS, specifically in the context of the *C9ORF72* mutation, where no multi-cellular models are available (to our knowledge). The altered barrier integrity, molecular changes, and neuronal consequences observed in this research provide compelling evidence for considering the BBB as a potential target for therapeutic interventions in ALS and certainly warrant further examination.

To conclude, my research explores the dysfunction of the BBB in the context of *C9ORF72* mutations, a prevalent genetic cause of ALS. By using hi-PSCs, I developed a BBB model and thoroughly assessed gene expressions and barrier integrity. Unexpectedly, we discovered that TJ genes are upregulated in C9-ALS cells, contrary to previous findings in *SOD1* murine models. Through co-culture and conditioned-media experiments, it was unveiled that C9-ALS iAstrocytes worsen barrier leakiness, affecting Claudin-5 and GLUT1 expression. Additionally, my research revealed that conditioned medium from C9-ALS BMEC-like cells has a toxic impact on MNs, leading to severe neurite length reduction. These insights provide fresh perspectives on BBB changes in C9-ALS, underscoring the vital role of BBB dysfunction in neurodegenerative conditions.

Chapter 4: A *MECP2*-Linked Mutations Blood-Brain Barrier Human-Derived *In Vitro* Model: a Valuable Resource for Researching Rett Syndrome Dynamics and Therapeutics

Chapter 4: Contents

4.1. Preface 84
4.2. Hypothesis and Aims 84
4.3. Results 85
4.3.1. Juvenile and RTT-derived BMEC-like cells are successfully differentiated from hi-PSCs 85
4.3.2. MECP2-RTT BMEC-like cells monolayer displays functional abnormalities 86
4.3.3. MECP2-RTT iAstrocytes conditioned medium is toxic to BMEC-like cells 89
4.3.4. MECP2-RTT BMEC-like cells display metabolic defects 90
4.3.5. MECP2-RTT iAstrocytes interfere with the endothelial barrier's dynamics and permeability 91
4.3.6. MECP2-RTT BMEC-like cells conditioned medium is non-toxic towards healthy neurons 94
4.4. Discussion 96

Chapter 4: Index of Figures

Figure 4. 1: MECP2-RTT BMEC-like cells display altered gene expression of key functional markers 87
Figure 4. 2: MECP2-RTT BMEC-like cells transcriptomic profile varies in a mutation-linked way 88
Figure 4. 3: MECP2-RTT BMEC-like cell lines form a leaky barrier 89
Figure 4. 4: MECP2-RTT iAstrocytes conditioned media is toxic but does not affect overall expression of key functional markers.....90
Figure 4. 5: MECP2-RTT BMEC-like cells have an upregulated mitochondrial respiration 91
Figure 4. 6 MECP2-RTT iAstrocytes affect the endothelial barrier's permeability 93
Figure 4. 7: MECP2-RTT BMEC-like cells are non-toxic to neurons 95

Chapter 4: Index of Tables

Table 4. 1: Rett Syndrome cell lines clinical information.....85

4.1. Preface

Rett Syndrome (RTT) is a predominately female neurodevelopmental disorder mainly caused by mutations in the *MECP2* gene (95 % of cases of typical RTT) located on the X chromosome (MECP2-RTT). *MECP2* acts as a transcriptional regulator through the interpretation of two epigenetic markers, DNA methylation and histone acetylation. Its correct function is required for proper neuronal development[126].

MECP2 influences neuronal differentiation, maturation, and synaptic plasticity. Mutations in *MECP2* lead to a spectrum of phenotypes, from mild to severe. Initially, disease severity was linked to the location, type, and severity of the *MECP2* mutation and X chromosome inactivation (XCI). However, factors beyond XCI, such as other genetic variations (e.g., *CDKL5* and *FOXG1* genes), and environmental elements, may play significant roles in shaping the RTT phenotype[32].

Individuals with RTT experience various neurovascular complications alongside neurological deficits. These include altered cerebral blood flow regulation, vascular endothelial dysfunction, and disruptions in neurovascular coupling - crucial for maintaining brain function. Additionally, RTT patients face increased risks of stroke-like episodes and seizures, potentially exacerbated by vascular abnormalities. However, little is known about the blood-brain barrier (BBB) in RTT patients. Understanding the neurovascular involvement is crucial for developing effective therapeutic strategies[3].

4.2. Hypothesis and Aims

As reviewed previously (Chapter 1), impairment in the BBB is a common feature in both neurodevelopmental and neurodegenerative pathologies, such as RTT and amyotrophic lateral sclerosis (ALS). However, the BBB is an often overlooked aspect in many disorders.

In the last year of my PhD project, I have focused on developing a MECP2-RTT BBB human-derived *in vitro* model. Through the Fulbright Spain pre-doctoral fellowship, I had the opportunity to visit a top research institute in the field, the Nationwide Children's Hospital in Columbus, OH.

As described in Chapter 3, RTT research is mainly developed on animal models. However, my project is aligned with the ongoing endeavour to minimise the use of animal models whenever feasible. Instead, I aim to replicate specific human molecular features that may differ across species, thus contributing to a more accurate representation of BBB dynamics in a human-derived *in vitro* model.

As mentioned in Chapter 1, there is evidence for cerebral blood flow dysfunction in RTT, but no study has focused on BBB dysfunction specifically. While *MECP2* is the most known genetic cause of RTT, the disorder is complex and multifactorial in nature. Hence, we decided to use cells donated from four patients with a range of different mutations and phenotype severity.

Therefore, I hypothesized that:

RTT-related mutations affect the function of cells involved in the BBB, thus leading to permeability defects, and causing BBB disruption, in a mutation-specific manner.

This led to the following aims:

1. To develop a fully human-derived *in vitro* BBB model to model paediatric disorders.

2. To assess BBB dysfunction in the context of MECP2-RTT-linked mutations.

3. To evaluate the role of the different cellular components of the BBB in relation to BBB dysfunction and neurotoxicity.

As mentioned in previous chapters, hi-PSCs can self-renew and be differentiated into any cell type. This feature makes them highly appealing for generating a BBB model. Using the same approach as described in Chapter 3 for ALS, I will use fibroblasts derived from patients carrying *MECP2* mutations (MECP2-RTT) and young healthy individuals to interrogate BBB dynamics in disease.

Briefly, to evaluate my MECP2-RTT BBB model I first checked typical BBB markers, including tight junctions (TJs) and transporters, together with permeability characteristics. Additionally, I studied interactions with other cell types involved in BBB function, such as astrocytes and neurons.

4.3. Results

4.3.1. Juvenile and RTT-derived BMEC-like cells are successfully differentiated from hi-PSCs

In Chapter 3, section 3.2.1, I tested 2 different protocols to obtain hi-PSCs derived brain microvascular endothelial (BMEC)-like cells. Briefly, the results showed that both protocols effectively produced cells expressing high levels of BBB markers (*OCLN*, *CLDN5*) and low levels of pluripotency markers (Chapter 3, Figure 3. 2). However, Protocol B produced a high-quality BMEC-like cell monolayer in a shorter timeframe, thus offering both time and cost advantages.

As outlined in Chapter 1, various *MECP2* point mutations can lead to a spectrum of disease severities. Among the 8 most prevalent mutations impacting MECP2 protein function[127] my focus was on three different point mutations: *R133C* (resulting in a mild phenotype), *R306C* (intermediate severity), and *R255X* (severe), along with a less frequent splicing mutation within *MECP2* intron 1, *c.62+1 del GT* (intermediate severity) (Table 4. 1). Because of the stochastic nature of the X inactivation process, I was able to work with isolated clone lines from the same patient as wild-type controls (isogenic control) and one juvenile control, non-RTT related (CTR-3). For additional genotypic and phenotypic details, thus including the healthy and wild-type cell lines, please refer to Chapter 2, Table 2. 2. All female RTT cell lines were generously provided by the Rett Syndrome Research Trust in the USA, in conjunction with the Coriell Institute for Medical Research.

Table 4. 1: Rett Syndrome cell lines clinical information

Cell line	ID	MECP2 Mutation	Type of mutation	Phenotype	Frequency
RTT 2036	RTT-1	*R133C*	Point	Mild	Common
RTT 2042	RTT-2	*R255X*	Point	Severe	Common
RTT 2047	RTT-3	*R306C*	Point	Intermediate	Common
RTT 2052	RTT-4	*c.62+1 del GT*	Splicing	Intermediate	Rare

Rett Syndrome (RTT) hi-PSCs lines clinical information is summarised in the table. Cell line refers to the company code and ID to the code used in this manuscript. Please refer to Chapter 2, Table 2. 2 for more detailed information.

To ensure the reproducibility of our model, I examined the expression of a set of BBB-related genes and proteins, like the methodology detailed in Chapter 3, section 3.2.1. This investigation encompassed the juvenile control line (CTR-3) and RTT-derived cell lines (WT/RTT 1 to 4). Additionally, transendothelial resistance measurements (TEER) were performed to evaluate the functionality of the cell model.

To summarize the findings and facilitate the results workflow, all data from healthy donors (CTR-3 and WT) were incorporated into the characterization of the model related to the disease, which is detailed in the following section.

4.3.2. MECP2-RTT BMEC-like cells monolayer displays functional abnormalities

RTT-derived hi-PSCs were successfully differentiated towards brain endothelial-like cells (BMEC-like cells), as shown by the expression of key BBB-related genes and proteins (Figure 4. 1).

As described above, 4 MECP2-RTT cell lines (RTT) and isogenic controls (WT) were used for the BMEC-like monolayer characterization; immunostaining showed that they expressed key endothelial proteins such as VEGFA and Claudin-5 with no significant differences when comparing WT vs RTT BMEC-like cells (Figure 4. 1A). Because different cell lines presented slightly different nuclei sizes when observing them under the optical microscope, I measured the BMECs using ImageJ's plugin CellProfiler, but no significant differences were identified (Figure 4. 1A).

Transcripts encoding TJ and adhesion proteins (*CDH5*, *CLDN5*, *OCLN*, *TJP1*); transporters (*ABCB1*, *ABCC1* and *SLC1A1*, *SLC16A1*, *SLC2A1*, *SLC7A5*); key receptors (*INSR*, *RAGE*); vascular (*PLVAP*) and clotting factors (*VWF*) were assessed via RT-qPCR. When analysing each cell line separately, there was no significant difference in gene expression when plotting the fold change over the CTR line (CTR-3) (Figure 4. 1B). In fact, some transcripts, such as *ABCB1* were upregulated or downregulated depending on the patient's cell line. However, when plotting the RNA fold change expression of the RTT BMEC-like cells against the isogenic WT lines, the average data showed an overall dysregulation of most genes when compared to the CTR line (Figure 4. 1B) yet was statistically significant for the genes encoding the glucose transporter *SLC2A1*, the amino acid transporter *SLC7A5* and *VWF* (Figure 4. 1B). Even though the isogenic WT cell lines are derived from different healthy individuals, yet their transcriptomic profiles are similar. Therefore, these were combined to enhance the statistical power during analysis. Next, because of the gene expression difference between the WT line and the CTR line (Figure 4. 1B), I plotted the data against the pooled WT isogenic control (Figure 4. 2) and used these as the control for future experiments.

Additionally, as the 4 different MECP2-RTT lines have different mutations (Table 4. 1), RNA expression was analysed for each cell line separately and was compared to the expression of the two pooled isogenic WT controls, as done previously (Figure 4. 1B). Hence, I could interpret the results in a clearer and mutation-specific way. Thus, showing that the RTT-1 cell line (*R133C* mutation) was the most altered one, with a significant upregulation for all the genes quantified except *ABCB1* (Glucoprotein-P) (Figure 4. 2). Surprisingly, RTT-2 (*R255X*), with a severe disease phenotype, presented fewer dysregulated genes, with downregulated expression of the transporter *ABCC1* only. Additionally, transporter *ABCB1*, TJ VE-Cadherin (*CDH5*) and the insulin receptor (INSR) were the only upregulated transcripts for RTT-2. For RTT-3 (*R306C*), *TJP1* expression was slightly upregulated. Finally, for the

rarest RTT cell line, RTT-4 (*c.62+1 del GT*), with an intermediate disease phenotype, only the transporters *ABCB1* and *SLC7A5* were upregulated.

Notably, the glucose transporter-1 (*SLC2A1*) emerges as the only consistently upregulated target across all patient cell lines, with RTT-2 exhibiting the highest levels (P≤0.0001).

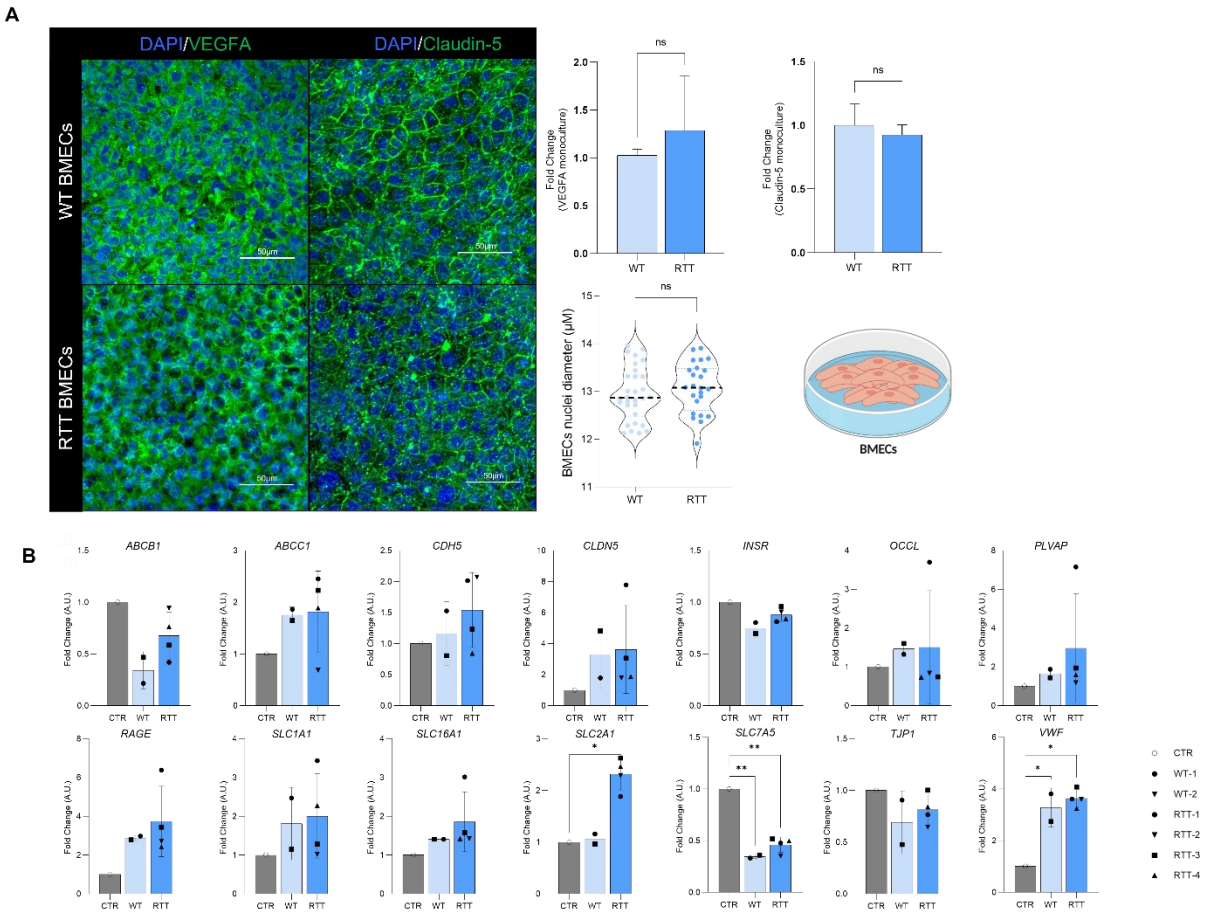

Figure 4. 1: MECP2-RTT BMEC-like cells display altered gene expression of key functional markers

A) Immunocytochemistry of BMEC-like cells differentiated from wild-type (WT) and Rett syndrome (RTT) human induced pluripotent stem cell (hi-PSC) donors. Vascular endothelial growth factor A (VEGFA) and Claudin-5 staining are shown. Images were acquired with a Nikon confocal microscope. Scale bar 50 µm. The protein quantification data are plotted as mean ± S.D. Statistical significance was determined using Student's unpaired t-test (****p < 0.0001), N=3. BMEC-like cells nuclei diameter violin plot. Each dot represents the average size per sample, with a total of 30 and 24 replicates for WT and RTT respectively. Statistical significance was determined by non-parametrical Kruskal-Wallis test (****p < 0.0001).

B) Blood-brain barrier phenotypic markers and transporters. Transcriptomic analysis representing the RNA fold change expression of each wild-type BMEC-like cells (WT-1 and WT-2) and Rett syndrome (RTT) cell lines (RTT-1, -2, -3 and 4) over the control cell line (CTR-3). Glucoprotein-P (*ABCB1*), MRP-1 (*ABCC1*), VE-Cadherin (*CDH5*), Claudin-5 (*CLDN5*), Insulin Receptor (*INSR*), Occludin (*OCLN*), Plasmalemma Vesicle Associated Protein (*PLVAP*), receptor for advanced glycation end products (*RAGE*), EAAT3 (*SLC1A1*), Monocarboxylate Transporter 1 (*SLC16A1*) EAAT2 (*SLC1A2*), L-Type Amino Acid Transporter 1 (*SLC7A5*) Zonula Occludens 1 (*TJP1*), and Von Willebrand factor (*VWF*). Statistical significance was determined using Two-Way ANOVA (****p < 0.0001). N=3. For further information please refer to Chapter 2, Table 2. 1.

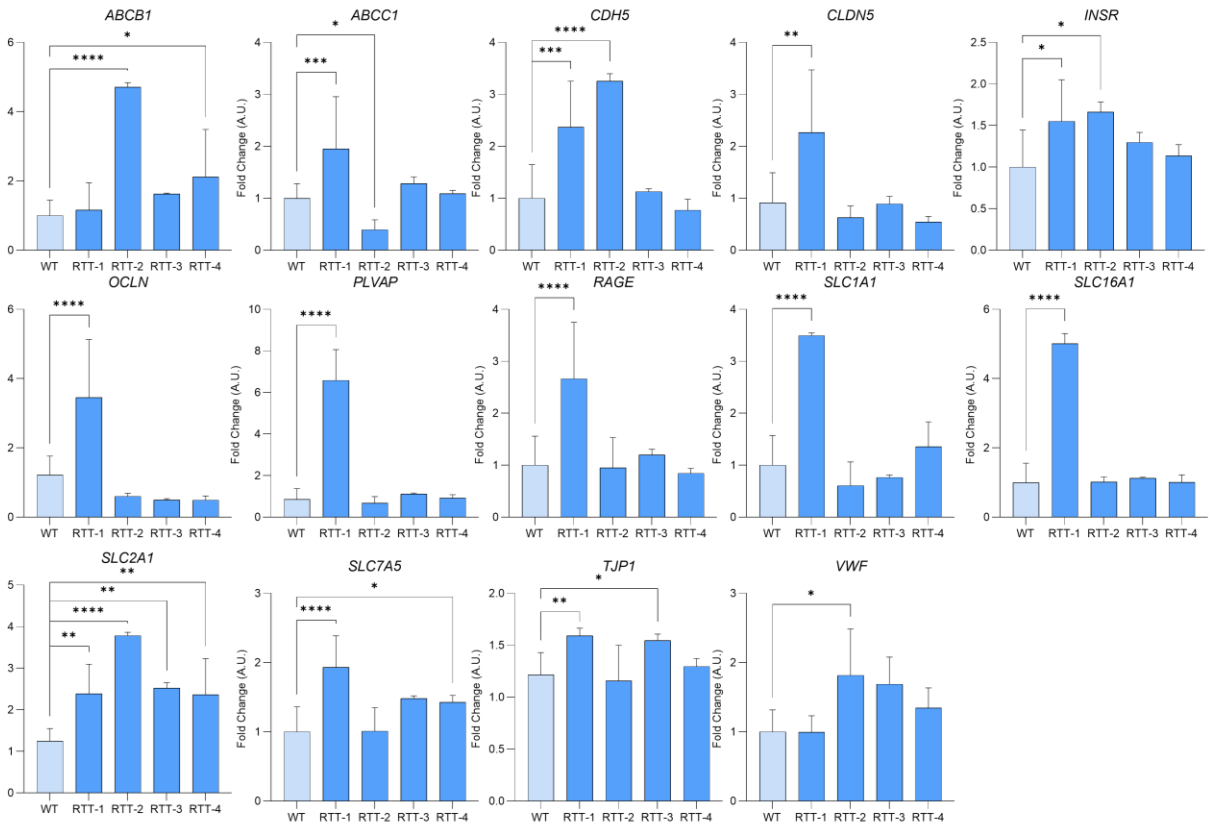

Figure 4. 2: MECP2-RTT BMEC-like cells transcriptomic profile varies in a mutation-linked way

Blood-brain barrier phenotypic markers and transporters. Gene quantification analysis representing the RNA fold change expression of each line over the wild-type BMEC-like cells (WT-1 and WT-2) and Rett syndrome (RTT) cell lines (RTT-1, -2, -3 and 4: *R133C*, *R255X*, *R206C* and *c.62+1 del GT* respectively). Glucoprotein-P (*ABCB1*), MRP-1 (*ABCC1*), VE-Cadherin (*CDH5*), Claudin-5 (*CLDN5*), Insulin Receptor (*INSR*), Occludin (*OCLN*), Plasmalemma Vesicle Associated Protein (PLVAP), Receptor for advanced glycation end products (RAGE), EAAT3 (SLC1A1), Monocarboxylate Transporter 1 (*SLC16A1*) EAAT2 (*SLC1A2*), L-Type Amino Acid Transporter 1 (*SLC7A5*) Zonula Occludens 1 (*TJP1*), and Von Willebrand factor (*VWF*). Statistical significance was determined using One-Way ANOVA (****$p < 0.0001$). N=3.

Another key feature of BMECs is their permeability properties. Similarly to the *C9ORF72* amyotrophic lateral sclerosis (C9-ALS) model, to assess whether these transcriptional alterations were associated with functional dysregulation, the monolayer permeability was tested by TEER measurements. The RTT BMEC-like monolayer appeared visibly intact and macroscopically indistinguishable from the WT (Figure 4. 3A).

The isogenic WT lines displayed high TEER values, comparable to those recorded in healthy adult lines examined previously in Chapter 3. Opposite to what I found for the C9-ALS monolayer, where on day 1 healthy control and C9-ALS BMEC-like cells displayed the same values, the RTT monolayer consistently maintained significantly low TEER values below 150 Ω x cm^2. Interestingly, high TEER values were maintained in the WT lines for three days, with a linear increase, averaging from 2222 to 4822 Ω x cm^2 on the first and third day respectively. Finally, on day 4, the TEER measurement declined below 1000 Ω x cm^2 (Figure 4. 3B), as expected in this cell culture paradigm[128].

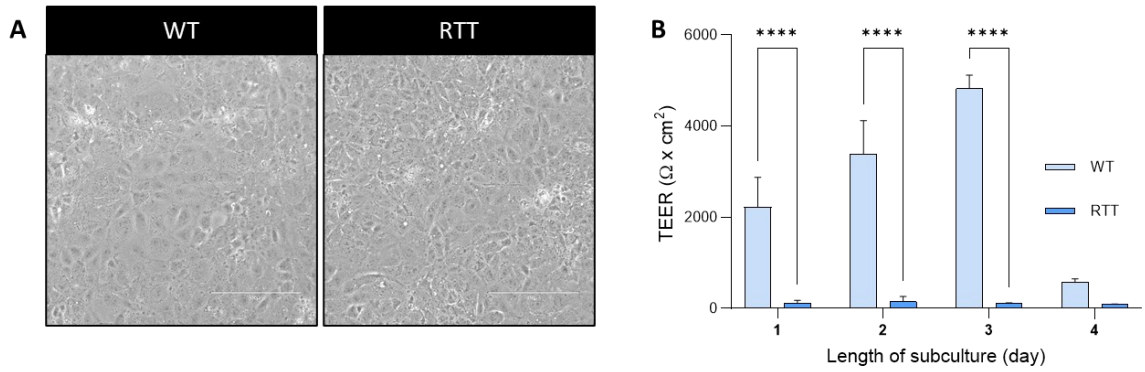

Figure 4. 3: MECP2-RTT BMEC-like cell lines form a leaky barrier

A) Brightfield images are shown as follows wild-type (WT) and Rett syndrome (RTT) BMEC-like cells. The scale bar equals 50 µM.

B) Brain endothelial (BMEC)-like cells passive barrier as shown by transendothelial resistance (TEER) following subculture for WT and RTT monolayers. Error bars represent the standard deviation of triplicate Transwell™ filters. Statistical significance was determined using Student's unpaired t-test (****$p < 0.0001$). N=3.

4.3.3. MECP2-RTT iAstrocytes conditioned medium is toxic to BMEC-like cells

As described in the previous Chapters 1 and 3, astrocytes are essential components of the BBB, as they support BMECs through the secretion of trophic factors and maintain brain homeostasis.

Several studies highlighted the relevance of astrocytes in RTT[129] and *Mecp2* knockout has been shown detrimental to astrocytes[130] as by altered glutamate clearance[131] or shown toxicity towards neurons, thus affecting neurites[132]. Moreover, that study also showed that conditioned medium from healthy astrocytes effectively corrected dendritic branching abnormalities in *Mecp2*-KO neurons in murine models[130].

Additionally, based on my previous research on C9-ALS (Chapter 3), I also wanted to explore the astrocyte-endothelial cellular interaction within the barrier features upon the addition of iAstrocytes conditioned media on juvenile BMEC-like cells. I used the LDH colourimetric assay to determine the media´s cytotoxicity. BMEC-like cells from healthy and patient donors were cultured in monoculture, and then iAstrocyte-conditioned media was added for 48 hours. Plain astrocyte medium-treated BMEC-like cells were used as controls (non-cond iA media).

MECP2-RTT iAstrocyte conditioned medium had a detrimental effect on both WT and RTT BMEC-like cells, as shown by an increase in LDH activity of over 50% and 38% respectively (Figure 4. 4A), in comparison to untreated and healthy astrocyte-conditioned media-treated cells. These results provide evidence that MECP2-RTT astrocyte toxicity extends beyond neurons, affecting other brain cells such as the BMECs.

To further investigate if the toxicity affected the cell dynamics as I reported previously in the context of C9-ALS (Annex2, Figure 3), the BMEC-like cells were incubated with iAstrocyte-conditioned media for 48 h. Subsequently, the protein expression levels of TJ Claudin-5 and glucose transporter GLUT1 were quantified using immunofluorescence. Intriguingly, in contrast to the findings in C9-ALS, neither protein showed alterations following the iAstrocyte-conditioned media treatment (Figure 4. 4B).

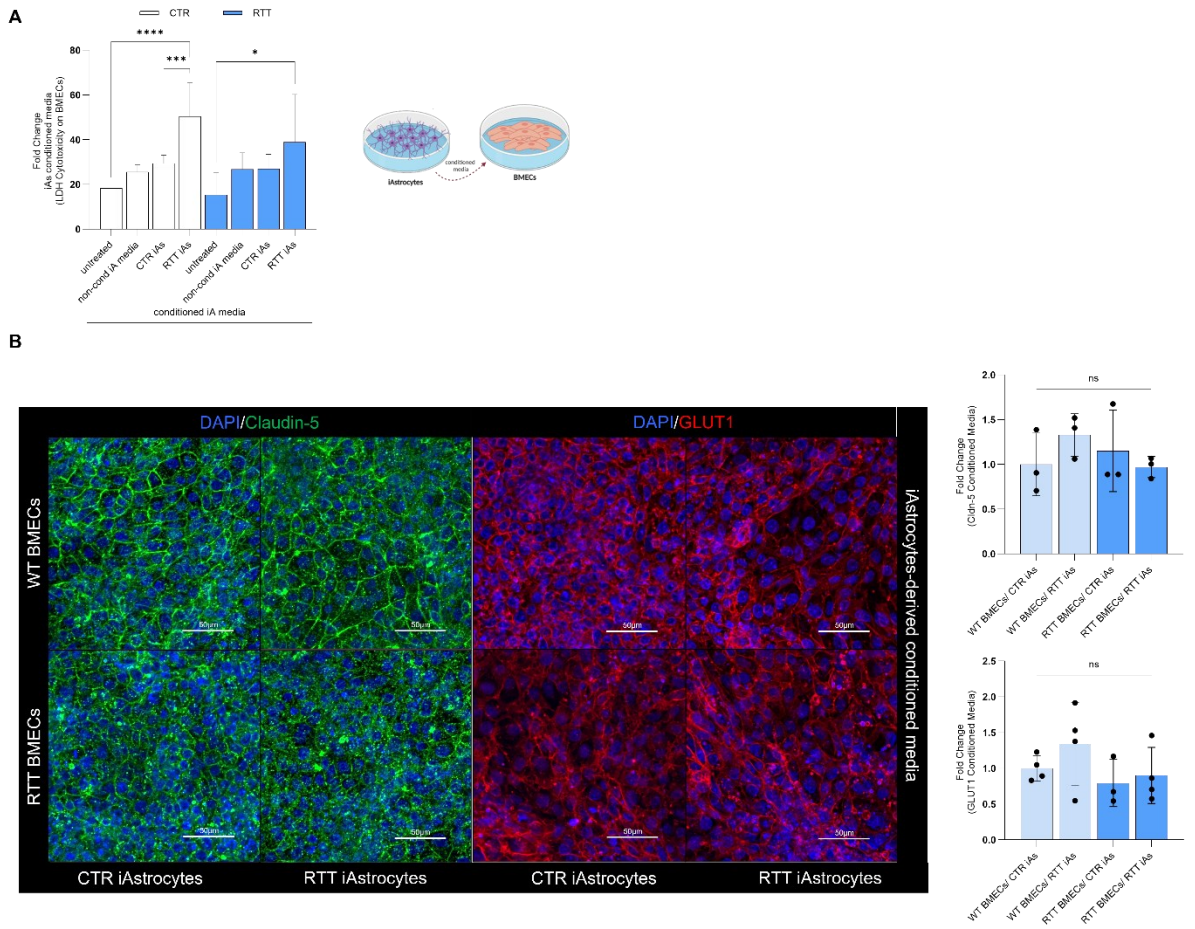

Figure 4. 4: MECP2-RTT iAstrocytes conditioned media is toxic but does not affect overall expression of key functional markers

A) The lactate dehydrogenase (LDH) assay was performed after 2 days of iAstrocytes conditioned media treatment on BMEC-like cells. Untreated refers to BMEC-like cells on their indicated endothelial media and non-conditioned iAstrocyte (non-cond iA) media are BMEC-like cells treated with plain iAstrocytes media to evaluate the effect of the media on the BMEC-like cells. Wild-type (WT) and Rett syndrome (RTT) media. Error bars represent the standard deviation of triplicate wells. Statistical significance was determined using One-Way ANOVA (****p < 0.0001). N=3. The diagram was created on Biorender.com.

B) BMEC-like cells were either co-cultured with WT or RTT-iAstrocytes. BMEC-like cells were fixed in 100% MeOH after 48 h of the experiment. Scale bar equals 50 µM. Plotted results represent confocal image z-stacks analysed in 3D volume. Claudin-5 is shown in green and Glucose-1 transporter (GLUT1) in red; and DAPI in blue for the nuclei staining. Error bars represent the standard deviation of triplicate Transwell™ filters. Statistical significance was determined using One-Way ANOVA (****p < 0.0001). N=3. At least a total of 5 images were acquired per condition, with a minimum of 3 technical replicates for a total of 3 biological replicates (N=3, total images per condition = 45). The diagram was created on Biorender.com.

4.3.4. MECP2-RTT BMEC-like cells display metabolic defects

Despite the clear upregulation of *SLC2A1* transcript encoding GLUT1 (Figure 4. 2), no significant dysregulation was found at the protein level when quantifying by immunofluorescence (Figure 4. 5A). Immunofluorescence quantification, however, is not always indicative of functionality, hence, to further explore the BMEC-like cells metabolism, the metabolic function of WT and MECP2-RTT BMEC-like cells using the Seahorse XF Real-Time ATP Rate Assay in the presence of mitochondria inhibitors was assessed (Figure 4. 5B). Even though the GLUT1 protein was not found to be dysregulated in the patient-derived BMEC-like cells, the data showed that they displayed a significant upregulation in basal respiration, basal glycolysis, and ATP-linked respiration (Figure 4. 5C).

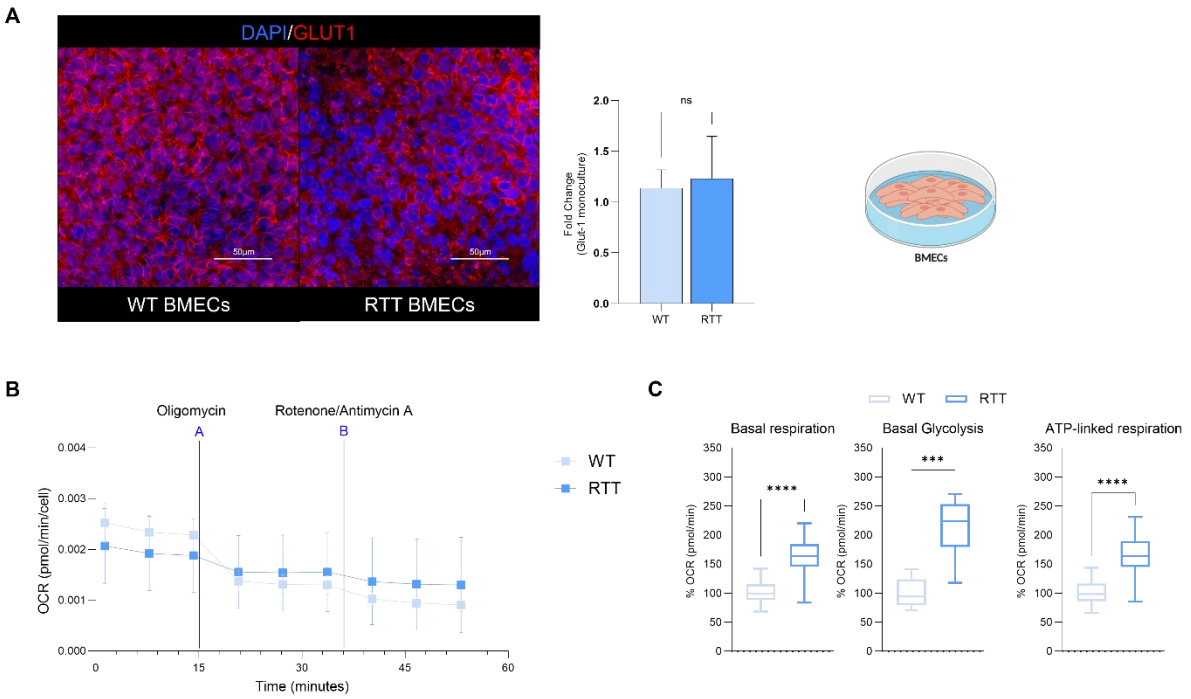

Figure 4. 5: MECP2-RTT BMEC-like cells have an upregulated mitochondrial respiration

A) Wild-type donor human induced pluripotent stem cells (hi-PSCs) derived brain endothelial (BMEC)-like cells (WT BMECs) and MECP2-Rett syndrome donor hi-PSCs derived BMEC-like cells (RTT BMECs) confocal images. BMEC-like cells were fixed in 100% MeOH. Scale bar equals 50 µM. Images and results represent confocal z-stacks analysed in 3D volume. Glucose-1 transporter (GLUT1) in red and DAPI in blue for the nuclei staining. Error bars represent the standard deviation of triplicate Transwell™ filters. Statistical significance was determined using Student's unpaired t-test (****p < 0.0001). At least a total of 5 images were acquired per condition, with a minimum of 3 technical replicates for a total of 3 biological replicates (N=3, total images per condition = 45). The diagram was created on Biorender.com.

B) Mitochondrial Real-Time ATP rate test was carried out on wild-type hi-PSCs derived BMEC-like cells (WT BMEC-like cells), and 4 MECP2-RTT donors hi-PSCs derived BMEC-like cells (RTT BMEC-like cells). Data were acquired and analysed using the Agilent Technologies Sea-horse platform and software. Oxygen consumption rate (OCR) measurement per cell is represented as a time curse. The addition of the mitochondrial drugs Olygomycin (A) and Rotenone/Antimycin A (B) are indicated in the graph.

C) Mitochondrial Real-Time ATP rate test was carried out on wild-type hi-PSCs derived BMEC-like cells (WT BMEC-like cells), and 4 MECP2-RTT donors hi-PSCs derived BMEC-like cells (RTT BMEC-like cells). Data were acquired and analysed using the Agilent Technologies Sea-horse platform and software. Error bars represent the standard deviation of triplicate wells N=3. Data is plotted as Min-Max Box and Whisker. Statistical significance was determined using Student's unpaired t-test (****p < 0.0001).

4.3.5. MECP2-RTT iAstrocytes interfere with the endothelial barrier's dynamics and permeability

The addition of iAstrocytes conditioned media did not induce changes in the protein expression of TJ Claudin-5 or the transporter GLUT1, as evidenced by immunofluorescence analysis (Figure 4. 4B). Nevertheless, the application of RTT-derived iAstrocytes medium had a harmful impact on both CTR and RTT, as shown by the LDH cytotoxicity test (Figure 4. 4A). In monoculture, there were no discernible differences in GLUT1 protein expression Figure 4. 5A); however, the mitochondrial metabolic analysis revealed a significant upregulation in RTT BMEC-like cells. Motivated by these

findings, I delved into investigating the co-culture of iAstrocytes, as prior research suggests their potential involvement in disrupting BBB, consequently leading to increased permeability, and altered dynamics[3] (Chapter 1).

For both WT and RTT BMEC-like cells, coculturing with RTT iAstrocytes reduced the TEER values, indicating compromised endothelial monolayer integrity (Figure 4. 6A). Interestingly, from day 2 onwards, when WT iAstrocytes were added to RTT BMEC-like cells, their TEER values improved, reaching the same values as the WT BMECs/WT iAstrocytes condition after one day of co-culture.

Then, I quantified by immunofluorescence the protein expression of Claudin-5 and GLUT1 the major TJ of the BBB and most expressed glucose transporter respectively. Claudin-5 expression decreased significantly in WT BMECs grown on RTT iAstrocytes when compared to WT BMECs grown on WT iAstrocytes Figure 4. 6B, left). However, no differences were reported in the GLUT1 transporter expression in any of these combinations (Figure 4. 6B, right). For the RTT BMEC-like cells, with an already diminished barrier permeability (Figure 4. 3B and Figure 4. 6A), Claudin-5 expression was severely downregulated and was not rescued by the addition of WT iAstrocytes (Figure 4. 6B, left). Remarkably, despite GLUT1 protein expression was not downregulated in the BMEC monolayer (Figure 4. 5A), the presence of RTT iAstrocytes reduced its expression when measured by immunofluorescence (Figure 4. 6B, right).

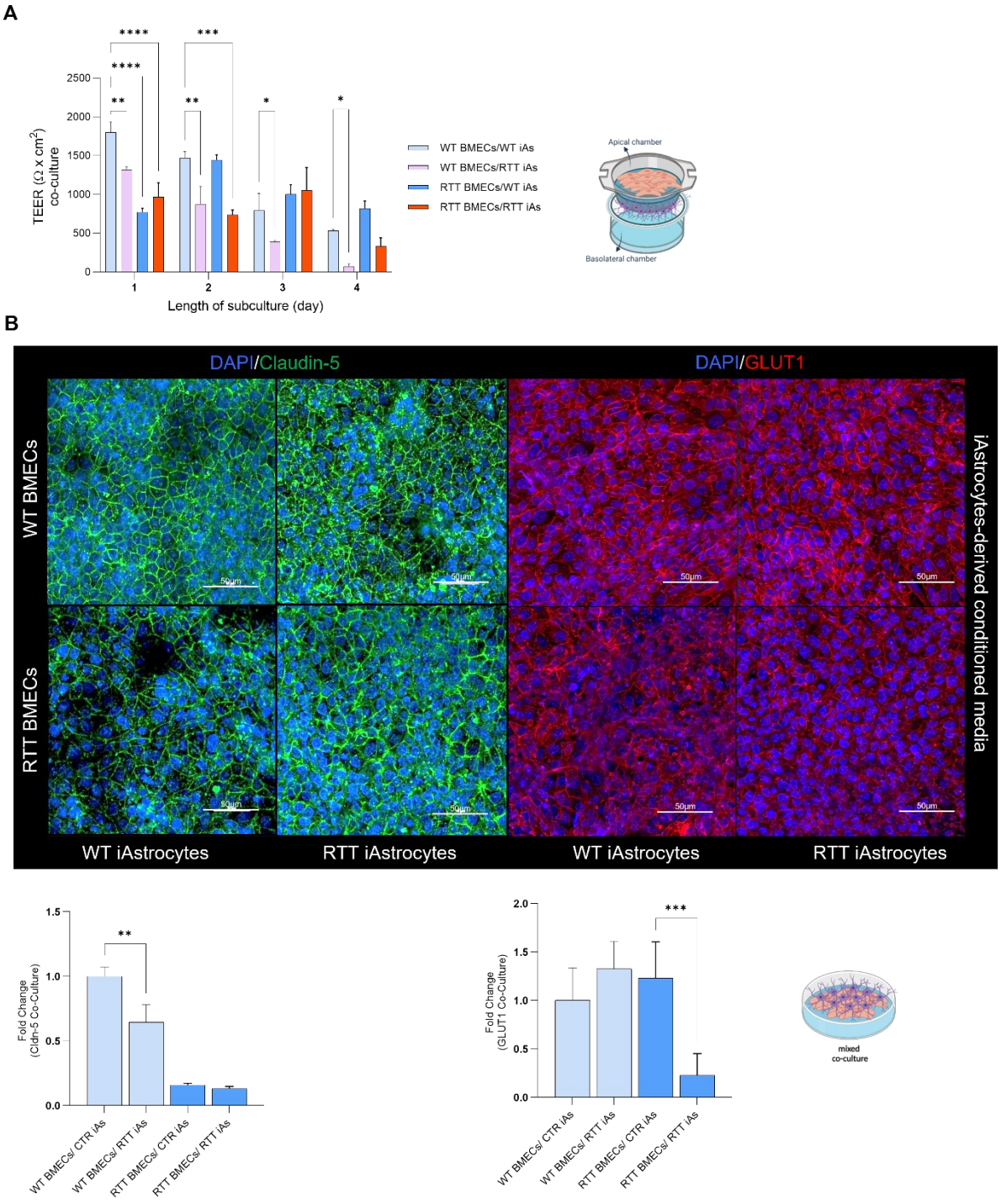

Figure 4. 6 MECP2-RTT iAstrocytes affect the endothelial barrier's permeability

A) BMEC-like cells passive barrier as shown by transendothelial resistance (TEER) following brain endothelial (BMEC)-like cells/iAstrocytes (iAs) co-culture for wild-type (WT) and MECP-Rett Syndrome (RTT) BMEC-like cells and iAstrocytes. Error bars represent the standard deviation of triplicate Transwell™ filters. Statistical significance was determined using One-Way ANOVA (****p < 0.0001). N=3. The diagram was created on Biorender.com.

B) BMEC-like cells were either co-cultured with WT or RTT-iAstrocytes. BMEC-like cells were fixed in 100% MeOH after 48h of the experiment. Scale bar equals 50µM. Plotted results represent confocal image z-stacks analysed in 3D volume. Claudin-5 is shown in green and Glucose-1 transporter (GLUT1) in red; and DAPI in blue for the nuclei staining. Error bars represent the standard deviation of triplicate Transwell™ filters. Statistical significance was determined using One-Way ANOVA (****p < 0.0001). N=3. At least a total of 5 images were acquired per condition, with a minimum of 3 technical replicates for a total of 3 biological replicates (N=3, total images per condition = 45). The diagram was created on Biorender.com.

4.3.6. MECP2-RTT BMEC-like cells conditioned medium is non-toxic towards healthy neurons

After confirming that MECP2-RTT BMEC-like cells exhibit cell-autonomous defects, such as impaired TEER and metabolism, I proceeded to investigate the influence of BMEC-like cells on isogenic control (WT) and RTT iNeurons. To minimise mutation-related confounding effects, I matched the cell lines, deriving both WT and RTT iNeurons as well as WT and RTT BMEC-like cells, from the same patient lines, totalling four lines (Table 4. 1).

Based on previous results, C9-ALS BMEC-like cells were shown to be cytotoxic, when measuring the lactate (LDH) release, as an indicator of cell death (Chapter 3, paper Figure 5A[128]). Moreover, RTT patients are known to display severe cortical neuronal damage, with a progressive loss of the synaptic connections[133]. Thus, I wanted to explore the effect of BMEC-like cells conditioned media on iNeurons. Patient-derived iNeurons are known to develop disease phenotypes, including reduced neurite length[134]. Hence, I used RTT-derived iNeurons to test the effect of BMEC-like cells conditioned media on neurite length. However, as opposed to C9-ALS BMEC-like cells, MECP2-RTT cells did not report toxicity levels compared to the wild-type (Figure 4. 7A).

In murine models, RTT-derived astrocytes have been shown to inadequately support normal neuronal growth. However, contrary to this, the addition of RTT BMEC-like cell conditioned medium did not adversely affect either WT or RTT iNeurons (Figure 4. 7B and C). Moreover, there was no observed increase in, or rescue of, neurite growth upon the addition of WT BMEC-like cell conditioned medium (Figure 4. 7B and C).

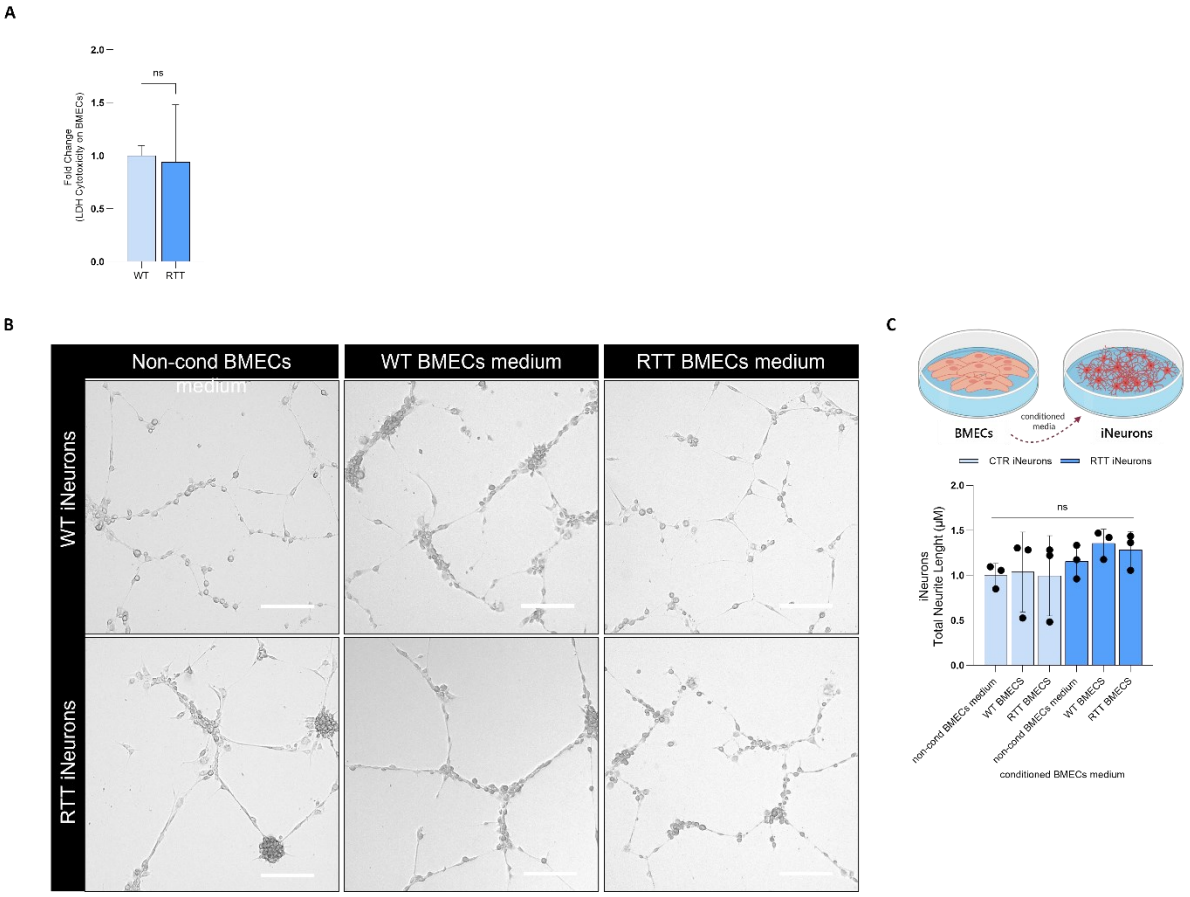

Figure 4. 7: MECP2-RTT BMEC-like cells are non-toxic to neurons

A) The Lactate Dehydrogenase Assay (LDH) assay was performed on 4 wild-type (WT) controls and 4 MECP2-Rett Syndrome (RTT) donors human induced pluripotent stem cells (hi-PSCs) derived brain endothelial (BMEC)-like cells. Statistical significance was determined using Student's unpaired t-test (****$p < 0.0001$).

B) Induced neurons (iNeurons) derived from WTT and RTT fibroblasts were fixed with 4% paraformaldehyde after 72h on 30% BMEC-like cells conditioned media treatment. Brightfield images are shown as follows: non-conditioned BMECs medium, WT BMEC-like cells medium and RTT BMEC-like cells medium treated iNeurons. The scale bar equals 50 µM. At least a total of 5 images were acquired per condition, with a minimum of 3 replicates for a total of 3 biological replicates per cell line (N=3, total images per condition = 45).

C) Neurite length analysis was performed with ImageJ software. Data are plotted as Mean ± SD. Statistical significance was determined using One-Way ANOVA (****$p < 0.0001$). N=3. The diagram was created on Biorender.com.

4.4. Discussion

In the previous Chapter, I highlighted the relevance of *in vitro* models for researching cell-to-cell interactions and dynamics.

In the BBB field, typically, BMECs are co-cultured with other components of the neurovascular unit (NVU), such as astrocytes, to replicate *in vivo* interactions.

The standard approach involves seeding BMECs as a flat monolayer, commonly cultured on a permeable transwell insert. This setup allows for the evaluation of TEER and co-culture experiments.

For this chapter of my doctoral project, I aimed to develop a human-derived *in vitro* model of the BBB with a specific focus on understanding its implications for RTT. Considering the essential functions of BBB in preserving CNS homeostasis and its relevance to a range of neurological disorders, including neurodevelopmental conditions such as RTT, this model is of great importance for research purposes. RTT is caused by mutations in the *MECP2* gene (X Chromosome) and is characterized by severe neurological and cognitive impairments. Hence, understanding BBB dysfunction in this context could provide crucial insights into unknown disease mechanisms and potential therapeutic targets.

Therefore, I hypothesise that RTT-related mutations affect the function of cells involved in the BBB, thus leading to permeability defects, and causing BBB disruption, in a mutation-specific manner. Hence, I developed a MECP2-RTT BMEC-like cells monolayer to investigate transcriptomic and proteomic patterns, alongside interactions with other components of the NVU, including astrocytes and neurons.

Despite the challenges involved in creating a functional and reproducible BBB model, I managed to develop a replicable *in* vitro system capable of investigating both ALS and RTT. As outlined in Chapters 1 and 3, hi-PSCs show significant promise, given their origin from patients, thus facilitating personalized medicine research.

As referenced earlier, generating an *in vitro* model of hi-PSCs-BBB presents significant challenges, as to culturing and maintaining hi-PSCs themselves. Notably, protocols developed by Lippmann[116,123] have been widely validated and successfully applied across all cell lines detailed in Chapter 2, Table 2. 2; 4 wild-types, 4 RTT and 1 control cell line.

The results demonstrated successful differentiation of BMEC-like cells from hi-PSCs using the chosen protocol. It yielded cells expressing key BBB markers and exhibiting functional characteristics. Hence, this differentiation protocol was applied to interrogate the effects of the *MECP2* mutation on BMEC-like cell morphology and function in a MECP2-RTT BBB model.

Henceforth, the data presented suggest the following:

1. Altered Gene Expressions and Compromised Barrier Integrity:

RTT and WT-derived hi-PSCs were successfully differentiated towards BMEC-like cells, as shown by the expression of key BBB-related genes and proteins, together with permeability properties. RTT and WT-derived hi-PSCs were successfully differentiated into BMEC-like cells, showing expression of key BBB-related genes such as Cadherin-5 (*CDH5*) and the *ABCB1* transporter, as well as proteins like Claudin-5 (*CLDN5*). These cells also exhibited permeability properties characteristic of BBB endothelial cells. Immunofluorescence analysis revealed no notable differences in the expression of VEGFA and Claudin-5 proteins between RTT and WT BMEC-like cells. Despite the absence of significant differences at the

translational level for most targets analysed, dysregulation was observed for the *SLC7A5* large neutral amino acids transporter, together with upregulation for the *SLC2A1* (GLUT1) transporter and clotting factor *VWF*.

SLC7A5 was found to be downregulated in both WT and RTT BMEC-like cells compared to the healthy control line. *SLC7A5* downregulation has been linked to a significant increase in the risk of developing autism spectrum disorders (ASD) by others, linked to a reduced aromatic amino acids intake, leading to a reduced availability during brain development [135,136]. RTT patients have a characteristic metabolic signature as shown by high glucose levels and insulin resistance [137]. Interestingly, upregulation of *SLC2A1* (GLUT1) transcript was specifically observed in RTT BMEC-like cells, especially for RTT-2 patient, the most severe case. This finding suggests a potential link between the dysregulated expression of *SLC2A1* and the metabolic abnormalities observed in RTT patients[138].

Similarly to the C9-ALS model, to assess whether these transcriptional alterations were associated with functional dysregulation, I quantified the monolayer permeability by TEER. RTT BMEC-like cells failed to maintain barrier permeability, as reported by others in RTT animal models [139].

2. Different MECP2-RTT mutations lead to diverse BBB gene-related expression:

MECP2 is situated within the nucleus, where it serves as a transcriptional regulator by binding to CpG islands in the cellular DNA. *MECP2* regulates the expression of a wide range of neuronal genes functioning as both an activator and a repressor of transcription[126].

According to the Human Gene Mutation Database, 651 mutations associated to RTT have been identified in the *MECP2* gene[140]. In my research, I have selected 4 mutations to recreate some aspects of disease variability, using three of the most common mutations [141]. This is also reflected in the transcriptomic analysis (unpublished), where each cell line reported a different spectrum of BBB genes affected in this context.

MECP2 has three functional domains: a DNA methyl-binding domain (MBD), a nuclear localization sequence domain (NLS), allowing trafficking to the nucleus, and a transcriptional repression domain (TRD)[142].

In a study exploring various mutations associated with RTT, patients carrying the missense mutation *R133C* (RTT-1) on the MBD domain demonstrated enhanced overall function. They exhibited a higher likelihood of acquiring walking skills and maintaining ambulation, displayed improved speech and mobility, and had fewer comorbidities[143]. In general, at the transcriptomic level, the RTT-1 cell line exhibited dysregulated expression of markers, consistent with the negative effect of *R133C* mutation in DNA binding domain[144].

On the other hand, the nonsense mutation *R255X* (RTT-2) represents a truncating mutation that lacks the nuclear localization signal (NLS) domain on *MECP2*. Thus, while these mutations may result in a more severe phenotype due to the inability of *MECP2* to localize to the nucleus [142], the transcriptional activity for the BBB genes analysed was more preserved than for the others. Surprisingly, even though complete loss of function would be predicted to result in a more severe phenotype, numerous studies have failed to establish a correlation between mutation type and severity of phenotype.

On the contrary, the *R306C* (RTT-3) mutation disrupts the binding of a *MECP2* transcriptional repressor (TRD), and hampers activity-dependent phosphorylation on the T308 site, which increases transcription; this, together with their known milder phenotype, may indicate that these domains are

not the only mechanisms regulating *MECP2* function[142]. My data suggests a modest BBB gene dysregulation for the R06C patient cell line, which may suggest a compensatory mechanism derived from TRD defects[142].

Finally, *c.62 + 1delGT* (RTT-4) is a *de novo* mutation consisting of a splice site mutation, resulting in a rare case of RTT with a classical phenotype with altered isoforms of *MECP2*[145]. For this patient, no overall dysregulation was found at the transcriptional level for the selected genes.

3. Impact of RTT Patient-Derived Astrocytes conditioned medium:

Astrocytes are essential for BBB establishment, maintenance, and maturation[3]. Moreover, conditioned medium from healthy astrocytes has been shown to effectively correct dendritic branching abnormalities in *Mecp2*-KO neurons[130]. However, there is limited understanding of astrocyte dynamics in the context of the BBB in RTT.

Despite the observed toxicity of RTT-iAstrocytes conditioned medium when added to BMEC-like cells, there were no discernible dysregulations in Claudin-5 or GLUT1 protein levels when assessed via immunofluorescence.

4. Energy homeostasis:

GLUT1 is the main transporter at the BBB and its malfunction is linked to a wide range of disorders, from cancer to Alzheimer's disease or Parkinson[146]. Additionally, endothelial cells are preferentially glycolytic[147], thus, glucose metabolism research is of great relevance for the BBB.

Interestingly, despite the lack of dysregulation in GLUT1 protein levels in the endothelial monolayer, the data revealed upregulated basal respiration, basal glycolysis, and ATP-linked respiration in MECP2-RTT BMEC-like cells compared to wild-type cells. This finding suggests alterations in cellular metabolism associated with MECP2-RTT, as shown by altered glucose and insulin tolerance in patients[138,148] and murine models[149].

5. RTT-MECP2 iAstrocytes disrupt the endothelial barrier:

The introduction of RTT-MECP2 iAstrocyte-derived medium did not induce significant changes in Claudin-5 or GLUT1 protein expression levels. However, co-culturing astrocytes with RTT-MECP2 BMEC-like cells led to a notable reduction in GLUT1 expression. Although astrocyte end-feet typically support endothelial cells in the NVU, the mixed co-culture of both cell types in this experiment may not fully replicate *in vivo* conditions, potentially influencing cell-to-cell interactions and worsening them[150,151]. Co-culturing RTT iAstrocytes not only impacted GLUT1 transporter expression but also Claudin-5 levels. The significant reduction in Claudin-5 observed when combining RTT-derived BMEC-like cells or RTT iAstrocytes with healthy counterparts was also evident in TEER measurements, indicating compromised barrier integrity in the BBB disease models.

6. BMEC-like cells toxicity towards other cells:

In contrast to the findings in the C9-ALS model, RTT-MECP2 BMEC-like cells did not exhibit toxicity towards iNeurons. The conditioned media from RTT BMEC-like cells showed comparable LDH release levels to that of WT cells, which could account for the observed lack of toxicity.

Although RTT BMEC-like cells did not display toxicity towards iNeurons, there may be variations in the cellular interactions between them compared to those between C9-ALS BMEC-like cells and C9-MNs. Additionally, the iNeurons utilised in the study represent a rapidly differentiating protocol, yielding impressive outcomes but resulting in immature neurons, whereas the MNs investigated in Chapter 3 had a clear spatial identity as demonstrated previously by the expression of motor neuron markers and were electrophysiologically active (unpublished data)[152]. A comprehensive understanding of the specific molecular mechanisms governing these cells with different identities, maturity and interconnections could offer insights into the observed differences in toxicity. Furthermore, it's important to note the substantial differences in the underlying pathophysiology of RTT-MECP2 and C9-ALS.

7. Implications for RTT Pathogenesis and Therapeutic Strategies:

Currently, there are no RTT-BBB models known to the author. It is notable that while there is limited knowledge about C9-ALS BBB, even less is understood about RTT, underscoring the significance of this research. Conducted within a relatively short timeframe of six months, my study sheds light on the complexities of this multifaceted disease. I acknowledge the model limitations, as the lack of different cell types involved in the NVU. However, a strength of this study is that it used cells from patients with 3 of the most common mutations, together with a rare mutation.

Understanding the expression of transporters at the RTT BBB is pivotal for devising effective therapeutic strategies. For instance, consider the case of the L-dopa dopamine precursor, widely utilized in treating Parkinson's disease[153]. L-dopa, being a large amino acid, crosses the BBB via the LAT-1 transporter[154]. Interestingly, in RTT BMEC-like cells, there was observed upregulation of the *SLC7A5* gene, which encodes LAT-1, compared to the wild-type. This finding suggests that alongside the upregulation of other transporters such as P-Glycoprotein, targeting these transporters could hold promise for the development of new therapies.

Chapter 5: Discussion and Conclusions

Chapter 5: Index of Tables

Table 5. 1: Main findings summary for C9-ALS and MECP2-RTT BBB models 104

Discussion

The blood-brain barrier (BBB) is a highly specialized and dynamic membrane composed of brain endothelial cells (BMECs), astrocytes, pericytes and neurons forming the neurovascular unit (NVU). It acts as a selective filter, allowing the diffusion of lipophilic compounds and gases while restricting larger and hydrophilic molecules. The BBB plays a crucial role in protecting the brain from exogenous substances and regulating blood flow. The neurodevelopmental period is critical for BBB formation, with various factors influencing its development and function[155–157]

BMECs express essential transporters and synthesize neurotransmitter molecules, contributing to neurodegenerative processes when dysregulated. Astrocytes also play a significant role in the BBB by secreting cytokines and exacerbating neuroinflammation[158].

Factors such as oxidative stress and hyperpermeability can disrupt the BBB and contribute to neurodegenerative and neurodevelopmental disorders like amyotrophic lateral sclerosis (ALS) and Rett Syndrome (RTT)[159].

Animal models serve as valuable tools in disease research, including ALS and RTT. Murine models have contributed to our understanding of their pathogenesis and potential therapeutics. *C9orf72* (C9-ALS) and *Mecp2* (MECP2-RTT) mouse models recapitulate pathological features; however, translation to the clinic has been challenging. Variations in disease onset and progression among different mutations, genders, and genetic strains highlight the influence of genetic background and epigenetic factors. Despite limitations such as cellular age reversal and interline variability, human induced pluripotent stem cells (hi-PSCs) provide insights into disease mechanisms[160].

Efforts to develop human BBB *in vitro* models have intensified over the past two decades. Co-culturing BMECs with other NVU cells like astrocytes has become common to simulate *in vivo* interactions. Traditional *in vitro* BBB modelling involves culturing BMECs as a flat monolayer, often on transwell inserts. These inserts allow for assessing transendothelial electrical resistance (TEER), tracer permeability, and sampling of different compartments[160].

Recent advancements include microfluidic models, which recreate blood flow between the body and brain. However, microfluidic prototypes are more complex, labour-intensive, and expensive compared to traditional transwell approaches. Currently, protocols for generating brain organoids show promise, but further research is needed to accurately replicate the brain's complexity. Moreover, organoids may not accurately measure key BBB characteristics like TEER[113].

Therefore, I opted for using hi-PSCs to model the BBB, considering their ethical advantages and patient origin. I selected a co-culture system in a transwell, which allows for the study of individual cell types and their interactions, although optimization is often required. Moreover, the transwell system is ideal for assessing barrier permeability and offers a convenient method for accurately measuring TEER without cell damage[161].

As mentioned above, the BBB is a highly intricate system, which protects the brain from external agents. BBB disruption has been studied in neurodegeneration, as shown by reduction in tight junction (TJ) expression, transporters dysregulation and, consequently cellular degeneration at the NVU[28]. However, our knowledge of C9-ALS and MECP2-RTT is very limited[3,139,162].

Overall, my research aims to elucidate if disease-related mutations, *C9ORF72* and *MECP2*, affect the function of cells involved in the BBB (BMECs, astrocytes and neurons), thus, leading to permeability defects and causing BBB disruption.

For this purpose, I developed a BBB *in vitro* model for both pathologies ALS and RTT (Chapter 3 and Chapter 4 respectively). Due to the lack of information for either of them, I started by researching differentiation protocols to obtain BMECs, the major cell type in the BBB[163]. After successfully obtaining a BMEC monolayer derived for multiple human cell lines, I decided to study them in the context of disease. Interestingly, my data showed an intrinsic alteration in transcript and protein signature, together with impaired permeability features (Table 5. 1).

Table 5. 1: Main findings summary for C9-ALS and MECP2-RTT BBB models

Model	Findings	*C9ORF72*-ALS 1 type of mutation	*MECP2*-RTT 4 different mutations
BMECs Monoculture	Tight junctions	Overall tight junctions' upregulation at transcriptomic level but not at protein level	No overall dysregulation at the transcript nor protein level
	Transporters and Receptors	Overall transporters upregulation at transcriptomic level. GLUT1 protein and P-glycoprotein receptor upregulated expression	*SLC2A1* (GLUT1) gene upregulation but not protein. No overall gene expression dysregulation
	Mitochondrial Activity	Downregulated basal glycolysis and upregulated basal and ATP-linked respiration	Overall upregulation
	Cytotoxicity	Increased LDH release	No significant LHD release
iAstrocytes conditioned media	Tight junctions	C9-ALS iAstrocytes media upregulated GLUT1 protein expression and downregulated Claudin-5 on BMECs	No effects
	Cytotoxicity	Toxic towards BMECs	Toxic towards BMECs
iAstrocytes/BMECs Co-culture	Tight Junctions	Not shown	Decreased Claudin-5 and GLUT1 protein expression
	TEER	C9-ALS iAstrocytes diminished the TEER measurements on BMECs	MECP2-RTT iAstrocytes diminished the TEER measurements on BMECs
BMECs conditioned media	Neurons	Toxicity towards healthy motor neurons	No toxicity towards iNeurons

This table summarises the main findings in Chapters 3 and 4, covering *C9ORF72*-amyotrophic lateral sclerosis (C9-ALS) and *MECP2*-Rett syndrome (MECP2-RTT) respectively. Briefly, it describes the results for all scenarios studies: brain endothelial-like cells (BMECs) monoculture, induced astrocytes (iAstrocytes) conditioned media treatments, iAstrocytes and BMECs co-culture set-ups and BMECs conditioned media treatments as well.

In our investigation of ALS, I discovered that C9-ALS BMEC-like cells exhibit upregulated expression of TJ-related genes such as Cadherin-5 and ZO-1, along with overexpression of transporters and receptors crucial for BBB function, contrary to what was found in a C9-ALS mouse model[26]. Despite the increased mRNA levels of TJ proteins like Claudin-5 in C9-ALS BMEC-like cells, protein levels remain unchanged, suggesting compensatory mechanisms and, perhaps technical limitations in the detection of changes in protein levels. Moreover, there is an upregulation in P-glycoprotein activity in C9-ALS, which, though controversial, is believed to be a compensatory strategy to protect the brain against neuroinflammation[164,165]. Notably, Riluzole, the first approved drug targeting ALS, is a substrate of P-

glycoprotein, and the receptor upregulation in the BBB has been linked to multidrug resistance in ALS patients[166].

After assessing the cell-autonomous properties of the endothelium, I moved on to investigating the impact of other components of the BBB, i.e., astrocytes, on endothelial cells. The addition of conditioned medium from C9-ALS iAstrocytes led to upregulation of GLUT1 expression, and co-culture experiments demonstrated that C9-ALS astrocytes exacerbate barrier leakiness, as evidenced by decreased TEER. This suggests potential effects on BBB dynamics and integrity.

Building on the metabolic features indicated by GLUT1 upregulation, C9-ALS BMEC-like cells also exhibited altered mitochondrial respiration, indicating disruptions in glucose metabolism and energy homeostasis. Additionally, these cells showed high levels of lactate release, a cytotoxicity indicator[167]. Consequently, conditioned medium from C9-ALS BMEC-lie cells proved to be toxic to healthy motor neurons (MNs), resulting in a significant reduction in neurite length. This underscores the downstream effects of BBB dysfunction on neuronal health and connectivity.

As opposed to these results, the dysregulated gene pattern in the MECP2-RTT BMEC-like cells was more irregular. Here, we must consider that, while for ALS, all the cells were carrying the same mutation and mostly similar repeat expansion size; for RTT we had 4 different mutations for the same gene (*R133C*, *R255X*, *R306C*, *c.62 + 1 del GT*). All these mutations affect the patients in a different way, resulting in a grade scale of severity[168].

All four RTT BMEC-like cell lines exhibited upregulation of the *SLC2A1* gene, encoding GLUT1. However, among them, the patient carrying the *R133C* mutation (RTT-1) displayed the most pronounced alteration in transcriptional profile. Consequently, this patient showed dysregulation in TJs and key transporters. The *R133C* mutation is situated in the DNA binding domain (MBD) of the *MECP2* gene, thereby impacting transcription. Surprisingly, the introduction of RTT-iAstrocytes did not result in any changes in Claudin-5 or GLUT1 protein expression within the endothelium. These alterations were only observed when evaluated in co-culture settings, resulting in a diminished TEER as well.

Moreover, in contrast to the C9-ALS BMEC-like cells, the MECP2-RTT BMEC-like cells displayed no significant differences in the GLUT1 transporter protein expression compared to the WT.

During childhood, there is typically a higher glucose consumption rate, reflecting the increased energy demands associated with growth and development[169]. RTT BMEC-like cells seahorse data analysis has shown an overall upregulation of mitochondrial respiration, which may indicate heightened cellular metabolism to support physiological processes. Conversely, in ALS BMEC-like cells, glycolysis appears to be downregulated, revealing a shift in metabolic priorities.

Ultimately, although the conditioned medium from C9-ALS BMEC-like cells exhibited toxicity towards healthy MNs, no such toxicity was observed when conducting a similar experiment using the MECP2-RTT conditioned medium. One potential explanation for this discrepancy could be attributed to variations in the neuronal models themselves. The MNs utilized in the experiment were at least 40 days old and derived from hi-PSCs, indicating a mature state. In contrast, the induced neurons (iNeurons) used in the MECP2-RTT experiments were generated through a rapid direct reprogramming protocol from fibroblasts, suggesting a different developmental stage and complexity. Another potential explanation relies on the inherent characteristics of the BMEC-like cells themselves, especially considering that RTT astrocytes have been demonstrated to induce non-cell-autonomous neuronal death in a mouse model[129]. In my research, ALS BMEC-like cells exhibited elevated rates of lactate release (LDH assay), indicative of cellular damage, along with more pronounced dysregulation

in gene and protein expression. In contrast, RTT cells did not demonstrate LDH levels approaching toxicity, suggesting less cellular damage compared to ALS cells.

Overall, my findings shed light on the complex interplay between genetic mutations, cellular mechanisms, and BBB integrity in ALS and RTT, and underscores the importance of developing accurate *in vitro* models for elucidating disease mechanisms and identifying therapeutic strategies.

Moving forward, several paths of research could build upon the findings of this study. For example, investigating the specific molecular mechanisms underlying the dysregulation of TJs, transporters, and other BBB components in ALS and RTT could provide deeper insights into disease pathogenesis.

Although my research has its limitations, such as the limited range of cell types investigated, it stands as an important attempt to unravel the complex interplay between the BBB and ALS, and RTT; particularly concerning the *C9ORF72* and *MECP2* mutations, for which no multi-cellular models were previously available for either of them. The observed changes in barrier integrity, molecular signatures, and neuronal outcomes offer compelling evidence to regard the BBB as a viable target for therapeutic strategies in ALS and RTT.

In addition, translating *in vitro* findings into clinical applications requires rigorous validation and optimization of therapeutic candidates. Due to the BBB's role in protecting the brain, conducting clinical trials to evaluate the safety and efficacy of BBB-targeted therapies, as well as their permeability properties, in ALS and RTT patients, while challenging, is essential for advancing novel treatments. Further research is necessary to elucidate the underlying mechanisms and explore potential therapeutic targets for these debilitating disorders.

Conclusions

To our knowledge, the *in vitro* model that has been generated is the first stem-cell derived human model of the BBB for ALS and RTT, which has been used to study its properties in both health and disease.

The main conclusions of my research are the following:

1. hi-PSCs were utilised, focusing on how *C9ORF72* and *MECP2* mutations affect BBB integrity. Various BBB *in vitro* models have been developed for ALS and RTT, starting with differentiation protocols for BMECs.

2. These findings showed that C9-ALS BMEC-like cells had upregulated gene expression of TJ-related genes and transporters; and receptors activity as P-glycoprotein, thus suggesting compensatory mechanisms.

3. In contrast, RTT BMEC-like cells showed varied gene dysregulation based on different *MECP2* mutations. Although *GLUT1* gene expression was upregulated in all RTT cell lines, the *R133C* mutation exhibited the most pronounced transcriptomic alterations.

4. Additionally, conditioned medium from C9-ALS iAstrocytes increased GLUT1 expression and reduced Claudin-5 and TEER, indicating barrier leakiness.

5. Furthermore, C9-ALS BMEC-like cells displayed altered glucose metabolism and toxicity to healthy MNs.

6. RTT-iAstrocytes in co-culture also reduced TEER and GLUT1 and Claudin-5 expression in BMEC-like cells, MECP2-RTT iAstrocytes conditioned medium did not affect healthy cells.

7. Moreover, MECP2-RTT BMEC-like cells had an altered glucose metabolism but did not show toxicity towards neuronal cells (iNeurons).

8. Lastly, while this study has limitations, it represents a pioneering effort to explore the complex role of BBB in neurodegenerative diseases.

Overall, this research highlights that genetic mutations causing neurodegenerative and neurodevelopmental disorders have a cell-autonomous impact on BMECs and a consequent effect on BBB function and integrity. In turn, these can affect neuronal health. Future research should further investigate the specific molecular mechanisms affecting BBB components in ALS and RTT to develop targeted therapeutic strategies.

References

1. Lenoir, T. Researches in the Kaiserreich: Paul Ehrlich. Scientist for Life. Ernst Bäumler. Holmes and Meier, New York, 1984. xvi, 288 pp. + plates. $39.50. Translated, from the German edition (Frankfurt-am-Main, 1984) by Grant Edwards. Science (1979) 227, 1026 (1985).

2. Sarikcioglu, L. Lina Stern (1878-1968): an outstanding scientist of her time. Child's nervous system : ChNS : official journal of the International Society for Pediatric Neurosurgery vol. 33 1027–1029 Preprint at https://doi.org/10.1007/s00381-017-3392-3 (2017).

3. Aragón-González, A., Shaw, P. J. & Ferraiuolo, L. Blood–Brain Barrier Disruption and Its Involvement in Neurodevelopmental and Neurodegenerative Disorders. Int J Mol Sci 23, (2022).

4. Song, I. & Dityatev, A. Crosstalk between glia, extracellular matrix and neurons. Brain Res Bull 136, 101–108 (2018).

5. Nimni, M. E. Collagen: Structure, function, and metabolism in normal and fibrotic tissues. Semin Arthritis Rheum 13, 1–86 (1983).

6. Antoine, E. E., Vlachos, P. P. & Rylander, M. N. Review of collagen I hydrogels for bioengineered tissue microenvironments: characterization of mechanics, structure, and transport. Tissue Eng Part B Rev 20, 683–696 (2014).

7. Pöschl, E. et al. Collagen IV is essential for basement membrane stability but dispensable for initiation of its assembly during early development. Development 131, 1619–1628 (2004).

8. Gaillard, P. J. et al. Establishment and functional characterization of an in vitro model of the blood-brain barrier, comprising a co-culture of brain capillary endothelial cells and astrocytes. Eur J Pharm Sci 12, 215–222 (2001).

9. Bell, A. H., Miller, S. L., Castillo-Melendez, M. & Malhotra, A. The Neurovascular Unit: Effects of Brain Insults During the Perinatal Period. Front Neurosci 13, 1452 (2019).

10. Kozberg, M. G., Ma, Y., Shaik, M. A., Kim, S. H. & Hillman, E. M. C. Rapid Postnatal Expansion of Neural Networks Occurs in an Environment of Altered Neurovascular and Neurometabolic Coupling. The Journal of Neuroscience 36, 6704 LP – 6717 (2016).

11. Lacoste, B. et al. Sensory-related neural activity regulates the structure of vascular networks in the cerebral cortex. Neuron 83, 1117–1130 (2014).

12. Boillée, S., Vande Velde, C. & Cleveland, D. W. ALS: A Disease of Motor Neurons and Their Nonneuronal Neighbors. Neuron 52, 39–59 (2006).

13. Asociación Española de Esclerosis Lateral Amiotrófica. adELA. https://adelaweb.org/.

14. Longinetti, E. & Fang, F. Epidemiology of amyotrophic lateral sclerosis: an update of recent literature. Curr Opin Neurol 32, 771–776 (2019).

15. Arthur, K. C. et al. Projected increase in amyotrophic lateral sclerosis from 2015 to 2040. Nat Commun 7, 12408 (2016).

16. Abel, O., Powell, J. F., Andersen, P. M. & Al-Chalabi, A. ALSoD: A user-friendly online bioinformatics tool for amyotrophic lateral sclerosis genetics. Hum Mutat 33, 1345–1351 (2012).

17. Smeyers, J., Banchi, E. G. & Latouche, M. C9ORF72: What It Is, What It Does, and Why It Matters. Frontiers in Cellular Neuroscience vol. 15 Preprint at https://doi.org/10.3389/fncel.2021.661447 (2021).

18. Petrov, D., Mansfield, C., Moussy, A. & Hermine, O. ALS Clinical Trials Review: 20 Years of Failure. Are We Any Closer to Registering a New Treatment? Front Aging Neurosci 9, 68 (2017).

19. Ng, L., Khan, F., Young, C. A. & Galea, M. Symptomatic treatments for amyotrophic lateral sclerosis/motor neuron disease. Cochrane Database Syst Rev 1, CD011776 (2017).

20. Moujalled, D. & White, A. R. Advances in the Development of Disease-Modifying Treatments for Amyotrophic Lateral Sclerosis. CNS Drugs 30, 227–243 (2016).

21. Jiang, J., Wang, Y. & Deng, M. New developments and opportunities in drugs being trialed for amyotrophic lateral sclerosis from 2020 to 2022. Front Pharmacol 13, 1054006 (2022).

22. Phukan, J., Pender, N. P. & Hardiman, O. Cognitive impairment in amyotrophic lateral sclerosis. Lancet Neurol 6, 994–1003 (2007).

23. Garbuzova-Davis, S. et al. Amyotrophic lateral sclerosis: A neurovascular disease. Brain Res 1398, 113–125 (2011).

24. Brundel, M. et al. High prevalence of cerebral microbleeds at 7Tesla MRI in patients with early Alzheimer's disease. J Alzheimers Dis 31, 259–263 (2012).

25. Cowley, P. M. et al. Oxidant production and SOD1 protein expression in single skeletal myofibers from Down syndrome mice. Redox Biol 13, 421–425 (2017).

26. Pan, Y. et al. Altered Blood–Brain Barrier Dynamics in the C9orf72 Hexanucleotide Repeat Expansion Mouse Model of Amyotrophic Lateral Sclerosis. Pharmaceutics vol. 14 Preprint at https://doi.org/10.3390/pharmaceutics14122803 (2022).

27. Sweeney, M. D., Zhao, Z., Montagne, A., Nelson, A. R. & Zlokovic, B. V. Blood-Brain Barrier: From Physiology to Disease and Back. Physiol Rev 99, 21–78 (2019).

28. Garbuzova-Davis, S. et al. Impaired blood–brain/spinal cord barrier in ALS patients. Brain Res 1469, 114–128 (2012).

29. Winkler, E. A. et al. Blood-spinal cord barrier disruption contributes to early motor-neuron degeneration in ALS-model mice. Proc Natl Acad Sci U S A 111, E1035–E1042 (2014).

30. National Health Service, Rett Syndrome. https://www.nhs.uk/conditions/rett-syndrome/ (2019).

31. Kirby, R. S. et al. Longevity in Rett syndrome: analysis of the North American Database. J Pediatr 156, 135-138.e1 (2010).

32. Percy, A. Natural History of Rett Syndrome & Related Disorders. beta.clinicaltrials.gov/study/NCT02738281 (2021).

33. Pejhan, S. & Rastegar, M. Role of DNA Methyl-CpG-Binding Protein MeCP2 in Rett Syndrome Pathobiology and Mechanism of Disease. Biomolecules 11, (2021).

34. Hoffbuhr, K. C., Moses, L. M., Jerdonek, M. A., Naidu, S. & Hoffman, E. P. Associations between MeCP2 mutations, X-chromosome inactivation, and phenotype. Ment Retard Dev Disabil Res Rev 8, 99–105 (2002).

35. Xiol, C. et al. X chromosome inactivation does not necessarily determine the severity of the phenotype in Rett syndrome patients. Sci Rep 9, 11983 (2019).

36. BARR, M. L. & BERTRAM, E. G. A Morphological Distinction between Neurones of the Male and Female, and the Behaviour of the Nucleolar Satellite during Accelerated Nucleoprotein Synthesis. Nature 163, 676–677 (1949).

37. Lyon, M. F. X-chromosome inactivation. Current Biology 9, R235–R237 (1999).

38. Knudsen, G. P. S. et al. Increased skewing of X chromosome inactivation in Rett syndrome patients and their mothers. European Journal of Human Genetics 14, 1189–1194 (2006).

39. Rett Syndrome Foundation. https://www.rettsyndrome.org.

40. Rett Syndrome Foundation. https://www.rettsyndrome.org.

41. National Institute of Neurological Disorders and Stroke, U.S. National Instute of Health (NIH). https://www.ninds.nih.gov/health-information/disorders/rett-syndrome.

42. Neul, J. L. et al. Specific mutations in methyl-CpG-binding protein 2 confer different severity in Rett syndrome. Neurology 70, 1313–1321 (2008).

43. Cronk, J. C., Derecki, N. C., Litvak, V. & Kipnis, J. Unexpected cellular players in Rett syndrome pathology. Neurobiol Dis 92, 64–71 (2016).

44. Maezawa, I., Swanberg, S., Harvey, D., LaSalle, J. M. & Jin, L.-W. Rett syndrome astrocytes are abnormal and spread MeCP2 deficiency through gap junctions. J Neurosci 29, 5051–5061 (2009).

45. Pejhan, S., Siu, V. M., Ang, L. C., Del Bigio, M. R. & Rastegar, M. Differential brain region-specific expression of MeCP2 and BDNF in Rett Syndrome patients: a distinct grey-white matter variation. Neuropathol Appl Neurobiol 46, 735–750 (2020).

46. Jackson, S. et al. Model systems for studying the blood-brain barrier: Applications and challenges. Biomaterials 214, 119217 (2019).

47. Williams-Medina, A., Deblock, M. & Janigro, D. In vitro Models of the Blood–Brain Barrier: Tools in Translational Medicine . Frontiers in Medical Technology vol. 2 Preprint at (2021).

48. Schreiner, T. G., Creangă-Murariu, I., Tamba, B. I., Lucanu, N. & Popescu, B. O. In Vitro Modeling of the Blood-Brain Barrier for the Study of Physiological Conditions and Alzheimer's Disease. Biomolecules 12, (2022).

49. Cecchelli, R. et al. Modelling of the blood–brain barrier in drug discovery and development. Nat Rev Drug Discov 6, 650–661 (2007).

50. Kaur, G. & Dufour, J. M. Cell lines: Valuable tools or useless artifacts. Spermatogenesis 2, 1–5 (2012).

51. Takahashi, K. & Yamanaka, S. Induction of Pluripotent Stem Cells from Mouse Embryonic and Adult Fibroblast Cultures by Defined Factors. Cell 126, 663–676 (2006).

52. Takahashi, K. et al. Induction of Pluripotent Stem Cells from Adult Human Fibroblasts by Defined Factors. Cell 131, 861–872 (2007).

53. Doss, M. X. & Sachinidis, A. Current Challenges of iPSC-Based Disease Modeling and Therapeutic Implications. Cells 8, 403 (2019).

54. Lippmann, E. S. et al. Derivation of blood-brain barrier endothelial cells from human pluripotent stem cells. Nat Biotechnol 30, 783–791 (2012).

55. Hollmann, E. K. et al. Accelerated differentiation of human induced pluripotent stem cells to blood-brain barrier endothelial cells. Fluids Barriers CNS 14, 9 (2017).

56. Qian, T. et al. Directed differentiation of human pluripotent stem cells to blood-brain barrier endothelial cells. 48–50 (2017).

57. Sun, N. et al. Applications of brain organoids in neurodevelopment and neurological diseases. J Biomed Sci 28, 30 (2021).

58. Van Damme, P., Robberecht, W. & Van Den Bosch, L. Modelling amyotrophic lateral sclerosis: progress and possibilities. Dis Model Mech 10, 537–549 (2017).

59. Mitsumoto, H., Brooks, B. R. & Silani, V. Clinical trials in amyotrophic lateral sclerosis: why so many negative trials and how can trials be improved? Lancet Neurol 13, 1127–1138 (2014).

60. Gurney, M. E. et al. Motor neuron degeneration in mice that express a human Cu,Zn superoxide dismutase mutation. Science 264, 1772–1775 (1994).

61. Philips, T. & Rothstein, J. D. Rodent Models of Amyotrophic Lateral Sclerosis. Curr Protoc Pharmacol 69, 5.67.1-5.67.21 (2015).

62. Storkebaum, E. et al. Treatment of motoneuron degeneration by intracerebroventricular delivery of VEGF in a rat model of ALS. Nat Neurosci 8, 85–92 (2005).

63. Van Damme, P. et al. Intracerebroventricular delivery of vascular endothelial growth factor in patients with amyotrophic lateral sclerosis, a phase I study. Brain Commun 2, fcaa160 (2020).

64. Pronto-Laborinho, A. C., Pinto, S. & de Carvalho, M. Roles of vascular endothelial growth factor in amyotrophic lateral sclerosis. Biomed Res Int 2014, 947513 (2014).

65. Meyer, K. et al. Direct conversion of patient fibroblasts demonstrates non-cell autonomous toxicity of astrocytes to motor neurons in familial and sporadic ALS. Proc Natl Acad Sci U S A 111, 829–832 (2014).

66. Majounie, E. et al. Frequency of the C9orf72 hexanucleotide repeat expansion in patients with amyotrophic lateral sclerosis and frontotemporal dementia: a cross-sectional study. Lancet Neurol 11, 323–330 (2012).

67. Kakaroubas, N., Brennan, S., Keon, M. & Saksena, N. K. Pathomechanisms of Blood-Brain Barrier Disruption in ALS. Neurosci J 2019, 2537698 (2019).

68. Lippmann, E. S., Al-Ahmad, A., Azarin, S. M., Palecek, S. P. & Shusta, E. V. A retinoic acid-enhanced, multicellular human blood-brain barrier model derived from stem cell sources. Sci Rep 4, 4160 (2014).

69. Neal, E. H. et al. A Simplified, Fully Defined Differentiation Scheme for Producing Blood-Brain Barrier Endothelial Cells from Human iPSCs. Stem Cell Reports 12, 1380–1388 (2019).

70. Katt, M. E., Linville, R. M., Mayo, L. N., Xu, Z. S. & Searson, P. C. Functional brain-specific microvessels from iPSC-derived human brain microvascular endothelial cells: the role of matrix composition on monolayer formation. Fluids Barriers CNS 15, 7 (2018).

71. Du, Z.-W. et al. Generation and expansion of highly pure motor neuron progenitors from human pluripotent stem cells. Nat Commun 6, (2015).

72. Meyer, K. et al. Direct conversion of patient fibroblasts demonstrates non-cell autonomous toxicity of astrocytes to motor neurons in familial and sporadic ALS. Proc Natl Acad Sci U S A 111, 829–832 (2014).

73. Stebbins, M. J. et al. Differentiation and characterization of human pluripotent stem cell-derived brain microvascular endothelial cells. Methods 101, 93–102 (2016).

74. Peerani, R. et al. Niche-mediated control of human embryonic stem cell self-renewal and differentiation. EMBO J 26, 4744–4755 (2007).

75. Chambers, S. M. et al. Highly efficient neural conversion of human ES and iPS cells by dual inhibition of SMAD signaling. Nat Biotechnol 27, 275–280 (2009).

76. Selekman, J. A., Grundl, N. J., Kolz, J. M. & Palecek, S. P. Efficient generation of functional epithelial and epidermal cells from human pluripotent stem cells under defined conditions. Tissue Eng Part C Methods 19, 949–960 (2013).

77. Lippmann, E. S., Estevez-Silva, M. C. & Ashton, R. S. Defined human pluripotent stem cell culture enables highly efficient neuroepithelium derivation without small molecule inhibitors. Stem Cells 32, 1032–1042 (2014).

78. Srinivasan, B. et al. TEER measurement techniques for in vitro barrier model systems. J Lab Autom 20, 107–126 (2015).

79. Wilson, H. K., Canfield, S. G., Hjortness, M. K., Palecek, S. P. & Shusta, E. V. Exploring the effects of cell seeding density on the differentiation of human pluripotent stem cells to brain microvascular endothelial cells. Fluids Barriers CNS 12, 13 (2015).

80. Fox, C. H., Johnson, F. B., Whiting, J. & Roller, P. P. Formaldehyde fixation. J Histochem Cytochem 33, 845–853 (1985).

81. Kim, S.-O., Kim, J., Okajima, T. & Cho, N.-J. Mechanical properties of paraformaldehyde-treated individual cells investigated by atomic force microscopy and scanning ion conductance microscopy. Nano Converg 4, 5 (2017).

82. Braet, F., Rotsch, C., Wisse, E. & Radmacher, M. Comparison of fixed and living liver endothelial cells by atomic force microscopy. Appl Phys A Mater Sci Process 66, (1998).

83. Schnell, U., Dijk, F., Sjollema, K. A. & Giepmans, B. N. G. Immunolabeling artifacts and the need for live-cell imaging. Nat Methods 9, 152–158 (2012).

84. Greer, S., Honeywell, R., Geletu, M., Arulanandam, R. & Raptis, L. Housekeeping genes; expression levels may change with density of cultured cells. J Immunol Methods 355, 76–79 (2010).

85. Li, T. et al. Identification of suitable reference genes for real-time quantitative PCR analysis of hydrogen peroxide-treated human umbilical vein endothelial cells. BMC Mol Biol 18, 10 (2017).

86. Desai, S. Y. et al. Mechanisms of endothelial survival under shear stress. Endothelium 9, 89–102 (2002).

87. Saunders, N. R., Daneman, R., Dziegielewska, K. M. & Liddelow, S. A. Transporters of the blood-brain and blood-CSF interfaces in development and in the adult. Mol Aspects Med 34, 742–752 (2013).

88. Richard, D. et al. Wnt/β-catenin signaling is required for CNS, but not non-CNS, angiogenesis. Proceedings of the National Academy of Sciences 106, 641–646 (2009).

89. McLoughlin, K. J., Pedrini, E., MacMahon, M., Guduric-Fuchs, J. & Medina, R. J. Selection of a Real-Time PCR Housekeeping Gene Panel in Human Endothelial Colony Forming Cells for Cellular Senescence Studies. Front Med (Lausanne) 6, 33 (2019).

90. Zhong, Z. et al. ALS-causing SOD1 mutants generate vascular changes prior to motor neuron degeneration. Nat Neurosci 11, (2008).

91. Winkler, E. A. et al. Blood-spinal cord barrier disruption contributes to early motor-neuron degeneration in ALS-model mice. Proc Natl Acad Sci U S A 111, E1035–E1042 (2014).

92. Van Mossevelde, S., van der Zee, J., Cruts, M. & Van Broeckhoven, C. Relationship between C9orf72 repeat size and clinical phenotype. Current Opinion in Genetics and Development vol. 44 Preprint at https://doi.org/10.1016/j.gde.2017.02.008 (2017).

93. Sareen, D. et al. Targeting RNA foci in iPSC-derived motor neurons from ALS patients with a C9ORF72 repeat expansion. Sci Transl Med 5, (2013).

94. Buchman, V. L. et al. Simultaneous and independent detection of C9ORF72 alleles with low and high number of GGGGCC repeats using an optimised protocol of Southern blot hybridisation. Mol Neurodegener 8, (2013).

95. Suh, E. R. et al. Semi-automated quantification of C9orf72 expansion size reveals inverse correlation between hexanucleotide repeat number and disease duration in frontotemporal degeneration. Acta Neuropathol 130, (2015).

96. Beck, J. et al. Large C9orf72 hexanucleotide repeat expansions are seen in multiple neurodegenerative syndromes and are more frequent than expected in the UK population. Am J Hum Genet 92, (2013).

97. Re, D. B. et al. Necroptosis drives motor neuron death in models of both sporadic and familial ALS. Neuron 81, (2014).

98. Lippmann, E. S., Estevez-Silva, M. C. & Ashton, R. S. Defined human pluripotent stem cell culture enables highly efficient neuroepithelium derivation without small molecule inhibitors. Stem Cells 32, 1032–1042 (2014).

99. Furuse, M. et al. Occludin: a novel integral membrane protein localizing at tight junctions. J Cell Biol 123, 1777–1788 (1993).

100. Morita, K., Sasaki, H., Furuse, M. & Tsukita, S. Endothelial Claudin: Claudin-5/Tmvcf Constitutes Tight Junction Strands in Endothelial Cells. Journal of Cell Biology 147, 185–194 (1999).

101. Shen, Q. et al. Endothelial Cells Stimulate Self-Renewal and Expand Neurogenesis of Neural Stem Cells. Science (1979) 304, 1338 LP – 1340 (2004).

102. Lim, J. C., Wolpaw, A. J., Caldwell, M. A., Hladky, S. B. & Barrand, M. A. Neural precursor cell influences on blood-brain barrier characteristics in rat brain endothelial cells. Brain Res 1159, 67–76 (2007).

103. Zhang, X. et al. Pax6 is a human neuroectoderm cell fate determinant. Cell Stem Cell 7, 90–100 (2010).

104. Nichols, J. et al. Formation of Pluripotent Stem Cells in the Mammalian Embryo Depends on the POU Transcription Factor Oct4. Cell 95, 379–391 (1998).

105. Dalla, C., Pavlidi, P., Sakelliadou, D.-G., Grammatikopoulou, T. & Kokras, N. Sex Differences in Blood-Brain Barrier Transport of Psychotropic Drugs. Front Behav Neurosci 16, 844916 (2022).

106. Peng, R., Zhang, H., Zhang, Y. & Wei, D.-Y. Effects of the ABCB1 (1199G > A) Polymorphism on Steroid Sex Hormone-Induced P-Glycoprotein Expression, ATPase Activity, and Hormone Efflux. Med Sci (Basel) 3, 124–137 (2015).

107. Huxley, V. H. et al. Sex differences influencing micro- and macrovascular endothelial phenotype in vitro. J Physiol 596, 3929–3949 (2018).

108. Zlokovic, B. V. The blood-brain barrier in health and chronic neurodegenerative disorders. Neuron 57, 178–201 (2008).

109. Kamm, D. R. The effects of diet and sex differences on cortical tight-junction protein expression in senescence-accelerated mouse-prone 8 (SAMP8) mice. Preprint at (2019).

110. McMillin, M. A. et al. TGFβ1 exacerbates blood-brain barrier permeability in a mouse model of hepatic encephalopathy via upregulation of MMP9 and downregulation of claudin-5. Lab Invest 95, 903–913 (2015).

111. Pardridge, W. M. Molecular biology of the blood-brain barrier. Mol Biotechnol 30, 57–70 (2005).

112. Garbuzova-Davis, S. & Sanberg, P. R. Blood-CNS Barrier Impairment in ALS patients versus an animal model. Front Cell Neurosci 8, 21 (2014).

113. Naik, P. & Cucullo, L. In vitro blood-brain barrier models: current and perspective technologies. J Pharm Sci 101, 1337–1354 (2012).

114. Majounie, E. et al. Frequency of the C9orf72 hexanucleotide repeat expansion in patients with amyotrophic lateral sclerosis and frontotemporal dementia: a cross-sectional study. Lancet Neurol 11, 323–330 (2012).

115. Abbott, N. J. Dynamics of CNS barriers: evolution, differentiation, and modulation. Cell Mol Neurobiol 25, 5–23 (2005).

116. Lippmann, E. S. et al. Derivation of blood-brain barrier endothelial cells from human pluripotent stem cells. Nat Biotechnol 30, 783–791 (2012).

117. Lippmann, E. S., Al-Ahmad, A., Azarin, S. M., Palecek, S. P. & Shusta, E. V. A retinoic acid-enhanced, multicellular human blood-brain barrier model derived from stem cell sources. Sci Rep 4, 4160 (2014).

118. Lippmann, E. S., Azarin, S. M., Palecek, S. P. & Shusta, E. V. Commentary on human pluripotent stem cell-based blood–brain barrier models. Fluids Barriers CNS 17, 64 (2020).

119. Di Marco, A. et al. Establishment of an in Vitro Human Blood-Brain Barrier Model Derived from Induced Pluripotent Stem Cells and Comparison to a Porcine Cell-Based System. Cells 9, (2020).

120. Obermeier, B., Daneman, R. & Ransohoff, R. M. Development, maintenance and disruption of the blood-brain barrier. Nat Med 19, 1584–1596 (2013).

121. Moretti, R. et al. Blood-brain barrier dysfunction in disorders of the developing brain. Front Neurosci 9, 40 (2015).

122. Stebbins, M. J. et al. Differentiation and characterization of human pluripotent stem cell-derived brain microvascular endothelial cells. Methods 101, 93–102 (2016).

123. Neal, E. H. et al. A Simplified, Fully Defined Differentiation Scheme for Producing Blood-Brain Barrier Endothelial Cells from Human iPSCs. Stem Cell Reports 12, 1380–1388 (2019).

124. Liu, G., David, B. T., Trawczynski, M. & Fessler, R. G. Advances in Pluripotent Stem Cells: History, Mechanisms, Technologies, and Applications. Stem Cell Rev Rep 10.1007/s12015-019-09935–x (2019) doi:10.1007/s12015-019-09935-x.

125. Wang, T. et al. C9orf72 regulates energy homeostasis by stabilizing mitochondrial complex I assembly. Cell Metab 33, (2021).

126. Chahrour, M. et al. MeCP2, a key contributor to neurological disease, activates and represses transcription. Science (1979) 320, (2008).

127. Neul, J. L. et al. Specific mutations in methyl-CpG-binding protein 2 confer different severity in Rett syndrome. Neurology 70, 1313–1321 (2008).

128. Aragón-González, A. et al. C9ORF72 patient-derived endothelial cells drive blood-brain barrier disruption and contribute to neurotoxicity. Fluids Barriers CNS 21, 34 (2024).

129. Ballas, N., Lioy, D. T., Grunseich, C. & Mandel, G. Non-cell autonomous influence of MeCP2-deficient glia on neuronal dendritic morphology. Nat Neurosci 12, (2009).

130. Cronk, J. C., Derecki, N. C., Litvak, V. & Kipnis, J. Unexpected cellular players in Rett syndrome pathology. Neurobiol Dis 92, 64–71 (2016).

131. Okabe, Y. et al. Alterations of gene expression and glutamate clearance in astrocytes derived from an mecp2-null mouse model of rett syndrome. PLoS One 7, (2012).

132. Williams, E. C. et al. Mutant astrocytes differentiated from Rett syndrome patients-specific iPSCs have adverse effects on wildtype neurons. Hum Mol Genet 23, (2014).

133. Armstrong, D., Dunn, J. K., Antalffy, B. & Trivedi, R. Selective dendritic alterations in the cortex of rett syndrome. J Neuropathol Exp Neurol 54, (1995).

134. Sinha Ray, S. et al. Mechanisms of IRF2BPL-related disorders and identification of a potential therapeutic strategy. Cell Rep 41, (2022).

135. Tărlungeanu, D. C. et al. Impaired Amino Acid Transport at the Blood Brain Barrier Is a Cause of Autism Spectrum Disorder. Cell 167, 1481-1494.e18 (2016).

136. Cascio, L. et al. Abnormalities in the genes that encode Large Amino Acid Transporters increase the risk of Autism Spectrum Disorder. Mol Genet Genomic Med 8, (2020).

137. Neul, J. L. et al. Metabolic Signatures Differentiate Rett Syndrome From Unaffected Siblings. Front Integr Neurosci 14, (2020).

138. Cooke, D. W., Naidu, S., Plotnick, L. & Berkovitz, G. D. Abnormalities of thyroid function and glucose control in subjects with Rett syndrome. Horm Res 43, (1995).

139. Pepe, G. et al. Blood–Brain Barrier Integrity Is Perturbed in a Mecp2-Null Mouse Model of Rett Syndrome. Biomolecules 13, (2023).

140. Stenson, P. D. et al. The human gene mutation database: 2008 update. Genome Medicine vol. 1 Preprint at https://doi.org/10.1186/gm13 (2009).

141. Gold, W. A., Krishnarajy, R., Ellaway, C. & Christodoulou, J. Rett Syndrome: A Genetic Update and Clinical Review Focusing on Comorbidities. ACS Chemical Neuroscience vol. 9 Preprint at https://doi.org/10.1021/acschemneuro.7b00346 (2018).

142. Cuddapah, V. A. et al. Methyl-CpG-binding protein 2 (MECP2) mutation type is associated with disease severity in rett syndrome. J Med Genet 51, (2014).

143. Leonard, H. et al. Patients with the R133C mutation: is their phenotype different from patients with Rett syndrome with other mutations? Journal of medical genetics vol. 40 Preprint at https://doi.org/10.1136/jmg.40.5.e52 (2003).

144. Kucukkal, T. G. & Alexov, E. Structural, dynamical, and energetical consequences of RETT syndrome mutation R133c in MeCP2. Comput Math Methods Med 2015, (2015).

145. Amir, R. E. et al. Mutations in exon 1 of MECP2 are a rare cause of Rett syndrome. J Med Genet 42, e15 LP-e15 (2005).

146. Shi, Y. et al. An arrayed CRISPR knockout screen identifies genetic regulators of GLUT1 expression. Sci Rep 13, 21038 (2023).

147. Leung, S. W. S. & Shi, Y. The glycolytic process in endothelial cells and its implications. Acta Pharmacologica Sinica vol. 43 Preprint at https://doi.org/10.1038/s41401-021-00647-y (2022).

148. Villemagne, P. M. et al. Brain glucose metabolism in Rett syndrome. Pediatr Neurol 27, (2002).

149. Golubiani, G., Lagani, V., Solomonia, R. & Müller, M. Metabolomic fingerprint of mecp2-deficient mouse cortex: Evidence for a pronounced multi-facetted metabolic component in rett syndrome. Cells 10, (2021).

150. Abbott, N. J., Rönnbäck, L. & Hansson, E. Astrocyte-endothelial interactions at the blood-brain barrier. Nat Rev Neurosci 7, 41–53 (2006).

151. Malekshah, A. K., Moghaddam, A. E. & Daraka, S. M. Comparison of conditioned medium and direct co-culture of human granulosa cells on mouse embryo development. Indian J Exp Biol 44, (2006).

152. Zhang, S. et al. Genome-wide identification of the genetic basis of amyotrophic lateral sclerosis. Neuron 110, (2022).

153. Davidson, L., Lloyd, K., Dankova, J. & Hornykiewicz, O. l-DOPA treatment in Parkinson's disease: Effect on dopamine and related substances in discrete brain regions. Experientia 27, (1971).

154. Kageyama, T. et al. The 4F2hc/LAT1 complex transports L-DOPA across the blood-brain barrier. Brain Res 879, (2000).

155. Engelhardt, B. & Sorokin, L. The blood-brain and the blood-cerebrospinal fluid barriers: function and dysfunction. Semin Immunopathol 31, 497–511 (2009).

156. Goasdoué, K., Miller, S. M., Colditz, P. B. & Björkman, S. T. Review: The blood-brain barrier; protecting the developing fetal brain. Placenta 54, 111–116 (2017).

157. Delaney, C. & Campbell, M. The blood brain barrier: Insights from development and ageing. Tissue Barriers 5, e1373897 (2017).

158. Alvarez, J. I., Katayama, T. & Prat, A. Glial influence on the blood brain barrier. Glia 61, 1939–1958 (2013).

159. Sweeney, M. D., Zhao, Z., Montagne, A., Nelson, A. R. & Zlokovic, B. V. Blood-Brain Barrier: From Physiology to Disease and Back. Physiol Rev 99, 21–78 (2019).

160. Jackson, S. et al. Model systems for studying the blood-brain barrier: Applications and challenges. Biomaterials 214, 119217 (2019).

161. Stone, N. L., England, T. J. & O'Sullivan, S. E. A Novel Transwell Blood Brain Barrier Model Using Primary Human Cells. Front Cell Neurosci 13, (2019).

162. Kakaroubas, N., Brennan, S., Keon, M. & Saksena, N. K. Pathomechanisms of Blood-Brain Barrier Disruption in ALS. Neurosci J 2019, 2537698 (2019).

163. Abbott, N. J., Patabendige, A. A. K., Dolman, D. E. M., Yusof, S. R. & Begley, D. J. Structure and function of the blood–brain barrier. Neurobiol Dis 37, 13–25 (2010).

164. Roberts, D. J. & Goralski, K. B. A critical overview of the influence of inflammation and infection on P-glycoprotein expression and activity in the brain. Expert Opinion on Drug Metabolism and Toxicology vol. 4 Preprint at https://doi.org/10.1517/17425255.4.10.1245 (2008).

165. Kooij, G. et al. P-Glycoprotein acts as an immunomodulator during neuroinflammation. PLoS One 4, (2009).

166. Calcagno, A., Kim, I.-W., Wu, C.-P., Shukla, S. & Ambudkar, S. ABC Drug Transporters as Molecular Targets for the Prevention of Multidrug Resistance and Drug-Drug Interactions. Curr Drug Deliv 4, (2007).

167. Chan, F. K. M., Moriwaki, K. & De Rosa, M. J. Detection of necrosis by release of lactate dehydrogenase activity. Methods in Molecular Biology 979, (2013).

168. Young, D. et al. The relationship between MECP2 mutation type and health status and service use trajectories over time in a Rett syndrome population. Res Autism Spectr Disord 5, 442–449 (2011).

169. Goyal, M. S., Hawrylycz, M., Miller, J. A., Snyder, A. Z. & Raichle, M. E. Aerobic glycolysis in the human brain is associated with development and neotenous gene expression. Cell Metab 19, (2014).

Abbreviations

AB I	Primary antibody
AB II	Secondary antibody
ABC	ATP binding cassette
AD	Alzheimer's disease
AGER	Rage receptor
AJ	Adherent junctions
ALS	Amyotrophic lateral sclerosis
APOE	Apolipoprotein e
ARE	Antioxidant response element
ASD	Autism spectrum disorder
ATP	Adenosine triphosphate
BBB	Blood-brain barrier
BDNF	Brain-derived neurotrophic factor
BFGF	Basic fibroblast growth factor
BM	Basement membrane
BMEC	Brain microvascular endothelial cell
BSA	Bovine serum albumin
BSCB	Blood-spinal cord barrier
C9-ALS	C9ORF72-ALS
CAU	Caucasian
CDH5	Cadherin-5
CHAT	Choline acetyltransferase
CLDN5	Claudin-5
CMT	Carrier-mediated transport
CNS	Central nervous system
CNTF	Ciliary neurotrophic factor
CSF	Cerebrospinal fluid
CTR	Control
DAPI	4’,6-diamidino-2-phenylindole

DHA	Dehydroascorbic acid
DIV	Dynamic in vitro models
DLB	Lewy body disease
DMEM	Dulbecco's modified eagle medium
DMSO	Dimethyl sulfoxide
DNA	Deoxyribonucleic acid
DPBS	Dulbecco's phosphate-buffered saline
DPDPE	D-pen^2, d-pen^5 enkephalin
DS	Down syndrome
EAAT	Excitatory amino acid transporters
EC	Endothelial Cell
EDTA	Ethylenediaminetetraacetic acid
EGF	Epidermal growth factor
EM	Endothelial medium
ETA/ETB	Endothelin receptors a/b
EW	Embryonic week
F-ALS	Familial amyotrophic lateral sclerosis
FBS	Foetal bovine serum
FDA	US food and drugs administration
FTD	Frontotemporal dementia
FZD	Frizzled receptors
G	G-force or relative centrifugal force
GAPDH	Glyceraldehyde 3-phosphate dehydrogenase
GDNF	Glial cell-derived neurotrophic factor
GFAP	Glial fibrillary acidic protein
GSH	Reduced glutathione
GSSG	Glutathione disulphide
H	Hours
HBSS	Hanks' balanced salt solution
HESFM	Human endothelial serum free medium
HIE	Hypoxic-ischaemic encephalopathy

HI-PSCS	Human induced pluripotent stem cells
HRE	Hexanucleotide repeat expansion
HUVECs	Human umbilical vein endothelial cells
ICC	Immunocytochemistry
IGF	Insulin-like growth factor i
INSR	Insulin receptor
IUGR	Foetal intrauterine growth restriction
IV	Intravenous
JAM	Junctional adhesion molecules
KO	Knock-out
LDH	Lactate dehydrogenase
L-DOPA	Levodopa
LEF	Lymphoid enhancer-binding factor 1
LPG	Lipoprotein glomerulopathy
LRP1	Low density lipoprotein receptor-related protein 1
MBD	DNA methyl-binding domain
MEM	Minimum essential medium
MIN	Minute
ML	Millilitre
MN	Motor neuron
MND	Motor neuron disorder
MRI	Magnetic resonance imaging
MS	Multiple sclerosis
N/A	Not applicable
NEST	Nestin
NG	Nanogram
NLS	Nuclear localization sequence domain
NMDA	N-methyl-d-aspartate receptor
NMO	Neuromyelitis Optica
NO	Nitric oxide
NP	Non-purified

NPC	Neuronal progenitor cell
NSC	Neural stem cell
NVU	Neurovascular unit
OCLN	Occludin
OCR	Oxygen consumption rate
OSA	Obstructive sleep apnoea
PBS	Phosphate buffered saline
PCR	Polymerase chain reaction
PD	Parkinson's disease
PDGF-B	Platelet derived growth factor subunit b
PET	Polyethylene terephthalate
PFA	Paraformaldehyde
PLVAP	Plasmalemma vesicle associated protein
POU5F1	Pou class 5 homeobox 1
PSP	Progressive supranuclear palsy
PTSD	Post-traumatic stress disorder
RA	Retinoic acid
RAGE	Receptor for advanced glycation end products
RBC	Red blood cell
RMT	Receptor-mediated transport
RNA	Ribonucleic acid
ROCK	Rho-kinase
ROS	Reactive oxygen species
RPL	Ribosomal protein l
RPM	Revolutions per minute
RT	Room temperature
RTT	Rett syndrome
S-ALS	Sporadic amyotrophic lateral sclerosis
SD	Standard deviation
SEM	Standard deviation of mean
SLC	Solute carrier transporter

SMAD	Transforming growth factor-beta signaling protein
SOD	Superoxide dismutase
SOD1-ALS	Superoxide dismutase 1-ALS
SVCT	Sodium-dependent vitamin c transporter
TBI	Traumatic brain injury
TC	Tissue culture
TCF	T cell-specific transcription factor
TEER	Trans-endothelial resistance
TGFB	Transforming growth factor beta
TJ	Tight junction
TJP1	Tight junction protein 1 or ZO-1
TNF	Tumor necrosis factor
TNFR	Tumor necrosis factor receptor
TRD	Transcriptional repression domain
UM	Unconditioned medium
UNK	Unknown
VEGF	Vascular endothelial growth factor
VWF	Von Willebrand factor
WT	Wild-type
XCI	X chromosome inactivation
XIST	X-inactive specific transcript
ZO-1	Zonula occludens protein or TJP-1

Annexes

Annexes: Contents

Annex 1: Review Article.....127

Blood–Brain Barrier Disruption and Its Involvement in Neurodevelopmental and Neurodegenerative Disorders

Annex 2: Research Article.....161

C9ORF72 patient-derived endothelial cells drive Blood-Brain Barrier disruption and contribute to neurotoxicity

Annex 1: Review Article

Blood–Brain Barrier Disruption and Its Involvement in Neurodevelopmental and Neurodegenerative Disorders

Ana Aragón-González [1,2], Pamela J. Shaw [1] and Laura Ferraiuolo [1,]*

[1]Sheffield Institute for Translational Neuroscience, University of Sheffield, SITraN, 385a Glossop Road, Sheffield S10 2HQ, UK; a.aragon@shefield.ac.uk or ana.aragon@uma.es (A.A.-G.); pamela.shaw@sheffield.ac.uk (P.J.S.)

[2]Facultad de Medicina, Universidad de Málaga, 29010 Málaga, Spain

*Correspondence: l.ferraiuolo@sheffield.ac.uk ; Tel: +44-(0)114-222-2257; Fax: +44-(0)114-222-2290

Citation: Aragón-González, A.; Shaw, P.J.; Ferraiuolo, L. Blood–Brain Barrier Disruption and Its Involvement in Neurodevelopmental and Neurodegenerative Disorders. Int. J. Mol. Sci. 2022, 23, 15271.

https://doi.org/10.3390/ijms232315271

Academic Editor: Hari Shanker Sharma

Received: 20 October 2022

Accepted: 30 November 2022

Published: 3 December 2022

Abstract: The blood–brain barrier (BBB) is a highly specialized and dynamic compartment which regulates the uptake of molecules and solutes from the blood. The relevance of the maintenance of a healthy BBB underpinning disease prevention as well as the main pathomechanisms affecting BBB function will be detailed in this review. Barrier disruption is a common aspect in both neurodegenerative diseases, such as amyotrophic lateral sclerosis, and neurodevelopmental diseases, including autism spectrum disorders. Throughout this review, conditions altering the BBB during the earliest and latest stages of life will be discussed, revealing common factors involved. Due to the barrier's role in protecting the brain from exogenous components and xenobiotics, drug delivery across the BBB is challenging. Potential therapies based on the BBB properties as molecular Trojan horses, among others, will be reviewed, as well as innovative treatments such as stem cell therapies. Additionally, due to the microbiome influence on the normal function of the brain, microflora modulation strategies will be discussed. Finally, future research directions are highlighted to address the current gaps in the literature, emphasizing the idea that common therapies for both neurodevelopmental and neurodegenerative pathologies exist.

Keywords: blood–brain barrier; neurodevelopment; neurodegeneration; therapies

1. Introduction

The blood–brain barrier (BBB) is a highly specialized and dynamic membrane formed by brain microvascular endothelial cells (BMVECs), astrocyte end-feet unsheathing the capillary, and pericytes embedded in the capillary basement membrane (BM), forming a functional element: the neurovascular unit (NVU) [1]. Due to its lipophilic nature, hydrophobic compounds and gases can diffuse across the BBB, but larger and hydrophilic compounds require specific transporters located within the barrier. A healthy BBB protects the brain from exogenous compounds and xenobiotics, filtering the blood flow [2]. Interestingly, there are BBB-absent regions in the central nervous system (CNS), including the circumventricular organs, the choroid plexus and the dura mater, allowing direct communication between them and blood [3–6]. These regions do not provide open circulation to the rest of the brain due to the presence of diffusion barriers such as the zonula occludens 1 (ZO-1) and glial fibrillary acidic protein (GFAP)-positive columnar cells between the area postrema (included in the circumventricular organs) and the nucleus tractus solitarius, which sends projections to the area postrema located in the brainstem [7].

As for brain formation and function, the neurodevelopmental period is a critical phase for the development of the BBB. This process will be briefly described to highlight the most important factors involved in each developmental step whose dysregulation may be implicated in various disorders [8].

BMVECs from the NVU are highly specialized cells and the major component of the barrier. They express important transporters such as ATP binding cassette (ABC) and synthesize relevant neurotransmitter molecules such as nitric oxide (NO), both of which are involved in neurodegenerative processes when dysregulated. Astrocytes, the most common cells in the brain, also have a relevant role in the BBB, secreting cytokines and exacerbating mechanisms contributing to neuroinflammation, a key player in both neurodevelopmental and neurodegenerative pathologies. In this review, the role of pericytes forming the barrier will be also discussed due to their part in the maintenance of BBB permeability. Moreover, basement membranes present in the BBB will be also described, offering to the reader a complete overview of the BBB anatomical structure [9].

To better understand the mechanisms by which the BBB could be altered, we will discuss the principal and most pathophysiological factors involved, including oxidative stress, hyperpermeability and, interestingly, the microbiota, dysfunction of which had been found in the context of neurodegenerative and neurodevelopmental disorders. Specific diseases such as amyotrophic lateral sclerosis (ALS), Alzheimer's disease (AD) and autism spectrum disorders (ASD) will be taken as examples to highlight concepts and failures in the BBB system [10].

Efforts to facilitate access of potential therapeutic agents across the BBB will be highlighted. Recent findings connecting the microbiome and CNS disorders open the pathway to microbiology-based therapies. Other methods such as molecular Trojan horses or nanotechnology-based approaches which use the barrier properties to achieve brain penetration will be also discussed. Finally, BBB breakdown in pathology will be examined as an opportunity for stem cell-based therapies.

The main objective of this review article is to highlight the common mechanisms between neurodevelopmental and neurodegenerative disorders, revealing their similarities and proposing the use of analogous therapies in both types of disorder.

2. Development of the Blood–Brain Barrier (BBB)

"Barriergenesis" comprises a multiple-phase process: angiogenesis, differentiation, and maturation. These phases overlap spatially, at the cell level, and physiologically, at the molecular level.

During **angiogenesis** (E9–E10.5 in mice and embryonic week (EW)-8 in humans [11]), endothelial progenitor cells (expressing the foetal liver kinase 1 receptor) from the perineural plexus invade the embryonic neuroectoderm following the concentration gradient of vascular endothelial growth factor (VEGF) and give rise to immature vessels [12]. VEGF is considered the major factor that controls brain angiogenesis. It is produced by cells in the subventricular neuroectoderm and reduced or absent neural VEGF results in impaired vascularization of the developing brain [13].

During this same period, the Wnt-β-catenin pathway plays an important role in the patterning and formation of the CNS. Neural progenitors express Wnt in the developing forebrain, the ventral regions of the neural tube, the dorsal spinal cord and the hindbrain. In particular, Wnt-7a and Wnt-7b have the broadest expression pattern in ventral regions of the developing CNS, and, in fact, Wnt-7b knock-out mice die by E11.5 [14].

Wnt ligands secreted by neural progenitor cells bind to frizzled receptors (FZD) expressed by endothelial progenitor cells responding to the VEGF gradient, leading to inhibition of β-catenin degradation via the proteasome. Subsequently, β-catenin accumulates in the cytoplasm and nucleus, where it induces transcription of target genes by interaction with transcription factors such as lymphoid enhancer-binding factor 1/T cell-specific transcription factor (LEF/TCF).

Wnt signalling activation leads to the transcription of BBB-related genes including those encoding glucose transporter 1 (Glut-1) and tight junction (TJ) molecules [15], such as *Cldn1* [16] and *Cldn3* [17] (Claudin). Hence, β-catenin is required for vessel formation as both the transducer of Wnt signalling and as a component of the adherent junctions (AJ) that join all the endothelial cells.

Some types of cells involved in BBB development, such as astrocytes, do not appear in a mature form until after birth. During the developmental phase, however, neural stem cells (NSCs), such as the radial glia, secrete transforming growth factor-β (TGF-β1) which plays a key role as a mediator of the interactions between glia and endothelial cells, contributing to the formation of the first blood vessels within the brain [18]. The interactions between these cells during this early phase give rise to the BBB, which in rodents is functional nearly as soon as it is established (E11 in mice), while TJs appear later in human development, at EW-14 [19].

Recent observations support the concept of ongoing barriergenesis in brain endothelial cells during angiogenesis [20,21]. Thus, barrier maturation in brain endothelial cells might not take place in two sequential phases as originally suggested [22].

Following BBB formation, the **differentiation** process (E15.5-E18.5 in mice) starts with pericytes and radial glia promoting barrier properties in the endothelial cells. Pericytes express the platelet-derived growth factor receptor β (PDGFR-β) at the endothelial surface, which acts as a signal for endothelial cells to be guided to the nascent vessel [23]. Pericyte recruitment to the developing endothelial capillaries is critical for the formation and maintenance of the BBB; in fact, PDGFR-β-deficient mice, which lack brain pericytes, die as a consequence of brain microhemorrhages [24]. Endothelial cell and pericyte interactions are mediated by bidirectional TGF-β–TGF-βR signalling. This signalling cascade leads to two crucial events: first, upregulation of endothelial N-cadherin, which promotes adhesion between pericytes and endothelial cells; second, pericytes are stimulated to deposit extracellular matrix components, such as angiopoietin-1 (Ang-1), contributing to basement membrane formation [25]. Moreover, Notch and sphingosine-1-phosphate signalling also contribute to the regulation of N-cadherin expression in brain endothelial cells [25,26]. The deficiency of PDGF-β or PDGFR-β leads to erroneous TJ distribution and increased vascular permeability [27]. As previously mentioned, radial glia contribute to the induction of barrier properties in endothelial cells, expressing SRC-suppressed

C-kinase substrate (SSeCKS) which decreases the expression of VEGF through transcription factor AP-1 (activator protein-1) reduction and stimulates the production of Ang-1 [28]. Ang-1 is essential for normal vascular development; it binds and activates the Tek/Tie-2 receptor by inducing its dimerization and tyrosine phosphorylation [29]. Additionally, Ang-1 enhances the TJ formation, limits BBB permeability and reduces the expression of leukocyte adhesion molecules. The radial glia are also involved in limiting BBB permeability, releasing sonic hedgehog protein (Shh) which activates hedgehog signalling in endothelial cells through the receptor Patched-1 (Ptc-1) [30] and upregulates TJ proteins (ZO-1, occludin, and cldn-5) [31].

Finally, the **maturation** and maintenance of the barrier is the last phase in BBB development. It takes place postnatally and the timing is species-dependent [32,33]. Maturation is accomplished through TJ protein expression and their redistribution within the barrier. In this phase, radial glia differentiate into mature astrocytes. Wnt signalling and astrocytes regulate TJ formation because of the FZD receptor expressed by the endothelial cells. BBB formation and maintenance are supported by TGF-β–TGF-βR and Ang-1–Tie-2 signalling through pericytes and endothelial cells. Retinoic acid (RA) also contributes to BBB maturation, enhancing expression of AJ and TJ proteins [34]. Maintenance of BBB integrity is supported by astrocytes, which also produce apolipoprotein E (ApoE). It was shown that ApoE knock-out mice present with a dysfunctional BBB and develop psychotic behaviour, suggesting a relationship between impaired BBB function and neuropsychiatric diseases [35]. Interestingly, ApoE4 is a major genetic risk factor for development of Alzheimer's disease (AD) [36]. In addition, astrocytes are the main cell type involved in the maintenance of the barrier, secreting Shh and Wnt in order to sustain BBB functionality throughout life [37].

3. Components of the Blood–Brain Barrier (BBB)

The neurovascular unit (NVU) has been described as a structure formed by microvascular endothelium, astrocytes, pericytes and neurons that are in physical proximity to the endothelium, basal lamina and parenchymal basement membrane. Each NVU component is intimately and reciprocally linked to each other, sharing several characteristics and establishing an anatomical and functional whole, which results in a highly efficient system regulating cerebral blood flow [38]. In this section, we will explore the main characteristics and functions of the NVU components.

3.1. Brain Microvascular Endothelial Cells (BMVECs)

BMVECs are a major cellular element of the BBB. They are extremely thin cells and present unique characteristics that distinguish endothelial cells of the brain from the vascular endothelium in the rest of the body, including tight junctions (TJs), absence of fenestrations, fewer or absent pinocytotic vesicles, expression of specialized transporters, and close association with other cell types comprising the NVU. These attributes allow them to tightly regulate the movement of ions, molecules, and cells between the blood and the brain [39].

The TJs are mainly composed of proteins such as ZO-1,-2,-3, occludins and claudins; adherens junctions (AJs), including cadherins, actinin and catenins, and junctional adhesion molecules, e.g., JAM-1. ZO-1 is located on the cytoplasmic side of the BMVEC plasma membranes and connects the TJs with the cytoskeleton. JAM-1, on the other hand, participates in TJs formation in conjunction with occludin and claudin and is involved in cell-to-cell adhesion. In addition, JAM-1 is involved in leukocyte migration. Therefore, its dysregulation has been associated with alterations of CNS immunity [40]. Overall, dysfunction of the molecular components of BMVECs are widely associated with increased BBB permeability, thus exacerbating some pathological mechanisms such as oxidative stress, neuroinflammation, stroke or trauma [41] that will be further discussed later in this review (see

Section 4). Additionally, BMVECs express two main types of transporters: efflux transporters [42] and highly specific nutrient/waste transporters [43]. Another remarkable difference between BMVECs and other endothelial cells is their higher content of mitochondria, which generate high levels of ATP used during active transport of ions and fluid [44,45].

Moreover, the quantity of leukocyte adhesion molecules is much lower in BMVECs compared to other endothelial cells, as these are involved in the interactions with leukocytes to regulate their transendothelial migration. In fact, the extremely low level of leukocyte adhesion molecules expressed in BMVECS is directly linked with the inability of immune cells to cross the barrier and enter into the CNS [40].

Interestingly, several biochemical studies have revealed the functional polarity present in the BMVECs, with different expression of enzymes, transporters, receptors and ion channels in the luminal and abluminal membrane surfaces of these endothelial cells to preserve brain homeostasis by controlling the exchanges between the blood and brain compartments [46].

Differences in enzymatic activity have also been found in BMVECs compared with other endothelial cells, with a high concentration of enzymes such as γ-glutamyl transpeptidase, alkaline phosphatase and aromatic acid decarboxylase. These enzymes take part in the assimilation of the neuroactive solutes originating from the blood, thus allowing BMVECs to metabolize drugs and nutrients for presentation to the brain [47].

BMVECs in Brain Vascular Contraction

BMVECs synthetize and release both endothelin-1 (ET-1) and NO which are in balance under healthy circumstances to maintain the function of the vascular tone. The disequilibrium of these molecules is involved in cerebral blood vessel dysfunction, such as in stroke [48]. ET-1 is one of the most potent vasoconstrictors known for mammalian blood vessels, with a relatively low concentration in plasma (0.2–5 pg/mL), while increased amounts have been reported in diseases such as hypertension and diabetes type 2 [49]. Endothelin receptors have been identified on platelets and blood vessels. Two subtypes of ET-1 receptors, ETA and ETB, have been described; however, the predominant subtype in the brain is B [50]. ETB opposes vasoconstriction by stimulating NO formation, acting as a feedback mechanism to limit the vasoconstrictor action of ET-1. NO inhibits platelet aggregation, the expression of adhesion molecules and the production of ET-1 [51]. The vasoconstriction mechanism through which ET-1 decreases the local brain flow is through platelet interaction, whereas a significant increase of ET-1 expression has been linked to haemorrhages [52]. Many physiological processes, including neurotransmission, are promoted by NO, which is mostly synthesized through endothelial NO synthase [53]. Interestingly, it has been reported that endothelial NO synthase knock-out mice have increased levels of amyloid-beta protein (Aβ) precursor, while expression of endothelial NO synthase and excess of NO have been associated with BBB disruption [54]. These data highlight the link between NO dysfunction, BBB disruption and some neurodegenerative disorders such as Alzheimer's disease (AD) [55].

3.2. Astrocytes

Astrocytes are the most abundant cells in the brain and play important roles in the establishment and maintenance of the BBB. They occupy a strategic position between capillaries and neurons. Astrocytic end-feet form a coating network around the brain vasculature, the glia limitans, and, together with endothelial cells and pericytes, they form the BBB, separating the bloodstream from the brain parenchyma. Astrocyte dysregulation is associated with neurodegenerative diseases such as

amyotrophic lateral sclerosis (ALS) [56] and AD [57] and paediatric neurological disorders such as Rett syndrome [58].

As mentioned in the previous section, astrocytes are in their immature form during BBB development; mature astrocytes, in fact, are not detected in the human foetal brain stem until the 15th week [59] and in foetal cortex until the 30th [60]. This late development, which continues even postnatally, offers a potential therapeutic window to reverse developmental dysregulation, thus making astrocytes an appealing therapeutic target.

Although the heterogeneity of the astrocyte population across the brain is well known, it is still poorly characterized and little is understood about its impact on BBB function. In the mature barrier, astrocytes secrete cytokines, growth factors and extracellular matrix proteins through their end-feet, including, in particular, proteoglycans of the lectican family and tenascins [61]. Other aspects of glial support include the signalling of reinforcing pathways such as sonic hedgehog protein (Shh), vascular endothelial growth factor (VEGF), angiopoietin-1 (Ang-1), retinoic acid (RA) [62]. The role of astrocyte-derived Shh was proposed in maintaining the BBB via a mechanism involving regulation of TJ protein expression by BVMECs [37]. Nevertheless, transcriptomic studies have begun to point out that post-mitotic astrocytes, and not BMECs, represent the primary responders to hedgehog signalling in the adult brain [63]. Astrocytes are also involved in strengthening the TJ, whose maturation is promoted by release of glial cell-derived neurotrophic factor (GDNF), an EC ligand for the GDNF family receptor alpha-1 (GFRA-1).

Furthermore, astrocytes play a crucial role in glutamate homeostasis, which is critical to maintain neuronal function and protect against excitotoxicity. Glutamate is known as the most abundant excitatory neurotransmitter in the mammalian nervous system, but its signalling is also important for the correct functioning of the BBB. Glutamate has been demonstrated to increase the permeability of BMVECs via activation of N-methyl-D-aspartate (NMDA) receptors [64,65]. For this reason, its clinical potential as a modulator of BBB permeability has been extensively explored in the context of neuroprotection and drug delivery [66]. Glutamate is also involved in blood flow regulation, since glutamate-mediated signalling prompts the release of NO from neurons, thus promoting vasodilation, and of arachidonic acid from astrocytes, which can have the double action of vasodilator or vasoconstrictor [67].

Considering the pivotal role of glutamate in the CNS and the injurious effects of its excessive accumulation in the synaptic cleft, astrocytes express excitatory amino acid transporters (EAATs), i.e., Na+-dependent glutamate transporters, in order to keep the concentration of glutamate tightly controlled in the extracellular space [68]. In addition, astrocytes are also involved in BM regulation by using ammonia in the synthesis of glutamine, metabolizing short-chain fatty acids, taking part in the regulation of brain nitrogen metabolism, and, finally, preventing the accumulation of ammonia, glutamine and glutamate in the CNS [69].

Another critical role of astrocytes in maintaining BBB function is the release of TGF-β, which regulates multiple biological processes, adult stem cell differentiation, immune regulation, apoptosis, and inflammation [70]. In addition to the pivotal role of TGF-β in TJ and blood vessel formation described above, TGF-β also downregulates endothelial anticoagulant factors, such as thrombomodulin, and increases blood flow under pathological conditions [71].

Similarly involved in fluid exchange and regulation, aquaporin-4 (AQP4) is the most abundantly expressed water channel in the brain and is predominantly expressed in the end-feet of astrocytes [72]. AQP4 regulates water permeability and plays an important role in neuroimmunological functions

too, but its role in brain physiology has remained elusive for years. AQP4 controls bidirectional fluid exchange [73] and has been linked to several pathological processes including paediatric brain neoplasms with dysfunctional BBB [74] and the neuroimmunological disorder neuromyelitis optica [75].

3.3. Pericytes

Pericytes coexist with the astrocytes in the abluminal compartment to maintain the BBB properties [76], located within the NVU between endothelial cells, astrocytes, and neurons. The relevant role of pericytes in the developmental phase of the barrier and their interaction with endothelial cells through PDGF-β signalling during the process has been described above.

It was shown that the number of pericytes involved in the barrier inversely correlates with its permeability, thus a decrease in the number of pericytes correlates with an increase in the BBB permeability [77]. In addition, reduction in pericyte coverage across the BBB is inversely correlated with ageing [78] and neurodegeneration, as in ALS [79].

In the case of pericyte loss, as it occurs in ageing, brain injury or neurodegeneration, these cells can actively adapt to ensure endothelial coverage by extending their wide-reaching processes [80]. Pericytes are major regulators of cerebral blood flow due to their sensitivity to glutamate signalling, which promotes the release of vasodilators such as NO and prostaglandin E2 [81]. They also help direct astrocyte foot projections and are responsible for reducing levels of leukocyte adhesion molecules [82].

Additionally, pericytes control the expression of TJ and AJ proteins and their alignment. They also regulate transendothelial vesicle trafficking across the barrier which is implicated in the transport of nutrients and essential molecules [82]. These cells also play a major role in blocking the entrance of xenobiotics, including therapeutic compounds, into the brain, which makes them a potential target for drug delivery [83].

The role of pericytes in neuroinflammation has been demonstrated by Olson et al. [84] in conditional PDGFR-β knock-in mice. These researchers showed the way in which a PDGFR-β-induced immune response could modulate the inflammatory properties of endothelial cells, leading to increased leukocyte adhesion and transmigration. They also revealed that amplified PDGFR-β signalling led to higher pericyte coverage of blood vessels and induced changes in pericyte differentiation. On the other hand, pericyte degeneration results in BBB breakdown with the accumulation of neurotoxic molecules leaking from the blood [82].

3.4. Basement Membrane (BM)

The BM is the non-cellular component of the barrier and it is a unique form of extracellular matrix. Its main functions are structural support, cell anchoring and signal transduction [85]. There are two types of BMs separating endothelium from astrocytes. One of the membranes is composed of fibronectin, collagen type IV, nidogen, perlecan and laminin and it is denominated as the endothelial BM. The other one is the perivascular glia limitans, also known as astroglial or parenchymal BM and is formed by fibronectin, agrin and laminins [86]. Consequently, the most important biochemical components of the BM are collagen type IV, fibronectin and laminin.

Collagen-IV and fibronectin are secreted by the cellular components of the NVU. **Collagen-IV**, the most abundant component of the BM, maintains BM stability by retaining other protein components such as laminin, perlecan and nidogen. Six collagen-IV isoforms have been identified of which collagen-IV α-1/2 are present in almost all BMs and are highly conserved across species [87]. Nonetheless, there

is evidence that collagen-IV is not necessary for early embryonic development, but it is indispensable for the structural integrity of the BMs at later stages [88]. To exemplify the importance of collagen-IV α-1 in BMVECs and astrocytes, mutations affecting the coding gene contribute to cerebrovascular defects resulting in intracerebral haemorrhages [89].

On the other hand, **fibronectin** stimulates the proliferation and survival of the endothelial cells in the BBB [90] and, in fact, both fibronectin and collagen-IV knock-out mice are embryonically lethal. Defects in the mesoderm, impaired neural tube and vascular development are caused by the absence of fibronectin [91], while collagen-IV deficient mice display structural deficiencies in the BMs with impaired integrity of Reichert's membrane, a basement heath between the parietal endoderm cells and trophoblast cells.

BMVECs, pericytes and astrocytes synthetize different **laminin** isoforms. There is a cell-specific expression pattern, hence laminin shows differential distribution between endothelial and parenchymal BMs. As an example, astrocytes produce different laminin isoforms depending on their BM location. Hence, laminin-211 is most abundant in the parenchymal membrane and laminins-411/511 are predominantly expressed in the endothelial membrane [92]. Deletion of laminin full isoforms is lethal during embryonic development. Similarly to fibronectin mutant mice, laminin-211 deletion leads to intracerebral haemorrhage and also age-dependent BBB breakdown [93].

To analyse the significance of laminin in the regulation of the BBB, Menezes et al. [94] generated mice lacking expression of the laminin α2 subunit within the laminin-211 heterotrimer expressed by astrocytes and pericytes. They reported altered integrity and composition of the endothelial basal lamina, inappropriate expression of embryonic vascular endothelial protein MECA-32, reduced pericyte coverage, and TJ abnormalities. Their data reveal the role of laminin in regulating the interactions of the NVU cellular components within the BBB.

The effect that lack of laminin chains has on the BM and BBB integrity was explored in several studies, but the mechanisms driving these phenomena are still largely unknown (see Yao et al. for a detailed review [95]).

3.5. Transport across the BBB

The BBB is lipophilic in nature, hence hydrophobic molecules and gases such as CO2 or O2 can cross it by passive diffusion [96]. However, only solutes of a molecular weight below 400 Daltons (Da) are able to circulate freely through the BBB endothelium [97]. Because it isolates the brain from the rest of the body, many polar nutrients are needed but cannot diffuse across the barrier. Thus, the main factors that influence the ability of circulating molecules to cross the BBB are their polarity and their size.

Additionally, the TJs forming the BBB act as a barrier to segregate transporters to the abluminal or luminal membrane face, thus preventing their movement across the endothelium and maintaining BBB polarity. Some transporters are present on both sides of the membrane or just in one of them, depending on the brain requirements for nutrients and the region [76].

In addition to passive transport, multiple molecules can be shuttled across the BBB through a variety of ion channels and selective transporters. The main transport mechanisms can be divided into endothelial cell and pericytal transport with machineries across both cell types including active efflux [98], carrier-mediated (CMT [99]) ion-transport [100] and receptor-mediated transport (RMT) [101], with exception of active efflux, which is a specific property of BMVECs. In addition to these, there is also a BMVEC/pericyte independent mechanism, vascular-mediated transport [102].

As mentioned before, BMVECs express two main categories of transporters: efflux transporters (i.e., ABC- and EEAT-transporters), which transport lipophilic compounds, and nutrient transporters, regulating the exchange of nutrients and removal of waste products. For example, essential nutrients such as glucose or amino acids are transported across the barrier by specific solute carriers to supply the essential substrates for brain metabolism [103].

These transport mechanisms and their functional relevance in health, together with their role in many disorders such as AD [104], ALS [105], Huntington's disease [106], schizophrenia [107], Parkinson's disease [108] and microcephaly [109], among others, have been extensively described previously [110].

4. Mechanisms Altering Blood–Brain Barrier (BBB) Function

The BBB is a complex system where cells and structural proteins create an environment in which any alteration can affect the normal activity of the others. For that reason, stress mechanisms such as oxidation, mechanical insults or genetic factors may result in an imbalance of the BBB. Several elements affecting the neurovascular unit components have been described elsewhere [111], but in this review we will focus on those most relevant for their impact on neurodegenerative and neurodevelopmental diseases (Figure 1).

4.1. Genetic Factors

4.1.1. APOE

APOE (chromosome 19) encodes apolipoprotein E which binds to a specific liver and peripheral cell receptor and is essential for the normal catabolism of triglyceride-rich lipoprotein constituents [112]. In the CNS, APOE is expressed mainly in astrocytes [113], but also microglia, vascular mural cells and choroid plexus cells. APOE modulates multiple pathways that affect cognition, thus involving lipid and glucose metabolism, synaptic function, neurogenesis and neuronal degeneration, neuroinflammation, mitochondrial function, tau phosphorylation, and Aβ metabolism. Moreover, APOE has a crucial role in amyloid beta-protein (Aβ) clearance, aggregation and deposition [114].

The ε4 allele of APOE (APOE4) constitutes the major susceptibility gene for late-onset Alzheimer's disease (AD) [36], and, in fact, it has been associated with both decreased neuroprotection and increased neurotoxicity [115].

In the context of the BBB, APOE4 affects barrier function by activating the pro-inflammatory protein cyclophilin A via the nuclear factor-kB (NFkB)–matrix-metalloproteinase-9 (MMP-9) or NF-kB-MMP-9 pathway in pericytes. Studies with transgenic APOE2 and APOE3 mice have indicated that ApoE2 and ApoE3 maintain the BBB structure by suppressing the NF-kB-MMP-9 pathway through activation of LRP1. On the contrary, ApoE4 fails to activate this protective mechanism, thus triggering tight junction (TJ) and basement membrane (BM) degradation, and therefore BBB breakdown [116]. This is supported by post-mortem human frontal cortex tissue samples where the pericytes of APOE4 carriers showed loss of integrity of the BBB [117].

That loss of typical BBB function is an important upstream event in AD and is supported by the fact that, although atrophy of the hippocampus is considered an early biomarker of disease [118], more recent studies demonstrate that BBB breakdown occurs even before atrophy [119]. This early BBB breakdown might appear as cerebral microbleeds, which are frequently seen in AD patients, particularly in APOE4 carriers, which involve severe BBB breakdown [120]. This suggests that BBB failure might precede neurodegeneration. Interestingly, APOE3 carriers have a reduced rate of BBB failure, in addition to a reduced risk for the development of AD [121].

The relevance of APOE is not only studied in AD progression, but it has also been related to ageing and neurodegeneration and in pathologies such as vascular dementia, Parkinson's disease (PD) or ischaemic stroke, where APOE seems to participate in the progression of these diseases, although the underlying mechanisms of action are still unclear [122].

In conclusion, more research is needed to clarify not only the role of APOE4 in neurodegeneration and ageing, but also in overall brain functioning.

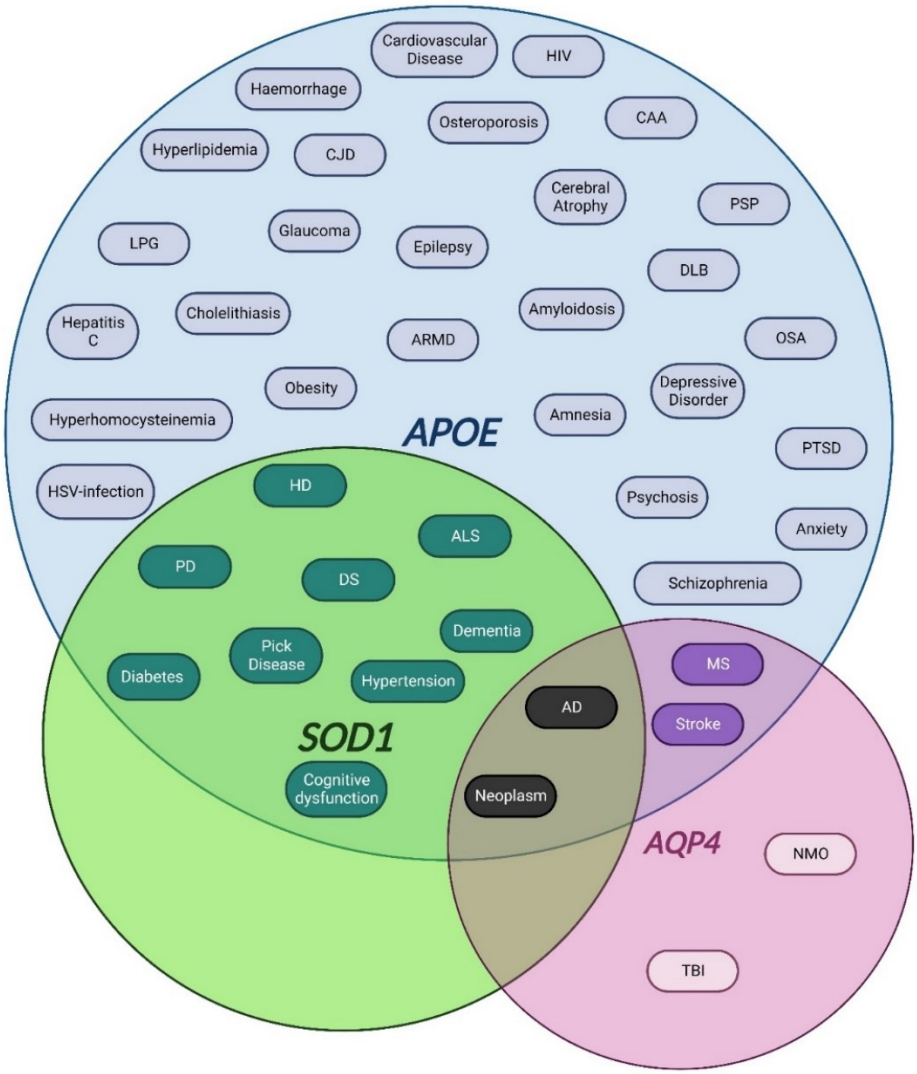

Figure 1. APOE, SOD1 and AQP4 genes are involved in multiple brain disorders and other pathologies. To create the Venn Diagram, diseases reported in ten or more research studies were selected. All the data related to APOE, SOD1, AQP4 and their variants associated with human diseases were explored in the platform DisGeNET. Acronyms used: Age-related Macular Degeneration (ARMD), Alzheimer's Disease (AD), Amyotrophic Lateral Sclerosis (ALS), Congenital Aural Atresia (CAA), Creutzfeldt–Jakob disease (CJD), Down Syndrome (DS), Herpes Simplex Virus Infections (HSV-infection), Huntington Disease (HD), Traumatic Brain Injury (TBI), Lewy Body Disease (DLB), Lipoprotein Glomerulopathy (LPG), Multiple Sclerosis (MS), Neuromyelitis Optica (NMO), Parkinson's Disease (PD), Post-Traumatic Stress Disorder (PTSD), Progressive Supranuclear Palsy (PSP), and Obstructive Sleep Apnoea (OSA).

4.1.2. SOD1

SOD1 (chromosome 21) encodes for the enzyme copper/zinc superoxide dismutase 1. SOD1 is widely expressed throughout the human body, particularly in liver, because of its detoxifying function, and in the CNS, probably due to the high metabolic rate in the region. SOD1 is located predominantly in the cytoplasm, but some pathogenic variants gradually aggregate and accumulate in mitochondria [123]. Mutations in SOD1 can cause conformational instability or misfolding of the SOD1 protein, and comprise the second major genetic risk factor associated with amyotrophic lateral sclerosis (ALS), accounting for 20% of familial ALS (fALS) cases [124].

Although rodent models have clarified that in general SOD1 mutations are not causative of ALS through a loss of function, some specific mutations result in decrease or loss of enzymatic activity and thus insufficient degradation of ROS [125]. The consensus is that SOD1 mutations cause ALS through a complex toxic gain of function which leads to an increase in oxidative stress, protein misfolding and aberrant protein interactions [126].

In terms of BBB function, mutant SOD1 rodent models develop a leaky BBB with higher permeability, enlarged astrocytic end-feet, interrupted BMs associated with a reduction of BMVECs and astrocytes, thus leading to oedema and microbleeds. This pathological phenotype is also observed in ALS patients [127].

SOD1 dysfunction has been linked not only with ALS. Due to triplication of chromosome 21, this protein is highly overexpressed in brains of patients with Down syndrome resulting in increased production of H2O2 [128]. This affects mainly the immune response and the microbiome through modification of signalling pathways leading to activation of phagocytosis as well as an imbalance in the concentration of superoxide free radicals [129]. Hence, greater SOD1 activity may impair neutrophil chemotaxis, thus increasing the risk of bacterial infections in patients [130].

4.1.3. AQP4

As previously mentioned, AQP4 (chromosome 18) encodes a water-selective channel 4 in the plasma membrane, the major water channel within the brain, which is concentrated in astrocytic foot processes at the BBB [131]. Apart from water, AQP4 conducts aquaglyceroporins that mediate diffusion of water, glycerol, and other small molecules without charge across membranes [73]. This channel is considered responsible for brain water homeostasis and central plasma osmolarity regulation, with a possible effect on the activity of inward rectifier potassium channel 4.1 (KIR4.1). AQP4 and KIR4.1 are co-expressed and together compose a multifunctional unit participating in the clearance of water and K+ following neural activity [132]. Additionally, this water channel appears to participate in neurotransmission [133], synaptic plasticity [134], astroglial cell migration during glial scar formation, stroke and tumours or abscesses [135]. AQP4 is known to be altered in several neurological conditions, including tumours, neuromyelitis optica [136], autism spectrum disorders [137], AD, ALS, multiple sclerosis (MS), stroke, epilepsy and as a consequence of traumatic brain injury [138].

Moreover, AQP4 is also related to Aβ clearance in AD. To explore the role of this channel in AD pathology progression, an AD mouse model lacking Aqp4 was used by Smith et al. to show that Aqp4-deficient mice displayed increased amyloid deposition, impairment of peri-plaque astrocyte structural organization and recruitment of microglia to plaques, thus amplifying the damage inflicted upon neurons adjacent to the plaques [139].

Some studies have also associated AQP4/KIR4.1 alteration to neurodevelopmental disorders. As previously highlighted, AQP4/KIR4.1 are key modulators of brain homeostasis, which is particularly critical during neurodevelopment. Disruption of the AQP4/KIR4.1 balance is likely to facilitate brain oedema formation possibly resulting in an increased risk for sudden infant death syndrome. Indeed, Opdal et al. conclude in their research that AQP4 may be a predisposing factor for this disorder [140].

In support of this hypothesis, a recent publication has explored the upregulation of AQP4 in a double knock-down mouse model with promising results when rescuing the channel activity by an enhancer. The authors suggest a pivotal role of AQP4 in suppressing oedema formation by maintaining BBB integrity and upregulating TJs [141].

4.2. Oxidative Stress

Oxidative stress is a phenomenon caused by an imbalance in the production and accumulation of reactive oxygen species (ROS) in cells and tissues and the ability of the biological system to detoxify them [142]. The most common ROS are superoxide anions (O2−), hydrogen peroxide (H2O2), hydroxyl radicals (.OH) and oxygen (O2). They are generated by physiological cell metabolism; in fact, the mitochondria are considered a primary site of ROS production from aerobic respiration. Increased oxidative stress has been extensively linked with different kinds of disorders such as cancer and diabetes or ALS and PD [143]. ROS sources can be also exogenous and can be found in pollutants, tobacco, xenobiotics, ultraviolet radiation, pesticides, etc. These particles can trigger the production of inflammatory cytokines, e.g., tumour necrosis factor-alpha (TNF-α) that operate through ROS-related mechanisms within the cell [144], involving neuroinflammation and oxidative stress.

In addition, ROS have been demonstrated to cause BBB dysfunction. One example is the way alcohol abuse can induce the activation of myosin light chain kinase, leading to phosphorylation of TJ proteins and enhanced monocyte migration across BBB, thus decreasing BBB integrity [145]. Similarly, ingestion of alcohol during pregnancy is associated with developmental diseases such as foetal alcohol syndrome. In this condition, neonates develop impairment of BBB function and neurodegeneration due to the increased production of ROS in the brain by catalase-mediated acetaldehyde production from alcohol [146].

4.2.1. Antioxidant Defences

The role of the antioxidants in combating oxidative stress is vital for physiological brain function. The reduction of this natural defence is a common factor in multiple pathologies which has attracted a lot of interest especially with the demographic increase in neurodegenerative diseases within the population in recent years [147].

Enzymes

Antioxidant enzymes constitute one of the principal intracellular defence mechanisms. The **Nrf2** (nuclear factor erythroid 2–related factor 2) is a transcription factor constitutively expressed in all tissues [148]. Nrf2 plays a key and complex role in the response to oxidative stress, it is a master regulator of a large transcriptional response to cellular stress. Nrf2, in fact, recognises an enhancer sequence known as the antioxidant response element (ARE), which is upstream of several antioxidant and anti-stress genes [149]. In addition, as part of its transcriptional response, Nrf2 downregulates the expression of some TJ proteins such as occludin and cldn-18 [150].

The therapeutic potential of Nrf2 activation has been and is still being explored in multiple disorders, including PD, AD and ALS, where various disease models highlight its importance in the pathophysiology of the disease [151].

Another important enzyme family implicated in the antioxidant defences is the family of the SOD proteins. SOD1 is a cytoplasmatic protein that catalyses the dismutation of superoxide anions to hydrogen peroxide and, interestingly, mutations in this enzyme have been the first associated with ALS. On the contrary, the SOD2 isoform is located in the mitochondria and dismutates superoxide to the less reactive hydrogen peroxide [152]. SOD2 reduction, as in the Sod2+/− mouse model, accelerates the onset of behavioural changes for AD. Interestingly, the reduction was associated with both a decrease in Aβ deposition in the brain parenchyma and an increase in amyloidosis in the brain vasculature [153]. Lastly, the isoform SOD3 is the extracellular anti-oxidant member of the family, which can be detected in fluids such as plasma or CSF. Furthermore, it has been shown that SOD3 synthesis by human bone marrow-derived mesenchymal stem cells is regulated synergistically in response to the inflammatory mediators TNF-α and interferon-gamma (IFN-γ). This induction in response to inflammation provides further evidence of the role of the SOD3 in preventing neuronal and axonal injury against NO or microglial-induced damage [154]. Additionally, SOD3 has been explored as a potential biomarker for neuroinflammation and neurodegeneration, since an increased level was reported in CSF from ALS patients [155].

Similarly, catalase is another important antioxidant enzyme which is ubiquitously expressed in tissues that utilise oxygen. By using an iron or manganese cofactor, it catalyses the reduction of hydrogen peroxide produced in the detoxifying cascade by SOD1 to form water and oxygen [156]. As previously mentioned, Shaw et al. demonstrated an increase of SOD3 in ALS along with the upregulation of catalase.

Non-Enzymatic Anti-Oxidants

Glutathione is a tripeptide containing cysteine, glycine and glutamic acid and its synthesis is carried out by two enzymes, glutamate cysteine ligase and glutathione synthetase. Glutathione can be found in two states, reduced (GSH) and oxidized (GSSG), and the ratio of GSH and GSSG is indicative of the redox status of the cell. In the brain, glutathione is considered the main antioxidant molecule, with an approximate concentration of 2 mM, much higher than in the CSF, where the concentration is only 4 µM, or in the plasma where it is around 2 µM [157]. Glutathione has critical roles in cellular antioxidant defence, including neutralizing oxygen, hydroxyl radicals, and superoxide radicals. In the brain, it also takes part in the detoxification of metals such as mercury, the regulation of cellular proliferation and apoptosis, mitochondrial function and the maintenance of its DNA, and it acts as a cofactor for signal transduction [158]. In the CNS, astrocytes have an elevated concentration of glutathione compared to neurons and they also secrete this molecule into the extracellular space for protection of neurons [159]. Huang et al. investigated the GSH shuttle from astrocytes to endothelial cells. GSH was found to preserve endothelial barrier stability by maintaining TJ proteins and preventing injury-induced TJ phosphorylation. In addition, supplementation with GSH analogues showed positive effects in supporting brain vascular stability and homeostasis [160].

Another important player in this regard is vitamin C or ascorbic acid, which is considered a vital antioxidant within the brain where it is more concentrated compared to blood levels. Besides the antioxidant role of ascorbic acid, this molecule is also implicated in other functions including neuronal maturation and differentiation, collagen maturation and modulation of neurotransmission. Vitamin C can cross the BBB in two ways, through the sodium-dependent vitamin C transporter (SVCT) or in its reduced form as dehydroascorbic acid (DHA) through the Glut family transporters [161]. Various studies have demonstrated the impact of vitamin C on neurodegenerative and neurodevelopmental disorders.

In particular, the importance of vitamin C during pregnancy to support normal foetal growth and development has been extensively explored [162]. For example, vitamin C deficiency has been linked to severe impairment of vascular development due to its relevance in angiogenesis, e.g., in collagen maturation [163]. Interestingly, a recent study reported that the parenteral administration of vitamin C significantly attenuates disruptions of BBB and protects TJs (i.e., Cldn-5 and ZO-1) in a rat model of cerebral ischaemia [164].

Vitamin E is also implicated in several cellular anti-oxidant defence mechanisms. In fact, it has been reported that a deficiency of vitamin E can trigger increased levels of oxidative stress, thus causing a disruption of the integrity of the BBB with important consequences for CNS function and maintenance [165]. Moreover, vitamin E supplementation seems to restore neuromuscular function in rodents and humans [166]. In this context, vitamin E deficiency has been linked with the pathogenesis of motor neuron diseases where oxidative stress plays a key role, including free radical damage to motor neurons in ALS [167]. In vivo studies assessing the effect of vitamin E treatment on disease progression in ALS mouse models are controversial, while some studies found a beneficial effect as vitamin E could reduce oxidative stress markers after 3 months of vitamin E supplementation with riluzole, even though no improvement of patient survival was reported [168]. Other studies have shown little or no effect and advised further investigation [169].

In summary, this evidence suggests a strong relationship between oxidative stress, BBB impairment and neuronal injury in various neurodegenerative and neurodevelopmental disorders.

4.3. Neuroinflammation

Neuroinflammation is a key pathophysiological factor in the exacerbation of neurodegeneration, but is also implicated in neurodevelopmental disorders and in BBB impairment [170]. The mechanisms by which neuroinflammation may disrupt the BBB are not fully understood. However, activation of microglia, astrocytes and endothelial cells leading to the secretion of pro-inflammatory cytokines such as TNFα and interleukin-1 beta (IL-1β) have been demonstrated as components of neuroinflammation [171]. In addition, increased expression of endothelial adhesion molecules, modifications of TJ proteins and upregulation of matrix metalloproteinases which increases BBB permeability by degrading TJs and extracellular matrix components of the endothelial BM have been described [172]. All these events lead to BBB leakiness, which in turn allows pathogen and immune cell invasion.

Immune cell infiltration and leakage of cytokines from the blood may aggravate brain damage after brain injury or under hypoxic conditions. Experiments using cromoglycate, a mastocyte stabilizer which inhibits cell degranulation, resulted in decreased BBB opening, reduced glial activation and neuronal death, allowing long-term neuroprotection [173]. Several studies have reported acute dysregulation of the immune system in ASD patients including chronic neuroinflammation. For example, elevated levels of pro-inflammatory cytokines such as IFN-γ, IL-1β, IL-6 and TNF-α and chemoattractant protein-1 (MCP-1) from macrophages accompanied by accumulation of microglia and astrocytes around the blood vessels have been reported in post-mortem ASD brain samples as reviewed by Bjorklund et al. [174]. Similar pathology has been described in several neurodegenerative diseases such as AD, PD or ALS, where activated microglia and reactive astrocytes exacerbate the inflammatory cascade and the disruption of the BBB [175].

However, the physiological role of inflammation cannot be overlooked, as clear evidence supports the idea that neuroinflammation may be favourable in the acute stage of traumatic brain injury to clear damage and set the stage for remodelling events [176].

4.4. Injures to the BBB

As highlighted earlier in this review, correct filtration of solutes, chemicals and cells through the BBB is essential for CNS homeostasis and physiological function, while several studies have implicated BBB disruption in neurodegenerative processes. One of the most common events reported in several neurodegenerative conditions is immune cell invasion from the blood stream, as observed in post-mortem CNS tissue from ALS patients. Studies have reported infiltration of mast cells and neutrophils along the motor pathways and at the neuromuscular junction, mediating degeneration [177]. Although some studies suggest that disruption of the BBB is an early event in ALS and others indicate that BBB hyperpermeability is involved in later disease stages, this process of BBB impairment has been associated with motor neuron degeneration [178]. Less debated is the involvement of microbleeds, with erythrocyte extravasation and brain infiltration by peripheral macrophages and neutrophils in AD post-mortem samples, which suggest that the brain's innate immunity is activated; this may exacerbate the neurodegenerative process [179]. Moreover, cerebral microhaemorrhages or microbleeds are known to occur in cerebrovascular-linked neurodegeneration, dementia and ageing. Although microbleeds have been linked with neurodegeneration [180], it is still unclear whether they precede and cause neuronal damage or whether they are a result of the neurodegenerative process.

One of the main mechanisms causing BBB damage is **traumatic brain injury (TBI)**, which encompasses a complex pathogenic process that results from primary and secondary injuries, thus leading to temporary or permanent neurological deficits [181]. Consequently, these processes greatly alter the normal functional interactions between glial cells and the cerebrovascular endothelium, including the expression of transporters and TJs across the BBB and increased oxidative stress among other pathophysiological processes [182]. Disruption of the BBB is such an important component of TBI-related neurodegeneration that the BBB is has been proposed as a target for therapeutic intervention.

In contrast, **hypoxic-ischaemic encephalopathy (HIE)** is the major cause of brain injury in neonates, resulting from oxygen and/or blood flow deficiency during the gestational period. As in TBI, the brain's response to global hypoxia-ischaemia is a multistep process. After an initial phase of cerebral flow alteration and vasoconstriction resulting in oedema [183], processes such as neuroinflammation, mitochondrial permeabilization and further oxidative stress take a central role [184]. Similarly to what happens in TBI, the hypoxic process causes disruption of TJ proteins and an increase in BBB permeability. These events are mediated by pro-inflammatory cytokines such as TNF-α and interleukins; common factors in neuroinflammation and also implicated in neurodegeneration [185].

Another gestational complication that compromises the BBB is **foetal intrauterine growth restriction (IUGR)**, affecting up to 10% of pregnancies and considered as the second most common cause of perinatal mortality. Most often it results from chronic hypoxia in utero caused by placental dysfunction, which entails a reduction in the transfer of oxygen and nutrients from the mother to the foetus, damaging the brain in several ways, with impairment of brain growth, vascular development and severe alterations of neurovascular unit organization [186]. Castillo-Melendez et al. reported a reduction in pericytic and astrocytic coverage and reduced BBB integrity in a lamb model of IUGR. These alterations may lead to cognitive impairment, defects in short term memory, speech delay, abnormal behaviour as attention deficit hyperactivity disorder or ASD, among others [187]. More long-term investigation is needed to better understand the implications in adult life, for example a higher predisposition to suffer from neurodegeneration for IUGR infants (see Kesavan et al. for a comprehensive review of IUGR and its complications [188]).

4.5. Gut–Brain Axis: Microbiota

During the last decade, increased interest in the importance of the gut microbiota in neuronal development and behaviour as well as neurodegeneration has created a "paradigm shift in

neuroscience" by indicating that the gut may play a pathophysiological role in several human brain diseases, including ASD, anxiety, depression, and chronic pain [189,190]. The emerging literature has demonstrated bidirectional signalling between the brain and the gut microbiome involving multiple neurocrine and endocrine signalling mechanisms [191].

An obvious area of investigation are the molecules involved in the communication between the gut microbiome and the brain. Mayer et al. have carefully reviewed this aspect, highlighting the endocrine, neurocrine and inflammatory-related signals generated by the gut microbiota that can affect the brain of mice. In turn, the brain can influence the microbial composition and function in the gut via endocrine and neural mechanisms including sensing luminal metabolites by intestinal enteroendocrine cells and communicating to the brain via activation of the vagus nerve by hormones and neurotransmitters, and via neural routes such as neuroepithelial connections [191,192].

Moreover, microbiota have been proposed to be involved in BBB modulation in health and its dysregulation could contribute to BBB dysfunction in neurodegenerative disorders, e.g., PD [193], and neurodevelopmental disorders, e.g., ASD [194]. Recent studies have highlighted a relationship between ASD, inflammation and the gut microbiome. ASD patients have been reported to demonstrate microbiota alterations and gastrointestinal abnormalities. The disruption of intestinal barrier integrity is implicated in both immune and inflammatory responses. What is even more interesting, research conducted on animals showed that the composition of gut microbiota also influences the integrity of the BBB, with evidence that the gut microbiota affects the prenatal development of the BBB and its permeability later in life [195]. Hsiao et al. found that Bacteroides fragilis caused an increased expression of the pro-inflammatory cytokine IL-6 in the colon [196]. In relation to this, one could speculate that if pregnant women experienced infections during critical periods of pregnancy, this could trigger systemic inflammation and influence the neural development of the developing foetus.

Interestingly, there is also a new field in neurodegenerative research related to the **oral microbiome** [197]. The mechanism of action is similar to that previously described, where oral microbiota could be transported from the mouth to the brain through the bloodstream during brushing, flossing, chewing, or toothpick use in patients with periodontitis, causing bacteraemia [198]. In addition, the increase in pro-inflammatory responses can weaken the BBB, promoting the penetration of pathogens as previously mentioned. In this context, elevated levels of periodontal disease bacteria were found in AD patients. Recent studies have identified oral microbiota that produce Aβ, referred to as microbiome-derived amyloid. This can access the rest of the body and may be able to promote chronic CNS pathologies with amyloidogenic features such as AD [199]. Studies in rodents also suggest that infections leading to an increase of the brain inflammatory state during early life and adulthood can promote cognitive decline and neurodegeneration progression in later life. In addition, they demonstrated that pathogen-free conditions slow the onset of neurodegeneration in transgenic mice [200].

To conclude, the essential role of the microbiome in health and disease may provide new insights in the field; despite the fact that our knowledge of this complex brain–gut microbiome cross-talk is currently limited, there is research impetus to generate greater understanding of this system in health and disease.

5. Potential Therapies

The unique properties of the blood–brain barrier (BBB) not only confer cerebral protection from toxic insults, but also underpin a major challenge to drug delivery within the CNS. Several drugs have been

developed to target CNS disorders but cannot cross the BBB. Therefore, great effort had made to design improved access to the CNS of potential therapeutic agents.

Even though the circumventricular organs were described by some researchers as “brain windows” due to the lack of BBB [3–6], it should be noted that in these regions the capillary endothelial cells display higher enzymatic activity which limits the entry of neurotransmitters, toxins and drugs, thus forming an “enzymatic barrier” [201].

As Dong. et al. reviewed extensively, there are multiple strategies for brain drug delivery that can be summarized into three main classes: neurosurgical-based, chemistry-based and biology-based strategies. The first is an invasive method involving intracranial surgery, the others are based on increasing the lipid solubility of the drug or the reformulation of molecules to cross the barrier utilising endogenous transporters within the BBB [202]. Lately, stem cell-based techniques are being considered a powerful therapeutic resource for some disorders (Figure 2).

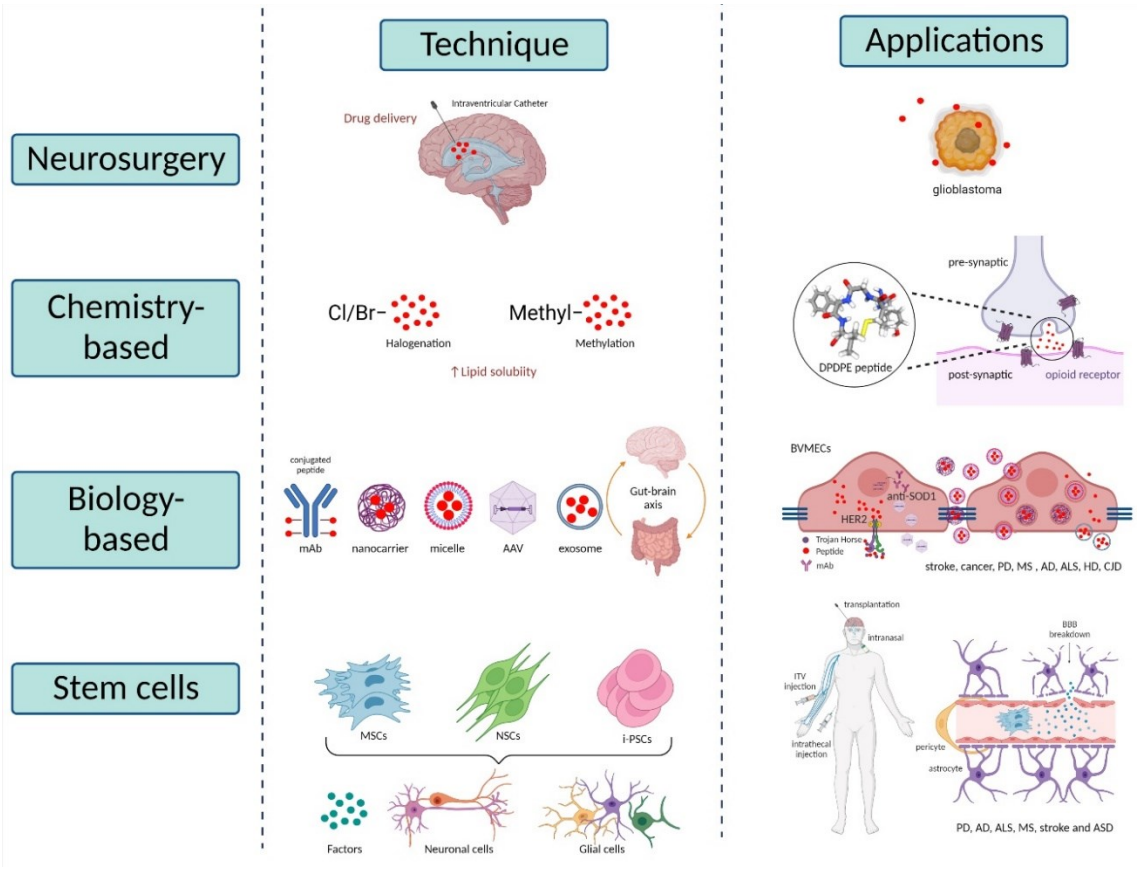

Figure 2. Main potential therapies and their most extended applications. The potential therapies described here are: neurosurgery [203,204], chemistry-based [202, 205-207], biology-based [208-236] and stem cell-based [237-255] approaches. Due to the brain’s lack of a lymphatic system, the drugs administrated by neurosurgical techniques preferentially move along white matter tracts, thus are widely utilised in glioblastoma treatment. Chemistry-based therapies are made to increase drug solubility and targeting scope, such as lipophilicity modulation, halogenation or methylation. Chemical approaches and biology-based therapies, as Trojan Horse technology or exosomes administration are often combined to treat a wide range of neurological disorders. Stem cells can exert their therapeutic effects either through their neurotrophic capacity or through cell replacement. This figure has been designed as a summary of the Potential Therapies section; please refer to the text for further details. This figure was created using biorender.com.

5.1. Neurosurgical-Based Techniques

With the administration of drugs by intracerebroventricular infusion, the compounds arrive at the ependymal surface and their concentration in the brain parenchyma decreases exponentially with the distance from the ependymal surface. On the other hand, with the delivery by intracerebral implantation, the drug distribution is restricted to the site of delivery and, consequently, the therapy may be restricted to a small region within the brain. Similar diffusion problems have been reported with the convection-enhanced diffusion technique, which aims to replace diffusion with convection. Nevertheless, these are promising techniques which are under investigation and which may be applied in the future to a variety of CNS disorders [203,204].

5.2. Chemistry-Based Techniques

With the increase in drug repurposing efforts for CNS disorders, the need to modify approved and effective molecules used for diseases affecting peripheral organs has also increased.

Another approach to increase drug delivery to the CNS is the chemical modification of small molecules in order to make them more BBB penetrant. To increase drug lipid solubility, various approaches can be employed, but the most common are the direct addition of lipophilic groups or halogenation. Halogenation is a chemical process consisting of the replacement of a hydrogen atom by a halogen atom as chloro or bromo, as shown by Gentri et al. [205]. Another chemical reaction often used is methylation; in fact, adding a methyl group can reduce the hydrogen bonding potential of peptides with enhancement of lipophilicity. Although there are successful examples of this process, chemical modifications leading to improvement in BBB permeability can also affect the properties of the original molecule, thus leading to potential decrease in specificity or potency. To illustrate the relevance of correct lipophilic mechanism and the intrinsic problems, Witt et al. explored the stereoselectivity differences in a synthetic opioid, DPDPE. They showed that the methyl group position on the phenol benzene ring can significantly modulate receptor selectivity, binding capacity, lipophilicity, or BBB penetration [206].

Lipophilicity has been shown to be a major determinant of drug diffusion across the BBB [207]. However, increasing the lipid solubility entails several problems such as drug-affinity reduction and increase in drug molecular weight, making BBB penetration potentially more difficult and resulting in higher non-specific tissue absorption [202].

5.3. Biology-Based Techniques

5.3.1. Trojan Horse Technology

To overcome the issues related to other approaches, researchers considered exploiting the properties of the BBB itself by using endogenous transporters to cross the barrier. One example is the molecular Trojan Horse technology, which by genetic engineering allows the use of peptides and recombinant proteins, enzymes and other large molecule drugs to cross the BBB via a receptor mediated transport (RMT) process [208]. Neurotrophins such as brain-derived neurotrophic factor (BDNF) or basic fibroblast growth factor (bFGF) have been frequently explored since they are secreted proteins which are essential for neuronal development and survival during the neurodevelopmental period, as well as neurogenesis in the adult brain [209]. Moreover, neurotrophins have been linked to neurodegenerative and neuropsychiatric diseases such as Alzheimer's disease (AD) [210] or bipolar disorder [211]. A successful example of this approach is adalimumab, a tumour necrosis factor-alpha (TNF-α) blocker, which was re-engineered for BBB penetration in a fusion protein with the human insulin receptor monoclonal antibody (HIRMAb). The fusion protein is known as HIRMAb-TNFR, which

undergoes receptor-mediated transport across the BBB via the endogenous insulin receptor, thus inhibiting TNF-α by releasing a fused TNF inhibitor [212]. The effectiveness of the molecular Trojan Horse approach has been tested in animal models of stroke, cancer, Parkinson's disease (PD), multiple sclerosis (MS), and AD, among others, as has been extensively reviewed by Pardridge [213].

5.3.2. Nanotechnology Approaches

Nanotechnology is an innovative resource to deliver drugs within the brain; a wide range of pharmaceutical nano-carriers including liposomes, micelles, dendrimers, and some others have been developed. For instance, a wide range of nano-treatments were generated as approaches for AD with the potential to produce a beneficial impact for patients [214]. Pai et al. revealed that stabilized polyethylene glycol phospholipid nano-micelles were effective in mitigating Aβ deposition and neurotoxicity in an SHSY-5Y human cell model [214]. Moreover, antibodies can be potential therapies, too, as it was demonstrated using an adeno-associated virus to deliver antibodies against mutant SOD1 in ALS mouse model, revealing an attenuation of motor loss, a reduction of neural stress and alleviation of gliosis [215].

5.3.3. Exosomes Therapies

Another remarkable potential therapy relates to exosomes, nano-vesicles secreted by the cells, acting as an intercellular communication and able to cross the BBB. Exosomes have been widely studied in disease since they are secreted into the extracellular space and may be useful diagnostically as well as in potential therapeutic approaches [216]. They participate in neurodegenerative diseases such as AD, ALS [217], HD [218], or CJD [219]. Kokubo et al. reported Aβ accumulation in exosomes within senile plaques in an AD mouse model [220]. In parallel, An et al. demonstrated that exosomes derived from human cerebrospinal fluid can reduce the action of Aβ in vivo [221].

Perets et al. reviewed the effects of the exosomes derived from bone marrow mesenchymal stem cells (MSCs) in different brain pathologies. They outlined an acute accumulation of exosomes in stroke, ASD, AD and PD, in contrast to a more diffuse pattern in healthy controls. The deposition of exosomes was found to be increased in disease-specific brain regions depending on the disease, for example, hippocampus in AD [222] or cerebellum in ASD [223]. With these findings, they proposed that exosomes could represent potential biomarkers or exploited to deliver therapeutic agents [224].

5.3.4. Microbiome Therapies

A body of evidence has emerged outlining the relationship between the altered microbiome and pathological conditions. Because of this, the use of microorganisms and probiotics as potential therapies had been explored due to their influence on neuroinflammation in neurodegenerative conditions [225].

Mancuso et al. reviewed the relationship between AD and gut microbiota in preclinical and clinical studies and proposed the modulation of the gut microbiota as a potential therapy for the disease [226]. This was based on clinical studies such as the report from Tillish et al. which demonstrated that the consumption of fermented milk enriched with probiotics modulates the activity in specific regions of the brain in healthy women [227]. Moreover, Messaoudi et al. observed improved human behaviour with reduced anxiety, stress, negative mood, as well as a decreased level of urinary cortisol after 30 days of probiotics administration [228,229].

In neurodegenerative diseases, microbiota, probiotics and even antibiotics as targets for potential therapies is an emerging field [230,231]. Clinical studies have shown the beneficial effects of probiotics in MS, as Kouchaki et al. demonstrated a more favourable score in the disability status scale,

inflammatory markers, mental health and lipid metabolism after a 12-week regimen of Lactobacilli and Bifidobacterium administered to patients [232].

The antibiotic doxycycline has been described to exhibit neuroprotective activity in animal models of PD [233], as well as reduced neurotoxic effects from microglia and astrocytes [234]. The main limitation of antibiotic administration is that it may affect non-target microorganisms with potential detrimental effects.

In parallel to neurodegenerative disease approaches, probiotics as a potential therapeutic strategy in neurodevelopmental pathologies had been explored, especially in relation to ASD. ASD patients have been reported to have an altered gastrointestinal barrier [235], and the use of probiotics may prevent ASD symptomatology, as it was reported by Hsiao et al. The authors demonstrated alteration in the maternal immune system, and with the administration of Bacteroides fragilis, the offspring developed correct gut permeability; Bacteroides fragilis, in turn, alters the microbial composition and reduces ASD-like behaviours including impairments of communication, anxiety and altered sensorimotor activities [236].

5.4. Stem Cell-Based Techniques

Lastly, stem cell-based therapies are changing scientist strategies toward the cure for neural disorders. In this context, BBB impairment can be used as an ally, as increased permeability can facilitate the migration of stem cells from the blood to the brain. Thus, BBB leakage and the pro-inflammatory environment caused by disease can be exploited for drug delivery or as coadjutants [237] for cell transplantation [238].

Embryonic stem cells (ESCs) are a great source for cell-based therapies, but, due to ethical concerns, adult stem cells are usually preferred for transplantation. There are three main types of adult-derived stem cell that are applied in neuroprotective therapeutic approaches: mesenchymal stem cells (MSCs), neural stem cells (NSCs) and induced-pluripotent stem cells (i-PSCs).

MSCs are the most widely used stem cells in brain-related treatments. Despite the migrating limitations enforced by the BBB in many situations such as TBI, MSCs can migrate across the endothelial cells via paracellular pathways through transiently formed inter-endothelial gaps [239]. Therefore, they can be used either for cell-mediated delivery of different elements, e.g., neuroprotective factors, or as a source for cellular regeneration. The applications of MSCs have been extensively employed in pre-clinical studies using various animal models as well as several clinical trials for PD, AD, ALS, MS, stroke [240] and ASD [241].

NSCs are widely found in foetal tissue and in a very limited region in adult brains, e.g., subventricular zone [242]. However, they can be generated in vitro using i-PSCs by passing the ethical issues derived from using foetal-derived tissue. NSC transplantation has been shown to improve AD features in animal models, e.g., memory deficit [243], by releasing neurotrophic factors such as BDNF [244] or participating in disaggregation of Aβ plaques [245].

Finally, since Takahashi and Yamanaka discovered the four transcriptional factors, i.e., Oct3/4, Sox2, c-Myc, and Klf4 that can induce pluripotency into adult cells [246,247], the use of **i-PSCs** for in vitro modeling has exponentially increased during the last decade [248]. Moreover, these cells can be used as therapeutic agents by differentiating them into the target cells altered in a disorder [249], as demonstrated in PD. In this pathology, the transplantation of dopaminergic progenitor cells into the putamen reported clinical changes gradually during the 18 to 24 months after implantation in the patient [250].

However, the safety and reliability of i-PSCs in the therapeutic arena is controversial and requires further efforts to overcome important key limitations, e.g., sporadic differentiation [251].

Overall, the delivery method is the main limitation for stem cell therapies. Direct transplantation at the site of injury is thought to be the more efficient, although this may cause injury at the site of injection [252]. Alternatively, intravenous injection has been reported to cause MSCs to be trapped in the lung vasculature [253]; nonetheless, they can migrate to other tissues, e.g., the brain, rescuing memory deficit and neuropathology in an AD mouse model [239]. Alternatively, stem cells may be delivered intranasally [254] and intrathecally [255], both feasible and accessible alternative routes by circumventing the BBB.

Notwithstanding, there is no consensus on either the adequate stem cell or the delivery route in the treatment of brain-related disorders.

6. Conclusions

The blood–brain barrier (BBB) is a unique structure consisting of different cell types such as brain endothelial cells, pericytes and astrocytes, thus constituting a functional entity, the neurovascular unit. The barrier's establishment and formation take time in a multistep and overlapping process, where BBB formation or angiogenesis and BBB differentiation occur at prenatal age; maturation and maintenance of the newly formed BBB happen postnatally. A wide range of publications reporting BBB integrity loss in pathological conditions are reviewed in this manuscript, from Alzheimer's disease (AD) to traumatic brain injury. A potential picture emerges indicating that BBB disruption might be not only a mechanism common to a variety of developmental and neurodegenerative conditions, but, in many cases, it might be a triggering event, leading to CNS dysfunction.

The correct function of the BBB rests on the interplay between many different cell types and the evolution of their cross-talk over time. Indeed, tuned expression of tight junctions (TJs), basement membrane components (BM) such as collagen IV or fibronectin, and proteins involved in the BBB maintenance and transport such as ATP-binding cassette (ABC) or excitatory amino-acid (EAAT) transporters are at the core of BBB functionality. As reviewed, many of the genetic causes linked to neurodegenerative diseases and many of the stressors that cause neurodevelopmental disorders trigger mechanisms such as neuroinflammation, oxidative stress and changes in neurotransmitter and ion homeostasis. The pathophysiology of these pathways has been associated with alterations in the function of astrocytes, which are, in fact, a common denominator in neuronal support and BBB function.

Indeed, although in neurodegenerative diseases such as AD, PD and ALS the focus has been specifically on neurons for many decades, astrocyte dysfunction in now well known. As we have moved away from the idea that astrocytes are simply reacting to neuronal death, and they might be affected directly by the same genetic and environmental factors that drive neuronal degeneration, we can hypothesize that these glial cells are intrinsically dysfunctional in disease and affect neurons and BBB function through the same pathways.

In the same context, dysfunction of brain microvascular endothelial cells, the main cell type forming the BBB, has been reported in the early stages of neurological disorders such as AD and neurovascular dementia. In fact, recent studies suggest an early BBB breakdown in patients, appearing as microbleeds. Therefore, brain endothelial cells must be considered as a potential therapeutic target, together with the other components of the NVU.

A remarkable new interest on microbiome modulation and its application as a therapeutic agent has arisen during the last decade. Therefore, the gut–brain axis involvement in health and disease progression is also a topic of interest in this review. Interestingly, microbiota may contribute to BBB modulation and disruption, triggering neuroinflammatory mechanisms. Autism spectrum disorders (ASD) are one of the most common pathologies where microbiome alteration has been reported. The concept that the microbiome may interfere with the BBB development leading to an alteration in the permeability of the barrier has raised many questions in the field and initiated new lines of research. The idea that BBB disruption during the prenatal period due to a maternal infection might predispose the person to neurological conditions later in life is one of the emerging new areas of investigation to understand the contribution of microbiota to BBB dysfunction.

In the last section, therapies commonly used and novel therapeutic approaches have been reviewed. Some classic approaches such as neurosurgery (widely applied in cancer); biology-based therapies including Trojan Horse technology, and chemistry-based therapies exemplified by halogenation were summarized. Furthermore, new trending treatments such as exosomes and nano-vesicles administration, microbiome modulation e.g., antibiotics, and stem-cell-based therapies including the mesenchymal stem cells (MSCs) were discussed. A great example of the Trojan Horse technology is adalimumab, a tumour necrosis factor-alpha blocker conjugated with a human insulin receptor antibody (HIRMAb-TNFR) able to penetrate the BBB. This drug has been tested in a variety of disorders, including AD and PD, due to the role of TNF-α in neuroinflammation, a common factor in several pathological conditions. The role of the microbiome in the maintenance of the BBB highlights the use of probiotics and antibiotics as potential therapies in some contexts such as ASD or PD.

In summary, several new techniques are being developed to allow therapeutic agents to cross the BBB and achieve innovative treatments for neurological disorders. However, the heterogeneity of brain pathologies means that scientists have a long way to go and more research is still needed.

The data reviewed here highlight the pathophysiological commonalities between neurodevelopmental and neurodegenerative disorders, including mechanisms such as hypoxia, neuroinflammation, physical injury and microbiota alterations. For this reason, research in both groups of disorders is necessary to understand whether there is a link between developmental and childhood disorders and the predisposition to develop neurodegenerative conditions later in life. We believe this is a compelling area of future research, where either chemistry-, biology- and or stem cell-based therapeutic approaches could be used for addressing a large variety of CNS pathologies.

Author Contributions: Writing—original draft preparation A.A.-G.; writing—review and editing A.A.-G., P.J.S. and L.F. All authors have read and agreed to the published version of the manuscript.

Funding: This research has received funding from the European Union's Horizon 2020 research and innovation programme under the Marie Skłodowska-Curie grant agreement No 765704 (EuroNeurotrophin project). PJS is supported by the NIHR Sheffield Biomedical Research Centre (BRC-1215-20017). LF is funded by the Medical Research Council (MR/V000470/1).

Acknowledgments: We thank the EuroNeurotrophin network for their support.

Conflicts of Interest: The authors declare no conflict of interest.

References

1. Zlokovic, B.V. The Blood-Brain Barrier in Health and Chronic Neurodegenerative Disorders. *Neuron* **2008**, *57*, 178–201. https://doi.org/10.1016/j.neuron.2008.01.003.
2. Sharif, Y.; Jumah, F.; Coplan, L.; Krosser, A.; Sharif, K.; Tubbs, R.S. Blood Brain Barrier: A Review of Its Anatomy and Physiology in Health and Disease. *Clin*. *Anat*. **2018**, *31*, 812–823. https://doi.org/10.1002/ca.23083.
3. Coomber, B.L.; Stewart, P.A. Morphometric Analysis of CNS Microvascular Endothelium. *Microvasc*. *Res*. **1985**, *30*, 99–115. https://doi.org/10.1016/0026-2862(85)90042-1.
4. Gross, P.M.; Sposito, N.M.; Pettersen, S.E.; Fenstermacher, J.D. Differences in Function and Structure of the Capillary Endothelium in Gray Matter, White Matter and a Circumventricular Organ of Rat Brain. *Blood Vessel*. **1986**, *23*, 261–270. https://doi.org/10.1159/000158652.
5. Zhao, R.; Pollack, G.M. Regional Differences in Capillary Density, Perfusion Rate, and P-Glycoprotein Activity: A Quantitative Analysis of Regional Drug Exposure in the Brain. *Biochem*. *Pharmacol*. **2009**, *78*, 1052–1059. https://doi.org/10.1016/j.bcp.2009.06.001.
6. Wilhelm, I.; Nyúl-Tóth, Á.; Suciu, M.; Hermenean, A.; Krizbai, I.A. Heterogeneity of the Blood-Brain Barrier. *Tissue Barriers* **2016**, *4*, e1143544. https://doi.org/10.1080/21688370.2016.1143544.
7. Wang, Q.-P.; Guan, J.-L.; Pan, W.; Kastin, A.J.; Shioda, S. A Diffusion Barrier Between the Area Postrema and Nucleus Tractus Solitarius. *Neurochem*. *Res*. **2008**, *33*, 2035–2043. https://doi.org/10.1007/s11064-008-9676-y.
8. Zhao, Z.; Nelson, A.R.; Betsholtz, C.; Zlokovic, B.V. Establishment and Dysfunction of the Blood-Brain Barrier. *Cell* **2015**, *163*, 1064–1078. https://doi.org/10.1016/j.cell.2015.10.067.
9. Delaney, C.; Campbell, M. The Blood Brain Barrier: Insights from Development and Ageing. *Tissue Barriers* **2017**, *5*, e1373897. https://doi.org/10.1080/21688370.2017.1373897.
10. Sweeney, M.D.; Zhao, Z.; Montagne, A.; Nelson, A.R.; Zlokovic, B.V. Blood-Brain Barrier: From Physiology to Disease and Back. *Physiol*. *Rev*. **2019**, *99*, 21–78. https://doi.org/10.1152/physrev.00050.2017.
11. Marín-Padilla, M. The Human Brain Intracerebral Microvascular System: Development and Structure. *Front*. *Neuroanat*. **2012**, *6*, 38. https://doi.org/10.3389/fnana.2012.00038.
12. Potente, M.; Gerhardt, H.; Carmeliet, P. Basic and Therapeutic Aspects of Angiogenesis. *Cell* **2011**, *146*, 873–887. https://doi.org/10.1016/j.cell.2011.08.039.
13. Raab, S.; Beck, H.; Gaumann, A.; Yüce, A.; Gerber, H.-P.; Plate, K.; Hammes, H.-P.; Ferrara, N.; Breier, G. Impaired Brain Angiogenesis and Neuronal Apoptosis Induced by Conditional Homozygous Inactivation of Vascular Endothelial Growth Factor. *Thromb*. *Haemost*. **2004**, *91*, 595–605. https://doi.org/10.1160/TH03-09-0582.
14. Daneman, R.; Agalliu, D.; Zhou, L.; Kuhnert, F.; Kuo, C.J.; Barres, B.A. Wnt/β-Catenin Signaling Is Required for CNS, but Not Non-CNS, Angiogenesis. *Proc*. *Natl*. *Acad*. *Sci*. *USA* **2009**, *106*, 641–646. https://doi.org/10.1073/pnas.0805165106.
15. Logan, C.Y.; Nusse, R. The Wnt Signaling Pathway in Development and Disease. *Annu*. *Rev*. *Cell Dev*. *Biol*. **2004**, *20*, 781–810. https://doi.org/10.1146/annurev.cellbio.20.010403.113126.
16. Tran, K.A.; Zhang, X.; Predescu, D.; Huang, X.; Machado, R.F.; Göthert, J.R.; Malik, A.B.; Valyi-Nagy, T.; Zhao, Y.-Y. Endothelial β-Catenin Signaling Is Required for Maintaining Adult Blood-Brain Barrier Integrity and Central Nervous System Homeostasis. *Circulation* **2016**, *133*, 177–186. https://doi.org/10.1161/CIRCULATIONAHA.115.015982.
17. Liebner, S.; Corada, M.; Bangsow, T.; Babbage, J.; Taddei, A.; Czupalla, C.J.; Reis, M.; Felici, A.; Wolburg, H.; Fruttiger, M.; et al. Wnt/Beta-Catenin Signaling Controls Development of the Blood-Brain Barrier. *J*. *Cell Biol*. **2008**, *183*, 409–417. https://doi.org/10.1083/jcb.200806024.
18. Siqueira, M.; Francis, D.; Gisbert, D.; Gomes, F.C.A.; Stipursky, J. Radial Glia Cells Control Angiogenesis in the Developing Cerebral Cortex Through TGF-B1 Signaling. *Mol*. *Neurobiol*. **2018**, *55*, 3660–3675. https://doi.org/10.1007/s12035-017-0557-8.
19. Daneman, R.; Zhou, L.; Kebede, A.A.; Barres, B.A. Pericytes Are Required for Blood-Brain Barrier Integrity during Embryogenesis. *Nature* **2010**, *468*, 562–566. https://doi.org/10.1038/nature09513.
20. Hupe, M.; Li, M.X.; Kneitz, S.; Davydova, D.; Yokota, C.; Kele, J.; Hot, B.; Stenman, J.M.; Gessler, M. Gene Expression Profiles of Brain Endothelial Cells during Embryonic Development at Bulk and Single-Cell Levels. *Sci*. *Signal*. **2017**, *10*, eaag2476. https://doi.org/10.1126/scisignal.aag2476.
21. Corada, M.; Orsenigo, F.; Bhat, G.P.; Conze, L.L.; Breviario, F.; Cunha, S.I.; Claesson-Welsh, L.; Beznoussenko, G.V.; Mironov, A.A.; Bacigaluppi, M.; et al. Fine-Tuning of Sox17 and Canonical Wnt Coordinates the Permeability Properties of the Blood-Brain Barrier. *Circ*. *Res*. **2019**, *124*, 511–525. https://doi.org/10.1161/CIRCRESAHA.118.313316.
22. Engelhardt, B.; Risau, W. *New Concepts of a Blood-Brain Barrier*; Springer: New York, NY, USA, 1995; Chapter 2.
23. Hellström, M.; Kalén, M.; Lindahl, P.; Abramsson, A.; Betsholtz, C. Role of PDGF-B and PDGFR-Beta in Recruitment of Vascular Smooth Muscle Cells and Pericytes during Embryonic Blood Vessel Formation in the Mouse. *Development* **1999**, *126*, 3047–3055.
24. Lindahl, P.; Johansson, B.R.; Levéen, P.; Betsholtz, C. Pericyte Loss and Microaneurysm Formation in PDGF-B-Deficient Mice. *Science* **1997**, *277*, 242–245. https://doi.org/10.1126/science.277.5323.242.
25. Winkler, E.A.; Bell, R.D.; Zlokovic, B.V. Central Nervous System Pericytes in Health and Disease. *Nat*. *Neurosci*. **2011**, *14*, 1398–1405. https://doi.org/10.1038/nn.2946.
26. Obermeier, B.; Daneman, R.; Ransohoff, R.M. Development, Maintenance and Disruption of the Blood-Brain Barrier. *Nat*. *Med*. **2013**, *19*, 1584–1596. https://doi.org/10.1038/nm.3407.
27. Hellström, M.; Gerhardt, H.; Kalén, M.; Li, X.; Eriksson, U.; Wolburg, H.; Betsholtz, C. Lack of Pericytes Leads to Endothelial Hyperplasia and Abnormal Vascular Morphogenesis. *J*. *Cell Biol*. **2001**, *153*, 543–553. https://doi.org/10.1083/jcb.153.3.543.

28. Lee, S.-W.; Kim, W.J.; Choi, Y.K.; Song, H.S.; Son, M.J.; Gelman, I.H.; Kim, Y.-J.; Kim, K.-W. SSeCKS Regulates Angiogenesis and Tight Junction Formation in Blood-Brain Barrier. *Nat*. *Med*. **2003**, *9*, 900–906. https://doi.org/10.1038/nm889.
29. Maisonpierre, P.C.; Suri, C.; Jones, P.F.; Bartunkova, S.; Wiegand, S.J.; Radziejewski, C.; Compton, D.; McClain, J.; Aldrich, T.H.; Papadopoulos, N.; et al. Angiopoietin-2, a Natural Antagonist for Tie2 That Disrupts in Vivo Angiogenesis. *Science* **1997**, *277*, 55–60. https://doi.org/10.1126/science.277.5322.55.
30. Nagase, T.; Nagase, M.; Machida, M.; Fujita, T. Hedgehog Signalling in Vascular Development. *Angiogenesis* **2008**, *11*, 71–77. https://doi.org/10.1007/s10456-008-9105-5.
31. Wang, Y.; Jin, S.; Sonobe, Y.; Cheng, Y.; Horiuchi, H.; Parajuli, B.; Kawanokuchi, J.; Mizuno, T.; Takeuchi, H.; Suzumura, A. Interleukin-1β Induces Blood-Brain Barrier Disruption by Downregulating Sonic Hedgehog in Astrocytes. *PLoS ONE* **2014**, *9*, e110024. https://doi.org/10.1371/journal.pone.0110024.
32. Saunders, N.R.; Daneman, R.; Dziegielewska, K.M.; Liddelow, S.A. Transporters of the Blood-Brain and Blood-CSF Interfaces in Development and in the Adult. *Mol*. *Aspects Med*. **2013**, *34*, 742–752. https://doi.org/10.1016/j.mam.2012.11.006.
33. Hagan, N.; Ben-Zvi, A. The Molecular, Cellular, and Morphological Components of Blood-Brain Barrier Development during Embryogenesis. *Semin*. *Cell Dev*. *Biol*. **2015**, *38*, 7–15. https://doi.org/10.1016/j.semcdb.2014.12.006.
34. Mizee, M.R.; Wooldrik, D.; Lakeman, K.A.M.; van het Hof, B.; Drexhage, J.A.R.; Geerts, D.; Bugiani, M.; Aronica, E.; Mebius, R.E.; Prat, A.; et al. Retinoic Acid Induces Blood-Brain Barrier Development. *J*. *Neurosci*. **2013**, *33*, 1660–1671. https://doi.org/10.1523/JNEUROSCI.1338-12.2013.
35. Hammer, C.; Stepniak, B.; Schneider, A.; Papiol, S.; Tantra, M.; Begemann, M.; Sirén, A.-L.; Pardo, L.A.; Sperling, S.; Mohd Jofrry, S.; et al. Neuropsychiatric Disease Relevance of Circulating Anti-NMDA Receptor Autoantibodies Depends on Blood-Brain Barrier Integrity. *Mol*. *Psychiatry* **2014**, *19*, 1143–1149. https://doi.org/10.1038/mp.2013.110.
36. Corder, E.H.; Saunders, A.M.; Strittmatter, W.J.; Schmechel, D.E.; Gaskell, P.C.; Small, G.W.; Roses, A.D.; Haines, J.L.; Pericak-Vance, M.A. Gene Dose of Apolipoprotein E Type 4 Allele and the Risk of Alzheimer's Disease in Late Onset Families. *Science* **1993**, *261*, 921–923. https://doi.org/10.1126/science.8346443.
37. Alvarez, J.I.; Dodelet-Devillers, A.; Kebir, H.; Ifergan, I.; Fabre, P.J.; Terouz, S.; Sabbagh, M.; Wosik, K.; Bourbonnière, L.; Bernard, M.; et al. The Hedgehog Pathway Promotes Blood-Brain Barrier Integrity and CNS Immune Quiescence. *Science* **2011**, *334*, 1727–1731. https://doi.org/10.1126/science.1206936.
38. Muoio, V.; Persson, P.B.; Sendeski, M.M. The Neurovascular Unit—Concept Review. *Acta Physiol*. **2014**, *210*, 790–798. https://doi.org/10.1111/apha.12250.
39. Villegas, J.C.; Broadwell, R.D. Transcytosis of Protein through the Mammalian Cerebral Epithelium and Endothelium. II. Adsorptive Transcytosis of WGA-HRP and the Blood-Brain and Brain-Blood Barriers. *J*. *Neurocytol*. **1993**, *22*, 67–80. https://doi.org/10.1007/bf01181571.
40. Henninger, D.D.; Panés, J.; Eppihimer, M.; Russell, J.; Gerritsen, M.; Anderson, D.C.; Granger, D.N. Cytokine-Induced VCAM-1 and ICAM-1 Expression in Different Organs of the Mouse. *J*. *Immunol*. **1997**, *158*, 1825–1832.
41. Cardoso, F.L.; Brites, D.; Brito, M.A. Looking at the Blood-Brain Barrier: Molecular Anatomy and Possible Investigation Approaches. *Brain Res*. *Rev*. **2010**, *64*, 328–363. https://doi.org/10.1016/j.brainresrev.2010.05.003.
42. Cordon-Cardo, C.; O'Brien, J.P.; Casals, D.; Rittman-Grauer, L.; Biedler, J.L.; Melamed, M.R.; Bertino, J.R. Multidrug-Resistance Gene (P-Glycoprotein) Is Expressed by Endothelial Cells at Blood-Brain Barrier Sites. *Proc*. *Natl*. *Acad*. *Sci*. *USA* **1989**, *86*, 695–698. https://doi.org/10.1073/pnas.86.2.695.
43. Mittapalli, R.K.; Manda, V.K.; Adkins, C.E.; Geldenhuys, W.J.; Lockman, P.R. Exploiting Nutrient Transporters at the Blood-Brain Barrier to Improve Brain Distribution of Small Molecules. *Ther*. *Deliv*. **2010**, *1*, 775–784. https://doi.org/10.4155/tde.10.76.
44. Oldendorf, W.H.; Cornford, M.E.; Brown, W.J. The Large Apparent Work Capability of the Blood-Brain Barrier: A Study of the Mitochondrial Content of Capillary Endothelial Cells in Brain and Other Tissues of the Rat. *Ann*. *Neurol*. **1977**, *1*, 409–417. https://doi.org/10.1002/ana.410010502.
45. Hladky, S.B.; Barrand, M.A. Fluid and Ion Transfer across the Blood-Brain and Blood-Cerebrospinal Fluid Barriers; a Comparative Account of Mechanisms and Roles. *Fluids Barriers CNS* **2016**, *13*, 19. https://doi.org/10.1186/s12987-016-0040-3.
46. Abbott, N.J. Dynamics of CNS Barriers: Evolution, Differentiation, and Modulation. *Cell*. *Mol*. *Neurobiol*. **2005**, *25*, 5–23. https://doi.org/10.1007/s10571-004-1374-y.
47. Pardridge, W.M. Molecular Biology of the Blood-Brain Barrier. *Mol*. *Biotechnol*. **2005**, *30*, 57–70. https://doi.org/10.1385/MB:30:1:057.
48. Yakubu, M.A.; Nsaif, R.H.; Oyekan, A.O. Peroxisome Proliferator-Activated Receptor Alpha Activation-Mediated Regulation of Endothelin-1 Production via Nitric Oxide and Protein Kinase C Signaling Pathways in Piglet Cerebral Microvascular Endothelial Cell Culture. *J*. *Pharmacol*. *Exp*. *Ther*. **2007**, *320*, 774–781. https://doi.org/10.1124/jpet.106.104992.
49. Kostov, K.; Blazhev, A.; Atanasova, M.; Dimitrova, A. Serum Concentrations of Endothelin-1 and Matrix Metalloproteinases-2, -9 in Pre-Hypertensive and Hypertensive Patients with Type 2 Diabetes. *Int*. *J*. *Mol*. *Sci*. **2016**, *17*, 1182. https://doi.org/10.3390/ijms17081182.
50. Maguire, J.J.; Davenport, A.P. Endothelin Receptors and Their Antagonists. *Semin*. *Nephrol*. **2015**, *35*, 125–136. https://doi.org/10.1016/j.semnephrol.2015.02.002.
51. Kelland, N.F.; Kuc, R.E.; McLean, D.L.; Azfer, A.; Bagnall, A.J.; Gray, G.A.; Gulliver-Sloan, F.H.; Maguire, J.J.; Davenport, A.P.; Kotelevtsev, Y. V; et al. Endothelial Cell-Specific ETB Receptor Knockout: Autoradiographic and Histological Characterisation and Crucial Role in the Clearance of Endothelin-1. *Can*. *J*. *Physiol*. *Pharmacol*. **2010**, *88*, 644–651. https://doi.org/10.1139/Y10-041.

52. Taddei, S.; Virdis, A.; Ghiadoni, L.; Salvetti, A. Vascular Effects of Endothelin-1 in Essential Hypertension: Relationship with Cyclooxygenase-Derived Endothelium-Dependent Contracting Factors and Nitric Oxide. *J. Cardiovasc. Pharmacol.* **2000**, *35*, S37–40. https://doi.org/10.1097/00005344-200000002-00009.
53. Mitsumori, T.; Furuyashiki, T.; Momiyama, T.; Nishi, A.; Shuto, T.; Hayakawa, T.; Ushikubi, F.; Kitaoka, S.; Aoki, T.; Inoue, H.; et al. Thromboxane Receptor Activation Enhances Striatal Dopamine Release, Leading to Suppression of GABAergic Transmission and Enhanced Sugar Intake. *Eur. J. Neurosci.* **2011**, *34*, 594–604. https://doi.org/10.1111/j.1460-9568.2011.07774.x.
54. Han, F.; Shirasaki, Y.; Fukunaga, K. Microsphere Embolism-Induced Endothelial Nitric Oxide Synthase Expression Mediates Disruption of the Blood-Brain Barrier in Rat Brain. *J. Neurochem.* **2006**, *99*, 97–106. https://doi.org/10.1111/j.1471-4159.2006.04048.x.
55. Austin, S.A.; d'Uscio, L.V.; Katusic, Z.S. Supplementation of Nitric Oxide Attenuates AβPP and BACE1 Protein in Cerebral Microcirculation of ENOS-Deficient Mice. *J. Alzheimers. Dis.* **2013**, *33*, 29–33. https://doi.org/10.3233/JAD-2012-121351.
56. Kushner, P.D.; Stephenson, D.T.; Wright, S. Reactive Astrogliosis Is Widespread in the Subcortical White Matter of Amyotrophic Lateral Sclerosis Brain. *J. Neuropathol. Exp. Neurol.* **1991**, *50*, 263–277. https://doi.org/10.1097/00005072-199105000-00008.
57. Acosta, C.; Anderson, H.D.; Anderson, C.M. Astrocyte Dysfunction in Alzheimer Disease. *J. Neurosci. Res.* **2017**, *95*, 2430–2447. https://doi.org/10.1002/jnr.24075.
58. Molofsky, A.V.; Krencik, R.; Ullian, E.M.; Tsai, H.; Deneen, B.; Richardson, W.D.; Barres, B.A.; Rowitch, D.H. Astrocytes and Disease: A Neurodevelopmental Perspective. *Genes Dev.* **2012**, *26*, 891–907. https://doi.org/10.1101/gad.188326.112.
59. Lippmann, E.S.; Azarin, S.M.; Kay, J.E.; Nessler, R.A.; Wilson, H.K.; Al-Ahmad, A.; Palecek, S.P.; Shusta, E.V. Derivation of Blood-Brain Barrier Endothelial Cells from Human Pluripotent Stem Cells. *Nat. Biotechnol.* **2012**, *30*, 783–791. https://doi.org/10.1038/nbt.2247.
60. Roessmann, U.; Gambetti, P. Astrocytes in the Developing Human Brain. An Immunohistochemical Study. *Acta Neuropathol.* **1986**, *70*, 308–313. https://doi.org/10.1007/bf00686089.
61. Wiese, S.; Karus, M.; Faissner, A. Astrocytes as a Source for Extracellular Matrix Molecules and Cytokines. *Front. Pharmacol.* **2012**, *3*, 120. https://doi.org/10.3389/fphar.2012.00120.
62. Alvarez, J.I.; Katayama, T.; Prat, A. Glial Influence on the Blood Brain Barrier. *Glia* **2013**, *61*, 1939–1958. https://doi.org/10.1002/glia.22575.
63. Wang, H.; Xu, Z.; Xie, Z.; Rallo, M.; Duffy, A.; Matise, M.P. Inactivation of Hedgehog Signal Transduction in Adult Astrocytes Results in Region-Specific Blood–Brain Barrier Defects. *Proc. Natl. Acad. Sci. USA* **2021**, *118*, e2017779118. https://doi.org/10.1073/pnas.2017779118.
64. András, I.E.; Deli, M.A.; Veszelka, S.; Hayashi, K.; Hennig, B.; Toborek, M. The NMDA and AMPA/KA Receptors Are Involved in Glutamate-Induced Alterations of Occludin Expression and Phosphorylation in Brain Endothelial Cells. *J. Cereb. blood flow Metab. Off. J. Int. Soc. Cereb. Blood Flow Metab.* **2007**, *27*, 1431–1443. https://doi.org/10.1038/sj.jcbfm.9600445.
65. Sharp, C.D.; Hines, I.; Houghton, J.; Warren, A.; Jackson, T.H. 4th; Jawahar, A.; Nanda, A.; Elrod, J.W.; Long, A.; Chi, A.; et al. Glutamate Causes a Loss in Human Cerebral Endothelial Barrier Integrity through Activation of NMDA Receptor. *Am. J. Physiol. Heart Circ. Physiol.* **2003**, *285*, H2592–2598. https://doi.org/10.1152/ajpheart.00520.2003.
66. Vazana, U.; Veksler, R.; Pell, G.S.; Prager, O.; Fassler, M.; Chassidim, Y.; Roth, Y.; Shahar, H.; Zangen, A.; Raccah, R.; et al. Glutamate-Mediated Blood-Brain Barrier Opening: Implications for Neuroprotection and Drug Delivery. *J. Neurosci.* **2016**, *36*, 7727–7739. https://doi.org/10.1523/JNEUROSCI.0587-16.2016.
67. Attwell, D.; Buchan, A.M.; Charpak, S.; Lauritzen, M.; Macvicar, B.A.; Newman, E.A. Glial and Neuronal Control of Brain Blood Flow. *Nature* **2010**, *468*, 232–243. https://doi.org/10.1038/nature09613.
68. O'Kane, R.L.; Martínez-López, I.; DeJoseph, M.R.; Viña, J.R.; Hawkins, R.A. Na(+)-Dependent Glutamate Transporters (EAAT1, EAAT2, and EAAT3) of the Blood-Brain Barrier. A Mechanism for Glutamate Removal. *J. Biol. Chem.* **1999**, *274*, 31891–31895. https://doi.org/10.1074/jbc.274.45.31891.
69. Cooper, A.J.; Plum, F. Biochemistry and Physiology of Brain Ammonia. *Physiol. Rev.* **1987**, *67*, 440–519. https://doi.org/10.1152/physrev.1987.67.2.440.
70. Yoshimura, A.; Wakabayashi, Y.; Mori, T. Cellular and Molecular Basis for the Regulation of Inflammation by TGF-Beta. *J. Biochem.* **2010**, *147*, 781–792. https://doi.org/10.1093/jb/mvq043.
71. Tran, N.D.; Correale, J.; Schreiber, S.S.; Fisher, M. Transforming Growth Factor-Beta Mediates Astrocyte-Specific Regulation of Brain Endothelial Anticoagulant Factors. *Stroke* **1999**, *30*, 1671–1678. https://doi.org/10.1161/01.str.30.8.1671.
72. Verkman, A.S.; Binder, D.K.; Bloch, O.; Auguste, K.; Papadopoulos, M.C. Three Distinct Roles of Aquaporin-4 in Brain Function Revealed by Knockout Mice. *Biochim. Biophys. Acta Biomembr.* **2006**, *1758*, 1085–1093. https://doi.org/10.1016/j.bbamem.2006.02.018.
73. Vandebroek, A.; Yasui, M. Regulation of AQP4 in the Central Nervous System. *Int. J. Mol. Sci.* **2020**, *21*, 1603. https://doi.org/10.3390/ijms21051603.
74. Mader, S.; Brimberg, L. Aquaporin-4 Water Channel in the Brain and Its Implication for Health and Disease. *Cells* **2019**, *8*, 90. https://doi.org/10.3390/cells8020090.
75. Takahashi, T.; Fujihara, K.; Nakashima, I.; Misu, T.; Miyazawa, I.; Nakamura, M.; Watanabe, S.; Shiga, Y.; Kanaoka, C.; Fujimori, J.; et al. Anti-Aquaporin-4 Antibody Is Involved in the Pathogenesis of NMO: A Study on Antibody Titre. *Brain* **2007**, *130*, 1235–1243. https://doi.org/10.1093/brain/awm062.

76. Abbott, N.J.; Patabendige, A.A.K.; Dolman, D.E.M.; Yusof, S.R.; Begley, D.J. Structure and Function of the Blood-Brain Barrier. *Neurobiol. Dis.* **2010**, *37*, 13–25. https://doi.org/10.1016/j.nbd.2009.07.030.
77. Winkler, E.A.; Sengillo, J.D.; Bell, R.D.; Wang, J.; Zlokovic, B.V. Blood-Spinal Cord Barrier Pericyte Reductions Contribute to Increased Capillary Permeability. *J. Cereb. Blood Flow Metab.* **2012**, *32*, 1841–1852. https://doi.org/10.1038/jcbfm.2012.113.
78. Bell, R.D.; Winkler, E.A.; Sagare, A.P.; Singh, I.; LaRue, B.; Deane, R.; Zlokovic, B.V. Pericytes Control Key Neurovascular Functions and Neuronal Phenotype in the Adult Brain and during Brain Aging. *Neuron* **2010**, *68*, 409–427. https://doi.org/10.1016/j.neuron.2010.09.043.
79. Winkler, E.A.; Sengillo, J.D.; Sullivan, J.S.; Henkel, J.S.; Appel, S.H.; Zlokovic, B.V. Blood-Spinal Cord Barrier Breakdown and Pericyte Reductions in Amyotrophic Lateral Sclerosis. *Acta Neuropathol.* **2013**, *125*, 111–120. https://doi.org/10.1007/s00401-012-1039-8.
80. Berthiaume, A.-A.; Grant, R.I.; McDowell, K.P.; Underly, R.G.; Hartmann, D.A.; Levy, M.; Bhat, N.R.; Shih, A.Y. Dynamic Remodeling of Pericytes In Vivo Maintains Capillary Coverage in the Adult Mouse Brain. *Cell Rep.* **2018**, *22*, 8–16. https://doi.org/10.1016/j.celrep.2017.12.016.
81. Hall, C.N.; Reynell, C.; Gesslein, B.; Hamilton, N.B.; Mishra, A.; Sutherland, B.A.; O'Farrell, F.M.; Buchan, A.M.; Lauritzen, M.; Attwell, D. Capillary Pericytes Regulate Cerebral Blood Flow in Health and Disease. *Nature* **2014**, *508*, 55–60. https://doi.org/10.1038/nature13165.
82. Armulik, A.; Genové, G.; Mäe, M.; Nisancioglu, M.H.; Wallgard, E.; Niaudet, C.; He, L.; Norlin, J.; Lindblom, P.; Strittmatter, K.; et al. Pericytes Regulate the Blood-Brain Barrier. *Nature* **2010**, *468*, 557–561. https://doi.org/10.1038/nature09522.
83. Upadhyay, R.K. Transendothelial Transport and Its Role in Therapeutics. *Int. Sch. Res. Not.* **2014**, *2014*, 309404. https://doi.org/10.1155/2014/309404.
84. Olson, L.E.; Soriano, P. PDGFRβ Signaling Regulates Mural Cell Plasticity and Inhibits Fat Development. *Dev. Cell* **2011**, *20*, 815–826. https://doi.org/10.1016/j.devcel.2011.04.019.
85. Baeten, K.M.; Akassoglou, K. Extracellular Matrix and Matrix Receptors in Blood–Brain Barrier Formation and Stroke. *Dev. Neurobiol.* **2011**, *71*, 1018–1039. https://doi.org/10.1002/dneu.20954.
86. Engelhardt, B.; Sorokin, L. The Blood-Brain and the Blood-Cerebrospinal Fluid Barriers: Function and Dysfunction. *Semin. Immunopathol.* **2009**, *31*, 497–511. https://doi.org/10.1007/s00281-009-0177-0.
87. Sado, Y.; Kagawa, M.; Kishiro, Y.; Sugihara, K.; Naito, I.; Seyer, J.M.; Sugimoto, M.; Oohashi, T.; Ninomiya, Y. Establishment by the Rat Lymph Node Method of Epitope-Defined Monoclonal Antibodies Recognizing the Six Different α Chains of Human Type IV Collagen. *Histochem. Cell Biol.* **1995**, *104*, 267–275. https://doi.org/10.1007/BF01464322.
88. Pöschl, E.; Schlötzer-Schrehardt, U.; Brachvogel, B.; Saito, K.; Ninomiya, Y.; Mayer, U. Collagen IV Is Essential for Basement Membrane Stability but Dispensable for Initiation of Its Assembly during Early Development. *Development* **2004**, *131*, 1619–1628. https://doi.org/10.1242/dev.01037.
89. Xu, L.; Nirwane, A.; Yao, Y. Basement Membrane and Blood-Brain Barrier. *Stroke Vasc. Neurol.* **2018**, *4*, 78–82. https://doi.org/10.1136/svn-2018-000198.
90. Wang, J.; Milner, R. Fibronectin Promotes Brain Capillary Endothelial Cell Survival and Proliferation through Alpha5beta1 and Alphavbeta3 Integrins via MAP Kinase Signalling. *J. Neurochem.* **2006**, *96*, 148–159. https://doi.org/10.1111/j.1471-4159.2005.03521.x.
91. George, E.L.; Georges-Labouesse, E.N.; Patel-King, R.S.; Rayburn, H.; Hynes, R.O. Defects in Mesoderm, Neural Tube and Vascular Development in Mouse Embryos Lacking Fibronectin. *Development* **1993**, *119*, 1079–1091.
92. Hallmann, R.; Horn, N.; Selg, M.; Wendler, O.; Pausch, F.; Sorokin, L.M. Expression and Function of Laminins in the Embryonic and Mature Vasculature. *Physiol. Rev.* **2005**, *85*, 979–1000. https://doi.org/10.1152/physrev.00014.2004.
93. Yao, Y.; Chen, Z.-L.; Norris, E.H.; Strickland, S. Astrocytic Laminin Regulates Pericyte Differentiation and Maintains Blood Brain Barrier Integrity. *Nat. Commun.* **2014**, *5*, 3413. https://doi.org/10.1038/ncomms4413.
94. Menezes, M.J.; McClenahan, F.K.; Leiton, C.V.; Aranmolate, A.; Shan, X.; Colognato, H. The Extracellular Matrix Protein Laminin A2 Regulates the Maturation and Function of the Blood-Brain Barrier. *J. Neurosci.* **2014**, *34*, 15260–15280. https://doi.org/10.1523/JNEUROSCI.3678-13.2014.
95. Yao, Y. Laminin: Loss-of-Function Studies. *Cell. Mol. Life Sci.* **2017**, *74*, 1095–1115. https://doi.org/10.1007/s00018-016-2381-0.
96. Atkinson, F.; Cole, S.; Green, C.; van de Waterbeemd, H.; Lipophilicity and Other Parameters Affecting Brain Penetration. *Curr. Med. Chem. Cent. Nerv. Syst. Agents* **2002**, *2*, 229–240.
97. Levin, V.A. Relationship of Octanol/Water Partition Coefficient and Molecular Weight to Rat Brain Capillary Permeability. *J. Med. Chem.* **1980**, *23*, 682–684. https://doi.org/10.1021/jm00180a022.
98. Strazielle, N.; Ghersi-Egea, J.-F. Efflux Transporters in Blood-Brain Interfaces of the Developing Brain. *Front. Neurosci.* **2015**, *9*, 21. https://doi.org/10.3389/fnins.2015.00021.
99. He, L.; Vanlandewijck, M.; Raschperger, E.; Andaloussi Mäe, M.; Jung, B.; Lebouvier, T.; Ando, K.; Hofmann, J.; Keller, A.; Betsholtz, C. Analysis of the Brain Mural Cell Transcriptome. *Sci. Rep.* **2016**, *6*, 35108. https://doi.org/10.1038/srep35108.
100. Liddelow, S.A.; Dziegielewska, K.M.; Ek, C.J.; Habgood, M.D.; Bauer, H.; Bauer, H.-C.; Lindsay, H.; Wakefield, M.J.; Strazielle, N.; Kratzer, I.; et al. Correction: Mechanisms That Determine the Internal Environment of the Developing Brain: A Transcriptomic, Functional and Ultrastructural Approach. *PLoS ONE* **2016**, *11*, e0147680.
101. Ray, R.; Juranek, J.K.; Rai, V. RAGE Axis in Neuroinflammation, Neurodegeneration and Its Emerging Role in the Pathogenesis of Amyotrophic Lateral Sclerosis. *Neurosci. Biobehav. Rev.* **2016**, *62*, 48–55. https://doi.org/10.1016/j.neubiorev.2015.12.006.

102. Bakker, E.N.T.P.; Bacskai, B.J.; Arbel-Ornath, M.; Aldea, R.; Bedussi, B.; Morris, A.W.J.; Weller, R.O.; Carare, R.O. Lymphatic Clearance of the Brain: Perivascular, Paravascular and Significance for Neurodegenerative Diseases. *Cell*. *Mol*. *Neurobiol*. **2016**, *36*, 181–194. https://doi.org/10.1007/s10571-015-0273-8.
103. Cederberg, H.H.C.; Uhd, N.C.; Brodin, B. Glutamate Efflux at the Blood-Brain Barrier: Cellular Mechanisms and Potential Clinical Relevance. *Arch*. *Med*. *Res*. **2014**, *45*, 639–645. https://doi.org/10.1016/j.arcmed.2014.11.004.
104. Wang, W.; Bodles-Brakhop, A.M.; Barger, S.W. A Role for P-Glycoprotein in Clearance of Alzheimer Amyloid β -Peptide from the Brain. *Curr*. *Alzheimer Res*. **2016**, *13*, 615–620. https://doi.org/10.2174/1567205013666160314151012.
105. Blasco, H.; Mavel, S.; Corcia, P.; Gordon, P.H. The Glutamate Hypothesis in ALS: Pathophysiology and Drug Development. *Curr*. *Med*. *Chem*. **2014**, *21*, 3551–3575.
106. Cowan, C.M.; Raymond, L.A. Selective Neuronal Degeneration in Huntington's Disease. *Curr*. *Top*. *Dev*. *Biol*. **2006**, *75*, 25–71. https://doi.org/10.1016/S0070-2153(06)75002-5.
107. Uno, Y.; Coyle, J.T. Glutamate Hypothesis in Schizophrenia. *Psychiatry Clin*. *Neurosci*. **2019**, *73*, 204–215. https://doi.org/10.1111/pcn.12823.
108. Deane, R.; Wu, Z.; Sagare, A.; Davis, J.; Yan, S.D.; Hamm, K.; Xu, F.; Parisi, M.; LaRue, B.; Hu, H.W.; et al. LRP/Amyloid β;-Peptide Interaction Mediates Differential Brain Efflux of A β; Isoforms. *Neuron* **2004**, *43*, 333–344. https://doi.org/10.1016/j.neuron.2004.07.017.
109. Harel, T.; Quek, D.Q.Y.; Wong, B.H.; Cazenave-Gassiot, A.; Wenk, M.R.; Fan, H.; Berger, I.; Shmueli, D.; Shaag, A.; Silver, D.L.; et al. Homozygous Mutation in MFSD2A, Encoding a Lysolipid Transporter for Docosahexanoic Acid, Is Associated with Microcephaly and Hypomyelination. *Neurogenetics* **2018**, *19*, 227–235. https://doi.org/10.1007/s10048-018-0556-6.
110. Qosa, H.; Miller, D.S.; Pasinelli, P.; Trotti, D. Regulation of ABC Efflux Transporters at Blood-Brain Barrier in Health and Neurological Disorders. *Brain Res*. **2015**, *1628*, 298–316. https://doi.org/10.1016/j.brainres.2015.07.005.
111. Iadecola, C. The Neurovascular Unit Coming of Age: A Journey through Neurovascular Coupling in Health and Disease. *Neuron* **2017**, *96*, 17–42. https://doi.org/10.1016/j.neuron.2017.07.030.
112. NCBI APOE Apolipoprotein E [Homo Sapiens (Human)] Available online: https://www.ncbi.nlm.nih.gov/gene/348 (accessed on 15 June 2020).
113. Boyles, J.K.; Pitas, R.E.; Wilson, E.; Mahley, R.W.; Taylor, J.M. Apolipoprotein E Associated with Astrocytic Glia of the Central Nervous System and with Nonmyelinating Glia of the Peripheral Nervous System. *J*. *Clin*. *Investig*. **1985**, *76*, 1501–1513. https://doi.org/10.1172/JCI112130.
114. Tai, L.M.; Thomas, R.; Marottoli, F.M.; Koster, K.P.; Kanekiyo, T.; Morris, A.W.J.; Bu, G. The Role of APOE in Cerebrovascular Dysfunction. *Acta Neuropathol*. **2016**, *131*, 709–723. https://doi.org/10.1007/s00401-016-1547-z.
115. Huang, Y.; Mucke, L. Alzheimer Mechanisms and Therapeutic Strategies. *Cell* **2012**, *148*, 1204–1222. https://doi.org/10.1016/j.cell.2012.02.040.
116. Bell, R.D.; Winkler, E.A.; Singh, I.; Sagare, A.P.; Deane, R.; Wu, Z.; Holtzman, D.M.; Betsholtz, C.; Armulik, A.; Sallstrom, J.; et al. Apolipoprotein E Controls Cerebrovascular Integrity via Cyclophilin A. *Nature* **2012**, *485*, 512–516. https://doi.org/10.1038/nature11087.
117. Halliday, M.R.; Rege, S.V.; Ma, Q.; Zhao, Z.; Miller, C.A.; Winkler, E.A.; Zlokovic, B.V. Accelerated Pericyte Degeneration and Blood-Brain Barrier Breakdown in Apolipoprotein E4 Carriers with Alzheimer's Disease. *J*. *Cereb*. *Blood Flow Metab*. **2016**, *36*, 216–227. https://doi.org/10.1038/jcbfm.2015.44.
118. Apostolova, L.G.; Mosconi, L.; Thompson, P.M.; Green, A.E.; Hwang, K.S.; Ramirez, A.; Mistur, R.; Tsui, W.H.; de Leon, M.J. Subregional Hippocampal Atrophy Predicts Alzheimer's Dementia in the Cognitively Normal. *Neurobiol*. *Aging* **2010**, *31*, 1077–1088. https://doi.org/10.1016/j.neurobiolaging.2008.08.008.
119. Montagne, A.; Barnes, S.R.; Sweeney, M.D.; Halliday, M.R.; Sagare, A.P.; Zhao, Z.; Toga, A.W.; Jacobs, R.E.; Liu, C.Y.; Amezcua, L.; et al. Blood-Brain Barrier Breakdown in the Aging Human Hippocampus. *Neuron* **2015**, *85*, 296–302. https://doi.org/10.1016/j.neuron.2014.12.032.
120. Brundel, M.; Heringa, S.M.; de Bresser, J.; Koek, H.L.; Zwanenburg, J.J.M.; Jaap Kappelle, L.; Luijten, P.R.; Biessels, G.J. High Prevalence of Cerebral Microbleeds at 7Tesla MRI in Patients with Early Alzheimer's Disease. *J*. *Alzheimers*. *Dis*. **2012**, *31*, 259–263. https://doi.org/10.3233/JAD-2012-120364.
121. Zipser, B.D.; Johanson, C.E.; Gonzalez, L.; Berzin, T.M.; Tavares, R.; Hulette, C.M.; Vitek, M.P.; Hovanesian, V.; Stopa, E.G. Microvascular Injury and Blood-Brain Barrier Leakage in Alzheimer's Disease. *Neurobiol*. *Aging* **2007**, *28*, 977–986. https://doi.org/10.1016/j.neurobiolaging.2006.05.016.
122. Yin, Y.; Wang, Z. ApoE and Neurodegenerative Diseases in Aging. *Adv*. *Exp*. *Med*. *Biol*. **2018**, *1086*, 77–92. https://doi.org/10.1007/978-981-13-1117-8_5.
123. Yonashiro, R.; Sugiura, A.; Miyachi, M.; Fukuda, T.; Matsushita, N.; Inatome, R.; Ogata, Y.; Suzuki, T.; Dohmae, N.; Yanagi, S. Mitochondrial Ubiquitin Ligase MITOL Ubiquitinates Mutant SOD1 and Attenuates Mutant SOD1-Induced Reactive Oxygen Species Generation. *Mol*. *Biol*. *Cell* **2009**, *20*, 4524–4530. https://doi.org/10.1091/mbc.e09-02-0112.
124. Rosen, D.R.; Siddique, T.; Patterson, D.; Figlewicz, D.A.; Sapp, P.; Hentati, A.; Donaldson, D.; Goto, J.; O'Regan, J.P.; Deng, H.-X.; et al. Mutations in Cu/Zn Superoxide Dismutase Gene Are Associated with Familial Amyotrophic Lateral Sclerosis. *Nature* **1993**, *362*, 59–62. https://doi.org/10.1038/362059a0.
125. Barber, S.C.; Shaw, P.J. Oxidative Stress in ALS: Key Role in Motor Neuron Injury and Therapeutic Target. *Free Radic*. *Biol*. *Med*. **2010**, *48*, 629–641. https://doi.org/10.1016/j.freeradbiomed.2009.11.018.
126. Allen, S.; Heath, P.R.; Kirby, J.; Wharton, S.B.; Cookson, M.R.; Menzies, F.M.; Banks, R.E.; Shaw, P.J. Analysis of the Cytosolic Proteome in a Cell Culture Model of Familial Amyotrophic Lateral Sclerosis Reveals Alterations to the Proteasome, Antioxidant Defenses, and Nitric Oxide Synthetic Pathways. *J*. *Biol*. *Chem*. **2003**, *278*, 6371–6383. https://doi.org/10.1074/jbc.M209915200.

127. Garbuzova-Davis, S.; Rodrigues, M.C.O.; Hernandez-Ontiveros, D.G.; Louis, M.K.; Willing, A.E.; Borlongan, C.V.; Sanberg, P.R. Amyotrophic Lateral Sclerosis: A Neurovascular Disease. *Brain Res*. **2011**, *1398*, 113–125. https://doi.org/10.1016/j.brainres.2011.04.049.
128. Cowley, P.M.; Nair, D.R.; DeRuisseau, L.R.; Keslacy, S.; Atalay, M.; DeRuisseau, K.C. Oxidant Production and SOD1 Protein Expression in Single Skeletal Myofibers from Down Syndrome Mice. *Redox Biol*. **2017**, *13*, 421–425. https://doi.org/10.1016/j.redox.2017.07.003.
129. Muchová, J.; Žitňanová, I.; Ďuračková, Z. Oxidative Stress and Down Syndrome. Do Antioxidants Play a Role in Therapy? *Physiol*. *Res*. **2014**, *63*, 535–542.
130. Ram, G.; Chinen, J. Infections and Immunodeficiency in Down Syndrome. *Clin*. *Exp*. *Immunol*. **2011**, *164*, 9–16. https://doi.org/10.1111/j.1365-2249.2011.04335.x.
131. Amiry-Moghaddam, M.; Otsuka, T.; Hurn, P.D.; Traystman, R.J.; Haug, F.-M.; Froehner, S.C.; Adams, M.E.; Neely, J.D.; Agre, P.; Ottersen, O.P.; et al. An Alpha-Syntrophin-Dependent Pool of AQP4 in Astroglial End-Feet Confers Bidirectional Water Flow between Blood and Brain. *Proc*. *Natl*. *Acad*. *Sci*. *USA* **2003**, *100*, 2106–2111. https://doi.org/10.1073/pnas.0437946100.
132. Nagelhus, E.A.; Mathiisen, T.M.; Ottersen, O.P. Aquaporin-4 in the Central Nervous System: Cellular and Subcellular Distribution and Coexpression with KIR4.1. *Neuroscience* **2004**, *129*, 905–913. https://doi.org/10.1016/j.neuroscience.2004.08.053.
133. Li, J.; Verkman, A.S. Impaired Hearing in Mice Lacking Aquaporin-4 Water Channels. *J*. *Biol*. *Chem*. **2001**, *276*, 31233–31237. https://doi.org/10.1074/jbc.M104368200.
134. Skucas, V.A.; Mathews, I.B.; Yang, J.; Cheng, Q.; Treister, A.; Duffy, A.M.; Verkman, A.S.; Hempstead, B.L.; Wood, M.A.; Binder, D.K.; et al. Impairment of Select Forms of Spatial Memory and Neurotrophin-Dependent Synaptic Plasticity by Deletion of Glial Aquaporin-4. *J*. *Neurosci*. **2011**, *31*, 6392–6397. https://doi.org/10.1523/JNEUROSCI.6249-10.2011.
135. Saadoun, S.; Papadopoulos, M.C.; Watanabe, H.; Yan, D.; Manley, G.T.; Verkman, A.S. Involvement of Aquaporin-4 in Astroglial Cell Migration and Glial Scar Formation. *J*. *Cell Sci*. **2005**, *118*, 5691–5698. https://doi.org/10.1242/jcs.02680.
136. Wingerchuk, D.M.; Lennon, V.A.; Lucchinetti, C.F.; Pittock, S.J.; Weinshenker, B.G. The Spectrum of Neuromyelitis Optica. *Lancet*. *Neurol*. **2007**, *6*, 805–815. https://doi.org/10.1016/S1474-4422(07)70216-8.
137. Fatemi, S.H.; Folsom, T.D.; Reutiman, T.J.; Lee, S. Expression of Astrocytic Markers Aquaporin 4 and Connexin 43 Is Altered in Brains of Subjects with Autism. *Synapse* **2008**, *62*, 501–507. https://doi.org/10.1002/syn.20519.
138. Hubbard, J.A.; Szu, J.I.; Binder, D.K. The Role of Aquaporin-4 in Synaptic Plasticity, Memory and Disease. *Brain Res*. *Bull*. **2018**, *136*, 118–129. https://doi.org/10.1016/j.brainresbull.2017.02.011.
139. Smith, A.J.; Duan, T.; Verkman, A.S. Aquaporin-4 Reduces Neuropathology in a Mouse Model of Alzheimer's Disease by Remodeling Peri-Plaque Astrocyte Structure. *Acta Neuropathol*. *Commun*. **2019**, *7*, 74. https://doi.org/10.1186/s40478-019-0728-0.
140. Opdal, S.H.; Vege, Å.; Stray-Pedersen, A.; Rognum, T.O. The Gene Encoding the Inwardly Rectifying Potassium Channel Kir4.1 May Be Involved in Sudden Infant Death Syndrome. *Acta Paediatr*. **2017**, *106*, 1474–1480. https://doi.org/10.1111/apa.13928.
141. Jeon, H.; Kim, M.; Park, W.; Lim, J.S.; Lee, E.; Cha, H.; Ahn, J.S.; Kim, J.H.; Hong, S.H.; Park, J.E.; et al. Upregulation of AQP4 Improves Blood-Brain Barrier Integrity and Perihematomal Edema Following Intracerebral Hemorrhage. *Neurotherapeutics* **2021**, *18*, 2692–2706. https://doi.org/10.1007/s13311-021-01126-2.
142. Pizzino, G.; Irrera, N.; Cucinotta, M.; Pallio, G.; Mannino, F.; Arcoraci, V.; Squadrito, F.; Altavilla, D.; Bitto, A. Oxidative Stress: Harms and Benefits for Human Health. *Oxid*. *Med*. *Cell*. *Longev*. **2017**, *2017*, 8416763. https://doi.org/10.1155/2017/8416763.
143. Lin, M.T.; Beal, M.F. Mitochondrial Dysfunction and Oxidative Stress in Neurodegenerative Diseases. *Nature* **2006**, *443*, 787–795. https://doi.org/10.1038/nature05292.
144. Churg, A. Interactions of Exogenous or Evoked Agents and Particles: The Role of Reactive Oxygen Species. *Free Radic*. *Biol*. *Med*. **2003**, *34*, 1230–1235. https://doi.org/10.1016/s0891-5849(03)00175-8.
145. Haorah, J.; Knipe, B.; Leibhart, J.; Ghorpade, A.; Persidsky, Y. Alcohol-Induced Oxidative Stress in Brain Endothelial Cells Causes Blood-Brain Barrier Dysfunction. *J*. *Leukoc*. *Biol*. **2005**, *78*, 1223–1232. https://doi.org/10.1189/jlb.0605340.
146. Haorah, J.; Schall, K.; Ramirez, S.H.; Persidsky, Y. Activation of Protein Tyrosine Kinases and Matrix Metalloproteinases Causes Blood-Brain Barrier Injury: Novel Mechanism for Neurodegeneration Associated with Alcohol Abuse. *Glia* **2008**, *56*, 78–88. https://doi.org/10.1002/glia.20596.
147. Ighodaro, O.M.; Akinloye, O.A. First Line Defence Antioxidants-Superoxide Dismutase (SOD), Catalase (CAT) and Glutathione Peroxidase (GPX): Their Fundamental Role in the Entire Antioxidant Defence Grid. *Alexandria J*. *Med*. **2018**, *54*, 287–293. https://doi.org/10.1016/j.ajme.2017.09.001.
148. Moi, P.; Chan, K.; Asunis, I.; Cao, A.; Kan, Y.W. Isolation of NF-E2-Related Factor 2 (Nrf2), a NF-E2-like Basic Leucine Zipper Transcriptional Activator That Binds to the Tandem NF-E2/AP1 Repeat of the Beta-Globin Locus Control Region. *Proc*. *Natl*. *Acad*. *Sci*. *USA* **1994**, *91*, 9926–9930. https://doi.org/10.1073/pnas.91.21.9926.
149. Itoh, K.; Chiba, T.; Takahashi, S.; Ishii, T.; Igarashi, K.; Katoh, Y.; Oyake, T.; Hayashi, N.; Satoh, K.; Hatayama, I.; et al. An Nrf2/Small Maf Heterodimer Mediates the Induction of Phase II Detoxifying Enzyme Genes through Antioxidant Response Elements. *Biochem*. *Biophys*. *Res*. *Commun*. **1997**, *236*, 313–322. https://doi.org/10.1006/bbrc.1997.6943.
150. Cuadrado, A.; Manda, G.; Hassan, A.; Alcaraz, M.J.; Barbas, C.; Daiber, A.; Ghezzi, P.; León, R.; López, M.G.; Oliva, B.; et al. Transcription Factor NRF2 as a Therapeutic Target for Chronic Diseases: A Systems Medicine Approach. *Pharmacol*. *Rev*. **2018**, *70*, 348–383. https://doi.org/10.1124/pr.117.014753.
151. Qu, Z.; Sun, J.; Zhang, W.; Yu, J.; Zhuang, C. Transcription Factor NRF2 as a Promising Therapeutic Target for Alzheimer's Disease. *Free Radic*. *Biol*. *Med*. **2020**, *159*, 87–102. https://doi.org/10.1016/j.freeradbiomed.2020.06.028.

152. Murphy, M.P. How Mitochondria Produce Reactive Oxygen Species. *Biochem*. *J*. **2009**, *417*, 1–13. https://doi.org/10.1042/BJ20081386.
153. Esposito, L.; Raber, J.; Kekonius, L.; Yan, F.; Yu, G.-Q.; Bien-Ly, N.; Puoliväli, J.; Scearce-Levie, K.; Masliah, E.; Mucke, L. Reduction in Mitochondrial Superoxide Dismutase Modulates Alzheimer's Disease-like Pathology and Accelerates the Onset of Behavioral Changes in Human Amyloid Precursor Protein Transgenic Mice. *J*. *Neurosci*. *Off*. *J*. *Soc*. *Neurosci*. **2006**, *26*, 5167–5179. https://doi.org/10.1523/JNEUROSCI.0482-06.2006.
154. Kemp, K.; Gray, E.; Mallam, E.; Scolding, N.; Wilkins, A. Inflammatory Cytokine Induced Regulation of Superoxide Dismutase 3 Expression by Human Mesenchymal Stem Cells. *Stem cell Rev*. *reports* **2010**, *6*, 548–559. https://doi.org/10.1007/s12015-010-9178-6.
155. Shaw, P.J.; Chinnery, R.M.; Thagesen, H.; Borthwick, G.M.; Ince, P.G. Immunocytochemical Study of the Distribution of the Free Radical Scavenging Enzymes Cu/Zn Superoxide Dismutase (SOD1); MN Superoxide Dismutase (MN SOD) and Catalase in the Normal Human Spinal Cord and in Motor Neuron Disease. *J*. *Neurol*. *Sci*. **1997**, *147*, 115–125. https://doi.org/10.1016/s0022-510x(96)05316-6.
156. Takeuchi, A.; Miyamoto, T.; Yamaji, K.; Masuho, Y.; Hayashi, M.; Hayashi, H.; Onozaki, K. A Human Erythrocyte-Derived Growth-Promoting Factor with a Wide Target Cell Spectrum: Identification as Catalase. *Cancer Res*. **1995**, *55*, 1586–1589.
157. Flagg, E.W.; Coates, R.J.; Jones, D.P.; Eley, J.W.; Gunter, E.W.; Jackson, B.; Greenberg, R.S. Plasma Total Glutathione in Humans and Its Association with Demographic and Health-Related Factors. *Br*. *J*. *Nutr*. **1993**, *70*, 797–808. https://doi.org/10.1079/bjn19930175.
158. Pizzorno, J. Glutathione! *Integr*. *Med*. *Encinitas* **2014**, *13*, 8–12.
159. Dringen, R. Metabolism and Functions of Glutathione in Brain. *Prog*. *Neurobiol*. **2000**, *62*, 649–671. https://doi.org/10.1016/s0301-0082(99)00060-x.
160. Huang, S.-F.; Othman, A.; Koshkin, A.; Fischer, S.; Fischer, D.; Zamboni, N.; Ono, K.; Sawa, T.; Ogunshola, O.O. Astrocyte Glutathione Maintains Endothelial Barrier Stability. *Redox Biol*. **2020**, *34*, 101576. https://doi.org/10.1016/j.redox.2020.101576.
161. Agus, D.B.; Gambhir, S.S.; Pardridge, W.M.; Spielholz, C.; Baselga, J.; Vera, J.C.; Golde, D.W. Vitamin C Crosses the Blood-Brain Barrier in the Oxidized Form through the Glucose Transporters. *J*. *Clin*. *Investig*. **1997**, *100*, 2842–2848. https://doi.org/10.1172/JCI119832.
162. Lykkesfeldt, J.; Tveden-Nyborg, P. The Pharmacokinetics of Vitamin C. *Nutrients* **2019**, *11*. https://doi.org/10.3390/nu11102412.
163. Telang, S.; Clem, A.L.; Eaton, J.W.; Chesney, J. Depletion of Ascorbic Acid Restricts Angiogenesis and Retards Tumor Growth in a Mouse Model. *Neoplasia* **2007**, *9*, 47–56. https://doi.org/10.1593/neo.06664.
164. Chang, C.-Y.; Chen, J.-Y.; Wu, M.-H.; Hu, M.-L. Therapeutic Treatment with Vitamin C Reduces Focal Cerebral Ischemia-Induced Brain Infarction in Rats by Attenuating Disruptions of Blood Brain Barrier and Cerebral Neuronal Apoptosis. *Free Radic*. *Biol*. *Med*. **2020**, *155*, 29–36. https://doi.org/10.1016/j.freeradbiomed.2020.05.015.
165. Mohammed, H.O.; Starkey, S.R.; Stipetic, K.; Divers, T.J.; Summers, B.A.; de Lahunta, A. The Role of Dietary Antioxidant Insufficiency on the Permeability of the Blood-Brain Barrier. *J*. *Neuropathol*. *Exp*. *Neurol*. **2008**, *67*, 1187–1193. https://doi.org/10.1097/NEN.0b013e31818f8f51.
166. Gohil, K.; Vasu, V.T.; Cross, C.E. Dietary Alpha-Tocopherol and Neuromuscular Health: Search for Optimal Dose and Molecular Mechanisms Continues! *Mol*. *Nutr*. *Food Res*. **2010**, *54*, 693–709. https://doi.org/10.1002/mnfr.200900575.
167. Muller, D.P.R. Vitamin E and Neurological Function. *Mol*. *Nutr*. *Food Res*. **2010**, *54*, 710–718. https://doi.org/10.1002/mnfr.200900460.
168. D'Antona, S.; Caramenti, M.; Porro, D.; Castiglioni, I.; Cava, C. Amyotrophic Lateral Sclerosis: A Diet Review. *Foods* **2021**, *10*, 3128. https://doi.org/10.3390/foods10123128.
169. Ng, L.; Khan, F.; Young, C.A.; Galea, M. Symptomatic Treatments for Amyotrophic Lateral Sclerosis/Motor Neuron Disease. *Cochrane database Syst*. *Rev*. **2017**, *1*, CD011776. https://doi.org/10.1002/14651858.CD011776.pub2.
170. Takata, F.; Nakagawa, S.; Matsumoto, J.; Dohgu, S. Blood-Brain Barrier Dysfunction Amplifies the Development of Neuroinflammation: Understanding of Cellular Events in Brain Microvascular Endothelial Cells for Prevention and Treatment of BBB Dysfunction. *Front*. *Cell*. *Neurosci*. 2021, *15*, 661838.
171. Simi, A.; Tsakiri, N.; Wang, P.; Rothwell, N.J. Interleukin-1 and Inflammatory Neurodegeneration. *Biochem*. *Soc*. *Trans*. **2007**, *35*, 1122–1126. https://doi.org/10.1042/BST0351122.
172. Rosenberg, G.A. Matrix Metalloproteinases and Their Multiple Roles in Neurodegenerative Diseases. *Lancet*. *Neurol*. **2009**, *8*, 205–216. https://doi.org/10.1016/S1474-4422(09)70016-X.
173. Strbian, D.; Karjalainen-Lindsberg, M.-L.; Tatlisumak, T.; Lindsberg, P.J. Cerebral Mast Cells Regulate Early Ischemic Brain Swelling and Neutrophil Accumulation. *J*. *Cereb*. *Blood Flow Metab*. *Off*. *J*. *Int*. *Soc*. *Cereb*. *Blood Flow Metab*. **2006**, *26*, 605–612. https://doi.org/10.1038/sj.jcbfm.9600228.
174. Bjorklund, G.; Saad, K.; Chirumbolo, S.; Kern, J.K.; Geier, D.A.; Geier, M.R.; Urbina, M.A. Immune Dysfunction and Neuroinflammation in Autism Spectrum Disorder. *Acta Neurobiol*. *Exp*. *Wars* **2016**, *76*, 257–268. https://doi.org/10.21307/ane-2017-025.
175. Ransohoff, R.M. How Neuroinflammation Contributes to Neurodegeneration. *Science* **2016**, *353*, 777–783. https://doi.org/10.1126/science.aag2590.
176. Russo, M.V.; McGavern, D.B. Inflammatory Neuroprotection Following Traumatic Brain Injury. *Science* **2016**, *353*, 783–785. https://doi.org/10.1126/science.aaf6260.
177. Trias, E.; King, P.H.; Si, Y.; Kwon, Y.; Varela, V.; Ibarburu, S.; Kovacs, M.; Moura, I.C.; Beckman, J.S.; Hermine, O.; et al. Mast Cells and Neutrophils Mediate Peripheral Motor Pathway Degeneration in ALS. *JCI insight* **2018**, *3*, e123249. https://doi.org/10.1172/jci.insight.123249.

178. Maiuolo, J.; Gliozzi, M.; Musolino, V.; Scicchitano, M.; Carresi, C.; Scarano, F.; Bosco, F.; Nucera, S.; Ruga, S.; Zito, M.C.; et al. The "Frail" Brain Blood Barrier in Neurodegenerative Diseases: Role of Early Disruption of Endothelial Cell-to-Cell Connections. *Int. J. Mol. Sci.* **2018**, *19*, 2693. https://doi.org/10.3390/ijms19092693.
179. Zenaro, E.; Pietronigro, E.; Bianca, V. Della; Piacentino, G.; Marongiu, L.; Budui, S.; Turano, E.; Rossi, B.; Angiari, S.; Dusi, S.; et al. Neutrophils Promote Alzheimer's Disease–like Pathology and Cognitive Decline via LFA-1 Integrin. *Nat. Med.* **2015**, *21*, 880–886. https://doi.org/10.1038/nm.3913.
180. Beaman, C.; Kozii, K.; Hilal, S.; Liu, M.; Spagnolo-Allende, A.J.; Polanco-Serra, G.; Chen, C.; Cheng, C.-Y.; Zambrano, D.; Arikan, B.; et al. Cerebral Microbleeds, Cerebral Amyloid Angiopathy, and Their Relationships to Quantitative Markers of Neurodegeneration. *Neurology* **2022**, *98*, e1605 LP-e1616. https://doi.org/10.1212/WNL.0000000000200142.
181. Cash, A.; Theus, M.H. Mechanisms of Blood-Brain Barrier Dysfunction in Traumatic Brain Injury. *Int. J. Mol. Sci.* 2020, *21*, 3344.
182. Price, L.; Wilson, C.; Grant, G. Chapter 4 Blood-Brain Barrier Pathophysiology Following Traumatic Brain Injury. In *Translational Research in Traumatic Brain Injury*; CRC Press/Taylor and Francis Group: Boca Raton, FL, USA, 2016.
183. Ferrari, D.C.; Nesic, O.; Perez-Polo, J.R. Perspectives on Neonatal Hypoxia/Ischemia-Induced Edema Formation. *Neurochem. Res.* **2010**, *35*, 1957–1965. https://doi.org/10.1007/s11064-010-0308-y.
184. Hamrick, S.E.G.; Ferriero, D.M. The Injury Response in the Term Newborn Brain: Can We Neuroprotect? *Curr. Opin. Neurol.* **2003**, *16*, 147–154. https://doi.org/10.1097/01.wco.0000063775.81810.79.
185. Disdier, C.; Stonestreet, B.S. Hypoxic-Ischemic-Related Cerebrovascular Changes and Potential Therapeutic Strategies in the Neonatal Brain. *J. Neurosci. Res.* **2020**, *98*, 1468–1484. https://doi.org/10.1002/jnr.24590.
186. Castillo-Melendez, M.; Yawno, T.; Allison, B.J.; Jenkin, G.; Wallace, E.M.; Miller, S.L. Cerebrovascular Adaptations to Chronic Hypoxia in the Growth Restricted Lamb. *Int. J. Dev. Neurosci. Off. J. Int. Soc. Dev. Neurosci.* **2015**, *45*, 55–65. https://doi.org/10.1016/j.ijdevneu.2015.01.004.
187. Baschat, A.A. Neurodevelopment Following Fetal Growth Restriction and Its Relationship with Antepartum Parameters of Placental Dysfunction. *Ultrasound Obstet. Gynecol.* **2011**, *37*, 501–514. https://doi.org/10.1002/uog.9008.
188. Kesavan, K.; Devaskar, S.U. Intrauterine Growth Restriction: Postnatal Monitoring and Outcomes. *Pediatr. Clin. N. Am.* **2019**, *66*, 403–423. https://doi.org/10.1016/j.pcl.2018.12.009.
189. Chandra, S.; Alam, M.T.; Dey, J.; Sasidharan, B.C.P.; Ray, U.; Srivastava, A.K.; Gandhi, S.; Tripathi, P.P. Healthy Gut, Healthy Brain: The Gut Microbiome in Neurodegenerative Disorders. *Curr. Top. Med. Chem.* **2020**, *20*, 1142–1153. https://doi.org/10.2174/1568026620666200413091101.
190. Zhu, X.; Li, B.; Lou, P.; Dai, T.; Chen, Y.; Zhuge, A.; Yuan, Y.; Li, L. The Relationship Between the Gut Microbiome and Neurodegenerative Diseases. *Neurosci. Bull.* **2021**, *37*, 1510–1522. https://doi.org/10.1007/s12264-021-00730-8.
191. Mayer, E.A.; Knight, R.; Mazmanian, S.K.; Cryan, J.F.; Tillisch, K. Gut Microbes and the Brain: Paradigm Shift in Neuroscience. *J. Neurosci.* **2014**, *34*, 15490–15496. https://doi.org/10.1523/JNEUROSCI.3299-14.2014.
192. Bohórquez, D.V.; Shahid, R.A.; Erdmann, A.; Kreger, A.M.; Wang, Y.; Calakos, N.; Wang, F.; Liddle, R.A. Neuroepithelial Circuit Formed by Innervation of Sensory Enteroendocrine Cells. *J. Clin. Investig.* **2015**, *125*, 782–786. https://doi.org/10.1172/JCI78361.
193. Breen, D.P.; Halliday, G.M.; Lang, A.E. Gut–Brain Axis and the Spread of α-Synuclein Pathology: Vagal Highway or Dead End? *Mov. Disord.* **2019**, *34*, 307–316. https://doi.org/10.1002/mds.27556.
194. Pulikkan, J.; Mazumder, A.; Grace, T. Role of the Gut Microbiome in Autism Spectrum Disorders. *Adv. Exp. Med. Biol.* **2019**, *1118*, 253–269. https://doi.org/10.1007/978-3-030-05542-4_13.
195. Braniste, V.; Al-Asmakh, M.; Kowal, C.; Anuar, F.; Abbaspour, A.; Tóth, M.; Korecka, A.; Bakocevic, N.; Ng, L.G.; Kundu, P.; et al. The Gut Microbiota Influences Blood-Brain Barrier Permeability in Mice. *Sci. Transl. Med.* **2014**, *6*, 263ra158. https://doi.org/10.1126/scitranslmed.3009759.
196. Hsiao, E.Y.; McBride, S.W.; Chow, J.; Mazmanian, S.K.; Patterson, P.H. Modeling an Autism Risk Factor in Mice Leads to Permanent Immune Dysregulation. *Proc. Natl. Acad. Sci. USA* **2012**, *109*, 12776–12781. https://doi.org/10.1073/pnas.1202556109.
197. Sureda, A.; Daglia, M.; Castilla, A.S.; Sanadgol, N.; Nabavi, S.F.; Khan, H.; Belwal, T.; Jeandet, P.; Marchese, A.; Pistollato, F.; et al. Oral Microbiota and Alzheimer's Disease: Do All Roads Lead to Rome? *Pharmacol. Res.* **2020**, *151*, 104582. https://doi.org/10.1016/j.phrs.2019.104582.
198. Olsen, I. Update on Bacteraemia Related to Dental Procedures. *Transfus. Apher. Sci.* **2008**, *39*, 173–178. https://doi.org/10.1016/j.transci.2008.06.008.
199. Shoemark, D.K.; Allen, S.J. The Microbiome and Disease: Reviewing the Links between the Oral Microbiome, Aging, and Alzheimer's Disease. *J. Alzheimers. Dis.* **2015**, *43*, 725–738. https://doi.org/10.3233/JAD-141170.
200. Capsoni, S.; Carucci, N.M.; Cattaneo, A. Pathogen Free Conditions Slow the Onset of Neurodegeneration in a Mouse Model of Nerve Growth Factor Deprivation. *J. Alzheimer's Dis.* **2012**, *31*, 1–6. https://doi.org/10.3233/JAD-2012-120427.
201. Ghersi-Egea, J.F.; Leninger-Muller, B.; Suleman, G.; Siest, G.; Minn, A. Localization of Drug-Metabolizing Enzyme Activities to Blood-Brain Interfaces and Circumventricular Organs. *J. Neurochem.* **1994**, *62*, 1089–1096. https://doi.org/10.1046/j.1471-4159.1994.62031089.x.
202. Dong, X. Current Strategies for Brain Drug Delivery. *Theranostics* **2018**, *8*, 1481–1493. https://doi.org/10.7150/thno.21254.
203. Cohen-Pfeffer, J.L.; Gururangan, S.; Lester, T.; Lim, D.A.; Shaywitz, A.J.; Westphal, M.; Slavc, I. Intracerebroventricular Delivery as a Safe, Long-Term Route of Drug Administration. *Pediatr. Neurol.* **2017**, *67*, 23–35. https://doi.org/10.1016/j.pediatrneurol.2016.10.022.
204. Huang, M.; Gu, X.; Gao, X. In *13-Nanotherapeutic Strategies for the Treatment of Neurodegenerative Diseases*; Gao, H., Gao, X.B.T.-B.T.D.D.S., Eds.; Academic Press: Cambridge, MA, USA, 2019; pp. 321–356. ISBN 978-0-12-814001-7

205. Gentry, C.L.; Egleton, R.D.; Gillespie, T.; Abbruscato, T.J.; Bechowski, H.B.; Hruby, V.J.; Davis, T.P. The Effect of Halogenation on Blood-Brain Barrier Permeability of a Novel Peptide Drug. *Peptides* **1999**, *20*, 1229–1238. https://doi.org/10.1016/s0196-9781(99)00127-8.
206. Witt, K.A.; Slate, C.A.; Egleton, R.D.; Huber, J.D.; Yamamura, H.I.; Hruby, V.J.; Davis, T.P. Assessment of Stereoselectivity of Trimethylphenylalanine Analogues of Delta-Opioid [D-Pen(2),D-Pen(5)]-Enkephalin. *J. Neurochem.* **2000**, *75*, 424–435. https://doi.org/10.1046/j.1471-4159.2000.0750424.x.
207. Banks, W.A.; Kastin, A.J. Peptides and the Blood-Brain Barrier: Lipophilicity as a Predictor of Permeability. *Brain Res. Bull.* **1985**, *15*, 287–292. https://doi.org/10.1016/0361-9230(85)90153-4.
208. Pardridge, W.M. Molecular Trojan Horses for Blood-Brain Barrier Drug Delivery. *Curr. Opin. Pharmacol.* **2006**, *6*, 494–500. https://doi.org/10.1016/j.coph.2006.06.001.
209. Pencea, V.; Bingaman, K.D.; Wiegand, S.J.; Luskin, M.B. Infusion of Brain-Derived Neurotrophic Factor into the Lateral Ventricle of the Adult Rat Leads to New Neurons in the Parenchyma of the Striatum, Septum, Thalamus, and Hypothalamus. *J. Neurosci.* **2001**, *21*, 6706–6717. https://doi.org/10.1523/JNEUROSCI.21-17-06706.2001.
210. Ventriglia, M.; Bocchio Chiavetto, L.; Benussi, L.; Binetti, G.; Zanetti, O.; Riva, M.A.; Gennarelli, M. Association between the BDNF 196 A/G Polymorphism and Sporadic Alzheimer's Disease. *Mol. Psychiatry* **2002**, *7*, 136–137.
211. Neves-Pereira, M.; Mundo, E.; Muglia, P.; King, N.; Macciardi, F.; Kennedy, J.L. The Brain-Derived Neurotrophic Factor Gene Confers Susceptibility to Bipolar Disorder: Evidence from a Family-Based Association Study. *Am. J. Hum. Genet.* **2002**, *71*, 651–655. https://doi.org/10.1086/342288.
212. Pardridge, W.M. Biologic TNFα-Inhibitors That Cross the Human Blood-Brain Barrier. *Bioeng. Bugs* **2010**, *1*, 231–234. https://doi.org/10.4161/bbug.1.4.12105.
213. Pardridge, W.M. Delivery of Biologics Across the Blood–Brain Barrier with Molecular Trojan Horse Technology. *BioDrugs* **2017**, *31*, 503–519. https://doi.org/10.1007/s40259-017-0248-z.
214. Naqvi, S.; Panghal, A.; Flora, S.J.S. Nanotechnology: A Promising Approach for Delivery of Neuroprotective Drugs. *Front. Neurosci.* **2020**, *14*, 494. https://doi.org/10.3389/fnins.2020.00494.
215. Patel, P.; Kriz, J.; Gravel, M.; Soucy, G.; Bareil, C.; Gravel, C.; Julien, J.-P. Adeno-Associated Virus–Mediated Delivery of a Recombinant Single-Chain Antibody Against Misfolded Superoxide Dismutase for Treatment of Amyotrophic Lateral Sclerosis. *Mol. Ther.* **2014**, *22*, 498–510. https://doi.org/10.1038/mt.2013.239.
216. Yáñez-Mó, M.; Siljander, P.R.-M.; Andreu, Z.; Zavec, A.B.; Borràs, F.E.; Buzas, E.I.; Buzas, K.; Casal, E.; Cappello, F.; Carvalho, J.; et al. Biological Properties of Extracellular Vesicles and Their Physiological Functions. *J. Extracell. Vesicles* **2015**, *4*, 27066. https://doi.org/10.3402/jev.v4.27066.
217. Silverman, J.M.; Fernando, S.M.; Grad, L.I.; Hill, A.F.; Turner, B.J.; Yerbury, J.J.; Cashman, N.R. Disease Mechanisms in ALS: Misfolded SOD1 Transferred Through Exosome-Dependent and Exosome-Independent Pathways. *Cell. Mol. Neurobiol.* **2016**, *36*, 377–381. https://doi.org/10.1007/s10571-015-0294-3.
218. Jeon, I.; Cicchetti, F.; Cisbani, G.; Lee, S.; Li, E.; Bae, J.; Lee, N.; Li, L.; Im, W.; Kim, M.; et al. Human-to-Mouse Prion-like Propagation of Mutant Huntingtin Protein. *Acta Neuropathol.* **2016**, *132*, 577–592. https://doi.org/10.1007/s00401-016-1582-9.
219. Saá, P.; Yakovleva, O.; de Castro, J.; Vasilyeva, I.; De Paoli, S.H.; Simak, J.; Cervenakova, L. First Demonstration of Transmissible Spongiform Encephalopathy-Associated Prion Protein (PrPTSE) in Extracellular Vesicles from Plasma of Mice Infected with Mouse-Adapted Variant Creutzfeldt-Jakob Disease by in Vitro Amplification. *J. Biol. Chem.* **2014**, *289*, 29247–29260. https://doi.org/10.1074/jbc.M114.589564.
220. Kokubo, H.; Saido, T.C.; Iwata, N.; Helms, J.B.; Shinohara, R.; Yamaguchi, H. Part of Membrane-Bound Abeta Exists in Rafts within Senile Plaques in Tg2576 Mouse Brain. *Neurobiol. Aging* **2005**, *26*, 409–418. https://doi.org/10.1016/j.neurobiolaging.2004.04.008.
221. An, K.; Klyubin, I.; Kim, Y.; Jung, J.H.; Mably, A.J.; O'Dowd, S.T.; Lynch, T.; Kanmert, D.; Lemere, C.A.; Finan, G.M.; et al. Exosomes Neutralize Synaptic-Plasticity-Disrupting Activity of Aβ Assemblies in Vivo. *Mol. Brain* **2013**, *6*, 47. https://doi.org/10.1186/1756-6606-6-47.
222. Vyas, Y.; Montgomery, J.M.; Cheyne, J.E. Hippocampal Deficits in Amyloid-β-Related Rodent Models of Alzheimer's Disease. *Front. Neurosci.* **2020**, *14*, 266. https://doi.org/10.3389/fnins.2020.00266.
223. Shpyleva, S.; Ivanovsky, S.; de Conti, A.; Melnyk, S.; Tryndyak, V.; Beland, F.A.; James, S.J.; Pogribny, I.P. Cerebellar Oxidative DNA Damage and Altered DNA Methylation in the BTBR T+tf/J Mouse Model of Autism and Similarities with Human Post Mortem Cerebellum. *PLoS ONE* **2014**, *9*, e113712. https://doi.org/10.1371/journal.pone.0113712.
224. Perets, N.; Betzer, O.; Shapira, R.; Brenstein, S.; Angel, A.; Sadan, T.; Ashery, U.; Popovtzer, R.; Offen, D. Golden Exosomes Selectively Target Brain Pathologies in Neurodegenerative and Neurodevelopmental Disorders. *Nano Lett.* **2019**, *19*, 3422–3431. https://doi.org/10.1021/acs.nanolett.8b04148.
225. Baizabal-Carvallo, J.F.; Alonso-Juarez, M. The Link between Gut Dysbiosis and Neuroinflammation in Parkinson's Disease. *Neuroscience* **2020**, *432*, 160–173. https://doi.org/10.1016/j.neuroscience.2020.02.030.
226. Mancuso, C.; Santangelo, R. Alzheimer's Disease and Gut Microbiota Modifications: The Long Way between Preclinical Studies and Clinical Evidence. *Pharmacol. Res.* **2018**, *129*, 329–336. https://doi.org/10.1016/j.phrs.2017.12.009.
227. Tillisch, K.; Labus, J.; Kilpatrick, L.; Jiang, Z.; Stains, J.; Ebrat, B.; Guyonnet, D.; Legrain-Raspaud, S.; Trotin, B.; Naliboff, B.; et al. Consumption of Fermented Milk Product with Probiotic Modulates Brain Activity. *Gastroenterology* **2013**, *144*, 1394–1401, 1401.e1-4. https://doi.org/10.1053/j.gastro.2013.02.043.
228. Messaoudi, M.; Lalonde, R.; Violle, N.; Javelot, H.; Desor, D.; Nejdi, A.; Bisson, J.-F.; Rougeot, C.; Pichelin, M.; Cazaubiel, M.; et al. Assessment of Psychotropic-like Properties of a Probiotic Formulation (Lactobacillus Helveticus R0052 and Bifidobacterium Longum R0175) in Rats and Human Subjects. *Br. J. Nutr.* **2011**, *105*, 755–764. https://doi.org/10.1017/S0007114510004319.

229. Messaoudi, M.; Violle, N.; Bisson, J.-F.; Desor, D.; Javelot, H.; Rougeot, C. Beneficial Psychological Effects of a Probiotic Formulation (Lactobacillus Helveticus R0052 and Bifidobacterium Longum R0175) in Healthy Human Volunteers. *Gut Microbes* **2011**, *2*, 256–261. https://doi.org/10.4161/gmic.2.4.16108.
230. Sasmita, A.O. Modification of the Gut Microbiome to Combat Neurodegeneration. *Rev*. *Neurosci*. **2019**, *30*, 795–805. https://doi.org/10.1515/revneuro-2019-0005.
231. Goyal, D.; Ali, S.A.; Singh, R.K. Emerging Role of Gut Microbiota in Modulation of Neuroinflammation and Neurodegeneration with Emphasis on Alzheimer's Disease. *Prog*. *Neuropsychopharmacol*. *Biol*. *Psychiatry* **2021**, *106*, 110112. https://doi.org/10.1016/j.pnpbp.2020.110112.
232. Kouchaki, E.; Tamtaji, O.R.; Salami, M.; Bahmani, F.; Daneshvar Kakhaki, R.; Akbari, E.; Tajabadi-Ebrahimi, M.; Jafari, P.; Asemi, Z. Clinical and Metabolic Response to Probiotic Supplementation in Patients with Multiple Sclerosis: A Randomized, Double-Blind, Placebo-Controlled Trial. *Clin*. *Nutr*. **2017**, *36*, 1245–1249. https://doi.org/10.1016/j.clnu.2016.08.015.
233. Cho, Y.; Son, H.J.; Kim, E.-M.; Choi, J.H.; Kim, S.T.; Ji, I.J.; Choi, D.H.; Joh, T.H.; Kim, Y.S.; Hwang, O. Doxycycline Is Neuroprotective against Nigral Dopaminergic Degeneration by a Dual Mechanism Involving MMP-3. *Neurotox*. *Res*. **2009**, *16*, 361–371. https://doi.org/10.1007/s12640-009-9078-1.
234. Lazzarini, M.; Martin, S.; Mitkovski, M.; Vozari, R.R.; Stühmer, W.; Bel, E. Del Doxycycline Restrains Glia and Confers Neuroprotection in a 6-OHDA Parkinson Model. *Glia* **2013**, *61*, 1084–1100. https://doi.org/10.1002/glia.22496.
235. McElhanon, B.O.; McCracken, C.; Karpen, S.; Sharp, W.G. Gastrointestinal Symptoms in Autism Spectrum Disorder: A Meta-Analysis. *Pediatrics* **2014**, *133*, 872–883. https://doi.org/10.1542/peds.2013-3995.
236. Hsiao, E.Y.; McBride, S.W.; Hsien, S.; Sharon, G.; Hyde, E.R.; McCue, T.; Codelli, J.A.; Chow, J.; Reisman, S.E.; Petrosino, J.F.; et al. Microbiota Modulate Behavioral and Physiological Abnormalities Associated with Neurodevelopmental Disorders. *Cell* **2013**, *155*, 1451–1463. https://doi.org/10.1016/j.cell.2013.11.024.
237. Labusca, L.; Herea, D.D.; Mashayekhi, K. Stem Cells as Delivery Vehicles for Regenerative Medicine-Challenges and Perspectives. *World J*. *Stem Cells* **2018**, *10*, 43–56. https://doi.org/10.4252/wjsc.v10.i5.43.
238. Wu, Y.-C.; Sonninen, T.-M.; Peltonen, S.; Koistinaho, J.; Lehtonen, Š. Blood-Brain Barrier and Neurodegenerative Diseases—Modeling with IPSC-Derived Brain Cells. *Int*. *J*. *Mol*. *Sci*. 2021, *22*, 7710.
239. Matsushita, T.; Kibayashi, T.; Katayama, T.; Yamashita, Y.; Suzuki, S.; Kawamata, J.; Honmou, O.; Minami, M.; Shimohama, S. Mesenchymal Stem Cells Transmigrate across Brain Microvascular Endothelial Cell Monolayers through Transiently Formed Inter-Endothelial Gaps. *Neurosci*. *Lett*. **2011**, *502*, 41–45. https://doi.org/10.1016/j.neulet.2011.07.021.
240. Volkman, R.; Offen, D. Concise Review: Mesenchymal Stem Cells in Neurodegenerative Diseases. *Stem Cells* **2017**, *35*, 1867–1880. https://doi.org/10.1002/stem.2651.
241. Perets, N.; Segal-Gavish, H.; Gothelf, Y.; Barzilay, R.; Barhum, Y.; Abramov, N.; Hertz, S.; Morozov, D.; London, M.; Offen, D. Long Term Beneficial Effect of Neurotrophic Factors-Secreting Mesenchymal Stem Cells Transplantation in the BTBR Mouse Model of Autism. *Behav*. *Brain Res*. **2017**, *331*, 254–260. https://doi.org/10.1016/j.bbr.2017.03.047.
242. Behnan, J.; Stangeland, B.; Langella, T.; Finocchiaro, G.; Tringali, G.; Meling, T.R.; Murrell, W. Identification and Characterization of a New Source of Adult Human Neural Progenitors. *Cell Death Dis*. **2017**, *8*, e2991. https://doi.org/10.1038/cddis.2017.368.
243. Liu, Y.; Weick, J.P.; Liu, H.; Krencik, R.; Zhang, X.; Ma, L.; Zhou, G.; Ayala, M.; Zhang, S.-C. Medial Ganglionic Eminence–like Cells Derived from Human Embryonic Stem Cells Correct Learning and Memory Deficits. *Nat*. *Biotechnol*. **2013**, *31*, 440–447. https://doi.org/10.1038/nbt.2565.
244. Wu, C.-C.; Lien, C.-C.; Hou, W.-H.; Chiang, P.-M.; Tsai, K.-J. Gain of BDNF Function in Engrafted Neural Stem Cells Promotes the Therapeutic Potential for Alzheimer's Disease. *Sci*. *Rep*. **2016**, *6*, 27358. https://doi.org/10.1038/srep27358.
245. Blurton-Jones, M.; Spencer, B.; Michael, S.; Castello, N.A.; Agazaryan, A.A.; Davis, J.L.; Müller, F.-J.; Loring, J.F.; Masliah, E.; LaFerla, F.M. Neural Stem Cells Genetically-Modified to Express Neprilysin Reduce Pathology in Alzheimer Transgenic Models. *Stem Cell Res*. *Ther*. **2014**, *5*, 46. https://doi.org/10.1186/scrt440.
246. Takahashi, K.; Yamanaka, S. Induction of Pluripotent Stem Cells from Mouse Embryonic and Adult Fibroblast Cultures by Defined Factors. *Cell* **2006**, *126*, 663–676. https://doi.org/10.1016/j.cell.2006.07.024.
247. Takahashi, K.; Tanabe, K.; Ohnuki, M.; Narita, M.; Ichisaka, T.; Tomoda, K.; Yamanaka, S. Induction of Pluripotent Stem Cells from Adult Human Fibroblasts by Defined Factors. *Cell* **2007**, *131*, 861–872. https://doi.org/10.1016/j.cell.2007.11.019.
248. Doss, M.X.; Sachinidis, A. Current Challenges of IPSC-Based Disease Modeling and Therapeutic Implications. *Cells* **2019**, *8*, 403. https://doi.org/10.3390/cells8050403.
249. Picanço-Castro, V.; Moreira, L.F.; Kashima, S.; Covas, D.T. Can Pluripotent Stem Cells Be Used in Cell-Based Therapy? *Cell*. *Reprogram*. **2014**, *16*, 98–107. https://doi.org/10.1089/cell.2013.0072.
250. Schweitzer, J.S.; Song, B.; Herrington, T.M.; Park, T.-Y.; Lee, N.; Ko, S.; Jeon, J.; Cha, Y.; Kim, K.; Li, Q.; et al. Personalized IPSC-Derived Dopamine Progenitor Cells for Parkinson's Disease. *N*. *Engl*. *J*. *Med*. **2020**, *382*, 1926–1932. https://doi.org/10.1056/NEJMoa1915872.
251. Madrid, M.; Sumen, C.; Aivio, S.; Saklayen, N. Autologous Induced Pluripotent Stem Cell–Based Cell Therapies: Promise, Progress, and Challenges. *Curr*. *Protoc*. **2021**, *1*, e88. https://doi.org/10.1002/cpz1.88.
252. Kondziolka, D. Reaching the Far Corners of Neurosurgery. *Neurosurgery* **2022**, *91*, 525–526.
253. Fischer, U.M.; Harting, M.T.; Jimenez, F.; Monzon-Posadas, W.O.; Xue, H.; Savitz, S.I.; Laine, G.A.; Cox, C.S. Pulmonary Passage Is a Major Obstacle for Intravenous Stem Cell Delivery: The Pulmonary First-Pass Effect. *Stem Cells Dev*. **2008**, *18*, 683–692. https://doi.org/10.1089/scd.2008.0253.

254. Zhang, Y.-T.; He, K.-J.; Zhang, J.-B.; Ma, Q.-H.; Wang, F.; Liu, C.-F. Advances in Intranasal Application of Stem Cells in the Treatment of Central Nervous System Diseases. *Stem Cell Res*. *Ther*. **2021**, *12*, 210. https://doi.org/10.1186/s13287-021-02274-0.
255. Berry, J.D.; Cudkowicz, M.E.; Windebank, A.J.; Staff, N.P.; Owegi, M.; Nicholson, K.; McKenna-Yasek, D.; Levy, Y.S.; Abramov, N.; Kaspi, H.; et al. NurOwn, Phase 2, Randomized, Clinical Trial in Patients with ALS: Safety, Clinical, and Biomarker Results. *Neurology* **2019**, *93*, e2294–e2305. https://doi.org/10.1212/WNL.0000000000000862

Annex 2: Research Article

C9ORF72 patient-derived endothelial cells drive Blood-Brain Barrier disruption and contribute to neurotoxicity

Ana Aragón-González[1,2,3*], Allan C Shaw[1], Jannigje R Kok[1], Florence S Roussel[3], Cleide dos Santos Souza[1], Sarah M Granger[1], Tatyana Vetter[3,4], Yolanda de Diego[5,6], Kathrin C Meyer[3,4], Selina N Beal[1], Pamela J Shaw[1,7], Laura Ferraiuolo[1*].

1 Sheffield Institute for Translational Neuroscience, University of Sheffield, 385 Glossop Road, Sheffield S10 2HQ, United Kingdom.

2 Facultad de Medicina, Universidad de Málaga, 29010 Malaga, Spain.

3 Center for Gene Therapy, The Abigail Wexner Research Institute, Nationwide Children's Hospital, Columbus, OH 43205, USA.

4 Department of Pediatrics, The Ohio State University, Columbus, OH, USA.

5 Research Group PAIDI CTS-546, Institute of Biomedical Research of Málaga (IBIMA), 29010 Malaga, Spain.

6 Department of Cell Biology, Physiology, and Immunology, Campus Rabanales, University of Córdoba, Cordoba, Spain.

7 NIHR Sheffield Biomedical Research Centre, Sheffield Teaching Hospitals NHS Foundation Trust, Glossop Road, United Kingdom.

* Corresponding authors:

Ana Aragón-González: a.aragon@sheffield.ac.uk

Laura Ferraiuolo: l.ferraiuolo@sheffield.ac.uk

Original Research Article

Citation: Aragón-González, A., Shaw, A.C., Kok, J.R. et al. C9ORF72 patient-derived endothelial cells drive blood-brain barrier disruption and contribute to neurotoxicity. Fluids Barriers CNS 21, 34 (2024). https://doi.org/10.1186/s12987-024-00528-6

Academic Editor: Matthew Campbell

Received: 18 December 2023

Accepted: 02 March 2024

Published: 11 April 2024

Abstract

The blood-brain barrier (BBB) serves as a highly intricate and dynamic interface connecting the brain and the bloodstream, playing a vital role in maintaining brain homeostasis. BBB dysfunction has been associated with multiple neurodegenerative diseases, including amyotrophic lateral sclerosis (ALS); however, the role of the BBB in neurodegeneration is understudied. We developed an ALS patient-derived model of the BBB by using cells derived from 5 patient donors carrying *C9ORF72* mutations. Brain microvascular endothelial-like cells (BMEC-like cells) derived from *C9ORF72*-ALS patients showed altered gene expression, compromised barrier integrity, and increased P-glycoprotein transporter activity. In addition, mitochondrial metabolic tests demonstrated that *C9ORF72*-ALS BMECs display a significant decrease in basal glycolysis accompanied by increased basal and ATP-linked respiration. Moreover, our study reveals that C9-ALS derived astrocytes can further affect BMECs function and affect the expression of the glucose transporter Glut-1. Finally, *C9ORF72* patient-derived BMECs form leaky barriers through a cell-autonomous mechanism and have neurotoxic properties towards motor neurons.

Key words: Stem Cells; Blood Brain Barrier; Amyotrophic Lateral Sclerosis; C9ORF72; *In vitro* modelling; Neurodegeneration

Introduction

The blood-brain barrier (BBB) serves as a highly intricate and dynamic interface connecting the brain and the bloodstream, carrying out several specialised functions. It comprises endothelial cells lining the capillary wall, astrocyte end-feet enveloping the capillary, and pericytes embedded in the capillary basement membrane [1]. The BBB permits the passive passage of hydrophobic molecules such as O2, CO2, and hormones, as well as small polar molecules. It regulates the exchange of metabolic substrates, such as glucose, using specific transport proteins across the barrier. Whilst tight regulation of molecular exchange between the blood and the brain is crucial for central nervous system function, the endothelial interface limits the entry of neuro-therapeutic molecules, thus making manipulations of BBB permeability an interesting target [2]. Conversely, disruptions in the BBB commonly occur in neurodegenerative diseases like Alzheimer's (AD) and amyotrophic lateral sclerosis (ALS). Despite growing evidence of BBB dysfunction in these conditions, further research is needed to understand its role in disease progression [3].

Graphical Abstract

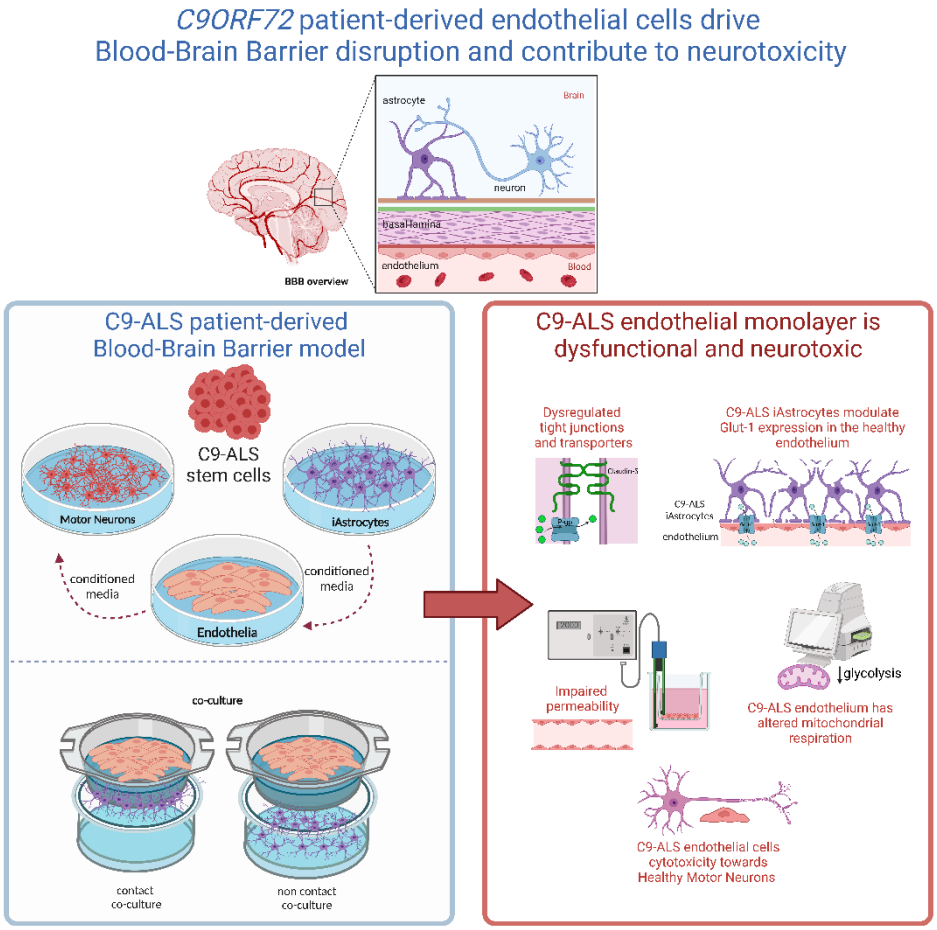

This graphical abstract was created on Biorender.com

Brain microvascular endothelial cells (BMECs) are the major cellular element in the BBB [4]. These cells present unique characteristics that distinguish them from the vascular endothelium in the rest of the body. BMEC-like cells lack fenestrations, express tight junctions (TJs) and specialised transporters, and interact with other cell types comprising the neurovascular unit (NVU). These attributes allow them to regulate the movement of ions, molecules, and cells between the blood and the brain [5].

The other main component of the BBB is the astrocyte [6], which plays an essential role in establishing and maintaining it. Astrocytic end-feet form a coating network around the brain vasculature, the glia limitans, and, together with endothelial cells and pericytes [7], they form the BBB, separating the bloodstream from the brain parenchyma. All components interact with each other, contributing to BBB function, development, and maintenance [4]. It is well documented that astrocyte function dysregulation is associated with neurodegenerative diseases such as ALS [8], AD [9]; and paediatric neurological disorders like Rett syndrome [10]. ALS, also known as motor neuron disease (MND), is a fatal neurodegenerative disorder characterised by progressive loss of upper and lower motor neurons (MNs), causing progressive paralysis, muscle atrophy due to denervation and, consequently, death due to respiratory failure. To date, there is no effective drug treatment for ALS. At present, Riluzole, Edaravone and Relyvrio are the only drugs approved by the US Food and Drugs Administration (FDA), providing modest benefits only in some patients [11].

Although most cases of ALS are sporadic (sALS) in origin, meaning that there is no family history of the disease, about 10% of patients are familial (fALS). Even though more than 35 genes have been linked with fALS, the most common disease-causing mutations are hexanucleotide (GGGGCC) intronic repeat expansions in the *C9ORF72* (C9) gene, followed by mutations in *SOD1* [12]. Remarkably, familial and sporadic ALS are for the most part clinically indistinguishable. Importantly, *C9ORF72* mutations are also known to cause frontotemporal dementia (FTD). Although the link between ALS pathology and BBB dysfunction is not clear, transgenic rodents expressing human *SOD1* mutations develop a leaky BBB with higher permeability, enlarged astrocytic end-feet, and an interrupted basement membrane associated with a reduction of BMEC-like cells and astrocytes, thus leading to oedema and microbleeds. This pathological phenotype is also observed in ALS patients [13]. The early BBB breakdown might appear as cerebral microbleeds, which are frequently seen in vascular dementia [14] and AD patients [15], suggesting that BBB failure might precede neurodegeneration.

Although vascular pathology has not been frequently studied in C9 mutation carriers, a recent publication reported increased glucose transport, together with enhanced Glucose-1 transporter expression in the BBB of a C9-ALS mouse model. In contrast, other permeability processes, such as passive diffusion or efflux transport, remained unaffected [16]. Consistently, P-glycoprotein transport was not altered in C9-ALS mice, and only a mild increase in ZO-1 expression was reported [16]. In addition, Sweeney et al. 2019 [17] proposed that BBB disruption due to endothelial cell degeneration causes extravasation of erythrocytes and accumulation of plasma-derived proteins such as Immunoglobulin G (IgG).

Currently, there is limited information available on how BBB breakdown affects the progression of ALS. However, a cross-sectional study by Prell et al. [18], focussing on cerebrospinal fluid and blood samples taken from ALS patients, found that there is no correlation between higher disease aggressiveness and markers of BBB breakdown. Thus, indicating that this pathological phenotype might be secondary to neurodegeneration.

Considering the knowledge gap in this area of ALS/ FTD pathology and the complexity of dissecting the contribution of different cell types to the neurodegenerative process, the present study sought to interrogate a human *C9ORF72* patient-derived model of the BBB to test the leakiness of such a system and unravel the role of endothelial cells in BBB dysregulation. We demonstrated that *C9ORF72* patient-derived endothelial cells form leaky barriers through a cell-autonomous mechanism and have neurotoxic properties towards healthy motor neurons.

Results

Hi-PSC-derived BMEC-like cells express a vascular/ endothelial profile and show barrier functionality

One of the most challenging aspects of studying the role of the BBB in neurodegenerative diseases is the limited availability of human in vitro models. Hence, we first set off to differentiate brain microvascular endothelial-like cells (BMEC-like cells) from a total of 2 human induced pluripotent stem cell lines (hi-PSCs) derived from healthy donor's fibroblasts, as previously described by others [19]. As reported, after 7 days of differentiation and subsequent subculture, hi-PSC-derived BMEC-like cells expressed various endothelial markers such as Claudin-5 and vascular endothelial growth factor A (VEGF-A) demonstrated by immunostaining (Fig. 1A). Indeed, upon differentiation, hi-PSCs derived BMEC-like cells showed a transcriptional reduction in the pluripotency marker POU5F1 (OCT4) and showed increased RNA expression of cell-specific genes encoding for tight junction molecules such as Cadherin-5 (CDH5 or VE-Cadherin), Claudin-5 (CLDN5) and Occludin (OCLN), as well as the platelet endothelial cell adhesion molecule 1 (PECAM1 or CD31) and the Von Willebrand factor (VWF) (Fig. 1B), which are involved in both the establishment and the maintenance of BBB permeability [20].

We then assessed BMEC functionality by measuring transendothelial electrical resistance (TEER) [21]. TEER measurement has been widely used and is the gold standard to assess the functionality of the BBB, both in vivo and in vitro. The maximum TEER recorded in vivo was 5400 Ω x cm^2, in adult rats [22]. In terms of in vitro modelling, Lippmann and colleagues successfully developed brain endothelial like-cells using human induced pluripotent stem cells, with a TEER of 4000 Ω x cm^2 [19].

Using a similar approach, BMEC-like cells were seeded onto Transwell™ inserts (Fig. 1C) and monitored daily for 4 days (Fig. 1D). Control BMEC-like cells displayed a typical increase in TEER values over time from day 1 to 3, as tight junctions developed and matured to achieve TEER values above 4000 Ω x cm^2 at day 3 of subculture across independent differentiations (*N* = 3). As previously reported by others, the resistance rapidly decreased on day 4 [19] (Fig. 1D).

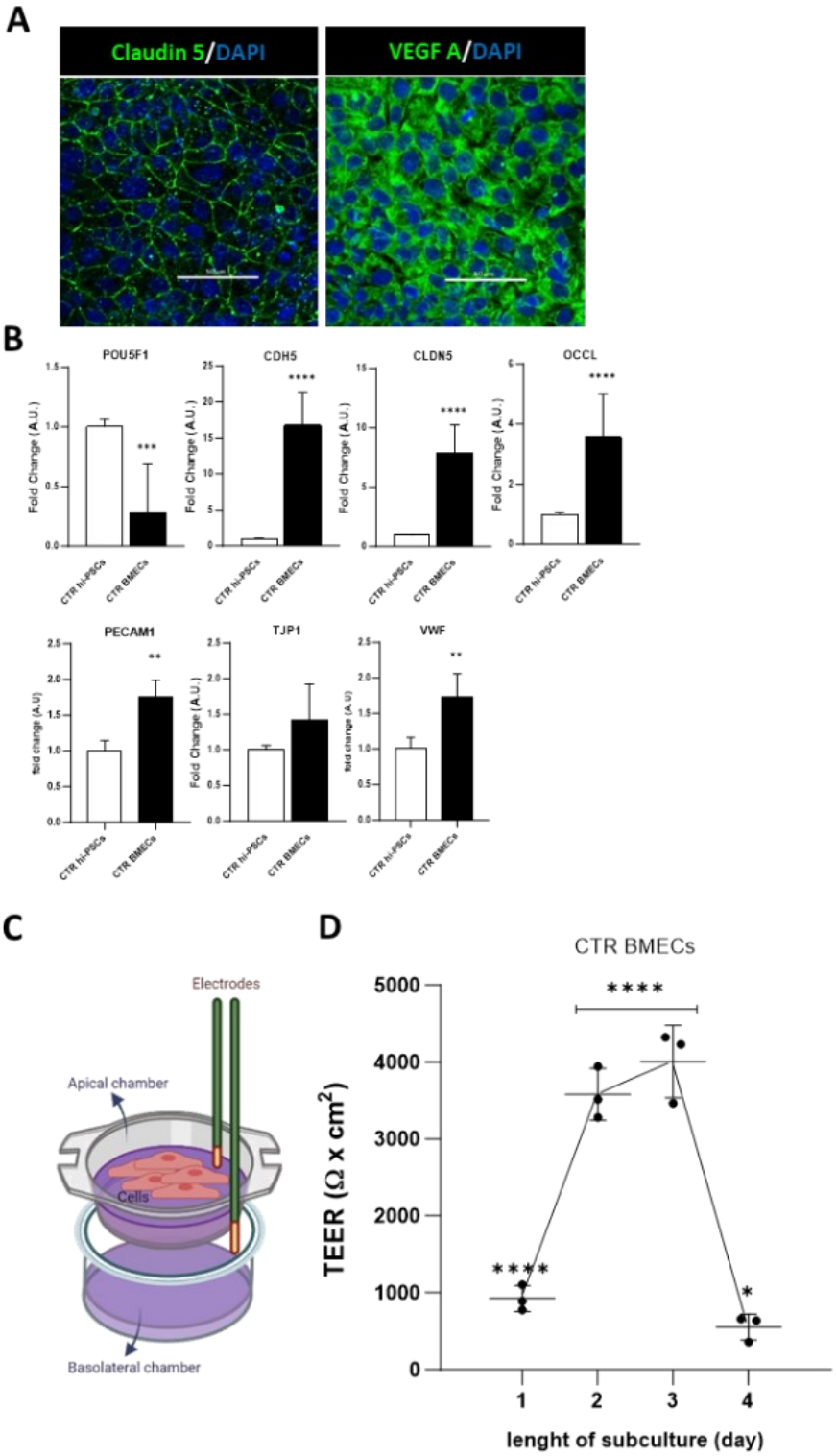

Fig. 1 BMEC-like cells can be differentiated from hi-PSCs and can produce a cell barrier *in vitro.* A) Immunocytochemistry of BMEC cells differentiated from a healthy hi-PSCs donor. Claudin-5 and Vascular endothelial growth factor A (VEGF-A) using the RA-enhanced Lippmann's laboratory protocol from 2019 [19]. Images were acquired with a Nikon confocal microscope. Scale bar 50 µm. B) Transcriptional expression of pluripotency and endothelial-specific markers in hi-PSCs and derived BMEC-like cells. Hi-PSC marker: POU5F1 (OCT4). Tight junctions: CDH5 (VE-CADHERIN), CLDN5, OCLN, PECAM1 (CD31), TJP1 (ZO-1) and VWF. The qRT-PCR data are plotted as mean±s.d. Student's unpaired t-test (****p<0.0001), N=3. C) Schematic representation of transendothelial resistance measurement (TEER). Cells plated on a permeable Transwell™ insert (0.4 µm PET) were assessed for TEER with an EVOM2 stx2 electrode. The diagram was created on Biorender.com D) BMEC passive barrier as shown by TEER following subculture for healthy donor hi-PSCs. Error bars represent the standard deviation of triplicate Transwell™ filters (N=3). Statistical significance was determined using One-Way ANOVA (****p<0.0001). N=3

C9-ALS BMEC-like cells monolayer displays functional abnormalities

Confident that the model developed from healthy hi-PSC recapitulated BMEC-like morphological and functional characteristics, we used the same differentiation protocol to interrogate the effects of the *C9ORF72* carriers and two healthy donors of similar age were differentiated into BMEC-like cells (Supplementary Table 1) and were interrogated by RT-qPCR for the expression of several BMEC-related markers that have been previously associated with ALS or BBB dysfunction in other pathologies (Fig. 2A, Supplementary Fig. 1) and immunocytochemistry (Supplementary Fig. 2). Briefly, we quantified transcripts encoding tight junction and adhesion proteins (VE-Cadherin, Claudin-5, JAM-2, Occludin, ZO-1); transporters (ABCB1 and SLC1A1, 2, 3); key receptors (INSR, RAGE); cytokines (TGFB1) and clotting factors (VWF). Overall, excluding Occludin and TGFB1, the data revealed a widespread transcriptional upregulation of BBB-associated structural proteins, transporters and receptors in C9-ALS BMEC-like cells compared to controls (Fig. 2A, Supplementary Fig. 1).

To assess whether these transcriptional alterations were associated with functional dysregulation, the monolayer permeability was tested by TEER measurements. The C9-ALS BMEC-like monolayer appeared visibly intact and macroscopically indistinguishable from its healthy counterpart (Fig. 2B and Supplementary Fig. 3). On day 1 of the assessment, TEER values for control and C9-ALS cells were comparable (1000 and 800 Ω x cm^2 respectively). However, on day 2, the TEER for C9-ALS BMEC-like cells failed to increase to the same level as the healthy control monolayer, with the C9-ALS BMEC-like TEER averaging approximately 2500 Ω x cm^2; whereas the control monolayer reached a TEER of 4000 Ω x cm^2. This significant difference was still present at day 3 with control BMEC-like cells sustaining a TEER measurement of 4000 Ω x $cm^2$and C9-ALS BMCs displaying a loss of membrane electrical resistance (900 Ω x cm^2). Finally, on day 4, both control and C9-ALS monolayers displayed the typical collapse in TEER measurement [19], which declined below 1000 Ω x cm^2 (Fig. 2C).

As we had identified a dysregulation in the P-glycoprotein (P-gp) transcript (ABCB1) (Fig. 2B), we next evaluated the efflux activity of this key transporter in BMEC-like cells. P-glycoprotein activity was tested by measuring the accumulation of its substrate, Rhodamine 123, via fluorescence, in the presence or absence of Cyclosporin A, a P-glycoprotein inhibitor (Fig. 2D). Both CTR and C9-ALS BMEC-like cells were incubated with Cyclosporin-A and showed a significant increase in fluorescence accumulation, indicating active P-glycoprotein function. However, patient P-glycoprotein efflux activity was significantly higher than control BMEC-like cells.

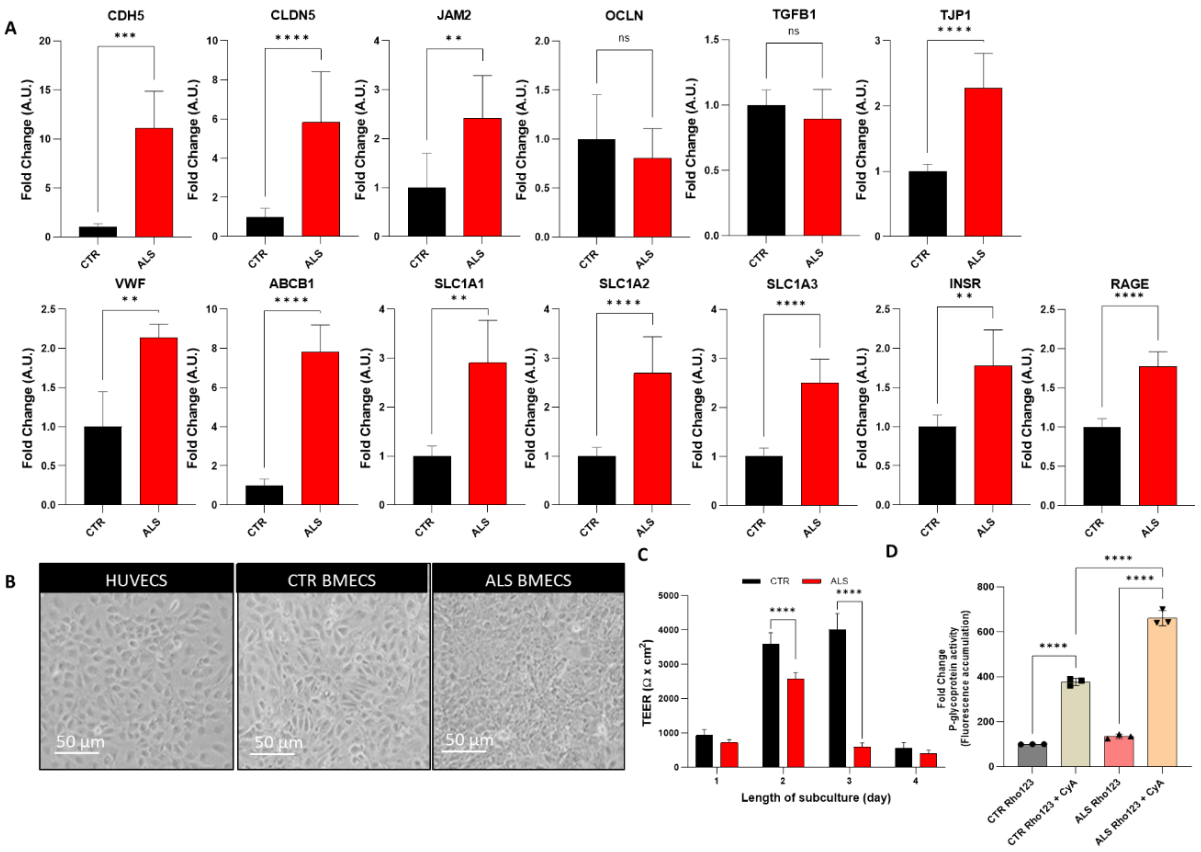

Fig. 2 C9-ALS BMEC-like cells form a dysfunctional barrier **A**) Blood-Brain Barrier phenotypic markers. VE-Cadherin (CDH5), Claudin-5 (CLDN5), Junctional Adhesion Molecule 2 (JAM2), Occludin (OCLN), Transforming growth factor beta 1 (TGFB1), Zonula Occludens 1 (TJP1) and, Von Willebrand factor (VWF), P-glycoprotein (ABCB1), EAAT3 (SLC1A1), EAAT2 (SLC1A2), EAAT1 (SLC1A3), Insulin receptor (INSR) and, receptor for advanced glycation end products (RAGE) transcriptional expression of 2 healthy donors and 3 C9-ALS donors hi-PSCs derived BMEC-like cells. qRT-PCR data are plotted as mean±s.d. Sta-tistical significance was determined using Student's unpaired t-test (****p<0.0001). N=3 per group. **B**) Brightfield images are shown as follows: HUVECs, CTR and C9-ALS BMEC-like cells. The scale bar equals 50 µM. **C**) BMEC passive barrier as shown by TEER following subculture for GM23338 male healthy donor hi-PSCs derived BMEC-like cells (CTR BMECs), CS52iALS-C9nxx and CS29iALS-C9nxx male C9-ALS donors (ALS BMECs). Error bars represent the standard deviation of triplicate Transwell™ filters. Statistical significance was determined using Student's unpaired t-test (****p<0.0001). **D**) BMEC-like cells were incubated with or without Cyclosporin-A, a P-glycoprotein inhibitor and, next with Rhodamine-123, a P-glycoprotein fluorescent substrate. Accu-mulation is normalised to the no-inhibitor samples. Error bars represent the standard deviation of triplicate wells. Statistical significance was determined using One-Way ANOVA (****p<0.0001). N=3

C9-ALS iAstrocytes conditioned medium is toxic to BMEC-like cells

Astrocytes are key players in BBB functionality, as they support BMECs through the secretion of trophic factors and maintain homeostasis. Research carried out by our group and others has shown that astrocytes are major players in ALS pathology [23, 24]. Above all, it has been reported that astrocytes derived from either post-mortem tissues or fibroblasts (iAstrocytes) from ALS patients are toxic towards motor neurons and this toxicity is also transferred through conditioned medium [25, 26]. Hence, we wanted to explore the effect of iAstrocytes on BMEC-like cells.

When C9-ALS BMEC-like cells were co-cultured either with healthy or with C9-ALS iAstrocytes, they displayed very poor TEER properties, comparable to the values obtained from the monocultures (Fig. 1D, Supplementary Fig. 4). Healthy astrocytes could not correct the cell-autonomous defects of the C9-ALS BMEC-like cells and C9-ALS iAstrocytes did not worsen their barrier phenotype (Supplementary Fig. 4).

We next interrogated the effect of C9-ALS iAstrocytes on BMEC-like cells from healthy individuals in a cell-to-cell contact as well as in a non-contact paradigm (Fig. 3A). For this experiment, BMEC-like cells were seeded on the apical chamber of the Transwell™ insert and iAstrocytes were placed either in the basal chamber (contact culture) or in the well underneath, with no physical contact but sharing the culture media (non-contact co-culture). Interestingly, the TEER of healthy BMEC-like cells co-cultured with C9-ALS iAstrocytes in the contact modality was unaffected (Fig. 3A) compared to BMEC-like cells in monoculture, while one would expect an increase in TEER when astrocytes and BMECs are cultured together. In contrast, a decrease in the TEER measurements of 36% (− 1400 Ω x cm^2) was recorded among the healthy BMEC-like cells when in non-contact co-culture with C9-ALS iAstrocytes.

To further explore the astrocyte-endothelial cells interaction within the barrier features, iAstrocyte conditioned media was added to BMEC-like cells for 48 h. Interestingly, the Glut-1 transporter protein was found to be upregulated in both healthy and C9-ALS BMEC-like cells after adding C9-ALS iAstrocytes conditioned media, thus indicating an active metabolic cross-talk between the two cell types through secreted factors. In contrast, the tight junction Claudin-5 protein expression decreased in the presence of C9-ALS iAstrocyte conditioned media (Fig. 3B). In the most severe condition, C9-ALS BMECs treated with C9-ALS iAstrocyte media, Claudin-5 staining while still junctional, it presents as puncta (Fig. 3B).

Finally, we used the LDH colourimetric assay to determine whether the differences observed in the TEER measurements and protein quantification were due to cytotoxicity. BMEC-like cells from healthy donors were assessed in monoculture at baseline and after 48 h in iAstrocyte conditioned medium **(**Fig. 3C). Plain astrocyte media-treated BMEC-like cells were used as controls (non-cond iA media).

C9-ALS iAstrocyte conditioned medium had a detrimental effect on healthy BMEC-like cells, as shown by an increase in LDH activity of over 60% (Fig. 3C) in comparison to untreated and healthy astrocyte-conditioned medium-treated cells. These results provide evidence that C9-ALS astrocyte toxicity extends beyond motor neurons.

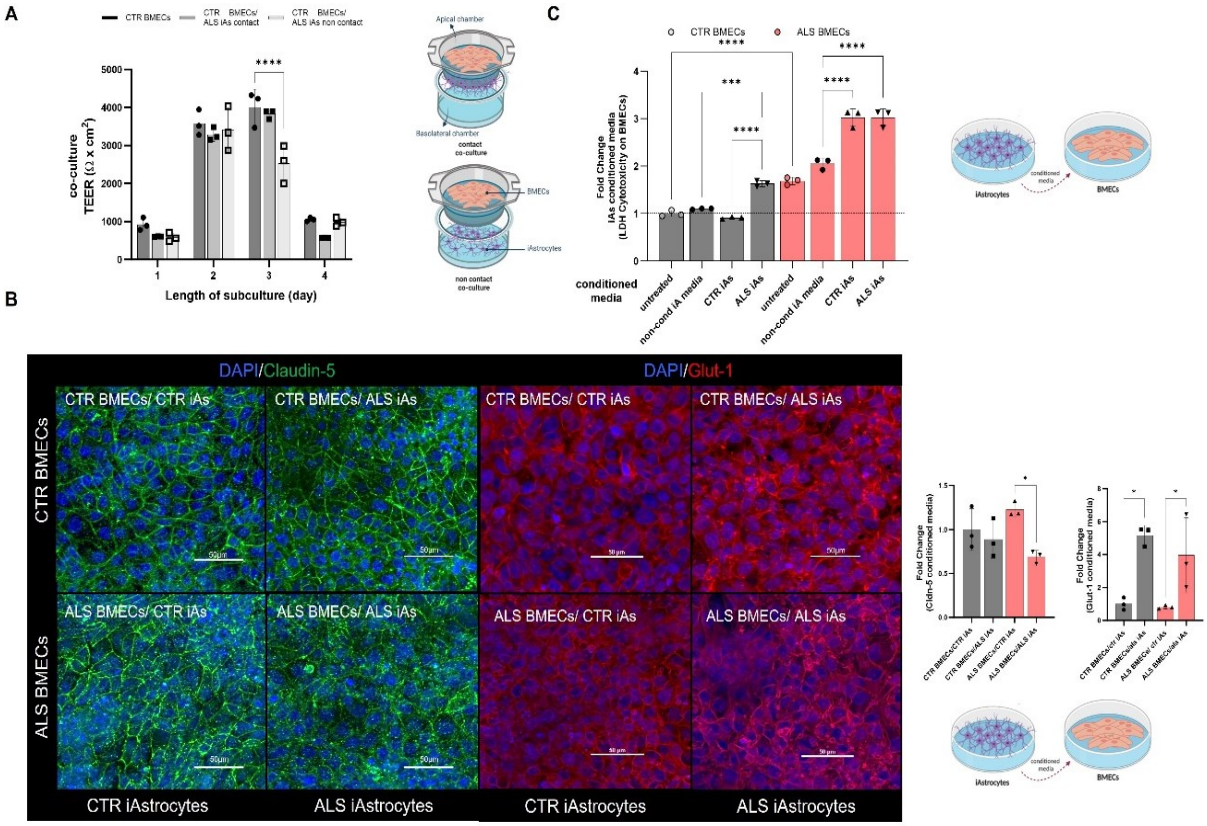

Fig. 3 C9-ALS iAstrocytes affect cell dynamics and paracellular permeability on BMEC-like cells **A**) BMEC passive barrier as shown by TEER following BMEC-like cells/iAstrocytes co-culture for C9-ALS BMEC-like cells. Error bars represent the standard deviation of triplicate Transwell™ filters. Statistical sig-nificance was determined using One-Way ANOVA (****p<0.0001). N=3. **B**) BMEC-like cells were either treated with control or C9-iAs-conditioned media. BMEC-like cells were fixed in 100% MeOH after 48 h of the experiment. Scale bar equals 50µM. Plotted results represent confocal image z-stacks analysed in 3D volume. Claudin-5 is shown in green and Glucose-1 transporter (Glut-1) in red; and DAPI in blue for the nuclei staining. Error bars represent the standard deviation of triplicate Transwell™ filters. Statistical significance was determined using One-Way ANOVA (****p<0.0001). N=3. At least a total of 5 images were acquired per each condition, with a minimum of 3 technical replicates for a total of 3 biological replicates (N=3, total images per condi-tion=45). **C**) The LDH assay was performed after 2 days of iAstrocytes conditioned media treatment on BMEC-like cells. Untreated refers to BMEC-like cells on their indicated endothelial media and non-cond iA media are BMEC-like cells treated with plain iAstrocytes media to evaluate the effect of the media on the BMEC-like cells. Control (CTR) and C9-ALS media (ALS). Error bars represent the standard deviation of triplicate wells. Statistical significance was determined using One-Way ANOVA (****p<0.0001). N=3

C9-ALS BMEC-like cells display metabolic defects

Since BMEC-like cells from C9-ALS donors displayed severe functional defects in a cell-autonomous fashion, we next decided to interrogate the expression and localisation of Claudin-5 and Glut-1, the major tight junction and main glucose transporter of the BBB respectively.

At the transcriptional level, C9-ALS BMEC-like cells displayed upregulation of CLDN5 (Claudin-5) (Fig. 1A), however, protein quantification and localisation were comparable to their healthy counterparts (Supplementary Fig. 2).

However, the expression of Glut-1 was significantly altered in C9-ALS BMEC-like cells, compared to controls, with an overall increase in protein immunofluorescence signal (Fig. 4A).

Due to the important metabolic role of BMECs at the BBB and the identified dysregulation in Glut-1, we decided to assess the metabolic function of healthy and C9-ALS BMEC-like cells using the Seahorse XF Real- Time ATP Rate Assay in the presence of mitochondria inhibitors (Fig. 4B). Consistent with the hypothesis that Glut-1 dysregulation would have downstream effects on metabolism; the data showed that C9-ALS BMEC-like cells display significantly higher basal respiration and ATP-linked respiration, while basal glycolysis is significantly downregulated (Fig. 4C).

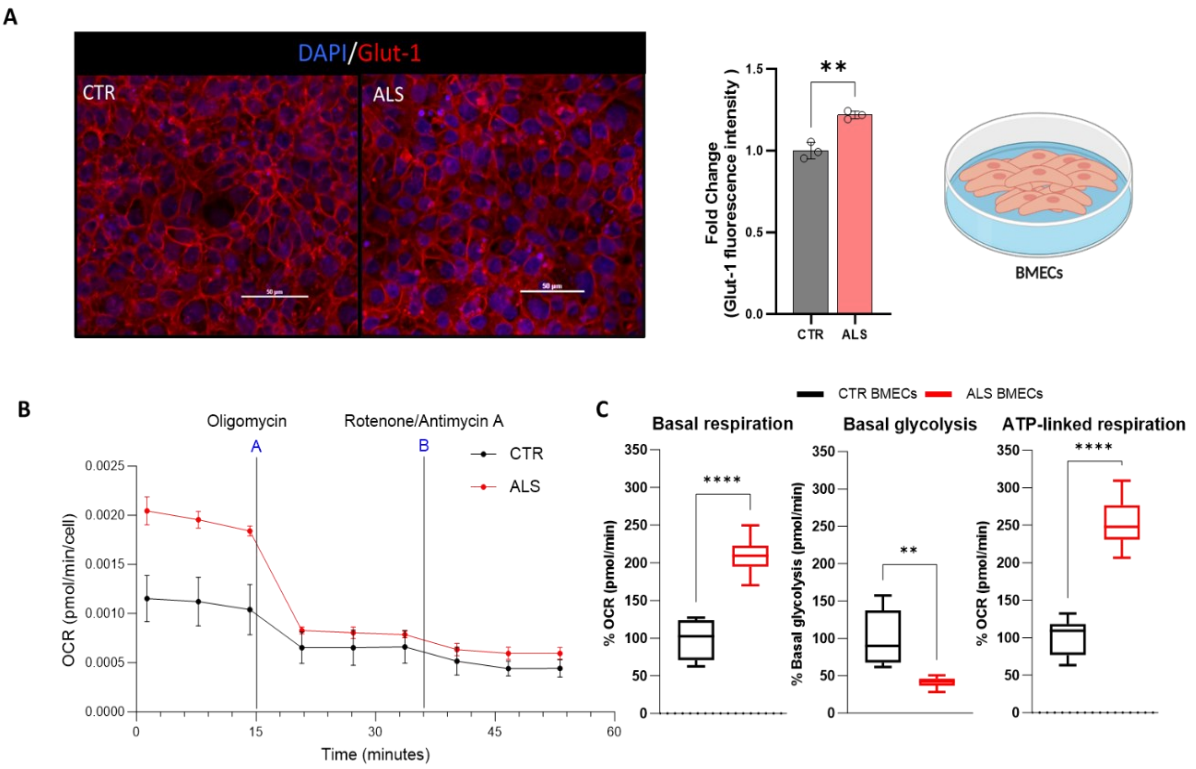

Fig. 4 C9-ALS BMEC-like cells have an increased glucose metabolism and altered mitochondrial respiration **A**) Healthy donor hi-PSCs derived BMEC-like cells (CTR BMECs) and C9-ALS donor hi-PSCs derived BMEC-like cells (ALS BMECs) confocal images. BMEC-like cells were fixed in 100% MeOH. Scale bar equals 50µM. Images and results represent confocal z-stacks analysed in 3D volume. Glucose-1 transporter (Glut-1) in red and DAPI in blue for the nu-clei staining. Error bars represent the standard deviation of triplicate Transwell™ filters. Statistical significance was determined using Student's unpaired t-test (****p<0.0001). At least a total of 5 images were acquired per each condition, with a minimum of 3 technical replicates for a total of 3 biological replicates (N=3, total images per condition=45). **B**) Mitochondrial Real-Time ATP rate test was carried out on healthy donor hi-PSCs derived BMEC-like cells (CTR BMEC-like cells), and 3 C9-ALS donors hi-PSCs derived BMEC-like cells (ALS BMEC-like cells). Data were acquired and analysed using the Agilent Technologies Sea-horse platform and software. Oxygen consumption rate (OCR) measurement per cells is represented as a time curse. The addition of the mitochondrial drugs Olygomycin (A) and Rotenone/Antimycin A (B) are indicated in the graph. **C**) Mitochondrial Real-Time ATP rate test was carried out on healthy donor hi-PSCs derived BMEC-like cells (CTR BMEC-like cells), and 3 C9-ALS donors hi-PSCs derived BMEC-like cells (ALS BMEC-like cells). Data were acquired and analysed using the Agilent Technologies Sea-horse platform and software. Error bars represent the standard deviation of triplicate wells N=3. Data is plotted as Min-Max Box and Whisker. Statistical significance was determined using Student's unpaired t-test (****p<0.0001)

C9-ALS BMEC-like cells conditioned medium reduce neurite length of healthy MNs

Once established that C9-ALS BMEC-like cells display cell-autonomous defects, such as impaired TEER and metabolism along with mild levels of cytotoxicity, we decided to explore the effect of BMEC-like cells on healthy control (CTR) motor neurons (MNs). To avoid confounding effects from contact cultures, we used the BMEC-like cells conditioned media, shown to be cytotoxic as per an increase in the lactate release, measured by the LDH test (Fig. 5A). MNs were derived from healthy hi-PSCs and treated with 30% BMEC-like cells conditioned medium for 3 days (Fig. 5B). No differences among MNs treated with CTR BMEC-like cells conditioned media or untreated were observed. Hence, contrary to what is reported for astrocytes [27], the BMEC-like cells conditioned media from healthy donors did not improve neurite length in healthy MNs (Fig. 5C, D). However, C9-ALS BMEC-like cells conditioned medium significantly decreased the total neurite length of treated CTR MNs by 93.8% (Fig. 5C and D), hence causing extensive cell death.

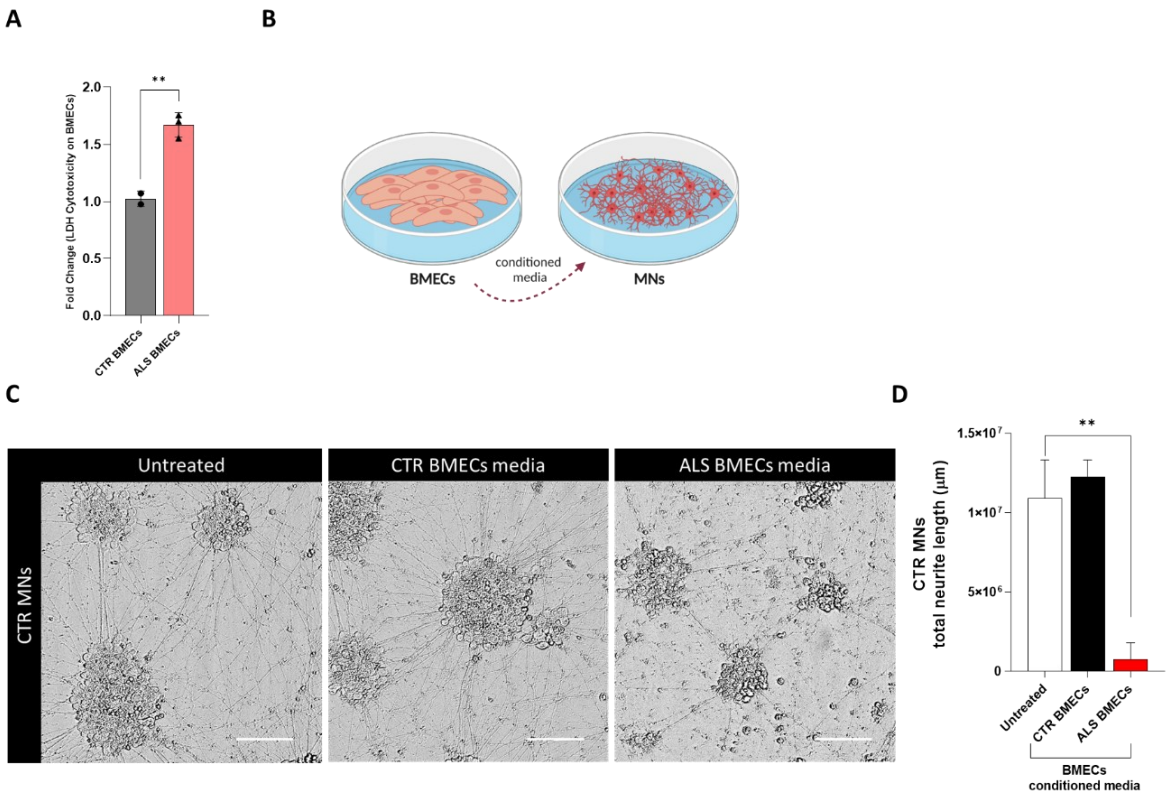

Fig. 5 C9-ALS BMEC-like cells restrict neurite length in healthy Motor Neurons A) The Lactate Dehydrogenase Assay (LDH) assay was performed on 2 healthy donors and 3 C9-ALS donors hi-PSCs derived BMEC-like cells. Statistical significance was determined using Student's unpaired t-test (****p<0.0001). B) The diagram was created on Biorender.com C) Control Motor Neurons (MNs) were fixed with 4%PFA after 72 h on 30% BMEC-like cells conditioned media treatment. Brightfield images are shown as follows: untreated MNs, control BMEC-like cells media (CTR BMECs) and ALS BMEC-like cells media (ALS BMECs) treated MNs. The scale bar equals 50 µM. At least a total of 5 images were acquired per each condition, with a media of 3 repli-cates for a total of 3 biological replicates (N=3, total images per condition=45). D) Neurite length analysis was performed with ImageJ software. Data are plotted as Mean±SD. Statistical significance was determined using One-Way ANOVA (****p<0.0001). N=5

Discussion

The BBB is a multi-functional compartment that shields the brain from external agents to protect it from infections and toxic molecules. It facilitates gas and nutrient exchange through a complex network of endothelial cells, astrocyte end-feet, and pericytes along capillaries.

BBB dysfunction is implicated in several neurodegenerative disorders [3]. While a clearer link has been described in dementia [28], little is known about the role of endothelial cells in ALS pathogenesis [29].

Given that *C9ORF72* (C9) repeat expansions are the most common genetic cause of ALS and frontotemporal dementia [12], we decided to investigate the characteristics and function of brain microvascular endothelial cells (BMEC-like cells) using 5 different C9-ALS patient-derived pluripotent stem cell lines (hi-PSCs).

First, we assessed the endothelial properties of BMEC-like cells. In contrast to the results reported in C9-ALS animal models, where most of the tight junctions seem to be downregulated at the protein level [16]; many of the transcripts were upregulated in C9-ALS BMEC-like cells. An example is Cadherin-5 (VE-Cadherin), which is exclusively expressed in endothelial cells and is involved in adherens junction assembly and maintenance [30, 31]. The junctional adhesion molecule Jam-2 (Jam-b) is involved in the regulation of cell polarity, endothelium permeability and leukocyte migration. Jam-2 downregulation might have a positive effect on immune disorders, suggesting a role in disease pathophysiology [32]. The tight junction 1 or ZO-1 transcript level was also higher in C9-ALS BMEC-like cells compared to CTR-BMEC-like cells. ZO-1 is essential for BBB assembly, as this protein is responsible for the organization of various components of the tight junction and for linking them to cytoskeletal actin [33].

Gene expression alterations do not always correspond to alterations in protein levels [34] due to the several processing steps between RNA and protein synthesis, especially in disease cases, such as C9-ALS, where RNA nucleo-cytoplasmic transport, as well as protein synthesis and turnover, are impaired [35].

In our study, Claudin-5 and other tight junctions were significantly upregulated at the mRNA level in C9-ALS BMEC-like cell monocultures compared to healthy BMECs, while protein levels in the membrane appeared unchanged via immunostaining. These results are inconsistent with the significant barrier defects detected via TEER measurements. In this context, transcriptional upregulation might reflect a compensatory mechanism to counteract a functional defect and failure to detect protein expression alterations could be explained by the technical limitations of immunostaining, which is only semi-quantitative and might fail to detect small changes. In addition, staining quantification was performed on the whole cell, rather than in the membrane, where tight junctions fulfil their function, hence potentially accounting for the difference between protein expression and functionality.

Of note, BBB integrity is not only linked to Claudin-5, in fact, several Claudins contribute to BBB electrical resistance [36]. Hence, our assessment of specific causative tight junction changes responsible for membrane permeability defects is limited. Several factors, such as an overall dysregulation of tight junction expression and membrane composition, post-translational modifications and splicing variants could cause defects in C9-ALS BMEC barrier properties. Subtle changes in BBB permeability can also be detected via tracer permeability assays, such as fluorescein and Evans blue-albumin, which were not performed in this study.

Lactate dehydrogenase (LDH) cytotoxicity or release test, which measures the LDH in the cell culture supernatant showed that C9-ALS BMEC-like cells showed a cytotoxicity value of over 50% compared to the healthy control cells. Although functional TEER defects could also be explained by the reported increased levels of cytotoxicity detected in C9-ALS BMEC-like cells, we have not observed macroscopic levels of cell loss in the cultures, as indicated by the Eosin Y staining or differences in cell numbers assessed during staining. It cannot be excluded, however, that cell death might occur over the 4-day assay during which TEER was measured.

The defects we have highlighted in this study, however, cannot be solely linked to cell death. C9-ALS BMEC-like cells displayed a significant increase in the expression and function of the P-glycoprotein transporter (ABCB1), which is crucial for drug delivery. P-glycoprotein upregulation is a very common feature in many diseases, including ALS, epilepsy and cancer in in vivo models [37, 38]. It is of great relevance for the development of disease-specific drug-permeability in vitro assays that the BBB model described here recapitulates increased P-gp functionality, thus providing a unique tool for the advancement of such pharmacodynamic assays.

Another membrane protein crucial for endothelial cell function and its relationship with neurons is Glut-1, the main glucose transporter expressed in the BBB. Our data highlighted increased expression of this protein in C9-ALS BMEC-like cells, with a concomitant severe decrease in basal glycolysis and a potentially compensatory increase in mitochondrial respiration. Recently, Kim et al. reported that brain endothelial cells are preferentially glycolytic, and this is associated with the maintenance and permeability of the BBB [39]. Kim and colleagues showed an impaired endothelial barrier permeability to molecules utilizing the transcellular pathway upon glycolysis inhibition [39]. Glycolysis therefore has a vital role in BBB homeostasis, promoting vessel branching and modulating angiogenesis [40].

Interestingly, this is dissimilar to the metabolic defects reported in other models of *C9ORF72* pathology, where neurons have mostly displayed defects in mitochondrial respiration [42]. Thus, while endothelial cells are preferentially glycolytic [41], motor neurons mostly use mitochondrial respiration to produce energy [42].

Our previous research on C9-ALS patient-derived astrocytes (iAstrocytes) demonstrated that *C9ORF72* astrocytes affect neuronal networks through cell-to-cell contact [25], as well as through the secretion of toxic factors [27]. Consequently, we decided to explore the effect of iAstrocytes on BMEC-like cells, given the crucial role of astrocytes in BBB homeostasis.

Consistent with the toxic properties of astrocytes towards motor neurons, C9-ALS iAstrocytes caused severe impairment of the TEER properties of healthy BMEC-like cells both through contact and conditioned medium, thus indicating that secreted factors might be the culprit. In fact, C9-ALS iAstrocyte conditioned medium treatment caused an upregulation in the Glut-1 transporter in both control and C9-ALS BMEC-like cells; while it caused a decrease in Claudin-5 expression in ALS BMECs. Although C9-ALS astrocytes only induced a decrease in TEER in non-contact cultures, the lack of an increase in TEER in the contact cultures with BMECs and C9-ALS astrocytes compared to BMECs only is unexpected. In fact, the electrical resistance of combined BMECs and astrocytes should be higher than BMECs on their own, thus suggesting that C9-ALS astrocytes affect healthy BMECs in both paradigms tested. Interestingly, C9-ALS iAstrocytes only mildly increased the already existing defects in C9-ALS BMEC-like cells, indicating that these cells are affected by the presence of mutations in *C9ORF72* in a cell-autonomous fashion.

Indeed, BMEC-like cells not only are intrinsically affected by the *C9ORF72* mutation, but they also display highly toxic properties against healthy human motor neurons via secreted factors, similar to

astrocytes. C9-ALS BMEC-like conditioned medium treatment significantly increased cell death and subsequently reduced motor neuron neurite length by more than 90% after only 3 days of exposure. As previously reported, neurotoxicity is not a property common to any cell type derived from ALS patients, in fact, fibroblasts do not display such characteristics [25].

Although genetic experiments in in vivo models of SOD1-ALS had led to the conclusion that endothelial cells played no role in disease pathogenesis [43], our data demonstrate that C9-ALS endothelial cells are intrinsically affected by the presence of the *C9ORF72* mutation. These cells display hyperactivation of P-gP transporters, which can cause pharmaco-resistance; and alterations in tight junction expression together with associated membrane permeability [44]. In addition, C9-ALS BMECs also displayed a marked decrease in glycolysis alongside an increase in mitochondrial energy production, thus indicating a metabolic shift that can affect membrane permeability [45] and substrate exchange with neurons [46]. Most importantly, our data demonstrate that C9-ALS BMECs can play a significant role in non-cell autonomous motorneuronal death through secreted factors.

Materials and Methods

Cell culture

Human umbilical vein endothelial cells (HUVECs)

Cells were purchased from ATCC (CRL-1730) and routinely seeded on uncoated flasks or 6-well plates. Following the manufacturer's recommendations, Human Endothelial Serum Free Medium (hESFM, Gibco), supplemented with 10% Foetal Bovine Serum (FBS, Gibco) and 1% penicillin/streptomycin media was replaced every 24-48 h, when cells reached 70% confluence. Cells were split when they approached 85% confluence by removing the media and washing twice with HBSS with no calcium/magnesium. Then, cells were incubated with trypsin for up to 10 min at 37 °C until the cells became completely round. Afterwards, the cell suspension was collected and subsequently centrifuged for 7 min / 100 g. Finally, the cell pellet was homogenised in 1 ml of fresh media, cells were counted with an automatic haemocytometer by mixing 10 µl of cell suspension with 10 µl of trypan blue and seeded following the supplier recommendations (2.3 × 103 viable cells / cm^2).

Human induced pluripotent stem cells derived brain endothelial-like cells

Brain endothelial-like cells (BMEC-like cells) were generated by culturing human induced pluripotent stem cells (hi-PSCs) in mTeSR plus media (STEMCELL Technologies) on Matrigel-coated (Corning) plates as previously described by Lippmann and Neal et al. protocols [19, 47, 48]. When hi-iPSCs reached more than 80% of confluence, they were detached by incubating the plate with accutase, for 5 min at 37 °C. Next, cells were collected and centrifuged for 4 min / 200 g and resuspended in TeSR™-E8™ media (STEMCELL Technologies). Subsequently, cells were counted with an automatic hemocytometer as described before and seeded at appropriate density (∼ 14 × 103 viable cells x cm^2) in matrigel coated 6w- plates.

Day 1 of differentiation began two days after seeding, or when cells reached 60–70% confluency, by switching the media to serum-free media TeSR™-E6™ (STEMCELL Technologies), refreshing it daily for 4 days. On day 5, during the expansion phase, the media was changed to EM+ (hESFM supplemented with 10 µM Retinoic Acid (RA, Sigma), 20 ng/mL bFGF (STEMCELL Technologies), 0.5% B-27 (Gibco), and maintained for 48 h). At day 7 of differentiation, cells were subcultured. Firstly, the media was removed, and cells were washed with HBSS with no calcium/magnesium and 1 ml of accutase (STEMCELL Technologies) was added per well and incubated at 37 °C 20–45 min until a single cell

suspension was formed. Then, cells were gently collected and centrifuged for 4 min/ 200 g. Optionally, cells can be stored in liquid nitrogen with 10% DMSO (Sigma). Finally, cells were reseeded or thawed in a mix of collagen IV and fibronectin pre-coated plates or cell culture inserts and maintained for one day in EM+ plus ROCK inhibitor (Tocris) at a final density of 1 million cells/ cm^2. At day 8, media was switched to hESFM supplemented with 0.5% B-27 only until the end point. At day 9 BMEC-like cells are ready to be tested.

Cell lines' relevant clinical information is described in Supplementary Table 1.

Hi-PSCs-derived motor neurons

Neural differentiation was performed using a modified version of the dual SMAD inhibition protocol [49]. Briefly, hi-PSCs in the presence of small molecules: ROCK inhibitor, SMAD inhibitors (SB431542 and DMH1) for 6 days, SB431542 (Tocris), DMH1 (Tocris), RA and Purmorphamine (Tocris) for another 6 days. At that point, all the hi-PSC lines generated more than 90% OLIG2 + Motor Neuron Progenitor Cells. Afterwards, the cells were expanded in the same media, supplemented with valproic acid (STEMCELL Technologies).

To induce MN differentiation, OLIG2 + MNPs were dissociated and cultured at a density of 1:6 in suspension in neural medium with RA and Purmorphamine. The medium was changed every other day for 6 days. Next, they were dissociated into single cells and plated on Matrigel-coated plates and cultured with RA, Purmorphamine and Compound E (γ-Secretase-IN-1, Sigma) for 10 days, after that, the media was replaced with neuronal media (neurobasal media supplemented with 1% of B27, BDNF 10ng/mL, CNTF 10ng/mL and IGF 10ng/mL). The cells were then fed on alternate days with neuronal medium until day 40 to mature into CHAT + MNs.

Cell lines relevant clinical information is described in Supplementary Table 1.

Hi-NPCs derived iAstrocytes

Fibroblasts were reprogrammed to human-induced neuronal progenitor stem cells (hi-NPCs) following the Meyer et al. 2014 protocol [25]. In brief, fibroblasts were seeded in a well of a six-well plate and treated with a mixture of retroviral vectors expressing Kruppel-like factor 4 (Klf4), POU transcription factor Oct-3/4 (Oct3/4), SRY-related HMG-Box Gene 2 (Sox2), and c-Myc for 12 h (System Biosciences). To promote neuroprogenitor cell conversion, the culture medium was switched 72 h after to a medium containing bFGF, epidermal growth factor (EGF, STEMCELL Technologies), and heparin (Sigma), and this was continued for 18 days.

To obtain iAstrocytes, hi-NPCs were seeded in 2.5 µg/ ml fibronectin-coated 10 cm dishes onto Knockout DMEM-Ham's F12 (Gibco), GlutaMAX supplement (STEMCELL Technologies); plus 10% FBS, 1.8% 100x diluted N2 (ThermoFisher) and 1% Penicillin/Streptomycin (Sigma); according to Meyer and Ferraiuolo's protocol [25], for 7 days.

Cell lines relevant clinical information is described in Supplementary Tables 1 and 2.

BMEC-like cells and iAstrocytes conditioned media and co-culture

At day 7 of BMEC-like cell differentiation cells were subcultured and seeded on the upper part of cell trans-well inserts (0.4µM, PET, Corning) or in 96-well clear bottom black (Fisher) at a density of 1 million cells/ cm^2. At day 8, BMEC-like cells were co-cultured with mature iAstrocytes. If performing conditioned media experiments, iAstrocytes conditioned media was collected and fast-frozen using dry ice. For co-culture, the iAstrocytes in dishes were washed once with PBS and detached by adding accutase at 37 °C. Then, the iAstrocyte suspension was collected and centrifuged for 4 min/200 g. At

that time, iAstrocytes were replated either at the bottom of the 2.5 µg/ml fibronectin-coated trans-well insert and incubated for 1 h at 37 °C (contact co-culture) or in the well below the Transwell™ insert (non- contact co-culture) at a density of 0.3 cells/cm^2. Finally, conditioned media and cells were tested after 2 or 3 days.

Barrier tightness and transport

Transendothelial resistance (TEER) measurements

BMEC-like cells were seeded in fibronectin/collagen (Corning/Sigma) 0.4 µm PET trans-well inserts when subculturing, as previously described. TEER (transendothelial resistance) measurements were monitored daily after day 8 of differentiation (day 1 of subculture), with an EVOM2 stx2 electrode. Before the TEER measurements, the cell's monolayer was visually checked, and only intact monolayers were used. Three measurements per insert were recorded at a standard time each day by placing the electrode chopsticks on the Transwell™ inserts containing the cells. One plate was recorded at a time to avoid artificially raising TEER because of having the plate a prolonged time outside the incubator as suggested by Stebbins et al. [50]. Finally, the plotted values were normalized by subtracting the blank (TEER from an empty insert) and then multiplied by the surface area (0.33 cm^2) of the transwell filter and reported as Ω × cm^2.

Efflux activity: P-glycoprotein transporter

Similarly, BMEC-like cells are tested on day 9 of the differentiation protocol. For this assay, cells were seeded in a 24-w plate at day 7. Later, at day 9, media was aspirated, and cells were washed with HBSS with no calcium/ magnesium. Next, 3 wells per condition were incubated for 1 h at 37 °C with HBSS only and 3 wells with HBSS + 10µM Cyclosporin A (CyA, R&D Systems), a P-glycoprotein inhibitor to inhibit transport. Then, the solution was aspirated, and the cells were incubated for 1 h at 37 °C with HBSS + 10µM Rhodamine 123 (ThermoFisher), a P-glycoprotein substrate; or with HBSS + Rhodamine 123 + CyA respectively. Afterwards, BMEC-like cells were rinsed with PBS twice and fluorescence was measured at Ex 488/ Em 530 nm with a PHERAstar® high-throughput screening microplate reader.

Transcription quantification by qRT-PCR

Cells were collected and washed twice with PBS and centrifuged for 4 min / 200 g subsequently. RNA was extracted following the manufacturer's instructions using the RNeasyPlus MiniKit (Qiagen). The RNA concentration was determined with a NanoDrop and the RNA to cDNA reverse transcription was performed following the manufacturer indications for the High-Capacity cDNA Reverse Transcription Kit (ThermoFisher). The RNA samples were standardised to 100 ng/µl. The qRT-PCR was finally completed by adding 50 ng of DNA per well in 384 well plates. The total volume per well was 10 µl, containing 50% SYBR Green, 5µM 2.5% forward Primer, 5µM 2.5% reverse Primer (Supplementary Table 3), 5% sterile ultra-pure water and 40% of cDNA. Transcripts were quantified by calculating the ratio between the expression of each transcript against the housekeeping gene and normalizing the expression to the reference control cell line, i.e., CTR hi-PSC in Fig. 1B or CTR BMEC-like cells in Fig. 2A.

Protein quantification by immunocytochemistry

Cells were washed twice with PBS and fixed either with 4% paraformaldehyde (ThermoFisher) for 20 min or 100% cold methanol for 10 min. Subsequently, the cells were incubated for 1 h at RT with a blocking solution of PBS, 5% animal serum and 0.3% Triton for non-membrane epitopes. Next, cells were rinsed 3 times with PBS. Then, they were incubated with the primary antibody at 4 °C overnight (Supplementary Table 3). The following day, cells were rinsed 3 times with PBS and incubated for 1 h at RT with the secondary antibody (Supplementary Table 3). Nuclei were stained with 1 µg/ml Hoechst

33342 for 5 min. Finally, the cells were washed 3 times with PBS and the images were normally acquired with a Nikon confocal microscope or with the Opera Phenix™ high-content screening system microscope.

Fluorescence image acquisition

Z-stack images were captured using an AX R confocal on a Ti2-E base with an LUA-S4 laser launch and a DUX-VB 4-channel GaAsP detector (Nikon Instruments). The images were captured as z-stacks in NIS-Elements AR software (Nikon Instruments) with a 0.5-µm step size in 2 K resonant mode using the 20x Plan Apochromat Lambda D objective (Nikon Instruments) and a 1AU pinhole for a final lateral resolution of 0.17 µm/pixel. For each experiment, at least a total of 5 images were acquired per condition, with a minimum of 3 technical replicates for each of the 3 biological replicates (*N* = 3, total images per condition = 45).

Fluorescence Images Analysis

NIS-Elements software (Nikon Instruments, v. 5.42) with the general analysis 3 (GA3) module was used to process and analyse images in 3D volume format. All images were pre-processed with Denoise.ai to remove confocal shot noise and facilitate segmentation. For each z-stack, an automatic threshold was calculated from the background signal intensity for each channel and was used to segment the volume that contained cells stained for the marker of interest. The total cell volume and the mean signal intensity in that volume were automatically measured, along with the mean signal intensity in the volume that did not contain cells (i.e., background intensity). The final reported mean signal intensity was corrected by subtracting the background intensity from the measured mean.

Cytotoxicity assay

To measure the cellular toxicity within the cells, a lactate dehydrogenase (LDH) assay was assessed following the manufacturer's indications (CyQUANT™, ThermoFisher). BMEC-like cells were seeded at appropriate density in a 96-w plate at day 7 of the differentiation protocol. After 2 days, the LDH test was done, and the absorbance was measured at 490/680 nm with a PHERAstar® high-throughput screening microplate reader. To determine LDH activity, 682 nm absorbance was subtracted from the 490 nm signal. Lysed cells were considered the maximum LDH activity control and media without cells was used as a blank.

Mitochondrial kinetics test

To test the effect of cell types on each other's function, BMEC-like cells were seeded at the desired density in a 96-w Agilent assay plate. The Agilent Seahorse XF Real-Time ATP Rate Assay evaluates key parameters of mitochondrial function by directly measuring the oxygen consumption rate (OCR) of cells on the Seahorse Analysers. It is a plate-based live cell assay that allows the monitoring of OCR in real-time. Non-mitochondrial respiration, which is the oxygen consumption that persists after the addition of rotenone and antimycin A (complex I and III electron transport chain inhibitors respectively) is used to obtain an accurate measure of true mitochondrial respiration. On the other hand, basal respiration which is being used to drive ATP production is measured upon injection of oligomycin (ATP synthase inhibitor) showing the ATP produced by the mitochondria.

Neurite length quantification

After 3 days of BMEC-like cells conditioned media treatment, motor neurons were fixed with 4% paraformaldehyde and brightfield images per were acquired with the Opera Phenix™ high-content

screening system microscope. In addition, ImageJ software was used for complementary image processing and neurite length quantification [51].

Data Analysis

All statistical analyses were undertaken with GraphPad Prism software (v.10); details of the statistical analyses have been indicated in each figure legend. Immunocytochemistry images were processed with either Columbus™ Image Data Storage and Analysis system software or Nikon NIS-Elements software (v. 5.42).

Supplementary Information

The online version contains supplementary material available at https://doi. org/10.1186/s12987-024-00528-6.

Supplementary Material 1

Supplementary Material 2

Acknowledgements

We thank the patients and healthy control participants who donated biosamples which supported this project. This project was funded by the 765704/European Union's Horizon 2020 research and innovation programme under the Marie Skłodowska-Curie grant agreement. The project was also supported by the NIHR Sheffield Biomedical Research Centre NIHR203321 and the Motor Neurone Disease Association AMBRoSIA 972-797. LF is also supported by the MRC (MR/W00416X/10).

Author contributions

L.F. and P.J.S. acquired the funding for the study as PIs within the EuroNeurotrophin Network, developed the original research idea and supervised the project. A.A-G. and L.F. developed the experimental design and prepared the manuscript. A.A-G. prepared the figures and performed the experiments. A.S. and S.G. cultured and prepared the iAstrocytes. J.K. and C.S. cultured and prepared the Motor Neurons. F.R. performed the mitochondrial assays. T.V. processed and assisted with acquiring and analysing the confocal images. S.B., Y.D. and K.M. reviewed and assisted in preparing the experiments. All authors reviewed the manuscript.

Data availability

The datasets used and/or analyzed are included in this manuscript and all materials are commercially available.

Declarations

Competing interests

The authors declare no competing interests.

Received: 18 December 2023 / Accepted: 2 March 2024

References

1. Muoio V, Persson PB, Sendeski MM. The neurovascular unit - concept review. Acta Physiol (Oxf). 2014;210:790–8.
2. Villegas JC, Broadwell RD. Transcytosis of protein through the mammalian cerebral epithelium and endothelium. II. Adsorptive transcytosis of WGA-HRP and the blood-brain and brain-blood barriers. J Neurocytol. 1993;22:67–80.
3. Aragón-González A, Shaw PJ, Ferraiuolo L. Blood–brain barrier disruption and its involvement in neurodevelopmental and neurodegenerative disorders. Int J Mol Sci 23, (2022).
4. Zlokovic BV. The blood-brain barrier in health and chronic neurodegenerative disorders. Neuron. 2008;57:178–201.
5. Obermeier B, Daneman R, Ransohoff RM. Development, maintenance and disruption of the blood-brain barrier. Nat Med. 2013;19:1584–96.
6. Alvarez JI, Katayama T, Prat A. Glial influence on the blood brain barrier. Glia. 2013;61:1939–58.
7. Benarroch E. What Are the Roles of Pericytes in the Neurovascular Unit and Its Disorders? *Neurology* 100, (2023).
8. Kushner PD, Stephenson DT, Wright S. Reactive astrogliosis is widespread in the subcortical white matter of amyotrophic lateral sclerosis brain. J Neuropathol Exp Neurol. 1991;50:263–77.
9. Acosta C, Anderson HD, Anderson CM. Astrocyte dysfunction in Alzheimer disease. J Neurosci Res. 2017;95:2430–47.
10. Molofsky AV, et al. Astrocytes and disease: a neurodevelopmental perspective. Genes Dev. 2012;26:891–907.
11. Petrov D, Mansfield C, Moussy A, Hermine OALS, Clinical Trials Review. 20 years of failure. Are we any closer to registering a New Treatment? Front Aging Neurosci. 2017;9:68.
12. Abel O, Powell JF, Andersen PM, Al-Chalabi A. ALSoD: a user-friendly online bioinformatics tool for amyotrophic lateral sclerosis genetics. Hum Mutat. 2012;33:1345–51.
13. Garbuzova-Davis S, et al. Amyotrophic lateral sclerosis: a neurovascular disease. Brain Res. 2011;1398:113–25.
14. Seo SW, et al. Clinical significance of microbleeds in subcortical vascular dementia. Stroke. 2007;38:1949–51.
15. Brundel M, et al. High prevalence of cerebral microbleeds at 7Tesla MRI in patients with early Alzheimer's disease. J Alzheimers Dis. 2012;31:259–63.
16. Pan Y et al. Altered Blood–Brain Barrier Dynamics in the C9orf72 Hexanucleotide Repeat Expansion Mouse Model of Amyotrophic Lateral Sclerosis. *Pharmaceutics* vol. 14 Preprint at https://doi.org/10.3390/pharmaceutics14122803 (2022).
17. Sweeney MD, Zhao Z, Montagne A, Nelson AR, Zlokovic BV. Blood-brain barrier: from physiology to Disease and back. Physiol Rev. 2019;99:21–78.
18. Prell T, Vlad B, Gaur N, Stubendorff B, Grosskreutz J. Blood–brain barrier disruption is not Associated with Disease aggressiveness in amyotrophic lateral sclerosis. Front Neurosci 15, (2021).
19. Neal EH, et al. A simplified, fully defined differentiation Scheme for producing blood-brain barrier endothelial cells from human iPSCs. Stem Cell Rep. 2019;12:1380–8.
20. Luissint AC, Artus C, Glacial F, Ganeshamoorthy K, Couraud PO. Tight junctions at the blood brain barrier: physiological architecture and disease-associated dysregulation. Fluids Barriers CNS. 2012;9:Preprintathttpsdoiorg1011862045–8118.
21. Srinivasan B, et al. TEER measurement techniques for in vitro barrier model systems. J Lab Autom. 2015;20:107–26.
22. Butt AM, Jones HC, Abbott NJ. Electrical resistance across the blood-brain barrier in anaesthetized rats: a developmental study. J Physiol. 1990;429:47–62.
23. Ferraiuolo L. The non-cell-autonomous component of ALS: New in vitro models and future challenges. Biochem Soc Trans 42, (2014).
24. Chen H, Kankel MW, Su SC, Han SWS, Ofengeim D. Exploring the genetics and non-cell autonomous mechanisms underlying ALS/FTLD. *Cell Death and Differentiation* vol. 25 Preprint at https://doi.org/10.1038/s41418-018-0060-4 (2018).
25. Meyer K, et al. Direct conversion of patient fibroblasts demonstrates non-cell autonomous toxicity of astrocytes to motor neurons in familial and sporadic ALS. Proc Natl Acad Sci U S A. 2014;111:829–32.
26. Re DB et al. Necroptosis drives motor neuron death in models of both sporadic and familial ALS. Neuron 81, (2014).
27. Varcianna A et al. Micro-RNAs secreted through astrocyte-derived extracellular vesicles cause neuronal network degeneration in C9orf72 ALS. *EBioMedicine* 40, (2019).
28. Hussain B, Fang C, Chang J. Blood–Brain Barrier Breakdown: An Emerging Biomarker of Cognitive Impairment in Normal Aging and Dementia. *Frontiers in Neuroscience* vol. 15 Preprint at https://doi.org/10.3389/fnins.2021.688090 (2021).
29. Kakaroubas N, Brennan S, Keon M, Saksena NK. Pathomechanisms of Blood- Brain Barrier Disruption in ALS. *Neurosci J* 2019, 2537698 (2019).

30. Giannotta M, Trani M, Dejana E. VE-cadherin and endothelial adherens junctions: Active guardians of vascular integrity. *Developmental Cell* vol. 26 Preprint at https://doi.org/10.1016/j.devcel.2013.08.020 (2013).
31. Li W, Chen Z, Chin I, Chen Z, Dai H. The role of VE-cadherin in blood-brain Barrier Integrity under Central Nervous System pathological conditions. Curr Neuropharmacol 16, (2018).
32. Tietz S et al. Lack of junctional adhesion molecule (JAM)-B ameliorates experimental autoimmune encephalomyelitis. Brain Behav Immun 73, (2018).
33. Fanning AS, Jameson BJ, Jesaitis LA, Anderson JM. The tight junction protein ZO-1 establishes a link between the transmembrane protein occludin and the actin cytoskeleton. J Biol Chem 273, (1998).
34. Taylor RC et al. Changes in translational efficiency is a dominant regulatory mechanism in the environmental response of bacteria. Integr Biology (United Kingd) 5, (2013).
35. Lehmkuhl EM, Zarnescu DC. Lost in translation: evidence for protein synthesis deficits in ALS/FTD and related neurodegenerative diseases. in Adv Neurobiol 20 (2018).
36. Günzel D, Yu ASL. Claudins and the modulation of tight junction permeability. Physiol Rev 93, (2013).
37. Van Vliet EA, et al. Expression and Cellular distribution of P-Glycoprotein and breast Cancer resistance protein in amyotrophic lateral sclerosis patients. J Neuropathol Exp Neurol. 2020;79:266–76.
38. Ahmed Juvale II, Hamid A, Abd Halim AA. K. B. & Che Has, A. T. P-glycoprotein: new insights into structure, physiological function, regulation and alterations in disease. *Heliyon* vol. 8 Preprint at https://doi.org/10.1016/j.heliyon.2022. e09777 (2022).
39. Kim ES et al. Brain endothelial cells utilize glycolysis for the maintenance of the Transcellular permeability. Mol Neurobiol 59, (2022).
40. De Bock K et al. Role of PFKFB3-driven glycolysis in vessel sprouting. Cell 154, (2013).
41. Leung SWS, Shi Y. The glycolytic process in endothelial cells and its implications. *Acta Pharmacologica Sinica* vol. 43 Preprint at https://doi.org/10.1038/ s41401-021-00647-y (2022).
42. Turner DA, Adamson DC. Neuronal-astrocyte metabolic interactions: Understanding the transition into abnormal astrocytoma metabolism. *Journal of Neuropathology and Experimental Neurology* vol. 70 Preprint at https://doi. org/10.1097/NEN.0b013e31820e1152 (2011).
43. Garbuzova-Davis S, et al. Ultrastructure of blood-brain barrier and blood-spinal cord barrier in SOD1 mice modeling ALS. Brain Res. 2007;1157:126–37.
44. Mohamed LA, Markandaiah S, Bonanno S, Pasinelli P, Trotti D. Blood–Brain Barrier Driven Pharmacoresistance in Amyotrophic Lateral Sclerosis and Challenges for Effective Drug Therapies. *AAPS Journal* vol. 19 1600–1614 Preprint at https://doi.org/10.1208/s12248-017-0120-6 (2017).
45. Fitzgerald G, Soro-Arnaiz I, De Bock K. The Warburg effect in endothelial cells and its potential as an anti-angiogenic target in cancer. *Frontiers in Cell and Developmental Biology* vol. 6 Preprint at https://doi.org/10.3389/ fcell.2018.00100 (2018).
46. Bell SM et al. Peripheral glycolysis in neurodegenerative diseases. *International Journal of Molecular Sciences* vol. 21 Preprint at https://doi.org/10.3390/ ijms21238924 (2020).
47. Lippmann ES, et al. Derivation of blood-brain barrier endothelial cells from human pluripotent stem cells. Nat Biotechnol. 2012;30:783–91.
48. Lippmann ES, Al-Ahmad A, Azarin SM, Palecek SP, Shusta E. V. A retinoic acid-enhanced, multicellular human blood-brain barrier model derived from stem cell sources. Sci Rep. 2014;4:4160.
49. Du Z-W, et al. Generation and expansion of highly pure motor neuron progenitors from human pluripotent stem cells. Nat Commun. 2015;6:6626.
50. Stebbins MJ, et al. Differentiation and characterization of human pluripotent stem cell-derived brain microvascular endothelial cells. Methods. 2016;101:93–102.
51. Schneider CA, Rasband WS, Eliceiri K. W. NIH image to ImageJ: 25 years of image analysis. Nat Methods. 2012;9:671–5.

Supplementary data

Supplementary Figure 1

Blood-Brain Barrier phenotypic markers. Ve-Cadherin (CDH5), Claudin-5 (CLDN5), Junctional Adhesion Molecule 2 (JAM2), Occludin (OCLN), Transforming growth factor beta 1 (TGFB1), Zonula Occludens 1 (TJP1) and, Von Willebrand factor (VWF), P-glycoprotein (ABCB1), EAAT3 (SLC1A1), EAAT2 (SLC1A2), EAAT1 (SLC1A3), Insulin receptor (INSR) and, receptor for advanced glycation end products (RAGE) relative transcriptional expression to the housekeeping of 2 healthy donors and 3 C9-ALS donors hi-PSCs derived BMEC-like cells. qRT-PCR data are plotted as mean ± SEM. N=3 per group.

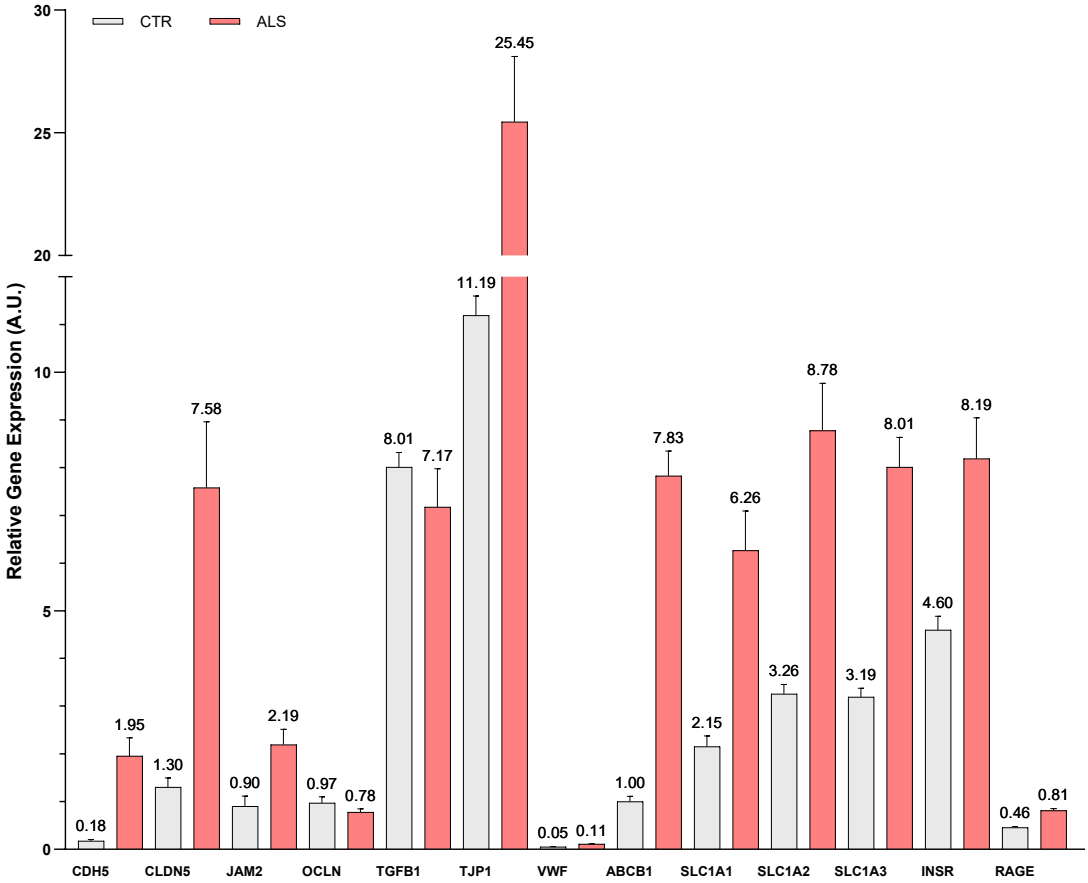

Supplementary Figure 2
Immunocytochemistry of BMEC cells differentiated from a healthy hi-PSCs donor total fluorescence intensity quantification. Claudin-5, Pecam-1 (CD31) and Vegf expression using the RA-enhanced Lippmann's laboratory protocol from 2019[23]. Scale bar 50um. N=3.

Claudin-5 and VEGF A images were acquired with a Nikon confocal microscope. In contrast, PECAM-1 was acquired with the Opera Phenix™ high-content screening system microscope. As a result, PECAM-1 images are not maximum projection and the 3D nature of the BMECs might look as gaps in the monolayer.

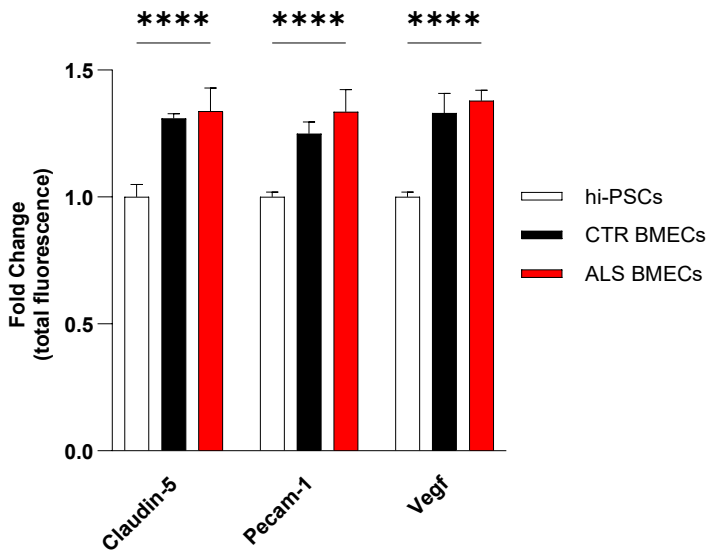

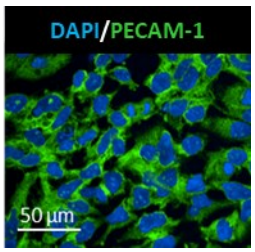

Supplementary Figure 3

BMEC barrier integrity was visually analysed by Eosin staining. Control and C9-ALS BMEC-like cells were stained with Eosin-Y and Hoechst solution for 1 and 5 minutes respectively. Brightfield images and EVOS fluorescence images (Eosin Y, Hoechst and combined) are shown. The scale bar equals 150 and 100 µM for the brightfield and fluorescence images respectively.

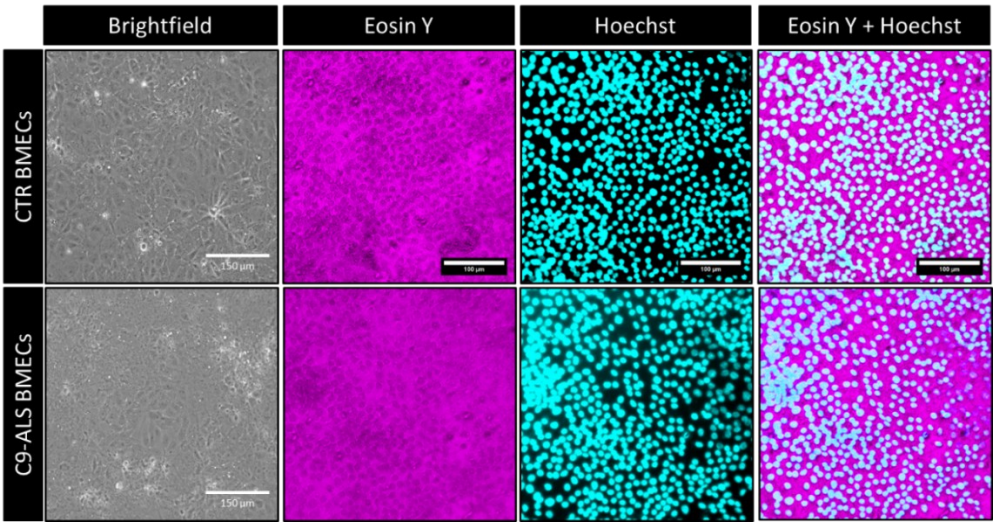

Supplementary Figure 4

BMEC passive barrier as shown by TEER following BMEC-like cells/iAstrocytes co-culture for C9-ALS BMEC-like cells. Error bars represent the standard deviation of triplicate Transwell™ filters. Statistical significance was determined using Two-Way ANOVA (****p < 0.0001). N=3.

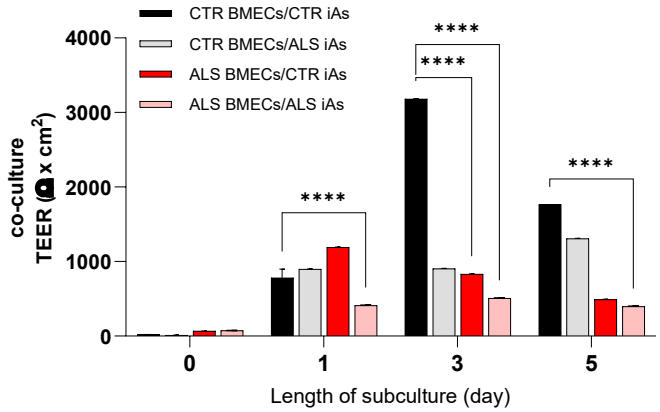

Supplementary Table 1
Hi-PSCs cell lines used for this research. All cell lines source tissue is fibroblasts.
(*)Cells available either as hi-PSCs or hi-NPCs.

Cell line	Supplier	Reprogramming Method	Clinical	Mutation protein	Ethnicity	Gender	Age at sampling
GM23338	Coriell Insitute	Retrovirus	**Control**	None	Caucasian	Male	55 years
CS14iCTR-21nxx*	Cedars Sinai	Episomal Plasmid Retrovirus	**Control**	None	Unknown	Female	52 years
CS52iALS-C9nxx*	Cedars-Sinai	Episomal Plasmid Retrovirus	**ALS**	*C9ORF72*	Caucasian	Male	49 years
CS29iALS-C9nxx*	Cedars-Sinai	Episomal Plasmid Retrovirus	**ALS**	*C9ORF72*	Caucasian	Male	47 years
CS28iALS-C9nxx*	Cedars-Sinai	Episomal Plasmid	**ALS**	*C9ORF72*	Caucasian	Male	47 years
ALS-183*	University of Sheffield	Sendai Virus	**ALS**	*C9ORF72*	Caucasian	Male	50 years
ALS-78*	University of Sheffield	Sendai Virus	**ALS**	*C9ORF72*	Caucasian	Male	66 years

Supplementary Table 2
Hi-NPCs cell lines used for this research. All cell lines source tissue is fibroblasts.
(NCH): Nationwide Children's Hospital, Columbus, OH

Cell line	Supplier	Reprogramming Method	Clinical	Mutation protein	Ethnicity	Gender	Age at sampling
161	NCH	Retrovirus	**Control**	None	Caucasian	Male	31 years
AG8620	NCH	Retrovirus	**Control**	None	Caucasian	Female	64 years
155	NCH	Retrovirus	**Control**	None	Caucasian	Male	40 years
S3	NCH	Retrovirus	**Control**	None	Asian	Male	Unknown
ZKW542	NCH	Retrovirus	**Control**	None	Unknown	Female	8 years

Supplementary Table 3

Primers used for qRT-PCR. Oligos designed and purchased from ThermoFisher.

Gene Name	Gene ID	Forward Sequence (5'-)	Reverse Sequence (5'-)
ABCB1	5243	TGAATCTGGAGGAAGACATGAC	CCAGGCACCAAAATGAAACC
ABCC1	4363	AATAGAAGTGTTGGGCTGAG	CGAGACACCTTAAAGAACAG
CDH5	1003	CGCAATAGACAAGGACATAACAC	GGTCAAACTGCCCATACTTG
CLDN5	7122	TTCGCCAACATTGTCGTCC	TCTTCTTGTCGTAGTCGCCG
INSR	3643	TGTTCATCCTCTGATTCTCTG	GCTTAGATGTTCCCAAAGTC
JAM2	58494	GCTCTAGAATAGACTTCCATGTCCTGCC	GGCAGGACATGGAAGTCTATTCTAGAG
OCLN	100506658	CTCGAGAAAGTGCTGAGTGCCTGGAC	AAGCTTTCGGTGACCAATTCACCTGA
POU5F1	5460	CCTGAAGCAGAAGAGGATCACC	AAAGCGGCAGATGGTCGTTTGG
RAGE	177	GTAGATTCTGCCTCTGAACTC	CTTCACAGATACTCCCTTCTC
RPL13	6137	TCAAAGCCTTCGCTAGTCTCC	GGCTCTTTTTGCCCGTATGC
RPL30	6156	GCTGGAGTCGATCAACTCTAGG	CCAATTTCGCTTTGCCTTGTC
RPL31	6160	CTCGGGCACTCAAAGAGATTC	CGGATTCGGTATGGCACATTC
RPL37	6167	CAAGCGCAAGAGAAAGTATAACTGG	CAGCTGCCCTCTTGGGTTTAG
SLC16A1	6566	GGTGTTTCTTAGTAGTTATGGG	TCTTATTGGCTTTGTGTTGG
SLC1A1	6505	GTTATTCTAGGTATTGTGCTGG	CTGATGAGATCTAACATGGC
SLC2A1	6513	ACGCTCTGATCCCTCTCAGT	GCAGTACACACCGATGATGAAG
SLC7A5	8140	TTAAAGTAGATCACCTCCTCGA	GGATGAGATTCGTACCAGAG
TJP1	7082	ACCAGTAAGTCGTCCTGATCC	TCGGCCAAATCTTCTCACTCC
vWF	7450	CCCGAAAGGCCAGGTGTA	AGCAAGCTTCCGGGGACT

Supplementary Table 4
Antibodies used for immunocytochemistry.

- Primary Antibodies

Antibody	Species	Company	Catalogue Number	Concentration	Fixation
CD31	Mouse	Proteintech	66065-1-Ig	1:300	MeOH
Claudin-5	Mouse	Invitrogen	35-2500	1:100	MeOH
Claudin-5	Rabbit	Abcam	Ab15106	1:100	MeOH
Glut-1	Rabbit	ProteinTech	21829-1-AP	1:150	MeOH
VEGF A	Rabbit	Proteintech	19003-1-AP	1:500	MeOH

- Secondary Antibodies

Antibody	Species	Wavelength (nm)	Company	Catalogue Number	Concentration
Anti-mouse	Donkey	568	Abcam	A10037	1:500
Anti-rabbit	Donkey	488	Abcam	A21206	1:500